# FOAM FRACTIONATION OF BIOPOLYMERS:

# STUDIES OF PROTEIN BEHAVIOUR

# IN ANALYTICAL AND PREPARATIVE SYSTEMS

by

**MARIA VELISSARIOU**

A thesis submitted to the

**FACULTY OF ENGINEERING**

of the

**UNIVERSITY OF BIRMINGHAM**

for the degree of

**DOCTOR OF PHILOSOPHY**

School of Chemical Engineering

University of Birmingham

P.O. Box 363

Birmingham B15 2TT

March 1992

## *SYNOPSIS*

The aim of the present work was to study the effects of molecular interactions between proteins upon foam quality in batch and continuous operations, and to investigate foam fractionation as a method of protein recovery from real biological feedstocks.

Foam stability studies of model protein solutions acted as engineering indicators and highlighted the importance of electrostatic interactions between basic (lysozyme and cytochrome-*c*) and acidic proteins (BSA) upon foamability and foam stability. Batch and continuous foam operations were employed in the study of electrostatic interactions between BSA and lysozyme and their effects upon foam quality. Batch foam production at pH 8.0 strongly demonstrated the importance of molecular stoichiometry upon individual protein partition into foam. Maximal lysozyme recovery was achieved at equimolar conditions and coincided with minimal fractionation between the two proteins. Continuous foaming demonstrated that foam positive proteins such as BSA (collector) can function as mobile ion-exchangers for poor foaming agents such as lysozyme (colligend). Experimentation with real biological systems such as brewer's yeast extract indicated that complex protein systems appear to behave like single protein solutions in terms of the effects of operating parameters upon foam performance. Such behaviour was confirmed by preliminary studies with bovine heart muscle homogenate. "Dry" foams, in continuous foam processing of brewer's yeast extract, were associated with dilute feedstocks, low gas flowrate and prolonged liquid residence times. They were characterised by high protein enrichment, low recovery, enhanced protein fractionation from RNA, but suffered extensive protein precipitation. Studies of dynamic changes in foam bubbles showed that such phenomena are associated with extensive coalescence.

It was concluded that, although single protein model systems can offer valuable information on foam fractionation, direct comparisons with real biological solutions should be treated with care. A need for further study on the role of protein interactions upon foaming was also identified. Finally, the currently held view of rejecting foaming as a source of protein precipitation should be reviewed and advancements in foam fractionation as a preliminary step in downstream processing should employ the development of semi-empirical predictive models.

ACKNOWLEDGEMENTS

This work was funded as part of the SERC Rolling Programme in the Centre for Biochemical Engineering in the School of Chemical Engineering at the University of Birmingham. I would like to take the opportunity to thank the following whose assistance and support was invaluable during my three years' research:

-My supervisor Dr Andrew Lyddiatt

-The members of the Biorecovery Group and in particular Dr Sudesh B. Mohan

-The technical staff in the Centre for Biochemical Engineering as well as the School of Chemical Engineering for general departmental technical support

-I acknowledge the assistance in computing offered by Miss J.F. Tidball and Mr R. M$^{C}$Iver and Mr A.B. Roberts.

-I am grateful to Dr I.E. Crompton and Dr P.K. Hegarty (Bass Brewers, Burton-upon-Trent) for their kind permission to use their image analysis facilities.

Finally, many thanks to Scott M$^{C}$Quiston for all his patience and understanding.

# CONTENTS

*CHAPTER 6*

*CONTINUOUS FOAM PRODUCTION FROM CLARIFIED BREWER'S YEAST EXTRACT*



*CHAPTER 7*

*DYNAMIC CHANGES IN FOAM BUBBLES AND EFFECTS UPON PROTEIN PARTITION*



*CHAPTER 8*



*APPENDICES*

## *LIST OF ILLUSTRATIONS*

### *FIGURES*

*PLATES*

## *LIST OF TABLES*

# *CHAPTER 1*

## *INTRODUCTION*

Throughout the chemical/biochemical process industries foams are of great importance. They can promote troublesome conditions causing adverse effects upon plant operations, but they are desirable and essential elements in processes such as foam fractionation and the manufacture of food products. The present chapter reviews foam phenomena and related applications of biological foams, first discussing the mechanism of foaming with particular emphasis on protein foams, and then elaborating on foam fractionation as a unit operation and its applicability to protein/enzyme recovery. Finally there is a brief presentation of the aims and objectives of the present thesis.

### 1.1 Theoretical Aspects of Foams

Foams are colloidal dispersions of gas in liquid or solid phases characterised by high volume fractions of the gas, and whose bulk density approaches that of the gas rather than the liquid. They are colloidal (Osipow (1962)) in the sense that the films separating the gas bubbles are of colloidal dimensions. In the present study only foams with liquid continuous phases will be considered. Such foams consist of bubbles whose walls are thin liquid films which exhibit rigidity and elasticity. Strong and cohesive viscoelastic films are a prerequisite for stable foam formation (Djabbarah and Wasan (1985)). Bubbles are separated by the so-called Plateau borders (see Figure 1.1), which are formed by the contact of three lamellae. Achievement of mechanical equilibrium necessitates the three angles formed by the contact of the three lamellae to be equal to $120^{\circ}$ (Bikerman (1973)). The diameter of foam bubbles can

**Figure 1.1: Idealised Cross-Sectional View of a Plateau Border**

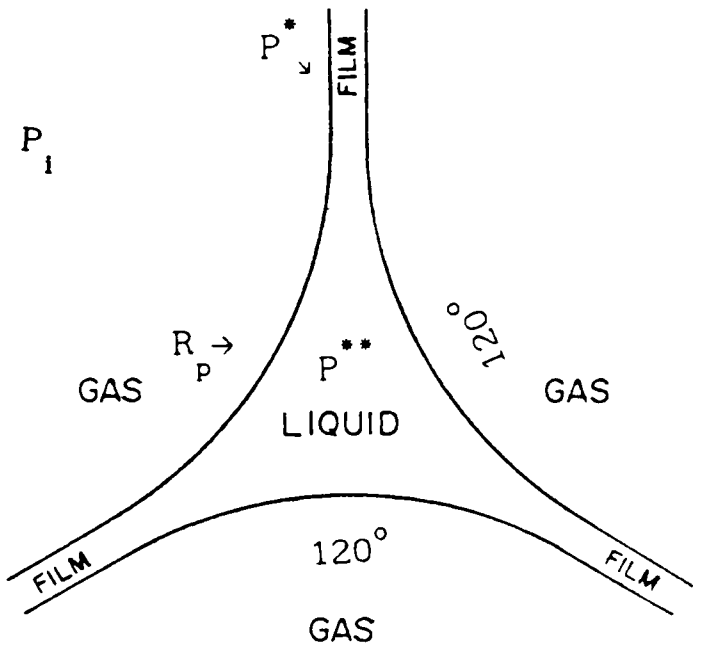


Legend

Plateau border (PB) is the intersection of 3 films

Film is the intersection of faces of 2 adjacent polyhedra

$R_p$ is the radius of curvature of the plateau border

$P^*$ the pressure inside the film

$P^{**}$ is the pressure inside the plateau border

$P_i$ is pressure inside a bubble i of radius $R_i$

vary from several inches down to fractions of a micron (Osipow (1962)).

Foams can cause severe problems in chemical processing steps involving gas-liquid interactions such as distillation, adsorption, evaporation, chemical reaction, and particle separation and settling. They can also be a problem in pulp and paper manufacture, coating and adhesive production, steam-boiler operation and foam control in products such as detergents, waxes, glycol anti-freeze and instant coffee (Perry and Green (1984); Kouloheris (1987)). They can interfere with process instruments, increase housekeeping costs (safety hazard) and impose a perceived negative environmental impact on discharge of frothy wastes (McGee (1989)). In contrast, fire-fighting foams are in great demand.

In biotechnological processes such as fermentation, foam is a very undesirable feature demanding close control though effective anti- and/or de-foaming actions. Contrary to their negative perception in fermentations, rapidly produced stable foams are desirable in the food industry for the manufacture of ice-cream, dessert topping, angel cakes and bread. The brewing industry is unique in the sense that foam generation in the early stages of fermentation can cause wasteful spillage, but brewers strive to manufacture and disperse a finished product with a good foaming "head". In wine making, however foam is undesirable both during fermentation and at dispense (Edwards et al. (1982)).

Foam formation necessitates the adsorption of a surface active component (surfactant) at the gas-liquid interface such that the rate of liquid drainage from the thin bubble films is reduced (Evans (1970)). Foams can be generated by whipping, shaking, bubbling or agitation of surfactant solutions. Surfactants lower the surface tension of solutions, but also permit gas bubbles to increase the total surface area of the gas-liquid interface (Davies and Rideal (1961)). Surfactants usually

**Figure 1.2: Concentration Gradient Between Surface and Bulk Phase at Equilibrium in Surfactant Systems** (from Charm (1973))

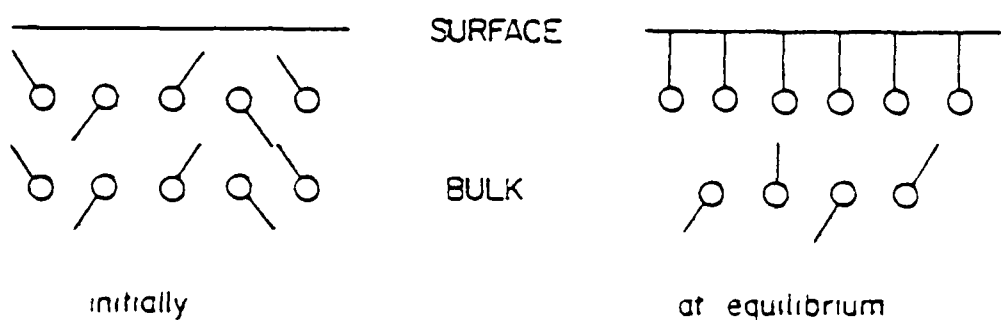


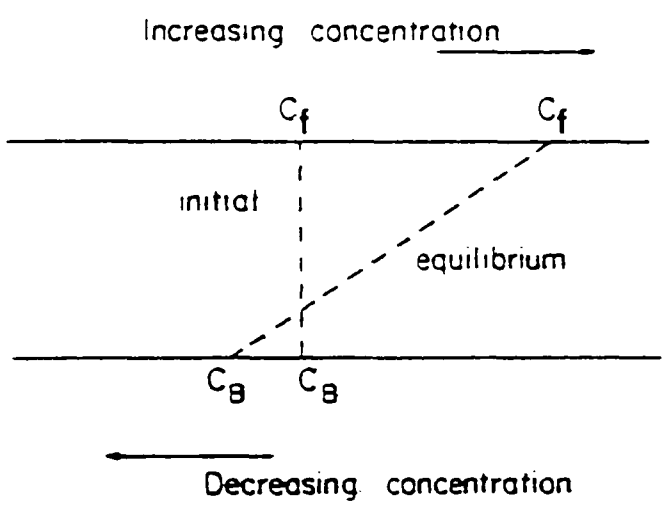

possess hydrophilic and hydrophobic groups, and concentrate at interfaces by orientating their hydrophobic moieties toward the gas phase while maintaining their hydrophilic domains in solution (the aqueous environment).

Given the availability of a surface, surfactant molecules in solution tend to migrate to the interface with a certain time delay (characteristic of each surfactant under comparable conditions), and thus increase the surface concentration. At equilibrium, whose establishment may vary from minutes to hours (Evans et al. (1970)), a concentration gradient exists between the surface (foam) and bulk phase (see Figure 1.2) and the chemical potentials of the two phases are equal as shown by Equation 1.1:

$$\mu_{iF} = \mu_{iB} \qquad \text{(Equation 1.1)}$$

where: $\mu_{iF}$ and $\mu_{iB}$ are the chemical potentials of the foam and bulk phase respectively.

The energy required for the movement of surfactant molecules from the bulk phase to the surface is provided by differences in the chemical potentials of the two phases referred to as the heat of desorption $\lambda$. The heat of desorption is described by Equations 2.5 and 2.6 in Chapter 2. At the onset of this surfactant migration, the concentration gradient is zero and the driving force is maximum, while at equilibrium the driving force is zero as $\mu_{iF} = \mu_{iB}$.

At constant pressure and temperature the Gibbs's adsorption theorem (Gibbs (1928)) is described by Equation 1.2:

$$d\sigma = -\{\Gamma_0 d\mu_0 + \sum_{i=1}^{n}(\Gamma_i \mu_i)\} \qquad \text{(Equation 1.2)}$$

where: $\sigma$ is the surface tension of the solution of n solutes.

$\Gamma_0$ and $\mu_0$ are the surface excess and the chemical potential of the solvent respectively

$\Gamma_i$ and $\mu_i$ are the surface excess and the chemical potential of the solutes present in the solution; $\Gamma$ [=] mass per surface area.

It is the usual convention to set $\Gamma_0 = 0$ as a standard of reference. For a single solute solution, where the activity coefficient of the solute is 1, Equation 1.2 can be reduced to Equation 1.3, which applies only to dilute solutions:

$$\Gamma = -(1/RT)(d\sigma/d\ln c) \qquad \text{(Equation 1.3)}$$

where: R is the ideal gas constant

T is temperature

c is the solute concentration.

Equation 1.3 shows that the surface excess depends on the slope of the line obtained by plotting $\sigma$ against ln c (see Figure 1.3), which theoretically determines foam concentration. At high solute concentrations, ie above critical micelle concentration (CMC), the monomolecular layer becomes saturated, whilst at very dilute solutions (below threshold concentration) bubbles cannot be stabilised. Both cases coincide with approximately zero slope in the curve of Figure 1.3 where surface excess is negligible. However, surface tension effects are time-dependent after the addition of protein in solution and tend to continuously decrease with time towards equilibrium. Bumbullis et al. (1981) have shown that the rate of change of surface tension depends upon the final protein concentration in solutions. Figure 1.4 (Lemlich (1973)) depicts a Langmuir type equilibrium isotherm for $\Gamma$. Graham and Phillips (1979b) described various types of adsorption isotherms for proteins such as lysozyme, $\beta$-casein and BSA respectively. In the case of a Langmuir type isotherm, $\Gamma$ is proportional to bulk solute concentration for very dilute solutions. Based on the same principle, fractionation of two solutes may

**Figure 1.3: Diagram of Surface Tension Against Concentration for Catalase and Amylase** (from Charm et al. (1966))

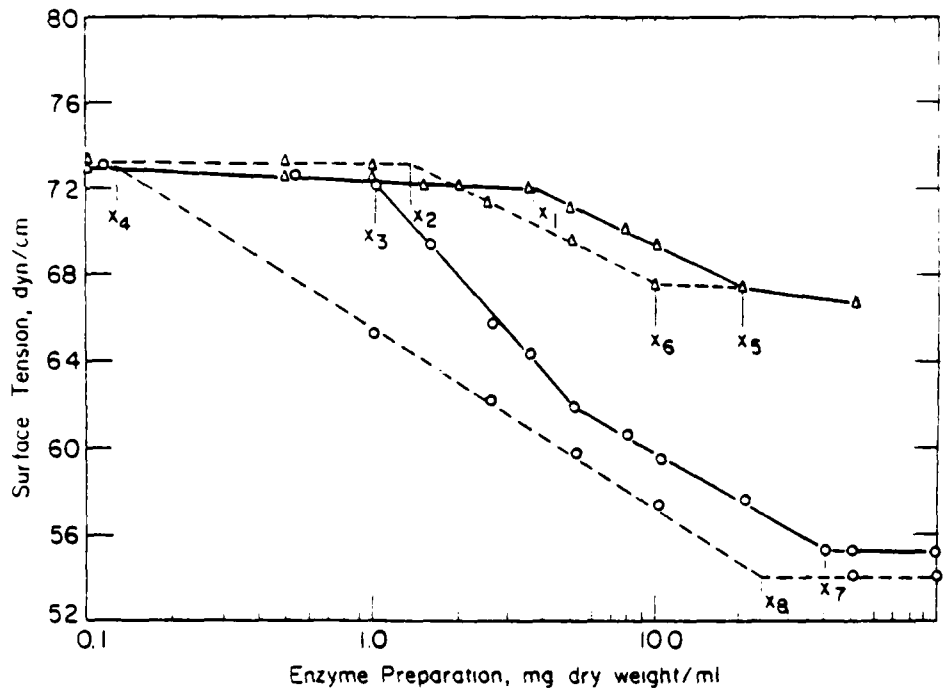


Surface tension-concentration diagram for catalase and amylase: (Δ — Δ) amylase in water; (Δ---Δ) amylase in 10% $(NH_4)_2SO_4$; (O——O) catalase in water; (O---O) catalase in 10% $(NH_4)_2SO_4$.

**Figure 1.4: Langmuir Isotherm for Protein Adsorption at the Gas-Liquid Interface**

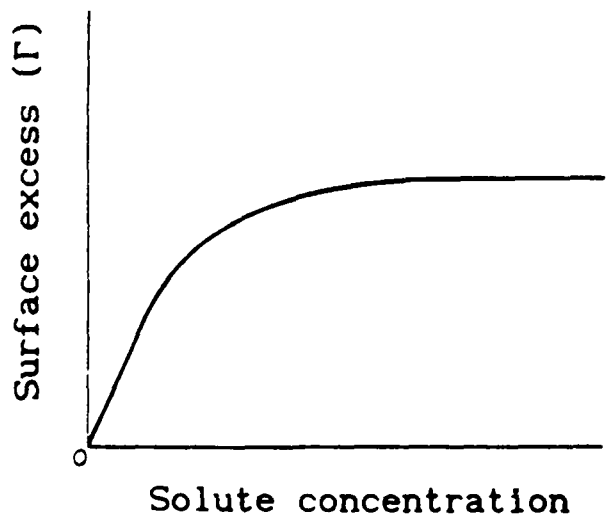

occur when their bulk concentrations lie in regions which give different $d\sigma/d\ln c$ values (see Figure 1.3). Best fractionation is expected to be achieved when one slope $d\sigma/d\ln c$ is negative and the other approximates zero values (threshold or CMC concentration values).

However, foams are thermodynamically unstable and tend to age rapidly by drainage and the formation of polyhedral bubbles. During drainage, the lamellae become increasingly thinner and brittle and, depending on the type of liquid film (Małysa (1985)), rupture may follow. Liquid from the films drains into the neighbouring plateau borders due to a combination of the actions of plateau border suction and the disjoining pressure associated with van der Waals attraction, and double layer and steric repulsions. Suction forces originate from the lower pressure present inside the intersection of the plateau border which creates a pressure difference as described by Equation 1.4 (Hansen and Derderian (1976)):

$$P^{*}-P^{**} = \sigma/R_{p} \qquad \text{(Equation 1.4)}$$

where: $\sigma$ is the surface tension

$R_p$ is the radius of curvature of the plateau border.

Inter-bubble gas diffusion, caused by pressure differences between bubbles of different size, promotes coalescence and disproportionation (Ronteltap et al. (1991)). The pressure difference between two bubbles is described by the equation of Laplace:

$$\Delta P_{total} = P_1 - P_2 = 2\sigma/R_1 - 2\sigma/R_2 \qquad \text{(Equation 1.5)}$$

where: $P_1$ and $P_2$ are Laplace pressures in the bubbles with radii $R_1$ and $R_2$ respectively

$\sigma$ is surface tension of both bubbles.

As drainage proceeds, weak areas in the lamellae may develop. However, the

presence of a higher surfactant concentration in the surface produces a lower surface tension. As the lamella starts to fail, exposing bulk liquid with higher surface tension, the surface is renewed and healed. This phenomenon is called the "Marangoni effect" (Marangoni (1871)). If drainage is faster than the Marangoni healing, then holes may develop in the lamella. Gradual film thinning below 20 nm thickness creates "black" films, so-called because they reflect virtually no light, which consist of simply two momolayers of surfactant molecules (Exerowa and Kashchiev (1986)). Collapse of the foam bed, ie a body of foam, occurs ultimately due to the rupture of thin liquid films unable to withstand mechanical and thermal disturbances.

Drainage of static foam beds have been described in various reports (Bikerman (1938); Jacobi (1956); Clark et al. (1987)) in terms of logarithmic expressions. However these do not account for foam collapse. Krugljakov et al. (1987) reported several characteristic kinetics (linear, stepped, logarithmic) associated with foam collapse in a gravitational field.

Wace at al. (1969) developed an empirical equation which related foam liquid hold-up to bubble size during foam drainage, and showed that foam stability is intricately related to the kinetics of liquid drainage. Factors which prevent drainage and increase foam stability may be summarised as follows :

-reduction in surface energy (high surfactant concentrations, low surface tension, molecular interactions between solutes, appropriate buffer conditions)

-increase in bulk and surface viscosity

-reduction in area (spherical bubbles)

-reduction in the adsorption rate of surfactant (Graham and Phillips (1976))

-increase in film elasticity (Małysa (1985))

-low rate of evaporation of the liquid phase

-prevention of mechanical and thermal stresses (Wrobel (1953))

-elimination of foam destabilisers such as lipids and solid impurities.

While detergents are ordinarily considered with regard to foaming systems, many other combinations are capable of producing stable foams. Aqueous solutions of proteins and other hydrophilic polymers can produce lasting foams, while even salts can marginally generate foams. Non-aqueous surfactants produce foams of high foam stability. The present work will concentrate on the study of protein stabilised foams only and the use of the general term surfactant will naturally account for protein molecules.

## 1.2 Protein Foams

The behaviour of proteins as foam stabilising agents is mainly attributed to their amphipathic nature. This enables them to be adsorbed at gas-liquid interfaces, where they undergo intermolecular rearrangement and form a stabilising film (Brooker (1985)). Hydrophobicity, molecular structure and rheological properties are also important in the foaming action of proteins. Halling (1981) has comprehensively discussed the foaming properties of proteins and Kinsella (1981) has presented a relationship between protein structure and foaming behaviour.

The adsorption characteristics of isolated proteins (homogeneous protein solutions) of varied molecular structures have been extensively studied in terms of kinetics of adsorption and surface denaturation (Graham and Phillips (1979a), adsorption isotherms (Graham and Phillips (1979b) and molecular structures of adsorbed films (Graham and Phillips (1979c)). Such proteins have included bovine serum albumin (BSA), lysozyme and $\beta$-casein. Based upon these data, Douillard et al. (1991) developed a

mathematical model for protein adsorption which correlated very satisfactorily with the experimental findings. The adsorption kinetics of ovalbumin and lysozyme have also been studied by de Feijter and Benjamins (1987), who concluded that, at low solute concentrations, the observed adsorption is diffusion controlled. Douillard and Teissié (1991) studied the stabilisation of interfacial films from solutions of ribulose-1,5-biphosphate carboxylase/oxygenase through adsorption from the bulk phase and lateral diffusion of already adsorbed molecules. Spectroscopic analysis showed that an intermediate and short state of protein molecules at the interface preceeds a stable stage associated with aging or compression. Considerable controversy surrounds the possibilities of reversibility of protein adsorption at interfaces, but reports both by Gonzalez et al. (1970) and Herrington and Sahi (1987) show that BSA adsorption is clearly reversible. Similar detailed studies of the surface properties of other important proteins such as $\beta$-lactoglobulin have also been reported (Waniska and Kinsella (1985); Murray (1987)), which indicate partial reversibility of adsorption.

The foaming properties of proteins are often categorised in terms of foamability or foam expansion (Poole et al. (1984)), which encompasses both the ability of a given protein to incorporate gas, and foam stability, ie the resistance of a foam bed to decay after foaming has ceased. Various foaming methods have been developed and applied to assess foam stability and are commonly visual, electrical, optical (Wilson and Mandy (1984)). Recently, studies of beer foam have exploited image analysis of the decaying head (Hegarty et. al. (1991)). Visual methods may include the Rudin test (Rudin (1957)) and volume reduction methods (Poole at al. (1984)). Electrical methods are based on conductivity measurements of foam (Kato et al. (1983b)). Stability assessment of foam subjected to enforced drainage by application of vacuum pressure at the bottom of a

sealed foam tower, as pioneered by Exerowa and colleagues (Lalchev et al. (1979); Khristov et al. (1978) and Khristov et al. (1983)) also employed conductivity measurements of foam. Such measurements offered vital information on foam liquid hold-up ($\varepsilon_l$). Equation 1.6 describes the liquid hold-up in a foam as a function of the electrical conductivity of foam.

$$\varepsilon_l = \eta(H_F/H_0) = \eta H_r \qquad \text{(Equation 1.6)}$$

where: $\varepsilon_l$ is the liquid hold-up in foam

$\eta$ is the shape coefficient ($\eta$ = 1.5-3)

$H_F$ and $H_0$ are the conductivities of foam and foaming solution respectively

$H_r$ is the reduced foam conductivity

Rapid adsorption of protein leads to the formation of a foam characterised by large bubbles, while slow adsorption leads to wetter foams of small bubbles. The foamability of protein solutions depends upon their surface activity, hydrophobicity and molecular structure of protein solutes. Experimental observations indicate that the foaming behaviour of random coil proteins is more advanced than that of globular proteins (Graham and Phillips (1976) and (1979c)). Disordered molecular structures (ie lacking intrachain restraints and secondary structure) are more surface active, form dilute films more easily and adsorb more rapidly at interfaces (Evans et al. (1970)). Lloppis and Albert (1959b) studied monolayers of bovine $\gamma$-globulin and found that, at alkaline conditions breakage of hydrogen bonds in the tertiary structure promoted greater molecular expansion of protein molecules in the monolayer. Thermally denatured proteins are also better foaming agents than untreated ones. O'Neill et al. (1989) studied the effects of thermal denaturation upon the surface activity of muscle proteins, such as myosin, F-actin, G-actin and actomyosin. They found that for all proteins heat treatment increased the

rate of surface tension decay. However Graham and Phillips (1976) have stated that globular proteins are likely to promote the best foam stability because they have a higher dynamic dilatational modulus $\tau$ (see Equation 1.7), which is the change in surface pressure ($d\pi$) caused by a relative change in surface area ($dA/A$). According to Phillips (1981), $\tau$ is important for foamability as well as foam stability.

$$\tau = -A(d\pi/dA) \qquad \text{(Equation 1.7)}$$

The effects of protein solubility upon foam stability are currently inconclusive and the object of some controversy. This contrast with emulsion stability, which is favoured by high solute solubility. Wang and Kinsella (1976) found that for alfalfa leaf protein the pH-foaming capacity curve paralleled its pH-solubility profile. Protein stability appears to be at a maximum at the isoelectric point of the protein (pI), where minimal protein solubility, maximal molecular association, and maximal rate of adsorption at interfaces is expected (Poole et al. (1984); Kim and Kinsella (1985); Waniska and Kinsella (1985)). Graham and Phillips (1976) showed that at the pI of a protein, the increase in surface rheological properties predominates over the observed decrease in electrostatic repulsions in the absence of net charge. However, these findings are at variance with results in O'Neill et al. (1989), which indicated that muscle proteins exhibited higher surface activity at strongly alkaline conditions (pH 11.0) far from their pI values (pH 5 to 6). Such a behaviour was attributed to pH-induced conformational changes of the muscle proteins studied, such as depolymerisation of F-actin followed by alkaline denaturation of its monomers, increase in myosin hydrophobicity and dissociation of the myosin-actin complex. Alkaline conditions reduce hydrogen bonding within protein structures allowing greater molecular expansion in foam monolayers (Llopis et al. (1959a-b)),

while acidic conditions reduce the surface pressure of the system. Increase in salt concentration suppresses electrostatic attractions and promotes hydrophobic interactions, particularly at gas-liquid interfaces where proteins are partially unfolded, with subsequent increase in film flexibility (Llopis et al. (1959b)).

Townsend and Nakai (1983) showed that molecular rigidity had a negative effect upon foaming properties. Thus the very rigid molecular structure of lysozyme, namely the number of disulphide linkages per molecular weight, yielded very poor foaming properties in contrast with the behaviour of the more flexible molecule of β-casein. BSA exhibited intermediate foam qualities, as its molecular flexibility lies between that of the other two proteins. The same workers also demonstrated a significant correlation between overall molecular hydrophobicity and foamability. Foamability was also favoured by increase in surface hydrophobicity in a curvilinear manner (Kato et al.(1983a)), but no significant correlation was found for foam stability. Slack and Bamforth (1983) demonstrated that hydrophobic polypeptides from beer and barley, which were separated by hydrophobic interaction chromatography, gave the most stable foams when compared with weak foams from hydrophilic proteins. Although an obvious correlation between polypeptide size and hydrophobicity was not found, it was demonstrated that larger polypeptides generated the most stable foams.

Townsend and Nakai (1983) found that charge density was disadvantageous to foam stability, and also reported that increase in bulk viscosity (a function of protein size, shape, structure, degree of hydration and intermolecular interactions) increased foam stability. Bikerman (1973) reported that solution viscosity was related to foam stability determined by drainage methods. At high surface viscosity, usually associated with globular proteins, foam stability is likely to be

enhanced due to reduction in drainage via forces of viscous drag. In beer foams, glycoproteins, which comprise a hydrophobic protein head and a hydrophilic carbohydrate tail, play a major role in foam stability by stabilising the bubble surface with their hydrophobic heads while inhibiting drainage by increasing local viscosity with their hydrophilic tails. Roberts (1977) proposed a theoretical model which attributes surface viscosity effects to glycoproteins and surface elasticity partially to the formation of complexes of denatured proteins cross-linked with small molecules. Controversy surrounding the importance of glycoproteins in beer foam stability is reviewed by Bamforth (1985).

Addition of short-chain alcohols do not appear to affect surface tension but increase surface viscosity and reduce film elasticity (Bucholtz et al. (1979)). Increased alcohol concentration results in higher protein solubility, with the occurrence of a maximum before decline. Such a behaviour coincides with identical trends in foam stability (Bumbullis and Schügerl (1979); Velissariou (1988); Ahmed and Dickinson (1990); Crompton and Hegarty (1991)).

Studies of protein mixtures (heterogeneous solutions) have shown that adsorption and foaming properties are not simply related to the properties of individual solutes. The adsorption of individual proteins at the gas-liquid interface may be competitive and therefore not simply related to the bulk phase concentration of individual components as implied by Equations 1.2 and 1.3. The adsorption of blood plasma is not only surface dependent (Brash and Uniyal (1979)) but also competitive in respect of component proteins. Thus fibrinogen and haemoglobin are preferentially adsorbed whilst the adsorption of albumin is inhibited (Morrissey (1977)). The same observations apply to milk proteins where the adsorption of $\beta$-casein is prevalent (Pegson et al. (1985)). Dalgleish et al. (1991) demonstrated that competition between $\alpha$-lactalbumin and

β-lactoglobulin (whey proteins) is partially established during adsorption at interfaces. Each of these proteins can displace the other to a limited extent, although rather high concentration of the displacing protein is required. However, they also found that once a layer of protein is formed it is very difficult to remove it with another protein. In contrast, cooperative protein-protein interactions between oppositely charged proteins have been found to improve foam stability. Thus mixed solutions have superior foaming properties when compared to these of the individual proteins alone at comparable conditions (Poole et al. (1984)). Mixtures of BSA and lysozyme were foamed in circumstances which encouraged electrostatic attractions between the two proteins (ie pH values between individual pI values) and indicated synergistic effects upon foam stability. This behaviour has relevance to egg white, a mixture of six main proteins among which the basic protein lysozyme. Johnson et al. (1981a-c) investigated the foaming properties of model systems of various combinations of the six proteins present in egg white using response surface methodology. Their findings were related to the performance of egg white in angel cakes, the foam structure of which was studied by Transmission Electron Microscopy (TEM). Studies concerned with the effects of lysozyme content in egg white upon foamability and stability (Sauter and Montoure (1972)) showed that there was an apparent improvement in both these parameters for low lysozyme contents. Such trends were more pronounced when fresh eggs were used. Peltonen-Shalaby and Mangino (1986) also found a strong correlation between the composition of whey protein concentrates and foaming properties.

The increasing demand for food functional proteins and the failure of cheap alternatives to replace the established soya proteins, caseinate and dried egg white (West (1984)) confirms scope for advancement in understanding of the foaming properties of interacting protein mixtures.

Experience of complex foaming systems such as beer foams, egg-white and whey proteins will clearly be advantageous.

## 1.3 Foam Fractionation

### 1.3.1: Principles and Applications of Foam Fractionation

Foam fractionation is a technique based upon the preferential adsorption of solutes at the gas-liquid interface of bubbles generated by gas sparging through a liquid solution. Figure 1.5 describes the classification of adsorptive bubble separation techniques as introduced by Karger et al. (1967). Foam fractionation refers to solute partition into foams as opposed to froth flotation which conventionally involves the recovery of particulate matter. However this distinction is less clear when colloids or high molecular weight solutes (eg. biopolymers) are concerned. Variation in solute adsorption reflect differences in the surface activity between constituent components in the foaming solution. Bubbles rise through the liquid and carry the surface active components to the top of the foam column, where the foam overhead may be collected. Foam fractionation is therefore analogous to distillation with entrainment. Rising bubbles correspond to vapour, and the interstitial liquid carried upwards is equivalent to the entrainment. Non-surface active components can also be efficiently collected in foam through the deliberate addition or presence of a surface active substance (collector); see Schnepf and Gaden (1959); Lee and Ryu (1979); Grieves et al. (1969). The collector interacts with the target substance (colligend), thus enabling its partition as part of a complex into the foam. The formation of the colligend-collector complex may be attributed to chelation, counterionic attraction or some other mechanism as solution conditions allow (Lemlich (1972)). As shown by Lee and Ryu (1979) and Grieves et al. (1969) the foam fractionation of a particular colligend can be maximised by judicious choice of the collector and an optimal collector:colligend ratio.

**Figure 1.5: Schematic Classification of the Adsorptive Bubble Separation Techniques** (from Karger et al. (1967))

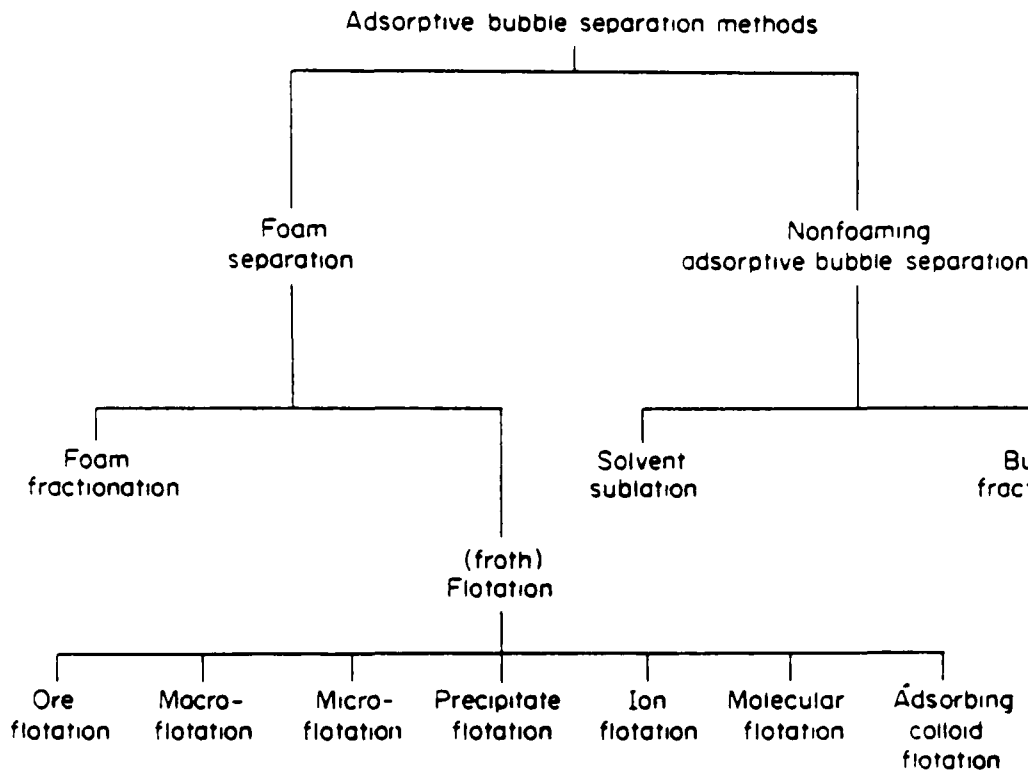

Foam fractionation has been extensively studied and applied in minerals engineering for particulate ore flotation (Osipow (1962); Hosten and Tezcan (1990)) and in the treatment of aqueous wastes including the removal of detergents and other pollutants from sewage (Stephan (1965); Jenkins et al. (1972)). Removal of metallic ions and complexes with the use of collectors (Wace et al. (1969)), the separation of radioactive contaminants from dilute feedstocks (Schonfeld and Kibbey (1967)) and the treatment of pulping wastes. Similarly, foam and bubble columns have been used by Harper and Lemlich (1966) and Shih (1971) to concentrate weakly surface active dyes, such as crystal violet chloride. Foam separation of microbial cells has also long been established following observations of the loss of micro-organisms in fermentation due to foaming. A wide range of species have been concentrated in foam in the presence of foaming stabilisers including *E. coli* (Grieves and Wang (1966)) and spores of *Bacillus subtilis* var. *niger* from autolysed cultures (Boyles and Lincoln (1958)). *Saccharomyces carlsbergensis* has been separated in foam without the use of a collector (Parthasarathy et al. (1988)). A parent-sake yeast was fractionated from its mutant (Ouichi and Akuyama (1971); Ouichi and Numokawa (1973)). Foam adsorption of yeast cells grown in a hydrocarbon medium was more effective than that of the same strain of yeast grown with glucose. In the former case the cell wall of the hydrocarbon-grown cells was shown to be seven times more hydrophobic (Miyazu and Yano (1974)).

The surface properties of proteins have constituted the basis for various studies concerned with their concentration and purification by foam fractionation. Application of foam fractionation to biologically active materials can be particularly attractive as a preliminary purification stage in downstream processing. It utilises mild conditions, has high separation efficiency at dilute conditions, can be operated batchwise or continuously in large scale processes, and is relatively

inexpensive in terms of capital, operational and maintenance costs. Foam fractionation can offer an attractive alternative where conventional techniques (precipitation, membrane separation, chromatography) fail due to close similarity of molecular size, shape, sedimentation constants and isoelectric point of system components. However, it has to be pointed out that there are significant differences between detergent and protein foam fractionation, due, at least in part, to the considerable differences in molecular size (eg. Triton X-100, a small molecule when compared with saponin and albumin; see Shih and Lemlich (1971)).

Foam fractionation was first applied by Ostwald and Siehr (1937) to recover albumin from potato and beet juices, which was subsequently dried and used for animal feed. Gonadotrophic hormones in the urine of pregnant women were concentrated in foam (Courrier and Dognon (1939)). Foaming has been the first step in the purification from urine of urokinase from young males. Urine is shaken to generate foam and dry foam is collected for further treatment after it has been allowed to drain statically (White et al. (1966)). A significant demonstration of the power of foam fractionation achievements was the separation of rennin and pepsin (Andrews et al. (1945)), which exploited the high surface activity of rennin at low pH (1.2-2.0). The two proteolytic enzymes had previously been thought to be identical. Urease was separated from catalase (London et al. (1954)) by foaming an impure mixture of the two enzymes, while Charm et al. (1966) achieved the fractionation of catalase in foam from a mixed solution with amylase. The underlying differences in the surface tension between the two enzymes are illustrated in Figure 1.3. Cholic acid was concentrated from its mixture with sodium cholate (Schutz (1937); Bader et al. (1944)). Streptokinase was isolated from streptococcal cultures (Holmstrom (1968)). It has been shown that BSA can be concentrated from dilute solutions by foaming (Schnepf and Gaden (1959);

Ahmad (1975); Gehle and Schügerl (1984b)), while Lalchev et al. (1982) showed that BSA can be purified from DNA by foaming a mixture of the two. In the latter report, it was also shown that lysozyme can be collected and purified in foam from a mixture with DNA when foamed at the isoelectric point of lysozyme. Total protein in chromatin solutions can also be fractionated from DNA by foaming. Protein recovery from potato juice waste water was accomplished by foaming (Weijenberg et al. (1978)). Chromatographic analysis of foam generated from a fermented mineral medium, in which a pure yeast culture of *Saccharomyces cerevisiae* had been added, highlighted the existence of specific protein species responsible for foaming in wine making (Molan et al. (1982)). Sarkar et al. (1987) achieved a twofold to fourfold increase in the specific activity of basic proteases from crude placental extracts in batch foaming processes. Recovery of antibiotics in foam was studied in model systems in the presence of collectors for penicillin (continuous operation) (Gehle et al. (1984a) and gentamicin (batch operation) (Lee and Ryu (1979)). Foam separation of a number of enzymes, such as lactate dehydrogenase (LDH) from chick heart (Charm (1972)) and choline esterase from pretreated horse serum (Bader et al. (1944)), can be achieved by successful removal of extraneous protein in the foam and increase in the target enzyme activity in the bottom product. In the case of LDH, a maximum fourfold increase in specific activity in respect with the feed was achieved, while the respective increase in the case of choline esterase was 8-16 fold. Foam separation is currently successful on an industrial scale for the separation of nisin (a polypeptide used as food preservative) by Aplin and Barrett, Trowbridge, Wilts.

Foam fractionation of biological molecules such as proteins and enzymes has neither enjoyed the wide range of applications found in mineral engineering nor the extensive study of the chemical engineering of

foam separation of small non-biological surfactants. The main reason for this is protein denaturation which can be observed during foaming. Some proteins are particularly prone to denaturation when in contact with surfaces, eg. albumin and hexokinase, whilst others (primarily enzymes) seem unaffected (eg. tripeptide synthetase, LDH, catalase, amylase) or exhibit varied degrees of activity loss. Thus a 5-20% loss in activity with five fold foam purification for human liver alcohol dehydrogenase was reported by Charm et al. (1966), and 25% loss in the activity of malate dehydrogenase isolated from chicken heart (Gehle and Schügerl (1984b)).

Proteins at interfaces are known to unfold to an extent dependent upon their native structures, local environmental conditions and process variables (Murray (1987)). Protein exposure to interfaces promotes stress in complex 3-dimensional structures with likely disruption and subsequent denaturation. Rupture of bonds remote from surface active sites in enzymes may lead to biological inactivation. Dilute films primarily host protein molecules which are extensively unfolded in contrast to more concentrated systems, which contain both native and small fractions of partially unfolded polypeptides (Evans at al. (1970)). It is therefore expected that the structure of proteins arranged at interfaces will be different from that in the bulk phase. In globular proteins the unfolding process may resemble heat denaturation. Surface denatured proteins are likely to renature after foaming as happens with some heat denatured proteins, eg. whey proteins (de Wit and Clarenbeck (1984); Kester and Richardson (1984)). In a similar fashion, surface denatured proteins are likely to form intermolecular complexes, such as those between $\beta$-lactoglobulin (highly susceptible to surface denaturation) with $\alpha$-lactalbumin and with $\beta$-casein in milk (Zittle et al. (1962); Sawyer (1969)). Murray (1987) showed that such complexes may be formed between these proteins on surfaces when aged, while the presence of $\beta$-casein may inhibit the surface

denaturation of β-lactoglobulin. Shear forces at gas-liquid interfaces and during mechanical foam breakage can cause protein denaturation and precipitation. Such effects depend upon protein structure and concentration, the magnitude of shear force and its duration, and the presence of other surfactant molecules (Thomas (1990)). Although denatured proteins may be biologically inactive, they can still be exploited as a food source or additive. Here, surface denaturation may be beneficial to foam stability in food fabrication. The varied resistance of protein molecules to surface denaturation implies that precipitation of denatured protein in foam does not necessarily involve the entire spectrum of constituent polypeptides to the same degree. Hence, there is a scope in determining the applicability of foam fractionation of target proteins from complex feedstocks by identifying the susceptibility of individual components to surface denaturation.

In contrast to foam fractionation of proteins, other aspects of foam stability and foamability, and foams in foods and beverages, have been exhaustively studied by a considerable body of researchers. Utilisation of such knowledge in conjunction with experience from foam separation of non-biological surfactants can be valuable in the design of foam fractionation of proteins/enzymes from complex biological feedstocks.

### 1.3.2: Modes of Operation and Effects of Operating Parameters in Foam Fractionation

Foam separation may be achieved in various modes of operation as shown in Figure 1.6(a-e). In the simple batch mode (Figure 1.6a), a volume of solution is foamed for a fixed period of time. Foam is collected at the top of the foam tower as specified by experimental design, and may necessitate breakage. Foam disruption usually involves mechanical means (Zlokarnik (1986)). In the current study, the collected foam overflow will

**Figure 1.6: Modes of Operation in Foam Fractionation**

(from Lemlich (1973))

Foam fractionation in the simple mode is described by **(a)** batch and **(b)** continuous operation. Continuous operations involving counterflow are described by **(c)** enriching, **(d)** stripping and **(e)** combined (stripping and enriching).

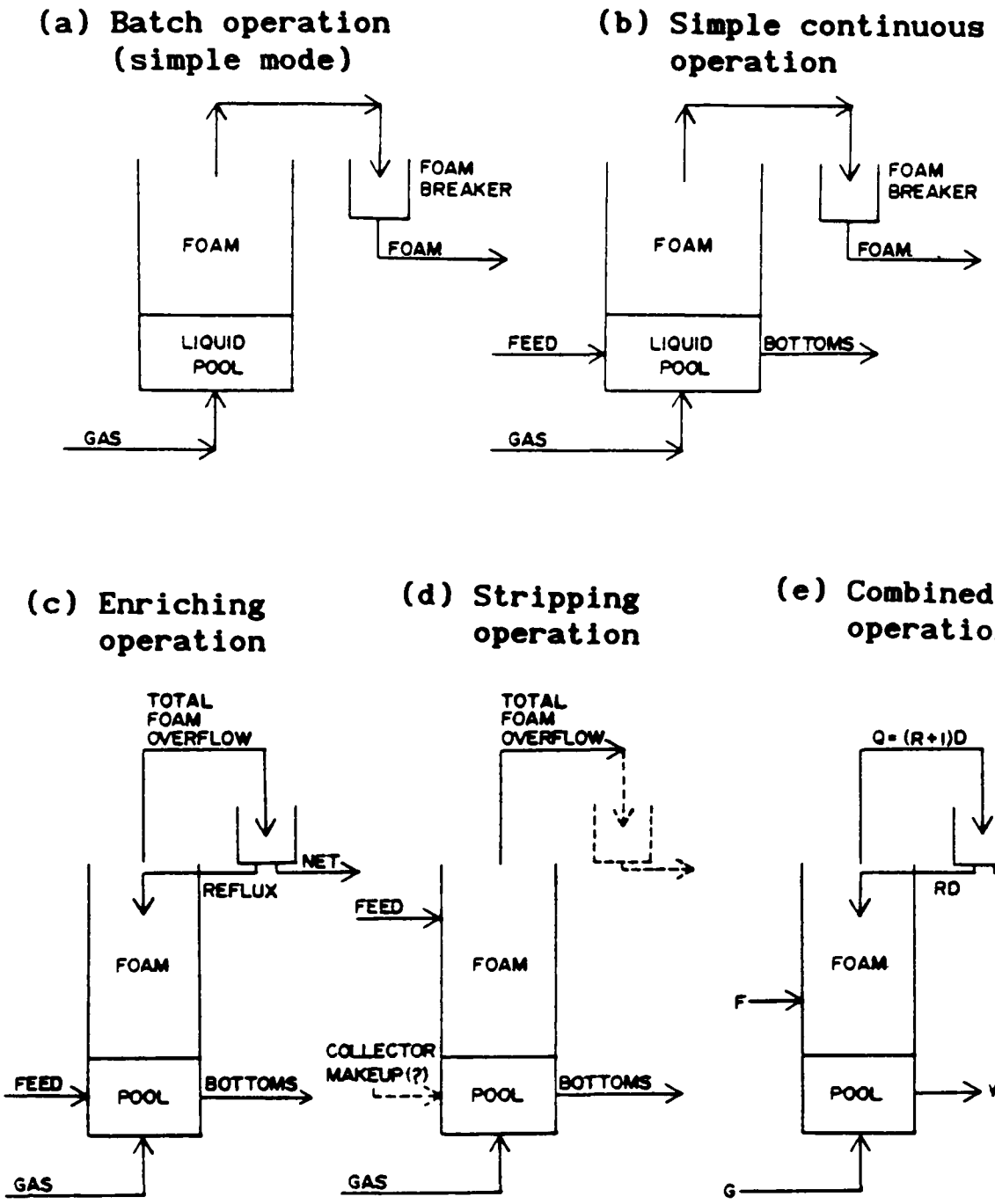

be referred to as foam, whilst the body of foam in the tower will be described as the foam bed. During batch foaming, a continuous decrease in the volume and surfactant concentration of the liquid pool is observed, while the surfactant concentration in the foam also varies. In simple continuous operations (Figure 1.6b), fresh feed is introduced continuously into the liquid pool, while foam and a proportion of the bulk liquid (bottoms) are removed from the top and bottom of the foam tower respectively. Collected foam is enriched in surfactant, while the bottoms are depleted. At steady-state conditions the mass and volumetric flowrates of the inlet and outlet streams are equal. A constant level of the foam-liquid interface is therefore maintained, which enables operation with defined heights of the foam bed as a fixed proportion of the height of the foam tower. These simple operations comprise one theoretical stage, under conditions where the liquid pool is well mixed, the sparger is sufficiently submerged, and no bubble coalescence occurs during foam ascension. Efficiency can be improved by elongated vertical pools, where mixing is not perfect, and additional separation can be achieved by bubble fractionation as described by Harper and Lemlich (1965).

Continuous operation with external reflux (enriching operation; see Figure 1.6c) allows a fraction of the collapsed foam to be returned to the foam tower at a short distance below the top of the foam bed. The refluxed foam trickles down the foam bed and enriches the rising foam by virtue of counterflow mass transfer. Experimental evidence (Lemlich and Levi (1961); Schonfeld and Kibbey (1967); Brunner and Lemlich (1963)) has demonstrated the benefit of external reflux, which is more pronounced at high foam bed heights. However these systems commonly require a very long period of operation to achieve steady-state conditions.

Introduction of the feed into the foam (stripping operation; see Figure 1.6d) results in a lower solute concentration in the pool and

bottoms due to resultant counterflow and mass transfer. Conversely, the volumetric flowrate of the bottoms also increases. When a colligend is stripped off, additional collector may require introduction to the pool to compensate for losses during stripping. Grieves and Wood (1964) demonstrated that, positioning the feed at the foam-liquid interface, at least a twofold increase in solute concentration in collected foam can be achieved. Feed location at different foam heights promoted a finite decrease in solute concentration in the bottoms, but showed a maximum in the bottoms volumetric flowrate. These effects were more pronounced in concentrated feedstocks and high gas rates.

Stripping and enriching may be combined as depicted in Figure 1.6e, with the optimum height of the feed input at approximately a mid-point of the operational foam bed (Grieves and Wood (1964)). Multi-stage columns yielded higher enrichment than single stage (Gehle et al. (1984b); Haas and Johnson (1965) and Fanlo and Lemlich (1965) have presented methods for calculating mass transfer coefficients, and the number and height of transfer units (NTU and HTU respectively) for diffusion controlled mass transfer. Combined foam fractionation with controlled reflux can be manipulated to maximise the solute concentration in foam and minimise the volume of collected foam (Schonfeld and Kibbey (1967)). Such approaches are essential to minimise storage or discharge costs of foams containing dangerous components, (eg. nuclear waste), and/or the scaling down of further treatment of the collected foam in processes such as recovery in foam of food functional protein. However, in cases of biological foams where enzyme activity in foam is desired, the practical benefits of foam fractionation with reflux are likely to be outweighed by extensive protein denaturation and loss of enzyme activity as relevant experience with LDH showed (Charm (1972)).

The main process parameters affecting the efficacy of foam

fractionation, as defined by the enrichment ratio $e_i$ (ratio of protein concentration in foam over that in the feedstock; see Equations 3.1 and 3.2 in Chapter 3) and recovery $R_i$ (percentage of feedstock protein collected in foam; see Equations 3.3 and 3.4 in Chapter 3), are:

-the surfactant concentration and its molecular, surface properties and rheological properties (viscoelasticity)

-the aqueous environment (type of buffer and salts, molarity, pH)

-the gas flowrate (G)

-the residence time of the liquid ($r_D$), ie the feed volumetric flowrate ($Q_0$) for fixed liquid pool heights

-the ratio of gas to liquid flowrate ($G/Q_0$)

-the height of the foam bed

-the height of the liquid pool

-the porosity and type of sparger

-the diameter of the foam tower

-the temperature of operation

-the mode of operation, ie batch or continuous (simple, enriching, stripping or combined)

The objectives of a successful foam fractionation/separation, are high enrichment ratios of the target surfactant molecule with efficient recovery. High enrichment is associated with dry foams, ie those subjected to extensive drainage and coalescence. Such foams usually originate from dilute feedstocks and are characterised by low liquid hold-up and density, and large bubbles of polyhedral shape (Haas and Johnson (1967); Narsimhan (1987)). However such conditions are likely to reduce solute recovery because of reduction in the volume of the collected foam. This may be orders of magnitude greater than the corresponding increase in enrichment. The priorities and objectives of each process must therefore be defined in order to specify and define optimal operating conditions.

The surfactant concentration and its properties have a direct effect on the foamability and stability of the generated foam as discussed. Single component systems (Ahmad (1975); Brown et al. (1990)) have shown that the enrichment ratio increases, while protein recovery decreases, with decreasing surfactant concentration in the bulk solution. This accords with the implications of decrease in surface tension at high bulk concentrations. However, a limiting concentration exists below which foam cannot be formed. Enzyme purification from crude extracts in batch operations (Sarkar et al. (1987); London et al. (1954); London and Hudson (1953)) has indicated the existence of maxima in enrichment of enzyme specific activity and enzyme recovery at varied total protein concentrations in the feedstock. This indicates an optimal feedstock concentration for enzyme fractionation, which does not coincide with a maximum in total protein recovery in the foam. At increasing total protein concentrations in the feedstock, a decline in total protein enrichment improves the enrichment of the target specific activity. However at very concentrated solutions the foam becomes "contaminated" with extraneous protein responsible for the observed decline in the enrichment of enzyme specific activity. Such findings highlight the complexity of biological feedstocks in foam performance. They also underline the limitations of conclusions derived from simple model systems, when applied to the fractionation of target enzymes. Studies of foam stability in complex systems (Poole et al. (1984)), where molecular interactions improve foam stability, indicated the importance of solution composition. Similarly, adsorption studies of plasma protein (Kochwa et al. (1977); Morrissey (1977); Brash and Uniyal (1979)) demonstrated that competitive adsorption at interfaces can also be related to solute concentration. The foregoing evidence draws attention to the importance of stoichiometry in protein adsorption, and its greater importance in process performance when

compared with that of total protein concentration in the feedstock.

In the absence of high salt concentrations in the foaming solution, the pH plays an important role in protein fractionation with most proteins exhibiting maximum values of recovery at their isoelectric point (Schnepf and Gaden (1959); Ahmad (1975)). However, under such conditions protein enrichment is likely to decrease, and this behaviour is the result of maximum foam stability and minimum drainage within the vicinity of the isoelectric point. Simultaneous variations in pH, ionic strength and bulk concentration have indicated the secondary importance of pH in determining protein recovery and enrichment (Brown et al. (1990)). An understanding of such behaviour necessitates the detailed study of surface forces and adsorption characteristics under defined conditions (Rao (1974)). Enzyme foam fractionation has yielded maximal purifications at the isoelectric point (London et al. (1954); Sarkar et al. (1987)). Weak foaming solutes, such as lysozyme, yielded collectable foam only when processed at their isoelectric point (Lalchev et al. (1982)). However, exceptions to these "rules" have also been reported, including a 40-50% loss in activity of streptokinase at its isoelectric point in contrast to 80% recovery at higher pH values (Holmström, 1968) and very unstable foam produced from catalase at its isoelectric point (Charm et al. (1966)). In addition, foam separation of the basic antibiotic gentamicin (Lee and Ryu (1979)) was maximal and constant in a wide range of pH values (2-9), where all amino groups are ionised ($NH_3^+$), but dropped to zero at pH 12. Foam fractionations involving collectors should account for pH effects in respect of the nature, the charge and surface adsorption of the collector. Increase in buffer molarity is beneficial to recovery but disadvantageous to enrichment. Manipulation of buffer conditions can be a powerful tool in controlling foam fractionation of those surfactants which interact to benefit foam stability in both biological (Clark et al. (1988); Clark et

al. (1989)) and non-biological systems (Shih Nan Hsu and Jer Ru Maa (1985)). Such manipulations can induce partition in the foam of the least surface active solute by enhancing molecular interactions. Wace and Banfield (1964) discussed the analogies between foam recovery of electrostatic colligend-surfactant complexes and ion-exchange adsorption.

Addition of low molecular weight agents, such as sucrose, ammonium sulphate and sodium chloride will alter the performance of foam fractionation in many ways, because of resultant variations in surface activity, surfactant threshold concentration and adsorption at the interface. For example, addition of 10% ammonium sulphate or sodium chloride increased catalase activity in foam while equal concentration of sucrose inhibited such partition (Charm et al. (1966)). The effects of ethanol addition may be both beneficial (Schnepf and Gaden (1959)) or detrimental (London et al. (1954)) depending on ethanol concentration. The role of this has already been discussed in Section 1.2 with respect to foam stability. The presence of solid impurities has been reported to reduce enrichment due to their scavenging action (Gehle and Schügerl (1984b)) while addition of small quantities of non-ionic emulsifiers improved protein enrichment (Ahmad (1975)). Shih Nan Hsu and Jer Ru Maa (1985) have shown that synergistic interactions between the anionic surfactant sodium benzenesulphonate and cationic dodecyl trimethylammonium chloride (a weak foaming agent) enabled efficient recovery of the latter in foam. As mentioned in Section 1.2, an important understanding has been accumulated in respect of the effects of molecular interactions between protein molecules upon foam stability of food systems (eg egg white, beer). However, little interest appears to have been shown in these advances possible in foam fractionation of interacting biological surfactants.

Enrichment ratios have been found to decrease and eventually level

off with increasing gas flowrates in both batch and continuous operations (Sarkar et al. (1987); Ahmed (1975); Brown et al. (1990)). This behaviour is associated with pronounced drainage and coalescence observed at low gas rates and several mechanisms have been proposed in explanation (Thomas and Winkler (1977)). At constant gas rates and varied sparger porosity, enrichment is increased with higher pore size due to the formation of larger bubbles (Koide et al. (1968)). Porous plates and frit glass spargers were found to give higher gas hold-up than orifice distributors (Fair et al. (1962)). Grieves and Wood (1964) showed that the ratio $G/Q_0$ is a prime factor in protein partition while Ahmad (1975) has demonstrated that increasing $G/Q_0$ finitely improves enrichment. Such effects are analogous to the heat input per unit weight of feed in continuous distillation processes. The same reports have also indicated the benefit of higher liquid residence times upon protein transfer from the bulk to foam phase. Mass transfer and optimal residence time are also very important scale-up parameters (Der Villar et al. (1992)). Temperature has been reported (Grieves and Wood (1964)) to favour enrichment (as opposed to recovery) by inducing drainage and coalescence. These effects can be attributed to the fact that high temperatures increase foamability but undermine stability.

Increased height of the foam bed is expected to increase enrichment and decrease recovery, since liquid drainage and bubble coalescence are prolonged. Ahmad (1975) observed a sharp decrease in recovery with foam height in continuous operations, which was followed by a plateau region at higher foam beds. Other reports however, in referring to batch operations (Sarkar et al. (1987)), indicated the existence of an optimal height of foam bed, above which enrichment sharply declined. These observations were consistent for a wide range of column diameters, with foam height optima lower for larger tower cross-sections. This behaviour however is not

associated with the dynamics of drainage and protein partition but instead with loss of enzyme activity due to extensive denaturation. The importance of this finding highlights the possibility of restrictions imposed by the complex nature of biological compounds upon the direct application of optimal conditions developed in non-biological surfactant systems.

Increase in column diameter was shown to enhance both enrichment and recovery in batch operations (London et al. (1954); Sarkar et al. (1987)). Optimum values were found above which foam became structurally unstable and detrimental to both enrichment and recovery. Large column diameters contribute to the formation of large bubbles which are conducive to better drainage and greater enrichment. However, values in excess of the optimum diameter cannot support the rising foam. Thus foam destruction occurs, which consequently leads to extensive protein denaturation. Experience from studies of bubble columns, reported by Shah et al. (1982), show that, for columns of diameters below 0.3 m, column diameter is related to interfacial area per unit volume ($f_{sp}$; see Equation 7.3 in Chapter 7) and gas hold-up ($\varepsilon_g$), both of which are important factors in surfactant partition into the foam. The observed effects of column geometry and sparger porosity upon process performance are also in accordance with the literature concerning the froth flotation of metal ores (Nieuwoudt at al. (1990)). Some column designs have varied cross-sections with larger diameters at either the bottom (liquid pool) or the top of the foam bed. Such designs respectively increase the volumetric capacity of the liquid pool and encourage increased foam drainage.

### 1.3.3: Mathematical Modelling and Performance Prediction of Foam Fractionation

The importance of operating parameters upon foam fractionation imposes a requirement to quantify effects upon process performance in

order to establish predictive mathematical models. Such efforts applied to biological compounds should take account of peculiarities and possible limitations associated with the large mass and vulnerable structural nature of proteins at gas-liquid interfaces.

Predictions of foam density and volumetric flowrate in continuous operations were developed by Leonard and Lemlich (1965a), where it was assumed that drainage occurs primarily through the plateau borders by force of gravity. The capillaries were considered to be randomly orientated, with non-circular cross section and non-rigid walls, which tend to flow along the direction of drainage. The model described the interstitial flowrate and drainage in a stationary or moving foam of non-coalescing bubbles. Flowrate predictions were obtained by solving the differential momentum and mass balances for a hydrodynamic model which accounted for the aforementioned capillary characteristics. The model was experimentally verified (Leonard and Lemlich (1965b); Fanlo and Lemlich (1965)) for small surfactant molecules of low surface viscosity, such as the non-ionic surfactant Triton X-100. The validity of this model was later tested for higher surface viscosity in saponin and albumin solutions, which closely represent those physical conditions of biological solutions (Shih and Lemlich (1971)). Predicted low values of surface viscosity raised questions about the initial assumptions of the model, such as mobile bubble walls and non-coalescence.

Haas and Johnson (1967) presented a model, which was based on the principle that drainage is mainly related to laminar flow through the plateau borders, and ignored the contribution of liquid from ruptured bubbles to drainage. A model for a cellular foam was first presented by Hartland and Barber (1974) in batch operations. It assumed that bubbles may be represented by a tessellated structure of pentagonal dodecahedra. Drainage comprised gravitational liquid flow through the plateau borders

and the films. Flow of liquid from the films is associated with plateau border suction. The model expressed foam height as a function of film density, gas velocity, bubble diameter and the physical properties of the solution (surface tension, density and viscosity). The liquid hold-up was also described by a correlation which included all these parameters.

Further studies by Desai and Kumar (1982), concerning semi-batch foams, showed that assumptions of rigid bubble walls (high surface viscosity), adopted by previous investigators, severely underestimate the velocity of liquid drainage. They found that such assumptions can be valid only when the inverse of the dimensionless surface viscosity is less than 0.044. Later work by the same investigators (Desai and Kumar (1983)) introduced a model, which predicted liquid hold-up profiles in semi-batch cellular foams. This model accounted for drainage from films and plateau borders. Thus the mobility of plateau border walls is decided by the surface viscosity, while the mobility of the film surface is dictated by the gradient of surfactant concentration of the film surface. Theoretically predicted liquid hold-up profiles compared reasonably well with those experimentally determined.

More recent work concerned with modelling of biological foams has attempted to address the special nature of proteins. Parthasarathy et al. (1988) proposed a model for microbial cell recovery in batch cellular foams. The model assumed a linear equilibrium relation between the cell concentration in the bulk and interface. The foam interface was also considered to be in equilibrium with its interstitial liquid, whose concentration is that of the bulk. Infinite surface viscosity (rigid walls) and constant drainage rate were also assumed. The model was found to correlate well with experimental data, particularly with respect to the effects of bubble size and gas rate. Thomas and Winkler (1977) developed a simplistic model, which correlated well on a semi-empirical basis with the

experimental results for BSA fractionation in a simple batch operation. The model assumed complete surface excess layers on bubble interfaces, and entrainment of bulk liquid in foam followed by drainage. Empirical expressions for the entrained liquid and the rate of drainage were established. Determination of the values of model coefficients were based on curve-fitting methods. The model expressed enrichment as a function of various operating parameters and gave accurate predictions.

Narsimhan and Ruckenstein (1986a) proposed a theoretical model for the hydrodynamics of foam bed in semi-batch foams. The model also accounted for the effects of capillary pressure and van der Waals attraction on liquid drainage from the thin films, and the rupture of thin films due to mechanical and thermal perturbations. The model predicted the liquid hold-up profile, enrichment factor and the critical residence time for the collapse of the foam bed under different operating conditions and physical properties. Narsimhan and Ruckenstein (1986b) proposed a comprehensive population balance model which accounted for bubble size distribution, bubble coalescence and gas diffusion between bubbles. The model indicated that the simplifying assumption, employed hitherto, for uniform bubbles can only be valid in a narrow range of bubble sizes. Narsimhan (1987) presented a model for the hydrodynamics of protein stabilised foams in semi-batch operations. The model can predict kinetics of protein adsorption, liquid drainage from films and plateau borders, and the dependence of surface viscosity on surface concentration. A model for the unsteady drainage of a standing foam was introduced by Narsimhan (1991) for protein foams and its theoretical predictions were compared with BSA stabilised foams. The model assumed dodecahedral bubbles of the same size, equilibrium surface protein concentration and negligible fraction of liquid in thin films. This latter assumption is in contrast with the model proposed by Desai and Kumar (1983), which accounted for the

contribution of liquid in the films to the liquid hold-up of the foam bed. Narsimhan's (1991) model was found to be in favourable agreement with simultaneous experimental results of BSA foams, but foam drainage was overestimated due to the assumption of equal bubble size. Adaptation of the above model for simple single stage continuous operations was introduced by Brown et al. (1990) which accounted for the prediction of enrichment and recovery. The model assumed adsorption equilibrium, infinite surface viscosity and uniform dodecahedral bubbles. When compared with experimental results for BSA foams, the model was simplified by assuming that no coalescence occurred along the foam bed and as a result the bubble size was constant. For this purpose, the height of the foam bed was maintained at low values. When compared with the model predictions, the experimental values for BSA enrichment were found to be higher, whilst the observed BSA recoveries were lower. These discrepancies were more pronounced at dilute feedstocks and low gas flowrates. Such deviation is attributed to bubble coalescence in the foam bed, which is more pronounced at low protein concentrations and gas rates, and results in broad bubble size distributions.

Application of such theoretical models and/or development of semi-empirical correlations necessitates experimental measurement of bubble size and liquid hold-up. Shah et al. (1982) reviewed a variety of methods for bubble size measurements, such as photography (the simplest and most commonly used), light scattering, light reflection, polarisation, and various optical and electrical probes. Photographs usually represent bubbles next to the glass wall and are likely to be distorted by wall effects. However, it has been shown (Ho and Prince (1971)) that bubbles adjacent to the wall surface are fairly representative of those in the interior of the foam, but are likely to yield a slightly overestimated average bubble diameter. This effect arises because bubbles near the wall

are more likely to be intercepted by a large area, such as the glass wall, than a small one. Małysa (1987) also showed that wall effects are eliminated at Reynolds numbers greater than 100 (characteristic of bubbles approaching the foam layer). Ronteltap and Prins (1989) introduced an optical glass-fibre technique which can measure the evolution of bubble-size distributions in foam, the rate of drainage, changes in gas content, the rate of foam collapse and changes in foam volume. Two-dimensional bubble size measurements can be statistically manipulated to calculate three-dimensional size distribution. Weaire (1989) highlighted the importance of foam structure in its mechanical properties and indicated that the validity for idealised bubble models must be checked in cases of seriously disordered systems. Developments in the potential for cryo-microscopical analysis of food foams (Wilson (1989)) and application of cryostage Scanning Electron Microscopy (SEM) to study bubble structure in beer foams (Hegarty et al. (1989)) may also provide an alternative way for bubble size measurement. Liquid hold-up is usually measured by $\gamma$-ray attenuation technique, which employs a radioactive tracer. Alternatively, liquid hold-up could be calculated from Equation 1.6, where foam conductivity at various heights of the foam bed could be measured with a conductivity bridge, while the size coefficient (see Equation 1.6) could be determined as described in Lemlich (1977).

The accuracy of existing theoretical models in predicting foam performance has been tested for model homogeneous feedstocks only, such as BSA solutions. The development of semi-empirical models has also been based on such simple foaming solutions. However, further research is required to establish performance prediction of foams generated by complex biological feedstocks, where competitive and/or synergistic action between protein molecules may occur, while various components, such as lipids could be deleterious to foam formation. Such studies may involve empirical

correlations based on the physical properties of simple and complex mixtures.

## 1.4 Aims and Objectives of the Current Research

The significance of molecular interactions upon foaming properties of mixed protein solutions, and existing misunderstanding regarding the merits of foam fractionation in protein recovery from real biological feedstocks, has been the main basis for the current research. Effects of protein-protein interactions were studied in foam model systems comprising basic and acidic proteins, while waste brewer's yeast extract was used to study the performance of foam fractionation in continuous operations. In addition, limited studies with muscle proteins were also conducted and are presented in Appendix V.

Chapter 3 examines the effects of operating conditions upon foam stability in homogeneous BSA and heterogeneous BSA-lysozyme solutions. Preliminary quantitation of protein partition in foam was also undertaken. The experience so gained established the objectives and enabled the experimental design of Chapters 4 and 5. The effects of molecular stoichiometry upon electrostatic interactions between BSA and lysozyme, and their partition in preparative foams was examined in Chapter 4. In Chapter 5, foam components were studied as mobile ion-exchangers and the magnitude of the electrostatic interactions between BSA and lysozyme was assessed, when imposed as a disturbance in a steady-state process.

In Chapter 6, an account of the partition of bulk protein from brewer's yeast extract into foam and its fractionation from RNA is presented for continuous foam production. Protein denaturation observed in foam was also quantified. The quality of the foam product was assessed with respect to its foaming capacity and response to further separation

steps. Chapter 7 relates dynamic changes in bubble size, liquid hold-up and protein partition in foam beds of various heights. Attempts were made to predict performance by application of a theoretical model (Brown et al. (1990)), which was reported to be in fairly good agreement with experimental results of BSA foam fractionation. Such attempts highlighted the significance of the complexity of real biological feedstocks with subsequent deviations from the qualities of model systems.

In Chapter 8 conclusions on the findings of the present study are summarised and a general assessment of foam fractionation of biopolymers is made. Conclusions refer to heterogeneous model systems of interacting protein molecules and real biological feedstocks. Chapter 8 also highlights areas of interest in the study of protein recovery by foaming, as emerged from experimental indications, and recommends directions in future research.

# CHAPTER 2

## EXPERIMENTAL PROCEDURE

### 2.1 Materials

Experimentation involved the following protein sources :

(a) Model Systems

1-Bovine Serum Albumin (BSA) supplied by Sigma Chemical Co., No A-7906. Molecular weight 66-67 kDaltons, pI 4.8, extinction coefficient $\varepsilon^{1\%}_{A280nm}$=6.7

2-Lysozyme Chloride (hen source) supplied by Sigma Chemical Co., No L-2879. Molecular weight 14.5 kDaltons, pI 10.5, extinction coefficient $\varepsilon^{1\%}_{A280nm}$=25.8

3-Cytochrome-*c* (from bovine heart) supplied by Sigma Chemical Co., No C-3006. Molecular weight 12.4 kDaltons, pI 10.0,

(b) Mixed protein Systems

1-Brewer's yeast extract. Spent yeast was supplied by Cape Hill Brewery. Cells were disrupted to release the intracellular content and the extract was clarified by centrifugation. Preparation procedure is described in detail in Section 6.2 (Chapter 6).

2-Beef heart extract. Fresh beef heart was homogenised to release muscle protein and the homogenate was clarified by centrifugation. Preparation procedure is described in detail in Appendix V.

The following reagents were utilised for biochemical analysis:

1-Pierce Coomassie Protein Assay supplied by Pierce, No 23200

2-RNA from Torrula Yeast supplied by Sigma Chemical Co., No R-6626

3-Orcinol supplied by supplied by Sigma Chemical Co., No O-1875

4-Glucose supplied by BDH Ltd., Prod. 28450

5-1-Naphthol supplied by BDH Ltd., Prod. 10162

6-Pepsin supplied by BDH Biochemicals, Prod. 39032

7-Haemoglobin supplied by Sigma Chemical Co., No H-2625

8-SDS Low and Heavy Molecular Weight standards for PAGE were supplied by Sigma Chemical Co..

The Low Molecular Weight (L.M.W) standards kit (MW-SDS-70L) included the following proteins:

L-6385 α-Lactalbumin, 14.2 kDaltons

T-9767 Trypsin Inhibitor, Soybean, 20.1 kDaltons

T-9011 Trypsinogen, 24 kDaltons

C-2273 Carbonic Anhydrase, 29 kDaltons

G-5262 Glyceraldehyde-3-phosphate Dehydrogenase, 36 kDaltons

A-7642 Albumin, egg, 45 kDaltons

A-7517 Bovine Serum Albumin, 66 kDaltons

The Heavy Molecular Weight (H.M.W) standards kit (MW-SDS-200) included the following proteins:

C-2273 Carbonic Anhydrase, 29 kDaltons

A-7642 Albumin, egg, 45 kDaltons

A-7517 Bovine Serum Albumin, 66 kDaltons

P-4649 Phosphorylase-β, 97.4 kDaltons

G-8511 β-Galactosidase, 116.1 kDaltons

M-3889 Myosin, 205 kDaltons

9-IEF standards (pI 3-9) were supplied by Pharmacia , Code No 17-0471-01, Lot No. 8109 and included the following markers:

Amyloglucosidase, pI 3.5

Soybean trypsin inhibitor, pI 4.55

β-Lactoglobulin, pI 5.20

Bovine carbonic anhydrase-β, pI 5.85

Human carbonic anhydrase, pI 6.55

Horse myoglobin, pI 6.85

Methyl red dye, pI 3.75

Horse myoglobin, pI 7.35

Lentil lectin, pI 8.15

Lentil lectin, pI 8.45

Lentil lectin, pI 8.65

Trypsinogen, pI 9.30

The following reagents were used for immunochemical analysis (ELISA):

1-Myosin from bovine muscle (antigen) supplied by Sigma Chemical Co., No M-6643

2-Anti-myosin (myosin skeletal and smooth, rabbit) supplied by Sigma Chemical Co., No M-7648

3-Conjugate (anti-anti rabbit) supplied by Sigma Chemical Co., No A-6154

## 2.2 Analytical Foaming Methods

### 2.2.1 Head Retention Measurements

The stability of the foaming solutions was measured as Head Retention Value (HRV) using the Rudin apparatus (Rudin (1957)) as shown in Figure 2.1. Volumes (60 $cm^3$) of sample, equilibrated at 20 $^{\circ}C$, were poured into the foam tube up to level A. Prior to sample loading gas (95% $CO_2$) had been sparged into the apparatus for $60\pm5$ sec. The gas supply was adjusted to an outlet of 1.5 bar and the gas flow indicator was calibrated for $CO_2$. The snap valve was opened to foam the sample up to level B in $60\pm5$ sec, whereupon the snap valve was closed. The time for the foam-liquid interface to rise from point C to point D (see Figure 2.1) represented the half-life ($t_{1/2}$) of the foam sample. During foaming the apparatus was thermostated at 20$^{\circ}C$. The experimental rig allowed retention of line pressure when the gas flow was directed off the sinter so that gravitational flow of liquid back through the sinter was avoided. The sinter used in comparable experiments was of porosity 3 (pore size 16-40

μm).

Duplicate samples were foamed as above and HRV measurements were considered as valid in average determinations only when they differed by less than 2 seconds.

Restricted availability of sufficient volume (>200 $cm^3$) of experimental samples such as freeze-dried foam from brewer's yeast, necessitated a 2 fold scale-down of the Rudin apparatus. This reduced the volume of the foaming sample by a factor of approximately 4 (13 $cm^3$). HRV determinations were carried out in an identical protocol. However the sparged gas was $N_2$ whose supply was adjusted to 0.5 bar. The gas was passed through a humidifier before reaching the sinter (porosity 3).

### 2.2.2 Assessment of Foam Stability by Conductivity Measurements and Lace Quality

Foam stability was determined by conductivity measurements of foam produced under set experimental conditions in the lacing funnel exploited by Jackson and Bamforth (1982) and others (Leeson (1989)). The experimental apparatus is illustrated in Figure 2.2. Foam quality was additionally assessed by quantitative analysis of the remaining foam adhered to the glass walls (lace). The protocol followed was an adaptation of the procedure reported by Jackson and Bamforth (1982) where the protein content of beer lace was measured at various stages of foam drainage.

The generation of foam took place in identical time scales used in the Rudin method. Since the apparatus could not be thermostated all experiments took place at room temperature (22.5-22.8 °C). Gas (95% $CO_2$) was sparged through a sinter of porosity 3 and was supplied at an outlet pressure of 1.5 bar. The gas flow indicator was calibrated for $CO_2$.

The conductivity probe comprised a pair of parallel stainless steel round wire electrodes and was connected to a conductivity meter calibrated

**Figure 2.1: Rudin Apparatus**

Schematic representation of Rudin Apparatus for foam stability measurements (see 2.2.1)

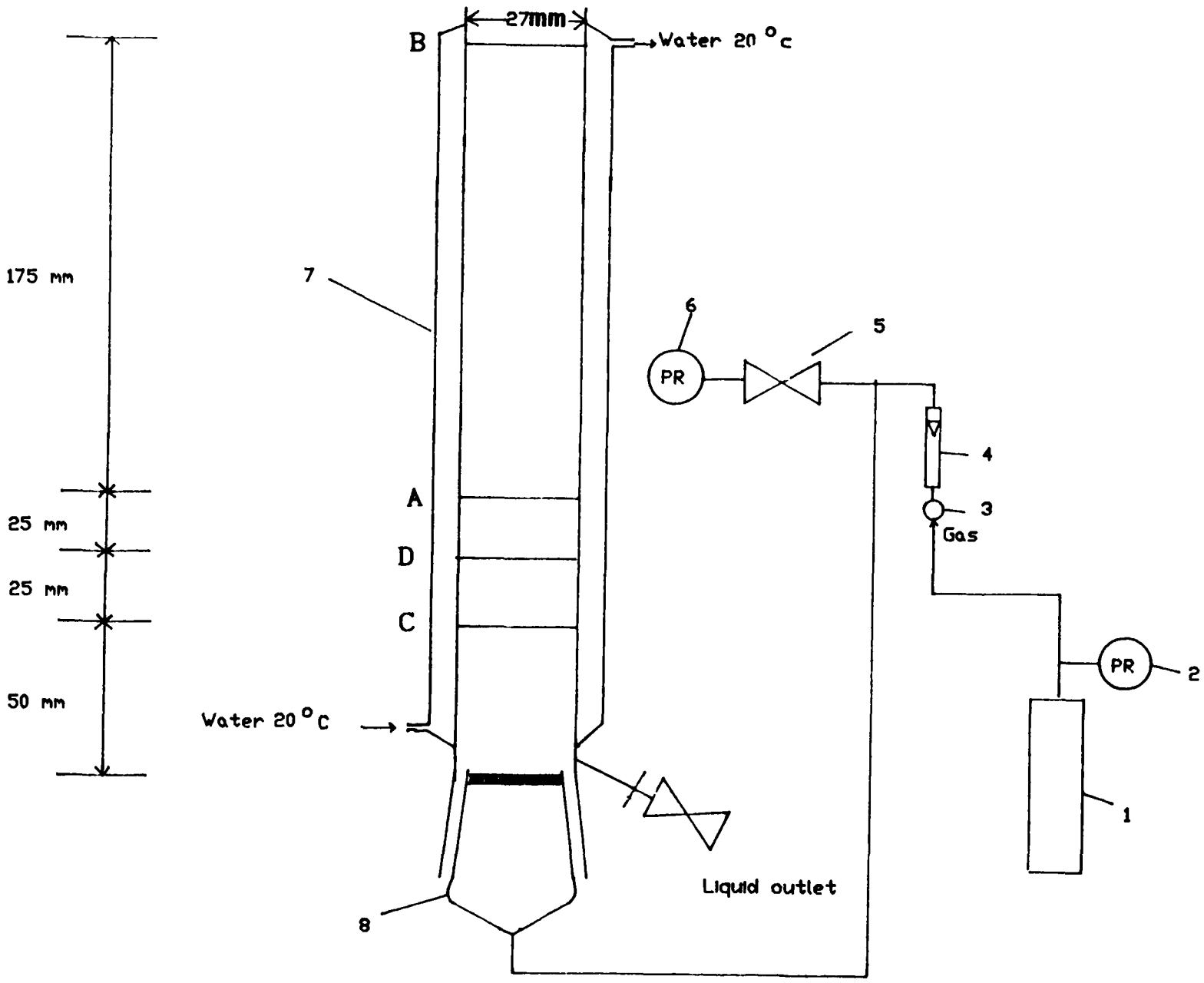


Legend

1. Gas cylinder
2. Pressure regulator
3. Gas flow control
4. Gas flow meter
5. Snap valve
6. Pressure regulator
7. Water jacket
8. Sinter

with 1M KCl. Conductivity readings were recorded on-line on a chart recorder. Prior to sample loading, gas was sparged through the sinter for $60^{+}_{-}5$ sec and then the gas was directed off the column. A volume of 60 $cm^3$ of foaming solution was loaded up to level A (see Figure 2.2) and the conductivity probe was carefully lowered to the surface of the liquid pool avoiding any contact with the liquid. The gas flowrate was then turned on appropriately adjusted so that the foam could reach level B within $60^{+}_{-}5$ sec. On reaching level B the gas was immediately turned off and the foam/liquid interface started to raise with foam drainage/collapse.

During foam generation and decay the recorded conductivity traces were characterised by an initial increase in conductivity during foam production followed by a decline during foam decay and a period of virtually constant foam conductivity (see Figure 3.8, Chapter 3). Results were recorded in terms of foaming power (FP), defined as the original conductivity of the foam (peak point in Figure 3.8) and conductivity half-life (CHL) equal to the time required to diminish that value by half. Conductivity half-life is a criterion of foam stability whereas foaming power is a measure of foam density. The latter can reveal physical differences between foams formed from protein preparations under identical conditions. Experiments were performed in triplicate and the average was considered. As with HRV determinations, conductivity half-life values were considered valid only when they differed by 2 sec. Duplicate foaming power readings were accepted when they were within 5% of each other.

The remaining liquid was completely drained 2 minutes after stabilisation in foam conductivity readings. Residual foam was removed from the vessel walls by careful rinsing with a known volume of buffer (identical to that in original sample) and the volume of the collected foam was calculated by mass differences. Calculations were based on the assumption that the density of the collapsed foam was that of the water.

**Figure 2.2: Apparatus for Determination of Foam Stability by Conductivity Measurements**

Schematic representation of dedicated apparatus for assessing foam stability by conductivity measurements of foam during drainage and decay. Removal of the foam lace, at the end of the decaying process, was followed by quantitative analysis of protein content.

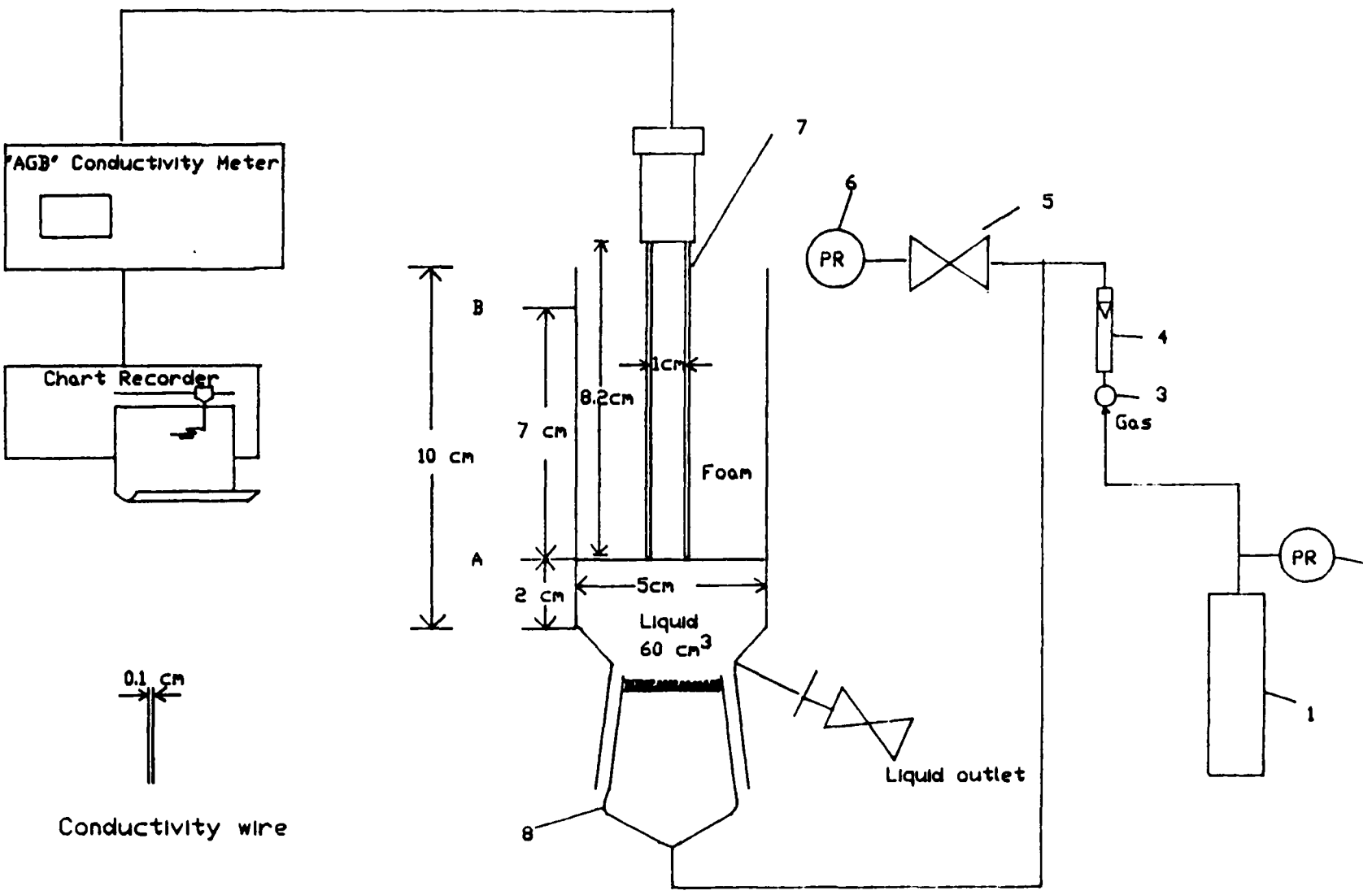


Legend

1. Gas cylinder
2. Pressure regulator
3. Gas flow control
4. Gas flow meter
5. Snap valve
6. Pressure regulator
7. Conductivity probe
8. Sinter

The time for foam collection was based on preliminary experimentation which showed that dry foams produced from a broad spectrum of feedstocks exhibited variations in protein composition from starting material. The recovered foams were collected in centrifuge pots and collapsed by centrifugation for periods of time depending on bubble resistance to centrifugal forces. Formed precipitates were carefully resuspended and sample compositions of foam and starting solutions were assayed by HPLC analysis.

## 2.3 Preparative Foam Production

### 2.3.1 Experimental Apparatus

Batch and continuous foam production was carried out in the 1,600 $cm^3$ foam tower illustrated in Figure 2.3. The final design of the tower took account of requirements for versatile use and the ability to apply a variety of continuous operations with counterflow (see Figure 1.6(a-e), Chapter 1). The tower consisted of a vertical glass column (6 cm in diameter and 57 cm in height), which could withstand pressures up to 60 psig. The tower could be thermostated by a water jacket, which was particularly important to operations involving thermosensitive enzymes. Gas was sparged through a sinter of a nominal diameter of 5 cm and porosity 3. The sinter was kept in an acidic solution of 20% $H_3NO_3$-20% HCl and was sonicated for approximately half an hour prior to use. At the bottom of the tower an effluent outlet enabled sampling of the bottom product. Outlet volumetric flowrate was controlled by a needle valve. There were 5 sampling ports (SP 1-5) to enable foam sampling at various heights in the foam column. The ports could also be used for introduction of the feed in stripping operations (see Figure 1.2) and facilitate the installation of a conductivity bridge to study variations in foam density throughout the foam column. SP 1 could additionally be used for sampling

**Figure 2.3: Experimental Set-up for Preparative Foam Production**
Schematic diagram (see Plate 2.1) of the 1600 $cm^3$ foam tower for batch and continuous foam production. The tower is connected to a centrifugal foam breaker, where foam is broken and collected in a fraction collector.

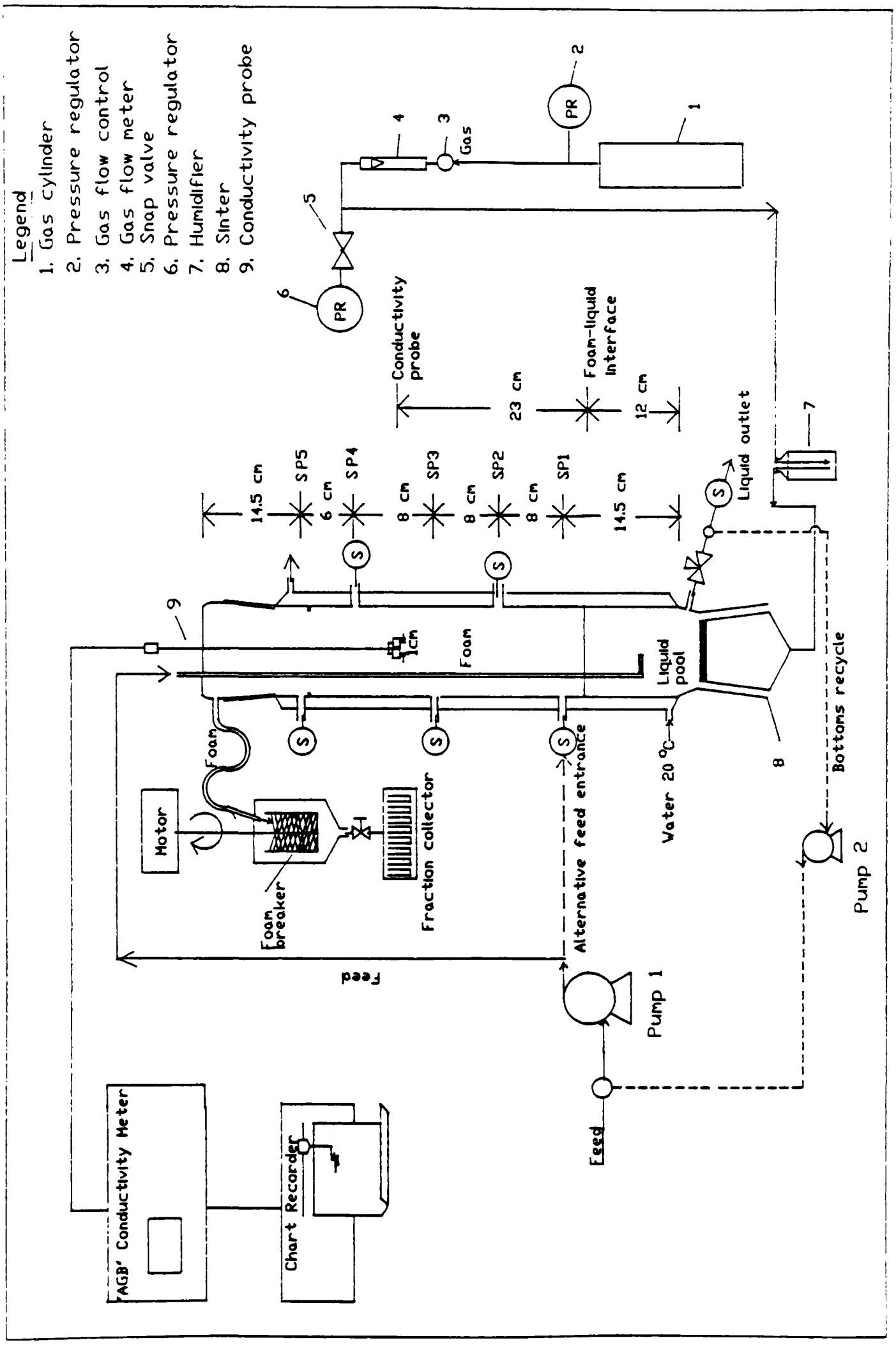

Plate 2.1: Experimental Set-up for Foam Fractionation: 1600 $cm^3$ Foam Tower

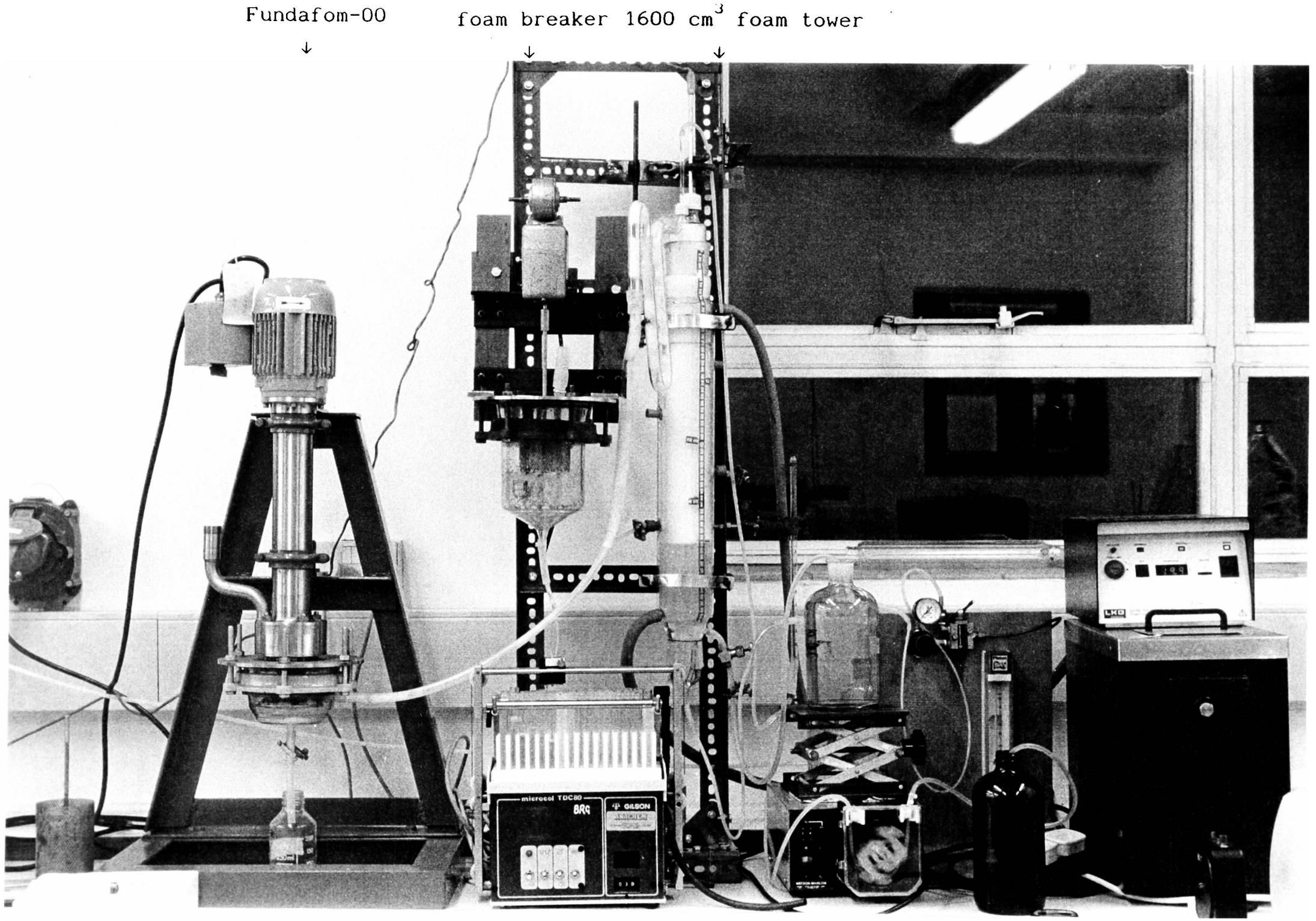

of, and access to, the liquid pool and could also serve as an alternative feed position in simple and/or enriching operations (see dotted line from Pump 1 to SP 1 in Figure 2.3). In operations with reflux (see Figure 1.6c, Chapter 1), foam could be introduced to the foam column via sampling port 5. For this reason, that part of the glass wall below it was appropriately constructed to support a spider-shaped drilled capillary tube to evenly distribute the recycled foam.

The top of the tower carried a ground joint to seal the tower when the tower cap was mounted so that the foam could be directed to the foam breaker. The tower cap added 2 cm in column height. Alternatively, the tower could be elongated by addition of glass sections in order to study height effects upon foam performance. The tower cap added 2 cm to the foam height and led the foam to the foam breaker through a U bend . The U bend was made of 4 glass pieces (2 cm in diameter) joined together with silicon tubing in order to secure flexibility. The cap had two ports through which the conductivity probe and the feed glass tube mounted. One port could also accommodate the introduction of reflux.

The conductivity probe consisted of 2 parallel stainless steel square electrodes of 1 cm side length. The distance between them was 1 cm. The probe was connected to a conductivity meter, which drove a chart recorder. The electrodes were submerged in the foam column at an immersion depth of 24 cm from the top of the tower, ie in the middle of the foam column for a liquid pool volume of 400 $cm^3$ (the pool volume applied in both batch and continuous experiments). The location of the conductivity probe was selected to reflect an average foam density in the foam bed.

The feed in continuous operations was pumped by a calibrated peristaltic pump (Pump 1 in Figure 2.3) to the liquid pool via a glass tube (ID=3 mm) ending in a perforated ring which achieved even feed distribution in the liquid pool through nine holes of 1.2 mm in diameter.

The feed was introduced in the middle of the liquid pool, although, as shown in Grieves and Wood (1964) and Ahmad (1975), the location of the feed element in the liquid pool does not affect the quality of foam.

The apparatus could accommodate enforced drainage of static foam by application of vacuum pressure. This could be applied by a vacuum pump connected to the sinter at the bottom of the tower and was measured by a manometer. Drained liquid from the foam could flow through the sinter in a trap along the vacuum line.

Foam breakage was achieved by means of a centrifugal foam breaker (Brunner and Lemlich (1963)), which consisted of perforated spinning can inside a tightly closed glass vessel. The diameter of the spinning basket was 6 cm while the inside diameter of the collecting vessel was 14 cm. The speed of rotation reflected the robustness of bubbles. The collector was made of 4 cm thick glass for safe operation. The glass surface was coated with Sigmacote, a commercially available silicone-based coating fluid (supplied by Sigma Co.) to minimise adsorption and encourage breakage of bubbles when centrifugally thrown against the walls. The broken foam drained into a fraction collector which was time-programed. Automated and regular foam collection in conjunction with foam conductivity traces indicated the attainment of steady-state conditions.

Alternative methods of foam breakage involved the use of a mini-Fundafom (Fundafom-00), supplied by Alfa-Laval Sharples Limited. Foam breaking action was based on centrifugal force. A schematic illustration of the Fundafom-00 is presented in Figure 2.4(a-b) and is depicted in Plate 2.1. Experimentation with this device was stimulated by its successful use in fermentation, chemical and oil drilling industries to break foam without the addition of antifoam reagents. As opposed to fermentation applications, where the Fundafom is mounted on the top of the fermenter vessel, it was connected in line with the foam tower in this

**Figure 2.4: Schematic Diagram of Fundafom-00**

Schematic description of Fundafom-00, for foam breakage based on centrifugal forces; **(a)** Foam flow when mounted on the top of a fermenter and **(b)** when used for foam disruption as a integral part of protein recovery by foam fractionation.

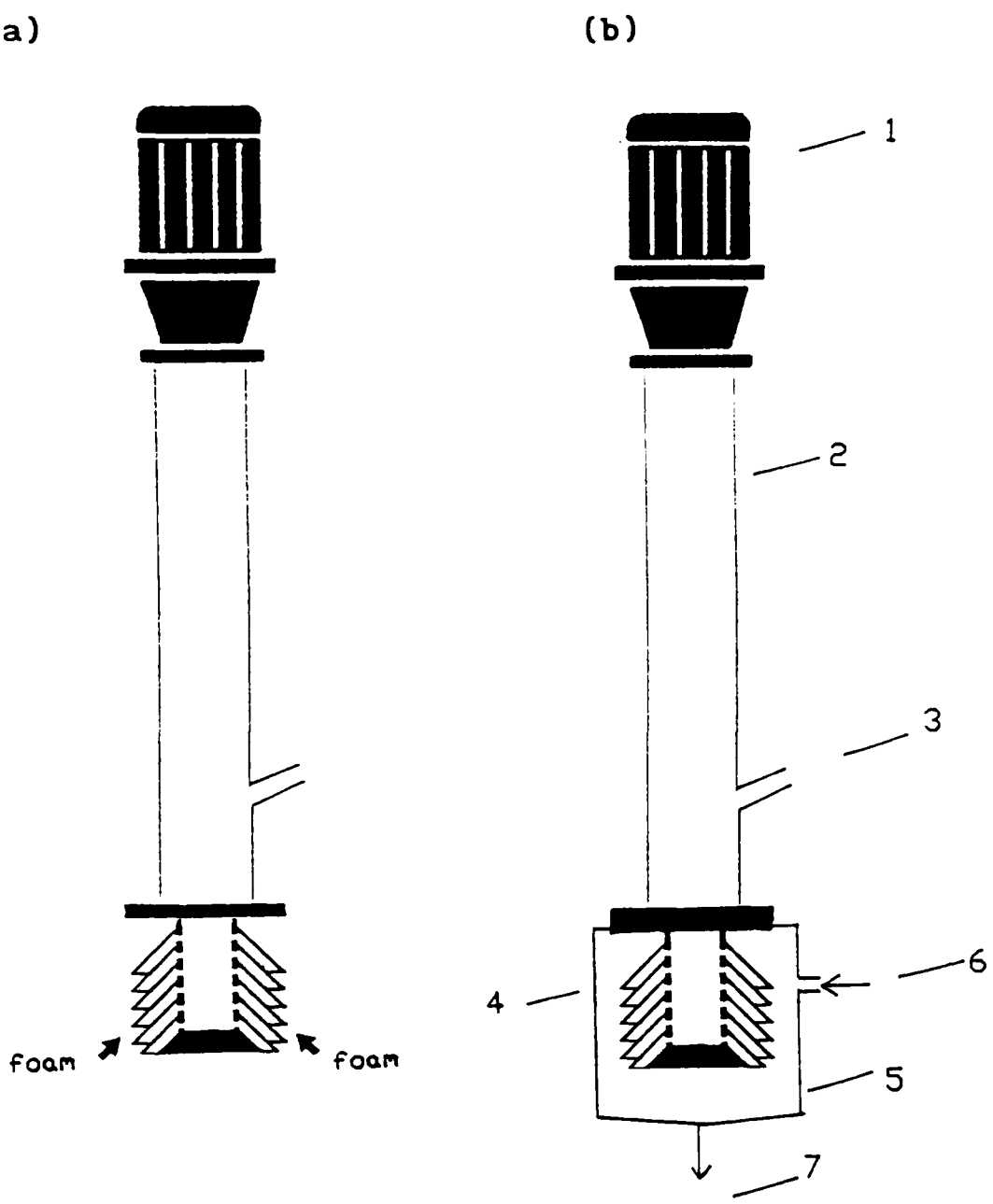


Legend

1. Motor
2. Rotating shaft
3. Ventilation port
4. Rotating disks
5. Glass Foam Collector
6. Foam entrance
7. Foam exit

study. A collecting vessel made of thick glass (4 cm wall thickness) was tightly fitted at the bottom of the Fundafom to enclose the rotating disks (see Figure 2.4b). Foam was introduced through a side port on the glass wall drilled at the height of the middle layer of rotating disks. The bottom of the vessel was nearly flat and the broken foam drained out through an outlet located in the middle. Overheating of the driving shaft caused increased temperatures in the collecting vessel and necessitated intermittent operation (see Appendix I).

Experimental determination and photographic illustration of physical parameters of foam, such as coalescence frequency, bubble size and liquid hold-up, led to the design of the glass foam tower depicted in Figure 2.5. The tower consisted of two vertical sections which could be held together by clamps. The internal diameter of the tower was 4.6 cm and the height of the bottom and top section was 31 and 35 cm respectively. The tower could withstand pressures up to 65 psig. Detachable sections enabled operation with low and high foam beds. The tower was not thermostated by a water jacket in order to avoid additional distortion of bubble photography. Gas was sparged through a sinter of a nominal diameter of 4 cm and porosity 3.

The level of the liquid pool was maintained constant at 26 cm from the tower bottom and the feed was introduced to the middle of the liquid pool. The bottom effluent was removed via a port located at the bottom of the tower and its flowrate was adjusted with a needle valve to maintain a constant level in the liquid pool. There were 11 sampling ports (3 in the bottom and 8 in the top section) evenly distributed along the foam column. Their internal diameter was 3 mm. The ports enabled determination of variations in liquid hold-up and protein concentration throughout the foam height. The tower cap was clamped on the top of the tower and channeled the rising foam to the foam breaker. Foam conductivity was not monitored during this set of experiments.

**Figure 2.5: Foam Tower for Bubble Studies**

Schematic diagram of apparatus dedicated to physical studies of foam bubbles during continuous foam production.

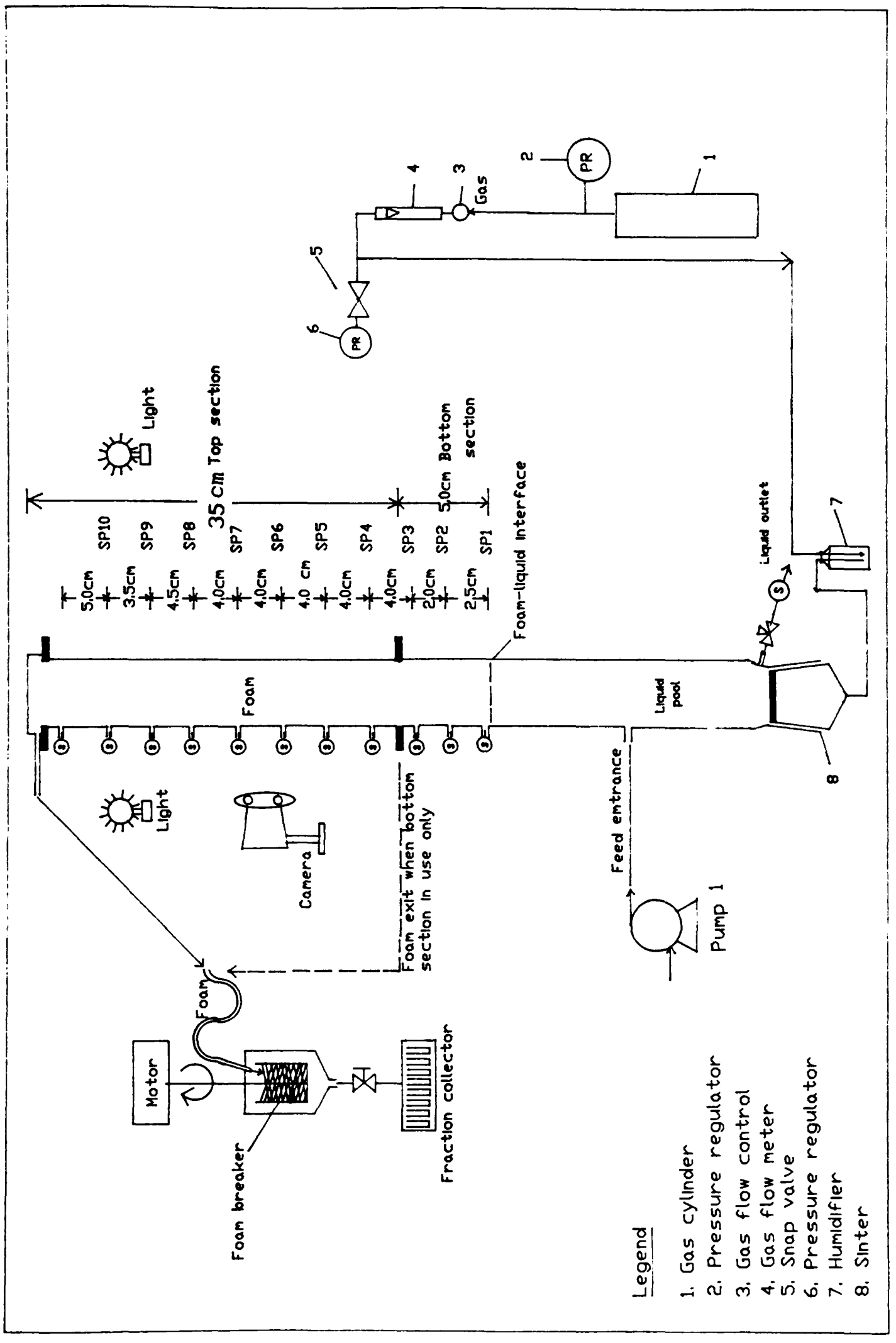

### 2.3.2 Batch operation

A selected volume of foaming solution was loaded into the foam tower and the gas supply was adjusted to a set flowrate. During operation, the level of the liquid pool dropped as liquid was carried to the foam phase and the reduction in the level of foam-liquid interface was noted at timed intervals. At these points, sampling of the bulk phase through SP 1 enabled determination of variations in solute concentration during batch foaming. The time of batch operation was constant throughout experimentation to ensure comparable results. Determination of volumes and solute concentrations in the liquid pool enabled calculation of the heat of desorption $\lambda$ of the surface active solutes and was based on Equation 2.8. At the end of operation, the volumes and solute concentrations of foam and bottom products were measured and compared with the original feedstock in order to evaluate individual processes.

### 2.3.3 Continuous operation

Continuous foam operation took place in the simple mode (see Figure 1.6**b**), by introducing the feed into the liquid pool without reflux. A predetermined initial volume of feedstock was loaded into the tower, and the gas and feed supplies were simultaneously switched on. Immediately the level of the liquid-foam interface was noted so that the level set point could be determined. There was an initial drop in the liquid level as thick foam was produced (high foam conductivity) and the bottoms outlet was closed. A gradual rise in the liquid level coincided with a reduction in the recorded foam conductivity until the level reached the set point, and thereafter the bottoms outlet was opened. The outlet flowrate was adjusted by a needle valve so that the liquid level remained constant. Assessment of the effectiveness of mixing in the liquid pool involved subsequent determination and comparison of protein concentrations.

Stabilisation in the liquid level for a constant bottoms outflow, constant foam conductivity and consistent volumes of collapsed foam collected at fixed time intervals, indicated the attainment of steady-state conditions. These were confirmed, when the protein concentration of foam fractions, foam samples at various tower heights, liquid pool, and bottoms were found to be constant at all times. A minimal average time of 90 minutes was needed for both model and yeast protein systems to attain steady-state operation.

During operation the inlet and bottom effluent flowrates were checked, and input adjustments were made to compensate for increases associated with dilated silicon tubing arising from prolonged operations of pumps. At the end of the steady-state operation, the volumes of feedstock processed and foam and bottom effluent collected were measured and compared with those observed during operation. Samples from individual foam fractions were taken before they were pooled for further protein determinations. In the case of turbid foams arising from molecular denaturation, the suspended particles were recovered by centrifugation and resolubilised in 2M NaOH for measurement of protein content.

The above procedure was also applied to experiments designed to study physical properties of the manufactured foam, with the exception that foam conductivity was not monitored whilst the pool concentration was measured by sampling the bottom effluent only (see dedicated apparatus in Figure 2.5).

Continuous foam production was also undertaken with partial recycle of the bottom effluent. For this purpose, a Y-shaped glass piece was used to divide the bottom effluent into two streams propelled by a peristaltic pump at a set recycle flowrate. The recycle was mixed with fresh feed, using a T-shaped glass piece and was pumped into the liquid pool. The inlet rate to the liquid pool was kept constant. Preliminary experiments,

designed to investigate the extent of mixing of the two streams and backflow action due to unequal flowrates, utilised pure water and an aqueous dye solution. Visual observations showed that there was no backflow and that the two streams mixed before the liquid reached the liquid pool. As a result, the use of a mixing valve was not found necessary. During operation, the protein concentration of the inlet stream, ie the resultant stream of effluent recycle and fresh feed, was determined and compared with the theoretical one.

## 2.4 Biochemical Characterisation

### 2.4.1 Spectrophotometric Determination at 280 nm.

Protein concentrations in homogeneous solutions, such as those of BSA and lysozyme, were determined by absorbance measurements at 280 nm using a 1 cm light path. The extinction coefficients of the proteins used are given in 2.1.

### 2.4.2 HPLC Analysis

Quantitation of BSA and lysozyme concentrations in heterogeneous solutions employed size-exclusion chromatography by HPLC analysis. The method exploited differences in molecular weight between the two proteins (67 and 14.5 kDaltons).

A Spherogel$^{TM}$ TSK 4000 PW column with a fractionation range of 2 to $10^3$ kDaltons was used. The average particle diameter was $\bar{d}_p$=10$\mu$m and the column dimensions were ID=7.5 mm and length=30cm. The column was equipped with a pre-column whose dimensions were ID=7.5 mm and length=7.5 cm and particle size was identical to the main column. Figure II1 in Appendix II shows the profile of protein elution with time for a variety of proteins with different molecular weights.

The column was equilibrated with 50 mM PBS (50 mM sodium phosphate

with 150 mM NaCl) at pH 7.0. The pumping rate was 1 $cm^3$ $min^{-1}$ and the sample loading was achieved by use of a 20 µl loop. Absorbance was read at 280nm and the column was calibrated for BSA and lysozyme solutions at both low and high protein concentrations, ie 0.01-0.5 mg $cm^{-3}$ and 0.5-5 mg $cm^{-3}$ (see Figures II2-II4 in Appendix II).

The method did not account for reported conformational changes induced in the BSA upon foaming. However such changes were not considered to influence the spectroscopic analysis in a significant way (Clark et al. (1989)).

### 2.4.3 Protein Determination by Coomassie Blue

Routine protein determination involved application of the Bradford assay (Bradford (1976)) as modified by Pierce (Pierce and Suelter (1977)). The method is based on the observation that the maximal absorbance for an acidic solution of Coomassie Brilliant Blue G-250 shifts from 465nm to 595nm when the dye binds stoichiometrically to protein molecules (Reisner et al. (1975)). This shift coincides with a transition from a brownish-orange (dye alone) to an intense blue colour in proportion to the amount and/or type of protein bound. Binding primarily involves arginine while other basic and aromatic residues give a slight contribution. It has been shown that there is minimal interference to this reaction from dissolved ions, detergents and carbohydrates, and the assay does not detect free amino-acids and small polypeptides (MW < 3 kDaltons) (Sedmak and Grossberg (1977)).

Equal volumes of dye (see Section 2.1) and sample were mixed and spectrophotometric absorbance was determined at 595nm relative to deionised water blank, within 30 minutes. Protein content was expressed in terms of the equivalent BSA concentration which gave the same $A_{595nm}$ in a standard test. Protein quantitation was based on a calibration curve

produced simultaneously BSA solutions of 0-25 $\mu g\ cm^{-3}$, range in which the absorbance at 595nm was found to increase linearly with BSA concentration (see Figure II5 in Appendix II). All samples were prepared in deionised water at room temperature. Sample concentrations were chosen to yield $A_{595nm}$ readings within this range. The assay was highly reproducible and could detect 1 $\mu g\ cm^{-3}$ BSA.

The precipitated protein was separated from turbid foam samples by centrifugation and the supernatant was discarded. The remainant precipitate was resolubilised in 2M NaOH (Mohan (1992)) by extensive stirring and its protein content was determined as previously described. A minimal amount of NaOH was used so that subsequent protein determinations demanded a minimal 10 fold dilution. This secured a NaOH concentration well below values of 0.5 M NaOH, above which interference with the assay takes place (Pierce specifications).

The above determinations facilitated confident comparison of the protein content of feedstock, foam and bottom product, although they could not reveal any variations in protein composition and structure taking place during foaming. Comparisons in respect of the protein composition of samples required gel electrophoresis (see 2.4.4).

Alternative protein assays such as the Lowry assay (Lowry et al. (1951)) were considered unsuitable for this study. Such assays are strongly influenced by free amino-acids and other solutes (particularly ammonium ions). In the case of the Lowry assay, interference is also associated with lipids, chelating agents (EDTA, GEDTA), sulphydryl reagents, nucleic acids, carbohydrates etc. Thus protein precipitation with trichloroacetic prior to quantitation may be essential. The lowest sensitivity of the Lowry assay is limited to 5-10 $\mu g\ cm^{-3}$ BSA as opposed to 1 $\mu g\ cm^{-3}$ BSA for the Bradford assay. The use of the Kjeldahl method for determination of nitrogen content also exhibits limitations when used

for the determination of protein content in beer foams. Reservations have also been expressed by Bamforth (1985) concerning the universal application of the conversion factor (6.25) for protein determination.

**2.4.4 RNA Assay**

The quantitation of RNA is based on reaction with an orcinol reagent at 100 $^{o}$C for 20 minutes (Herbert et. al. (1971)). The orcinol reagent comprises 1 volume of 1.25% w $v^{-1}$ orcinol in water and 4 volumes of 0.09% w $v^{-1}$ $FeCl_3$ in concentrated HCl. During the reaction a transition from a bright yellow to a green colour takes place. Colour intensity is directly related to the amount of RNA reacted.

Samples were added to orcinol reagent (1:3) and the mixtures were heated at 100 $^{o}$C for 20 minutes. The absorbance of samples was determined spectrophotometrically at 672nm in respect of a distilled water blank. RNA concentration was expressed as RNA equivalents determined for a standard RNA from Torrula yeast. A calibration curve of reaction of 0-120 $\mu g\ cm^{-3}$ RNA was used (see Figure II6 in Appendix II). Sample absorbance was read against blank of distilled water.

A major disadvantage of the method is that it depends on an estimation of ribose released by acid hydrolysis of RNA, but is complicated by other sugar reactions (free ribose in particular). Carbohydrate contamination of crude extracts is therefore expected to interfere to a greater or lesser extent. Sample pretreatment with concanavalin A may reduce this interference but is unlikely eliminate. Differential colour response by different interfering substances may enable the development of assays at various wavelengths to compensate for the presence of other substances. In the present study no remedial alternative was applied. RNA values obtained for feedstock and foam and bottom products were used in the assembly of mass balances.

### 2.4.5 Carbohydrate Assay

The assay is based on the development of a bright deep purple colour when 4 volumes of 0.4% 1-napthol in concentrated $H_2SO_4$ react with 1 volume of carbohydrate sample at 100 $^{o}C$ for 10 minutes (Plummer (1978)). The absorbance was determined at 555nm against a distilled water blank. The intensity of the colour was directly related to the quantity of reacted carbohydrate. The carbohydrate content was expressed as glucose equivalents derived from a calibration curve established for 0-40 $\mu g\ cm^{-3}$ glucose (see Figure II7, Appendix II). Determination of the carbohydrate content of freeze-dried foam, feedstock and bottom product was applied to assessment of product quality.

### 2.4.6 Acidic Protease Assay

The method applied herein was described by Kassell et al (1970). Its principle is based on the proteolytic activity of acidic proteases upon haemoglobin whose cleaved fragments are soluble in trichloroacetic acid. The tyrosine and tryptophan content of these compounds can be determined by the Folin and Ciocalteu Phenol reagent, or by measurement of the extinction at 280 nm. The latter was applied in this study.

Samples were prepared in 0.1 M citrate buffer pH 3.2. Acidic denatured haemoglobin was prepared by allowing 1 g of haemoglobin to dissolve in 20 $cm^3$ water with simultaneous pH adjustment to 3.2. The solution was made to 100 $cm^3$ with citrate buffer. Sample of 0.1 $cm^3$ was mixed with 0.4 $cm^3$ of acid denatured haemoglobin in duplicate. Duplicates were incubated in a water bath at 37$^{o}C$ for 30 minutes (reacted samples). Trichloroacetic acid (1 $cm^3$ of 5% w $v^{-1}$) was added to precipitate undigested haemoglobin fragments insoluble in trichloroacetic acid. A further set of duplicates included simultaneous mixing of 0.1 $cm^3$ of

sample, 0.4 $cm^3$ of acid denatured haemoglobin and 1 $cm^3$ trichloroacetic acid (control). Both reacted and control samples were centrifuged in a microfuge for 5 minutes and the absorbance of the supernatant was measured at 280nm against distilled water. The difference in the absorbance of the reacted and the control samples, $\Delta A_{280nm}$(reaction-control) was determined.

Calculation of the acidic protease concentration was based on a calibration curve established by a standard solution of 0-100 $\mu g\ cm^{-3}$ pepsin (Figure II8 in Appendix II). The enzyme concentration was expressed in $\mu g\ cm^{-3}$ pepsin (dry w $v^{-1}$). Determination of the acidic protease content of foam, feedstock and bottom product was part of the product quality assessment.

### 2.4.7 Gel electrophoresis

Polyacrylamide gel electrophoresis was employed to investigate and compare the polypeptide profiles of complex feedstocks and respective foams and bottom products. Analysis was dependent on molecular weight and pI distribution. Electrophoretic analysis was performed automatically using a Pharmacia Phast System (Pharmacia Ltd., Uppsala, Sweden). Sample preparation, separation procedures and development techniques were based on the Phast System Manual (Pharmacia (1987)). Polyacrylamide gels were also supplied by Pharmacia Ltd. and included 8-25% gradient and isoelectric focusing (IEF) gels (pI 3-9).

Study of the molecular weight distribution involved SDS-PAGE ($\beta$-mercaptoethanol reduced conditions) on 8-25% gradient gels, which offered a linear relationship between the logarithm of molecular weight (log(mw)) and the relative mobility distance ($R_f$) for a mass range of 6-300 kDaltons (see Figure II9(a-b) in Appendix II). Sample load was 1 $\mu$l and up to 8 samples could be analysed on the same gel. Samples typically included the starting material, bottom product, foam and resolubilised

foam precipitate. Estimation of polypeptide molecular weights was based upon the mobilities of low and heavy molecular weight standard proteins (LMW and HMW respectively). Post electrophoretic visualisation exploited silver diamine staining (Pharmacia (1987)) as opposed to Coomassie Blue treatments because of the dilute conditions of applied foaming systems. However, silver staining created a dark backround which hampered attempts to quantify discrete bands by gel scanning.

Isoelectric focusing electrophoresis (IEF) was applied to identify the isoelectric points of yeast extract polypeptides in feedstocks and foam and bottom products. Characterisation was based on a calibration with standard markers having pI values in the range of pH 3-9. Gels were stained with silver diamine. Experience indicated that application of silver diamine staining, was more efficient that silver nitrate staining specifically developed for IEF gels. Therefore identical development procedures were applied for both SDS-PAGE and IEF gels.

### 2.4.8: Cytochrome-*c* Assay

Determination of the concentration of cytochrome-*c* in muscle heart extract was based upon the method of Cole and Rittenberg (1971). Samples were reduced with sodium dithionite ($Na_2S_2O_4$) and the absorbance spectrum was determined in the region of 400-650 nm against blank of distilled water. Followingly, reduced samples were oxidised with potassium ferricyanide ($K_3Fe(CN)_6$) and their spectrum was measured in the same region (400-650 nm) against distilled water. The presence of cytochrome-*c* in its oxidised form gave a distinct peak at 550 nm. Subtraction of the reduced spectrum from the oxidised one and application of the folowing formula yielded the concentration of cytochrome-*c* as a fraction of the mass of total protein:

$$(\text{pmole cytochrome-}c)(\text{mg protein})^{-1} = 10^6 \Delta A_{550nm}/20$$

Investigation of the likelihood of interference by the presence of haemoglobin, due to the peak at 559 nm of single haemoglobin solutions when the assay procedure is applied, included experimentation with commercially available cytochrome-*c* (see Section 2.1) in the presence and absence of various amounts of haemoglobin. Such interference was found to be negligible (see Table II1(a-c) in Appendix II).

### 2.4.9: Immunochemical Determination of Myosin Concentration

An ELISA assay was established to determine the concentration of myosin from bovine muscle (see Appendix V). Commercially available myosin antigen (see 2.1) was used to establish a calibration curve. The observed absorbance of commercial myosin antigen was compared with that of myosin samples of comparable concentrations, courtesy of Drs D. Bandari and Prof. I.P. Trayer, School of Biochemistry, University of Birmingham.

Aliquots of myosin of various concentrations (0-5 $\mu g\ cm^{-3}$) were prepared in 0.6 M KCl. Preparations in 0.05 M sodium carbonate ($Na_2CO_3$); pH 9.6 were characterised by extensive myosin precipitation. Myosin aliquots ( 100 $\mu$l) were pipetted into the plate wells, which had been previously coated with 0.05 M $Na_2CO_3$ buffer; pH 9.6, and were incubated for 3 hours at room temperature. The liquid content of the wells was then discarded and the plate was dried. 100 $\mu$l of a 2% casein solution were added in each well and the plate was incubated for 1 hour at room temperature. The casein solution was then shaken off and the wells were thoroughly washed with a mixture of PBS; pH 7.4 and 0.05% Tween-20. 1 l of PBS solution comprised 40 g of NaCl, 1 g $KH_2PO_4$, 14.46 g $N_2HPO_4.12H_2O$ and 1 g KCl. Followingly, 100 $\mu$l myosin antibody (see 2.1) was added in each well and the plate was incubated for 3 hours at room temperature. The myosin antibody was diluted 200 and 400 fold in a mixture of 1 volume 2% casein, 3 volumes PBS and 1 volume 0.05% Tween-20. After incubation, the

plate was exhaustively washed, as previously described. 100 μl of conjugate solution (see 2.1), diluted 5000 and 10000 fold in the same mixture as the antibody, were applied in each well and the plate was incubated for approximately 1 hour at room temperature. Thorough wash followed prior to the addition of 100 μl of substrate (pH 4.3) in each well. The substrate comprised a mixture of 12 $cm^3$ 0.1 M citric acid, 8 $cm^3$ 0.2 M $Na_2H_2PO_4.12H_2O$, 8 $cm^3$ $H_2O_2$ and 8 mg of OPD (o-phenylene diamine). When colour developed in the most dilute wells in the plate, the reaction was stopped with the addition of 75 μl of 12% $H_2SO_4$ to each well. Readings were taken at 492nm against blank of empty wells.

## 2.5 Physical Characterisation

### 2.5.1 Surface Tension Measurements

Surface tension was measured with a Torsion Balance, type "OS", using a glass test plate (see Figure 2.6(a-b)). The balance was calibrated from 0-0.12 N $m^{-1}$, with 240 equal divisions. Measurements took place at room temperature (22.5-22.8 °C) and, since surface tension is sensitive to temperature, regular checks of the temperature of the solutions were undertaken to ensure experimental accuracy. Solutions were prepared 90 minutes prior to foaming to ensure equilibrium of air-liquid adsorption and were used that day. Hazy solutions were centrifuged prior to surface tension determination and protein concentrations were determined by appropriate assay methods. The balance was initially set up and zeroed with the glass test plate in air. The glass test plate was then lowered to the liquid surface so that its edge was parallel to the surface of the liquid. The plate was completely immersed into the liquid phase, and the platform was gradually lowered while the index pointer was moved anticlockwise so as to maintain the beam pointer at a zero value. The value indicated by the index pointer at the moment the glass plate parted

**Figure 2.6 : Surface Tension Measurements**

Experimental apparatus for surface tension measurements with the method of the glass test plate **(a)** using a the Torsion Balance Type "OS" **(b)**.

(a) Surface tension measurement

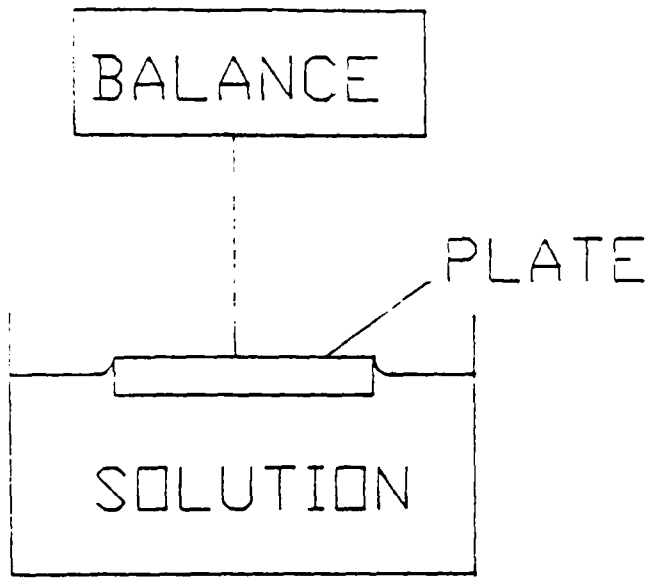


(b) Torsion balance type "OS"

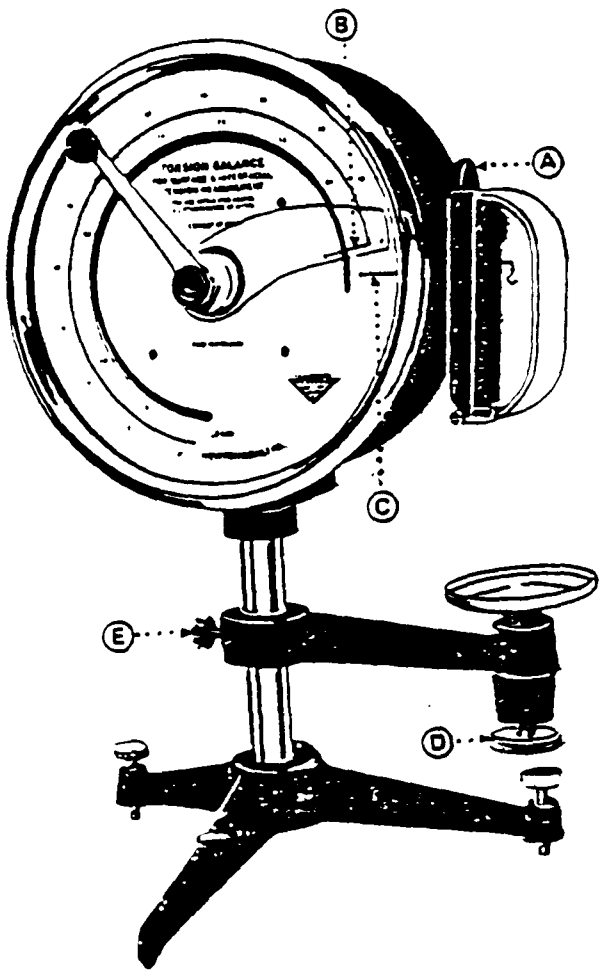

from the interface gave an estimate of the surface tension of the solution and could be read directly from the balance dial in N $m^{-1}$. Experiments were performed in triplicate and the average values were determined.

### 2.5.2 Bubble Photography

Foam bubbles adjacent to the glass wall of the foaming tower, illustrated in Figure 2.5, were photographed in motion using a Nikon FN, 35mm SLR camera. A fast (400 ASA) black-and-white film was used and the exposure time was 1/125-1/250 sec. The apparatus was lit from the back with a fibre optic cold light source. The camera was focused on a small area of the glass wall to avoid distortion due to the cylindrical surface of the tower. Photographs included adjacent graduated tape to enable calibration and determination of bubble size. Photographs were printed on matt paper to avoid reflection during image analysis.

Bubble size measurements were made with a Seescan Solitaire image analysis system (supplied by Seescan Ltd., Cambridge, UK) operating in an interactive mode in order to overcome limitations of picture quality. These were associated with poor resolution between the bubble edge and its interior, bubble overlapping, and interference from background bubbles when the bubble walls were very thin. Results were expressed in terms of bubble feret diameter (which compensates for deviations from perfect circular cross-sections of bubbles), bubble area and perimeter. Statistical analysis on the obtained values gave average feret diameter values and bubble size distribution.

## 2.6 Material Balances

### 2.6.1 Batch Operation

A material balance on component i for the batch foaming system is illustrated in Figure 2.7 is given by equation 2.1 (Charm (1973)):

$$(V-dV)(c_{iB}-dc_{iB})+dV(c_{iF}+dc_{iF}) = Vc_{iB} \qquad \text{(Equation 2.1)}$$

where: V is the volume of the bulk phase

$c_{iB}$ is the concentration of component i in the bulk phase

$dV$ is the differential volume foamed from the bulk phase

$c_{iF}$ is the concentration of component i in the foam

Simplifying and dropping second order differentials Equation 2.1 becomes:

$$dV/V = dc_{iB}/(c_{iF}-c_{iB}) \qquad \text{(Equation 2.2)}$$

The driving force for transferring a component i from the bulk to the foam phase is determined by the chemical potential difference between the two phases. The chemical potentials for component i in the foam and bulk phase are given by Equations 2.3 and 2.4 respectively

$$\mu_{iF} = \mu_{iF}^{\circ} + RT \ln c_{iF} \qquad \text{(Equation 2.3)}$$

$$\mu_{iB} = \mu_{iB}^{\circ} + RT \ln c_{iB} \qquad \text{(Equation 2.4)}$$

where: $\mu_{iF}$ is the chemical potential of component i in the foam

$\mu_{iF}^{\circ}$ is the chemical potential of component i in the foam under standard conditions

$\mu_{iB}$ is the chemical potential of component i in the bulk phase

$\mu_{iB}^{\circ}$ is the chemical potential of component i in the bulk phase under standard conditions

$c_{iF}$ is the concentration of component i in the foam

$c_{iB}$ is the concentration of component i in the bulk phase

R and T are the gas constant and absolute temperature respectively

At equilibrium the chemical potentials of the two phases are equal, and therefore Equations 2.3 and 2.4 result in Equation 2.5

$$\lambda = \mu_{iB}^{o} - \mu_{iF}^{o} = -RT\ln(c_{iB}/c_{iF}) \qquad \text{(Equation 2.5)}$$

or equivalently

$$c_{iF} = c_{iB}e^{(\lambda/RT)} \qquad \text{(Equation 2.6)}$$

where: $\lambda$ is the heat of desorption

Substitution of $c_{iF}$ and integration of Equation 2.2 give Equation 2.7:

$$\int_{V}^{V_o} dV/V = \int_{c_{iB}}^{c_{iBo}} dc_{iB}/\{c_{iB}(e^{\lambda/RT}-1)\} \qquad \text{(Equation 2.7)}$$

where: $V_o$ and $c_{iBo}$ are the initial bulk volume and concentration respectively.

Equation 2.7 yields Equation 2.8 which describes the relationship between the volume and composition of the bulk phase, assuming that equilibrium was achieved between the bulk and the foam phase. It is also an experimental tool to calculate the heat of desorption $\lambda$.

$$\ln(V_o/V) = \{1/(e^{\lambda/RT}-1)\}\{\ln(c_{iBo}/c_{iB})\} \qquad \text{(Equation 2.8)}$$

### 2.6.2 Continuous Operation

For a simple continuous operation at steady-state conditions the material balances for the streams and component i (see Figure 2.8a) will be

$$Q_O = Q_F + Q_B \qquad \text{(Equation 2.9)}$$

$$Q_O c_{iO} = Q_F c_{iF} + Q_B c_{iB} \qquad \text{(Equation 2.10)}$$

where: $Q_O$, $Q_F$ and $Q_B$ are the volumetric flowrates of feed, foam and bottoms respectively

$c_{iO}$, $c_{iF}$ and $c_{iB}$ the concentrations of component i in the feed, foam and bottom effluent respectively.

In the case of bottoms recycle (see Figure 2.8b) material balances around point 1 for streams and component i are described by Equations 2.11 and 2.12 respectively:

$$Q_0^* = Q_0 + R \qquad \text{(Equation 2.11)}$$

$$c_{i0}^* = (c_{i0}Q_0 + c_{iB}R)/Q_0^* \qquad \text{(Equation 2.12)}$$

where: $c_{i0}^*$ and $Q_0^*$ are the concentration and volumetric flowrate of the stream at the entrance of the foam tower

R is the bottoms recycle.

**Figure 2.7: Schematic Representation of Material Balances in Batch Foam Production**

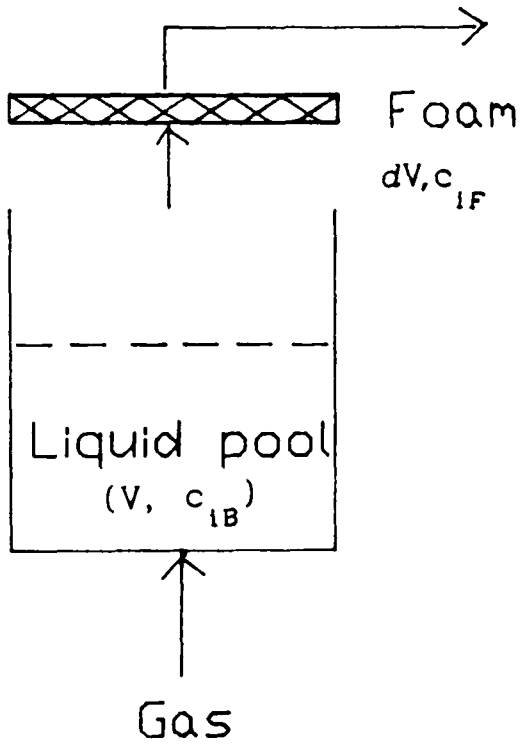


Legend

V -volume of the bulk phase

$c_{iB}$-concentration of component i in the bulk phase

*d*V -differential volume foamed from the bulk phase

$c_{iF}$-the concentration of component i in the foam

**Figure 2.8: Material Balances in Continuous Foam Production**

Schematic representation of material balances in **(a)** simple continuous operation and **(b)** simple continuous operation with bottoms recycle.

**(a)**

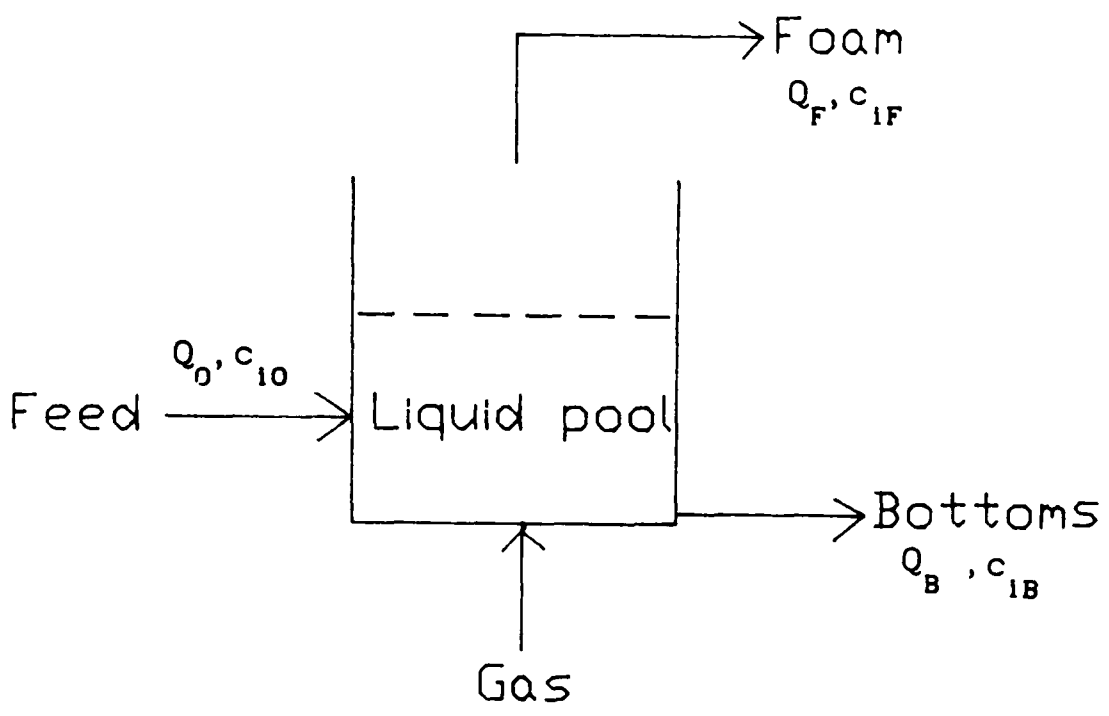


**(b)**

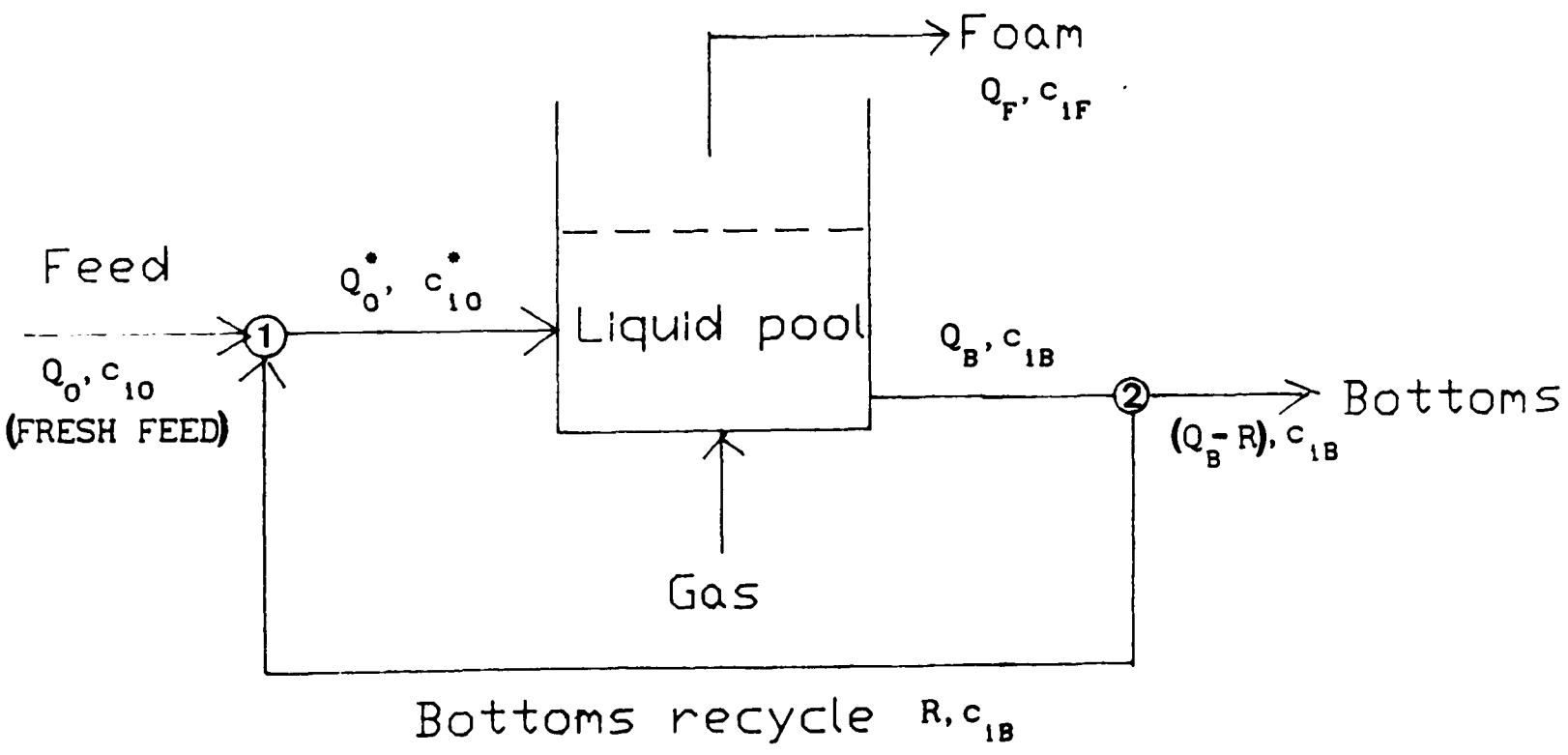

# CHAPTER 3

## FOAMING PROPERTIES OF DEFINED PROTEIN SYSTEMS

### 3.1 Preface

The importance of protein foams in the food industry and in the positive recovery of proteins from complex feedstocks by foaming has confirmed a role for the study of the foaming behaviour of both defined homogeneous and heterogeneous protein solutions (see Chapter 1). Such solutions are closely representative of real systems and characterised by quantifiable foaming qualities. Understanding of the molecular interactions which underpin these foaming systems is essential to the development of controlled foam fractionation as a separation unit in downstream processing.

Foam stability of homogeneous and heterogeneous model systems of proteins was assessed from head retention values (HRV) obtained by the Rudin method (Rudin, 1957), well established in the Brewing Industry (Bamforth (1985); Hegarty et al. (1989)), and conductivity measurements of foam generated under selected conditions. In contrast to the Rudin method, which can only trace liquid drainage, conductivity measurements of foam address both the time-dependent decay of dry foams and foaming power (Kato et al. (1983b)). In tandem with foam stability assessment by conductivity measurements, foam lace was collected to analyse the protein concentration of individual components and hence determine the degree of protein partition in foams of known stability.

Homogeneous protein preparations comprised solutions of bovine serum albumin (BSA), an acidic protein of pI 4.8 and molecular mass 67 kDaltons. In heterogeneous preparations, basic proteins such as lysozyme (pI 10.5; molecular mass 14.5 kDaltons) and cytochrome-*c* (pI 10; molecular mass 12.4

kDaltons) were added to BSA solutions to assess both the nature and the influence of protein-protein interactions upon foam stability. The basic proteins were added at concentrations which yielded no measurable foam in their own right, ie 1 mg $cm^{-3}$ lysozyme and 0.1 mg $cm^{-3}$ cytochrome-*c* (Velissariou (1988)). The foam stability of the BSA-lysozyme and BSA-cytochrome-*c* systems was evaluated with reference to that observed in homogeneous solutions under identical conditions (control). Experimentation was undertaken with a view to investigate the influence of BSA concentration, pH conditions (at, above and below the isoelectric point of BSA) and ionic strength upon foam stability.

## 3.2 Experimental Description

Foaming was undertaken in the Rudin apparatus (Figure 2.1, Chapter 2) and the lacing funnel (Figure 2.2, Chapter 2) by sparging $CO_2$ gas (95 % purity) as described in Chapter 2. Thus foam stability was expressed in terms of head retention value (HRV) and conductivity half-life (CHL) respectively (see Section 2.2, Chapter 2). Conductivity measurements also enabled determination of the foaming power (FP, defined in Chapter 2 (2.2.2) and Figure 3.8 in Chapter 3) of foams from solutions prepared in comparable buffer systems. As already mentioned in Chapter 2, the same sinter (porosity 3) was used throughout experimentation with the exception of HRV determinations of homogeneous and heterogeneous solutions at various pH conditions (Figure 3.5). Here a spare sinter of the same porosity was used as a temporary replacement.

Foam collection from the lacing funnel (see Chapter 2) was undertaken 2 minutes after the establishment of constant foam conductivity (Region "C" in Figure 3.8, Chapter 3). Determination of BSA and lysozyme concentration by HPLC gel electrophoresis (see Chapter 2) was based on respective calibration curves shown in Figure II1(a-b) (see Appendix II).

Proteins were dissolved in 50 mM citrate buffer (distilled water), unless stated otherwise, containing 4 % v $v^{-1}$ ethanol. The ethanol concentration applied throughout experimentation was found to maximise foam stability of a 2 mg $cm^{-3}$ BSA solution in 100mM citrate buffer, pH 4.8 (Velissariou (1988)). The use of citrate buffer enabled application of a wide range of pH below and above the isoelectric point of BSA, ie pH 3.4 to 6.0. Individual protein solutions were carefully stirred separately in ethanol free buffer, to effect dissolution and to avoid foam head formation. Components were mixed 15 min prior to foaming with simultaneous addition of the required amount of ethanol under mild continuous stirring. Lysozyme required extended dissolution by extensive stirring for approximately two hours, as opposed to 45 min for BSA. Remaining solids were removed by centrifugation at 30,000 g for 60 minutes. Working lysozyme concentrations were determined spectrophotometrically at 280 nm using the published extinction coefficients (Jollès et al. (1977); Clark et al. (1989)). The reported concentrations of BSA and cytochrome-*c* assumed molecular purity and complete dissolution and are based upon dry weight per volume. The selection of protein concentrations for assessment of foam stability by conductivity measurements of foam was based upon previous experience gained with HRV measurements and trends in the diagrams of surface tension ($\sigma$) against ln c as shown in Figure III1(a-b) in Appendix III.

## 3.3 Results and Discussion

Presentation of results on foam stability of protein systems, as determined by the Rudin method and conductivity measurements, is followed by relevant discussion. Subsequently the protein content of foams generated during CHL determinations is presented and discussed, and results are related to observed trends in foam stability of respective

samples.

### 3.3.1 Foam Stability of Defined Protein Systems: HRV and CHL Determinations

The effects of various operating conditions upon foam stability of protein systems determined by application of the Rudin method are described in Figures 3.1-3.7. In homogeneous BSA solutions of constant pH, foam stability was enhanced with increasing BSA feed stock concentration in a similar manner at all three pH conditions applied, ie at,above and below the isoelectric point of BSA (see Figure 3.1). However, across the range of BSA concentrations studied, it can be seen that pH variations resulted in varied HRV for identical BSA concentrations. The most stable foams were formed at the isoelectric point of BSA (pH 4.8). At a constant BSA concentration (2 mg $cm^{-3}$) and varied pH conditions, it was found that foam stability was maximum at the isoelectric point of BSA, namely pH 4.8 (see lower plot in Figure 3.5). In heterogeneous solutions of BSA and lysozyme at pH 6.0, where proteins are oppositely charged, addition of a fixed amount of lysozyme (1 mg $cm^{3}$) in BSA solutions of increasing concentration (1 to 6 mg $cm^{-3}$) enhanced foam stability in a steady manner as shown in Figure 3.2. Application of 0.1 mg $cm^{-3}$ of cytochrome-*c* in the place of lysozyme yielded moderate degrees of synergistic enhancement in foam stability (see Figure 3.3) for BSA concentrations up to 4 mg $cm^{-3}$. Further increase in BSA concentration eliminated any effects associated with the presence of cytochrome-*c* and established the former as the determining factor of foam stability in heterogeneous solutions. The applied concentration of cytochrome-*c* (0.1 mg $cm^{-3}$) was insufficient alone to generate foam of measurable HRV under comparable buffer conditions. The effects upon foam stability of increasing salt dosage in heterogeneous solutions of 2 mg $cm^{-3}$ BSA and 1 mg $cm^{-3}$ lysozyme are described in Figure

**Figure 3.1: HRV Response with Increasing BSA Concentration at Various pH Conditions**

Dependence of foam stability (HRV) upon BSA feedstock concentration at pH 3.8, 4.8 and 6.0, ie at, above and below the isoelectric point of BSA (pI 4.8). Protein solutions were prepared in 50 mM citrate buffer in the presence of 4 % ethanol.

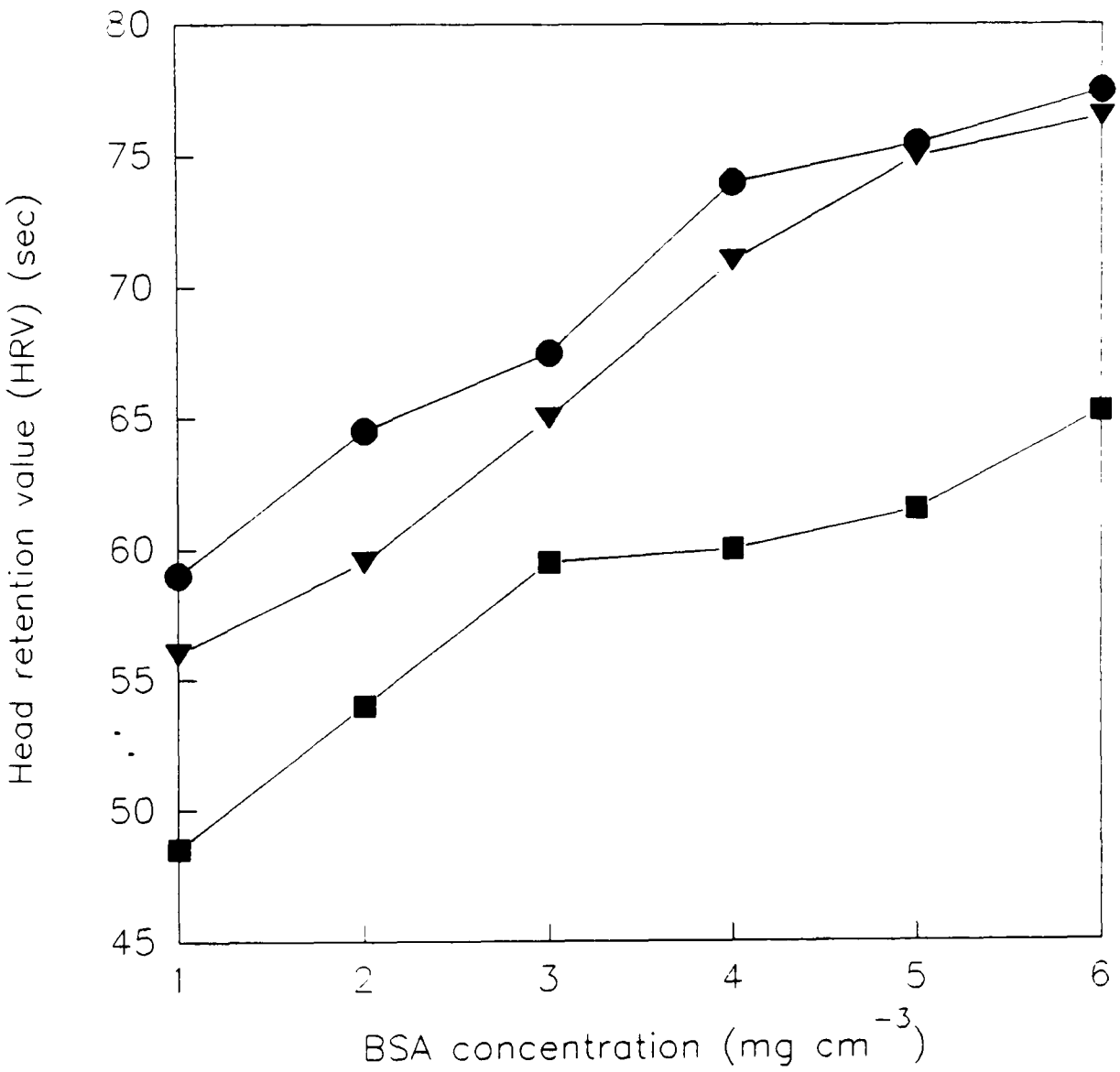

**Figure 3.2: HRV Enhancement in BSA-Lysozyme Solutions at pH 6.0**

Synergistic effects upon foam stability (HRV) of BSA solutions in the presence of 1 mg $cm^{-3}$ lysozyme at pH 6.0. BSA solutions of varied concentration (1 to 6 mg $cm^{-3}$) were prepared in 50 mM citrate buffer in the presence of 4 % ethanol.

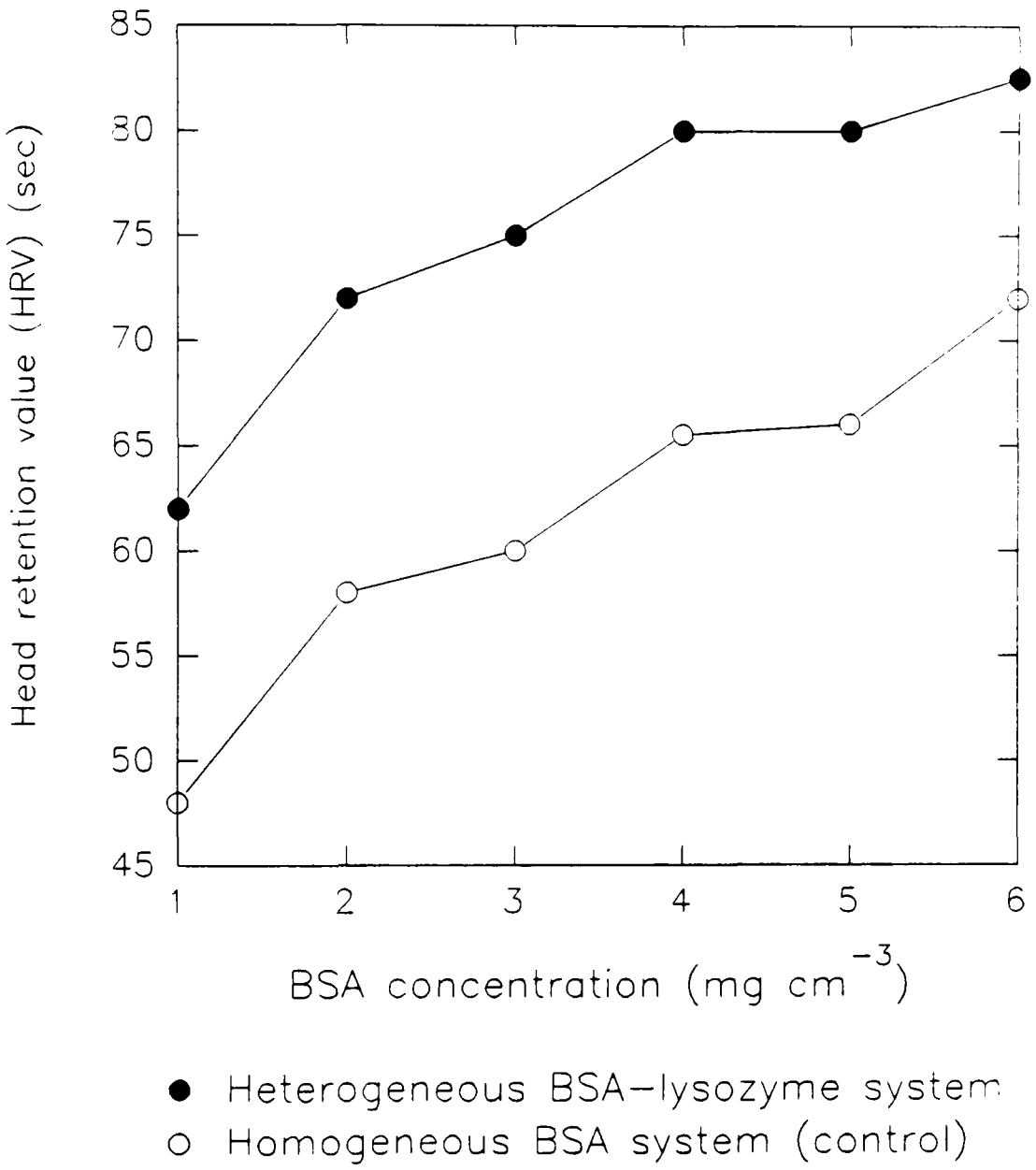

**Figure 3.3: HRV Enhancement in BSA-Cytochrome-*c* Solutions at pH 6.0**

Description of the effects upon foam stability (HRV) of the addition of 0.1 mg $cm^{-3}$ cytochrome-*c* in solutions of varied BSA concentration (1 to 6 mg $cm^{-3}$) at pH 6.0. Protein solutions were prepared in 50 mM citrate buffer in the presence of 4 % ethanol.

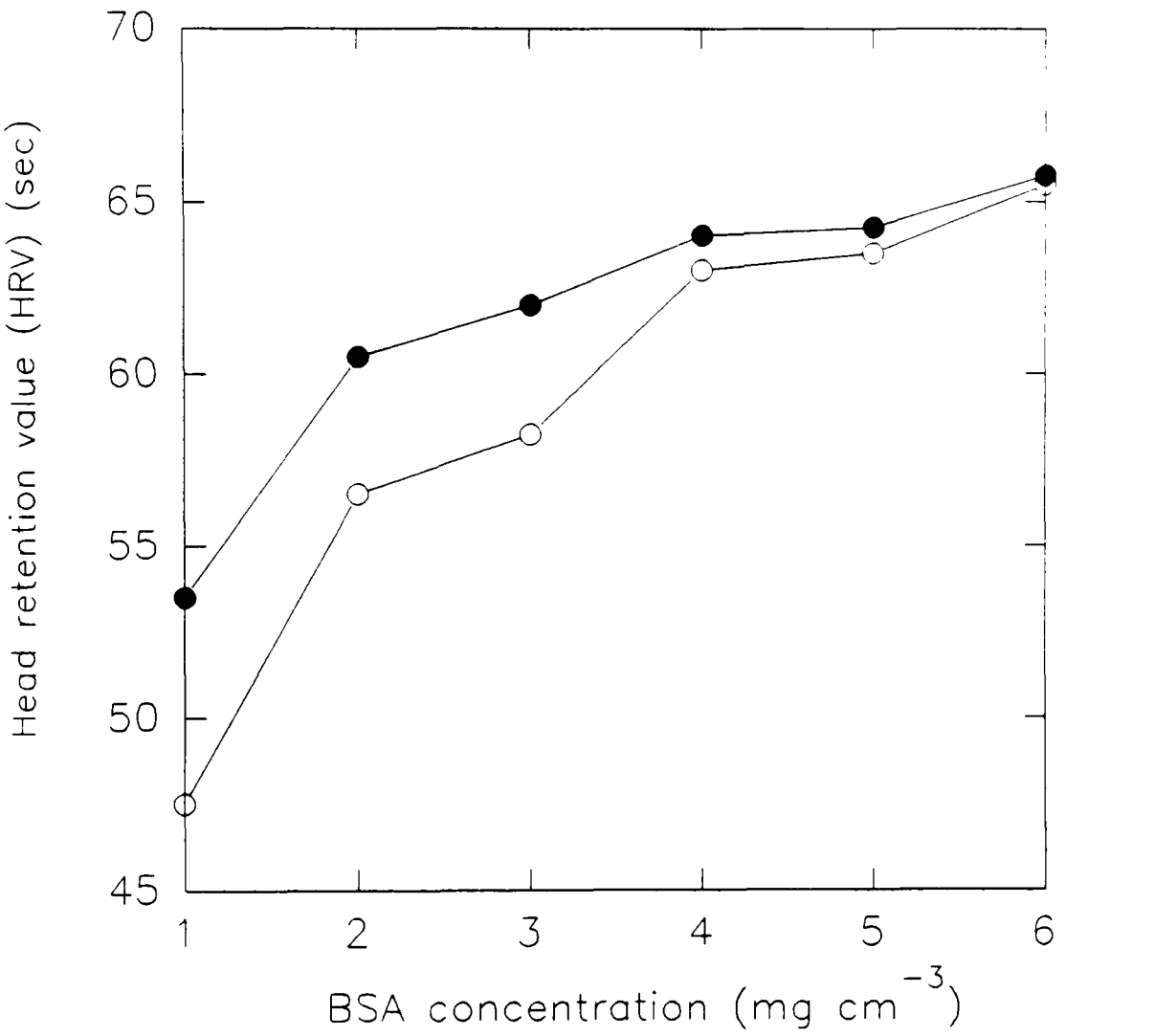

**Figure 3.4: Effects of NaCl upon HRV in BSA-Lysozyme Solutions at pH 6.0**

Variations in HRV with the addition of increasing amounts of NaCl in heterogeneous (2 mg $cm^{-3}$ BSA mixed with 1 mg $cm^{-3}$ lysozyme) and homogeneous (2 mg $cm^{-3}$ BSA ) at pH 6.0. Protein solutions were prepared in 50 mM citrate buffer in the presence of 4 % ethanol.

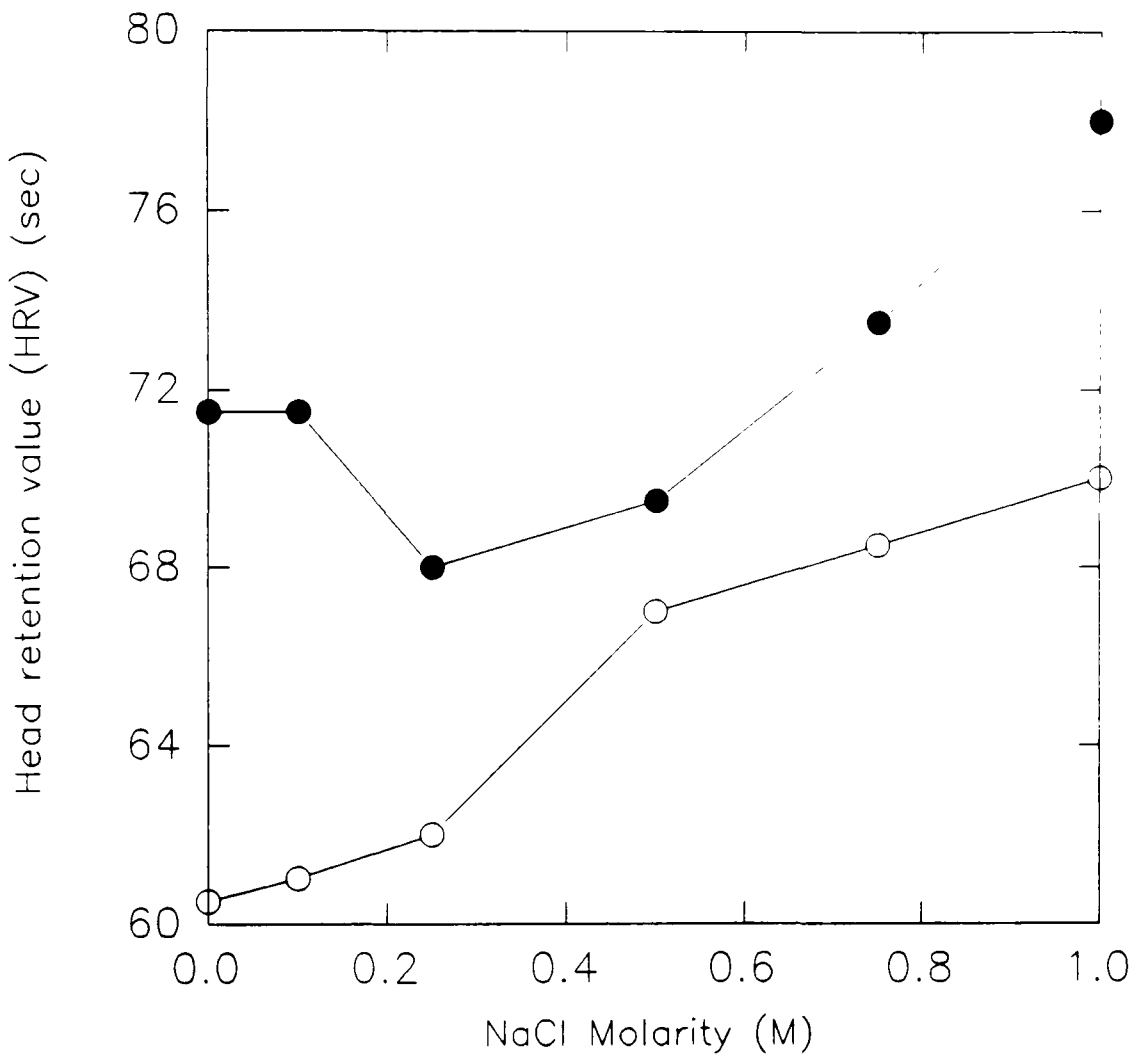


● Heterogeneous system of 2 mg $cm^{-3}$ BSA and 1 mg $cm^{-3}$ lysozyme

○ Homogeneous 2 mg $cm^{-3}$ BSA system (control)

3.4. In the presence of salt the synergistic enhancement of foam stability of a 2 mg $cm^{-3}$ BSA solution by 1 mg $cm^{-3}$ lysozyme was reduced as the salt concentration approached 0.5 M. Further increase in salt concentration up to 1 M enhanced HRV to a magnitude previously seen with 4 mg $cm^{-3}$ BSA mixed with 1 mg $cm^{-3}$ lysozyme mixtures (see Figure 3.2). In homogeneous BSA solutions of a fixed concentration of 2 mg $cm^{-3}$ (see lower plot in Figure 3.4) foam stability was moderately enhanced at higher salt concentrations. Subsequent experiments, undertaken in the pH range 3.6-6.4 with heterogeneous solutions of 2 mg $cm^{-3}$ BSA mixed with 1 mg $cm^{-3}$ lysozyme, revealed that the presence of lysozyme in BSA solutions had an insignificant effect upon HRV at pH 4.8 but favoured formation of more stable foams above and below that point (Figure 3.5). Two additional experiments were performed at pH 4.8 and 3.8, where a fixed amount of lysozyme (1 mg $cm^{-3}$) was added to BSA solutions of various concentrations (1 to 6 mg $cm^{-3}$) and results are illustrated in Figures 3.6 and 3.7 respectively. At pH 4.8 (Figure 3.6) negligible improvement in foam stability was observed throughout the range of BSA concentrations applied. In contrast, at pH 3.8 (Figure 3.7) the presence of lysozyme resulted in distinct enhancement of foam stability at BSA concentrations up to 4 mg $cm^{-3}$, where the BSA:lysozyme molar ratio was below unity. Such effects were eliminated at and above BSA:lysozyme equimolar conditions, namely for BSA concentrations of 5 and 6 mg $cm^{-3}$ where the molar ratios became 1.07 and 1.28 respectively.

Foam stability and foaming power of protein systems expressed as conductivity half-life (CHL) and foaming power (FP) under various operating conditions are described in Figures 3.9-3.11 and Table 3.1. A typical profile of the recorded conductivity during foam generation and decline is presented in Figure 3.8, and is based on an experimental trace of foam conductivity. Region "A" represents the period of foam generation

**Figure 3.5: Effects of pH upon HRV of BSA-Lysozyme Solutions**

Variations in HRV of heterogeneous solutions (2 mg $cm^{-3}$BSA mixed with 1 mg $cm^{-3}$ lysozyme) and homogeneous (2 mg $cm^{-3}$ BSA) with pH. Protein solutions were prepared in 50 mM citrate buffer in the presence of 4 % ethanol. The observed effects reflect variations in the nature of protein-protein interactions at different pH values.

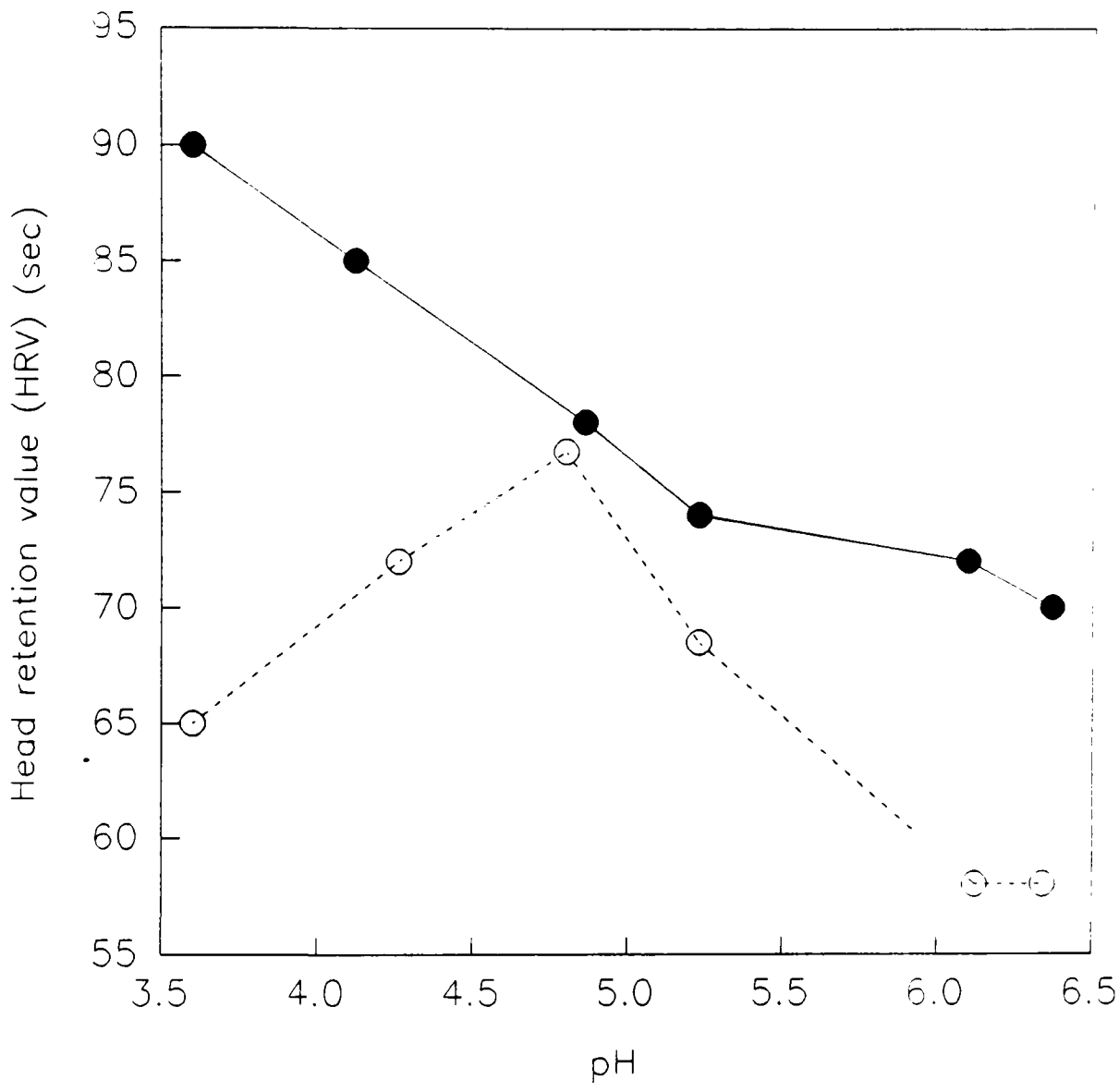

**Figure 3.6: HRV Response to the Presence of Lysozyme in BSA Solutions at pH 4.8**

HRV response to the addition of 1 mg $cm^{-3}$ lysozyme in BSA solutions of various concentrations (1 to 6 mg $cm^{-3}$) at the isoelectric point of BSA (pH 4.8). Protein solutions were prepared in 50 mM citrate buffer in the presence of 4 % ethanol.

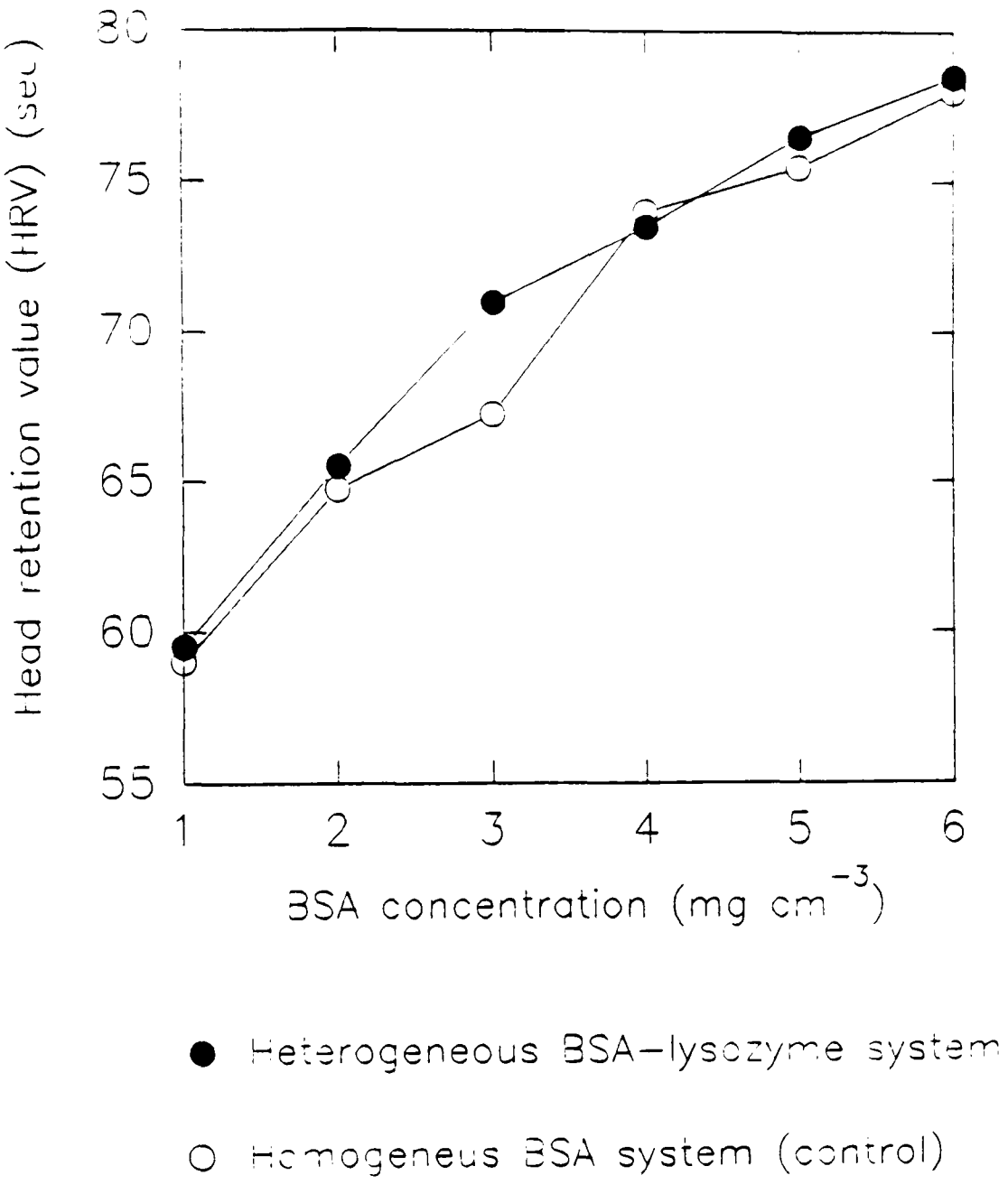

**Figure 3.7: HRV Response to the Presence of Lysozyme in BSA Solutions at pH 3.8**

HRV response to the addition of 1 mg $cm^{-3}$ lysozyme in BSA solutions of varied concentrations (1 to 6 mg $cm^{-3}$) at pH 3.8. Protein solutions were prepared in 50 mM citrate buffer in the presence of 4 % ethanol.

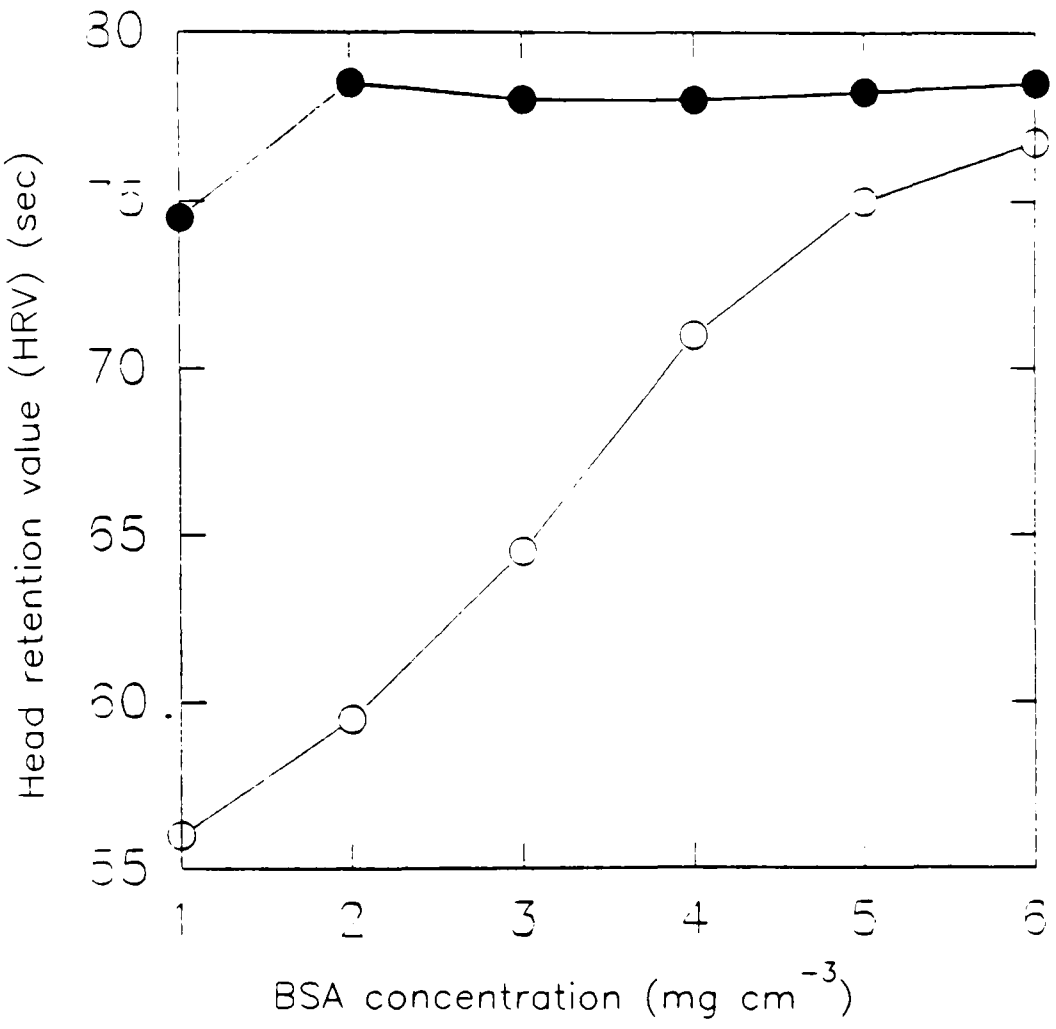

**Figure 3.8: Conductivity Profile of Foam during Generation and Decay**

Typical conductivity profile of foam during generation and decay, conducted as outlined in Chapter 2 (2.2.2).

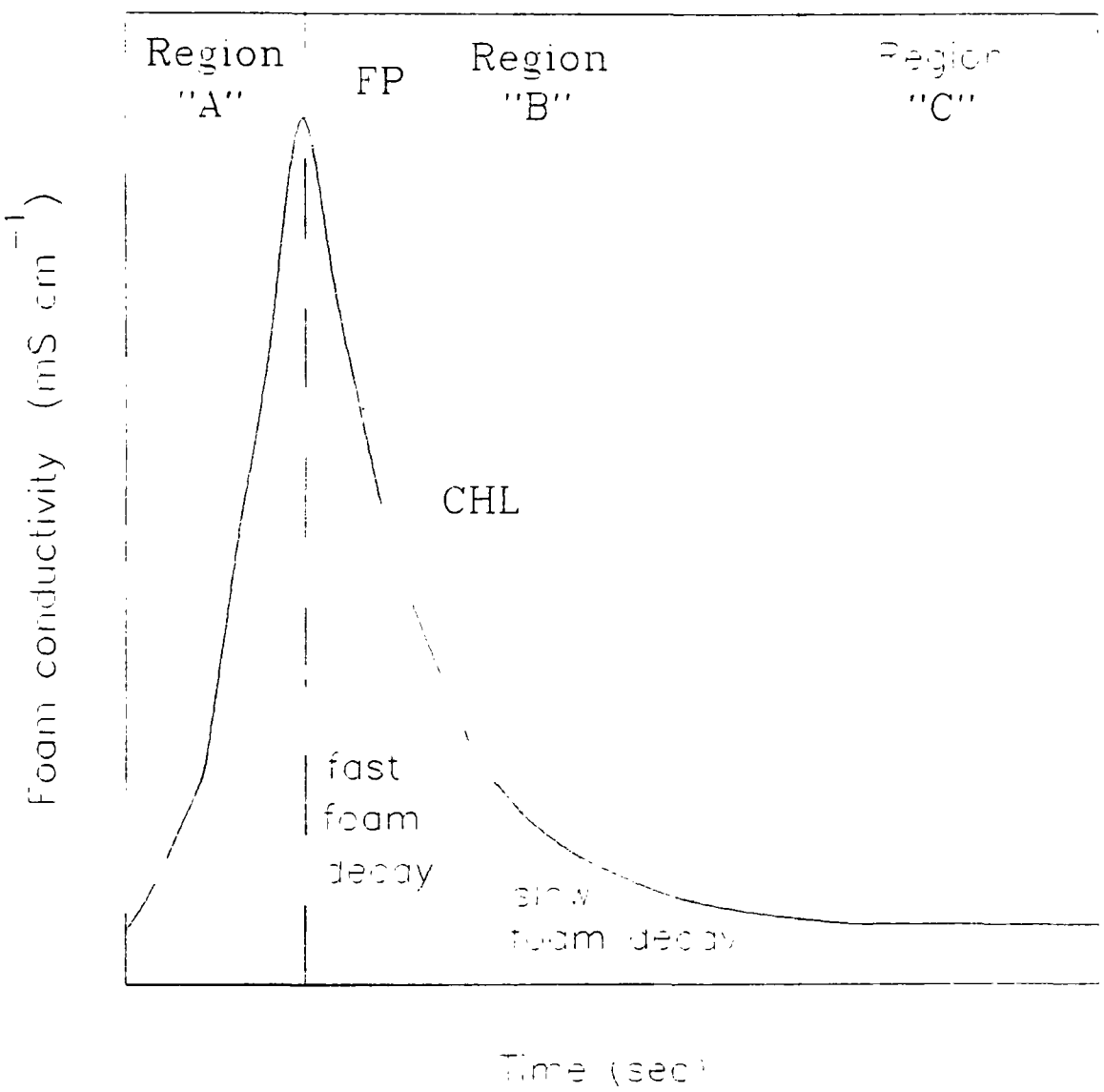


FP = Foaming power

CHL = Conductivity half-life of foam

(defined by experimental procedure), region "B" is the trace of "double-logarithmic" decline of conductivity, which describes the liquid drainage from the foam, and region "C" reflects the termination of foam decay due to liquid drainage and bubble collapse.

Foams produced from homogeneous BSA solutions of increasing concentration at pH 6.0 were more stable (higher CHL), and incorporated more liquid into the foam (higher FP)) as Figure 3.9 shows. Addition of a fixed amount of lysozyme (1 mg $cm^{-3}$) in BSA solutions of 0.5 and 2 mg $cm^{-3}$ at pH 6.0 increased both conductivity half-life and foaming power (see Table 3.1). The effects of pH upon stability of foams generated by BSA solutions (0.5 and 2 mg $cm^{-3}$) in the absence and presence of 1 mg $cm^{-3}$ lysozyme are described in Figure 3.10(a-b). It can be seen that homogeneous solutions exhibited relatively poor foam stability at pH 6.0, which improved at and below the isoelectric point of BSA. A maximum in foam stability was observed at pH 4.8 for the most concentrated BSA solution (Figure 3.10b). However, instead of a peak at pH 4.8, a gradual decline in CHL with pH was observed for foams formed by 0.5 mg $cm^{-3}$ BSA solutions (see Figure 3.10b). In heterogeneous solutions, the presence of lysozyme greatly favoured foam stability at pH 6.0, whereas such effects were reduced or negligible at pH 4.8 and limited at pH 3.8 at both 0.5 and 2 mg $cm^{-3}$ BSA. Figure 3.11 illustrates the effects of increasing buffer molarity/ionic strength (0 to 100 mM citrate buffer) upon foam stability of a heterogeneous system comprising 2 mg $cm^{-3}$ BSA mixed with 1 mg $cm^{-3}$ lysozyme at pH 6.0. Foam stability declined with increasing buffer molarity and remained practically constant in the region of 25-100 mM citrate buffer.

Trends in foam stability at various operating conditions, determined by the Rudin method and conductivity measurements of foam, showed good agreement and the conclusive evidence can be summarised as follows. It is

**Table 3.1: Conductivity Measurements of Foams in BSA Solutions in the Presence and Absence of Lysozyme**

Variations in conductivity half-life (CHL) and foaming power (FP) of foams generated by 0.5 and 2 mg $cm^{-3}$ BSA solutions in the absence (homogeneous) and presence (heterogeneous) of 1 mg $cm^{-3}$ lysozyme at pH 6.0. Protein solutions were prepared in 50 mM citrate buffer in the presence of 4 % ethanol. CHL and FP are average values of three individual determinations.

| BSA Feedstock Concentration (mg $cm^{-3}$) | Conductivity Half-Life (CHL) (sec) | | Foaming Power (FP) ($mS\ cm^{-1}$) | |
|---|---|---|---|---|
| | Homogeneous | Heterogeneous | Homogeneous | Heterogeneous |
| 0.5 | 16.0 | 26.0 | 2.10 | 2.60 |
| 2.0 | 26.5 | 39.0 | 5.05 | 6.15 |

**Figure 3.9: Conductivity Measurements of BSA foams at pH 6.0**

Variations in conductivity half-life (CHL) and foaming power (FP) of foams formed by BSA solutions of increasing concentration (0.5 to 3 mg $cm^{-3}$) in 50 mM citrate buffer in the presence of 4 % ethanol; pH 6.0.

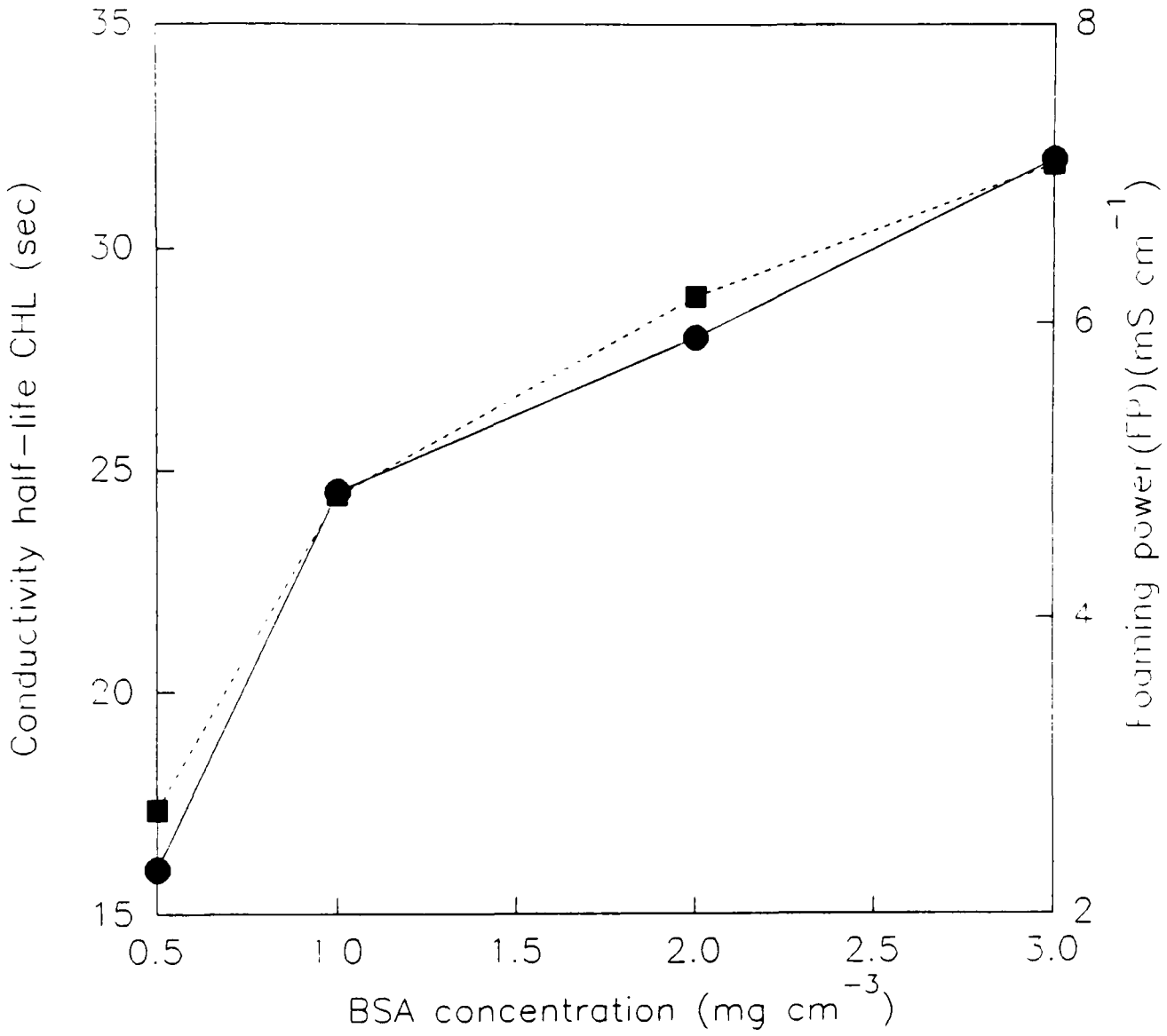

**Figure 3.10: Effects of pH upon Conductivity Half-Life of Foams from Homogeneous and Heterogeneous Solutions**

Variations in conductivity half-life of foams formed by homogeneous (0) and heterogeneous (1) solutions at pH 3.8, 4.8 and 6.0; Proteins solutions comprised **(a)** 0.5 mg $cm^{-3}$ BSA and **(b)** 2 mg $cm^{-3}$ BSA while the concentration of lysozyme in heterogeneous solutions was fixed to 1 mg $cm^{-3}$. Protein solutions were prepared in 50 mM citrate buffer in the presence of 4 % ethanol.

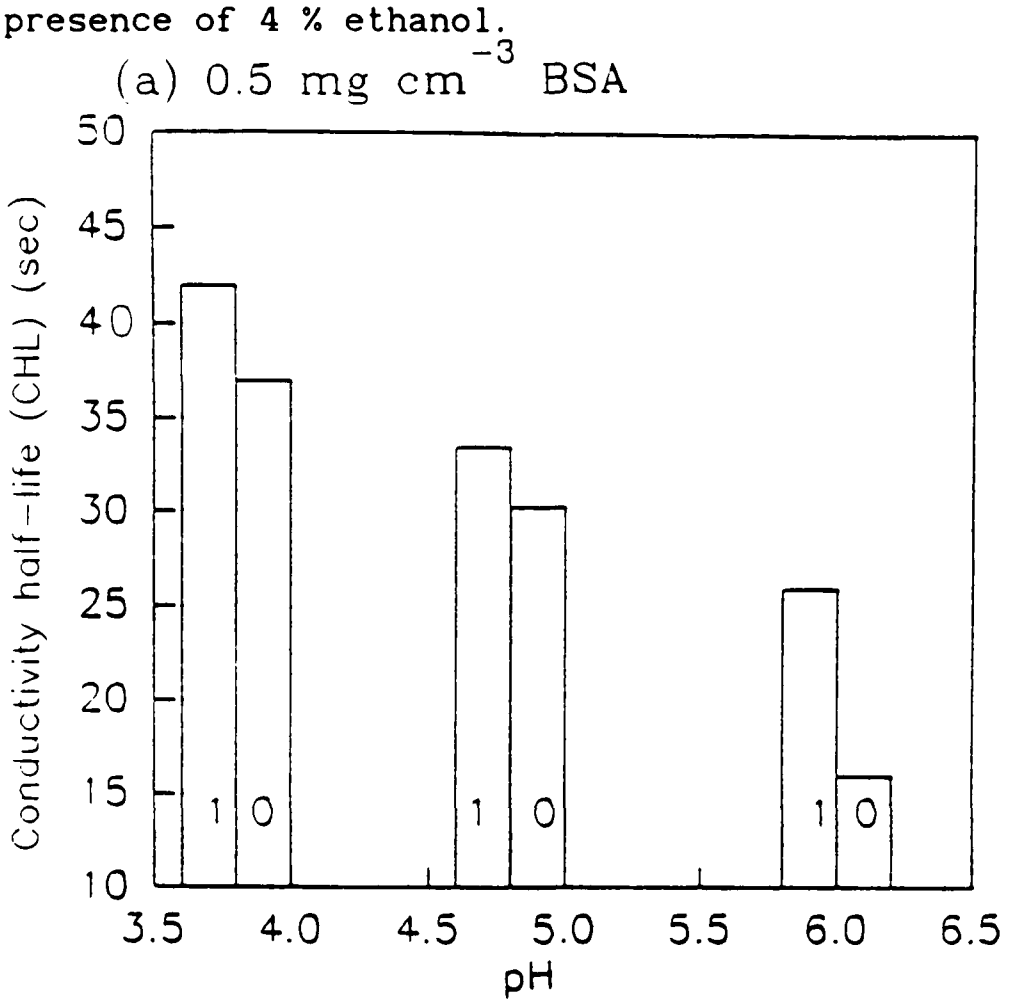


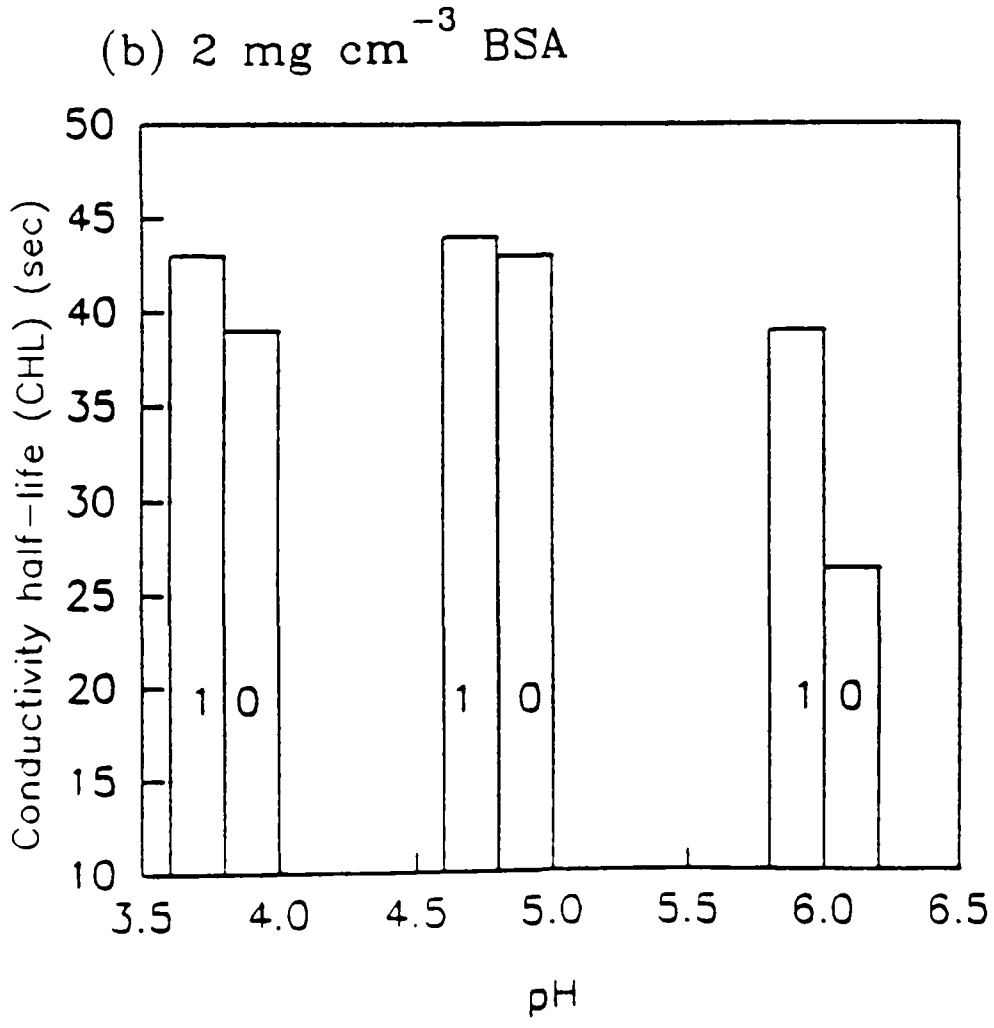


0–Homogeneous BSA solutions

1–Heterogeneous BSA–lysozyme solutions

**Figure 3.11: Effects of Ionic Strength upon Conductivity Half-Life of Foams (CHL) in Heterogeneous Solutions**

Decline in conductivity half-life (CHL) of foams with increasing citrate buffer molarity (0-100 mM) in heterogeneous solutions at pH 6.0. Protein solutions comprised 2 mg $cm^{-3}$ BSA and 1 mg $cm^{-3}$ lysozyme. Foaming solutions contained 4 % ethanol.

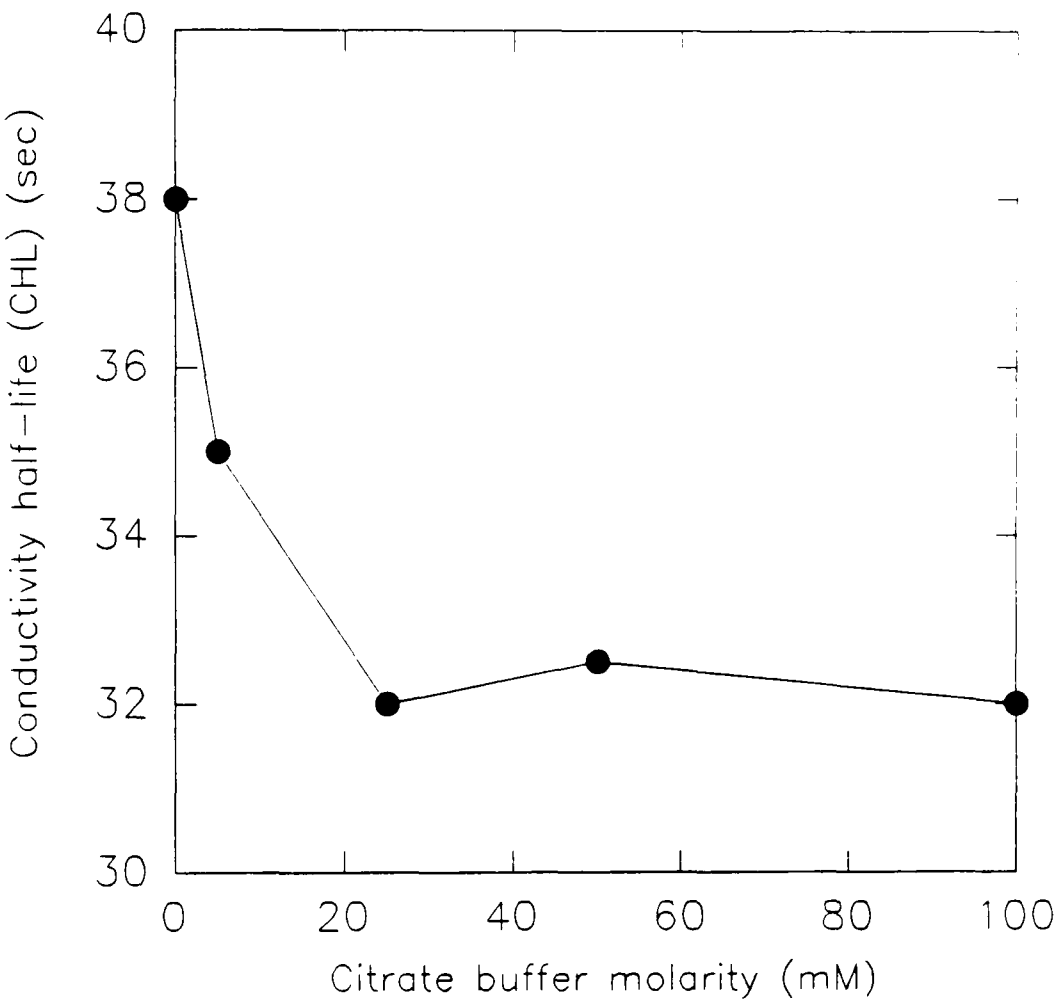

evident that in homogeneous BSA solutions, foam stability and foaming power increase with higher feedstock concentration. At comparable BSA concentrations it appears that foam stability is maximum at the isoelectric point of BSA. In heterogeneous solutions where proteins carry opposite charges, foam stability is profoundly enhanced and there is evidence that such behaviour is dependent upon the composition of the foaming solution. Suppression of such positive behaviour can be achieved by salt addition to a certain concentration before reverse effects appear, or by increase in buffer molarity. The presence of lysozyme in BSA solutions at pH 4.8 has negligible effects upon foam stability, while at pH < 4.8 it appears that there is an improvement in foam stability, the magnitude of which increases with increasing distance from the pI of BSA. Such behaviour appears to be controlled by solution composition and is eliminated at and above BSA: lysozyme equimolar ratio.

Determination of foam stability by HRV and CHL measurements is based on the rate of liquid drainage from foam after cessation of gas supply and cannot distinguish foam drainage from collapse. Various workers (Jacobi (1956); Wace et al. (1969)) demonstrated that foam drainage is governed by exponential decay and that drainage rate is directly proportional to wetness. Conductivity traces of draining foam (see Figure 3.8) appear to follow a pattern of logarithmic decline. However, semi-logarithmic plots of foam conductivity in region "B" against time failed to yield a straight line. Division of region "B" into two zones comprising an initial fast logarithmic decline and a sluggish phase, which appears to prolong foam life, was validated by respective semi-logarithmic plots of conductivity against time. These yielded individual straight lines. It is therefore clear that the decline of foam conductivity can be described by a double-exponential equation, the coefficients of which could be calculated by statistical analysis based on the recorded data. This approximates to

similar findings of Clark et al. (1987) and expands upon evidence reported in Leeson (1989). Mathematical determination of the double-exponential equation for each sample studied was felt to exceed the scope of the present work.

Comparison between foaming power (FP) values taken from conductivity traces such as that of Figure 3.8 can only be reliable for protein solutions prepared in equivalent aqueous environments. Otherwise they are likely to reflect differences in both FP and buffer ionic strength. The latter may be overcome by conductivity measurements of the original solution under identical conditions (temperature, concentration and electrode surface submerged), and subsequent calculation of the reduced foam conductivity $H_r$ (see Equation 1.6 in Chapter 1).

The observed increase in foam stability at higher BSA concentrations in homogeneous solutions at constant pH (Figures 3.1 and 3.9) is attributed to more effective bubble stabilisation due to the greater number of adsorbed molecules at the gas-liquid interface. Under such conditions, the ability to incorporate gas bubbles in the liquid is enhanced as the trends in foaming power indicate (Figure 3.9). At low protein concentration, monolayer formation occurs by irreversible adsorption, and provides saturated surface coverage and a film thickness of about 50-60 Å. At low surface coverage, adsorption is diffusion controlled (Graham and Phillips (1979a)). In more concentrated bulk phases, protein adsorption can continue via multilayer formation of reversibly adsorbed molecules which yield film thicknesses greater than 100 Å and create a more stable foam (Graham and Phillips (1979b)). Effective foam stability is synonymous with reduced drainage and slower foam decay, and therefore a higher foam density.

The achievement of maximal foam stability at the isoelectric point of BSA (Figures 3.5 and 3.10b) is associated with its solubility and

charge. At the isoelectric point, a protein carries zero net charge and therefore is characterised by minimal repulsive forces and solubility. As a result, attractive forces between the molecules, mainly short-range hydrogen, Van der Vaals and hydrophobic interactions, are maximal (Halling (1981); Kim and Kinsella (1985)). The predominant regime of such forces, as opposed to electrostatic repulsion and steric stabilisation, fortifies the strength of the bubble film by increasing its shear rheological properties to a maximum (Graham and Phillips (1976)). Kim and Kinsella (1985) showed that yield stress, elasticity and foam stability are maximal at the isoelectric point. For a given concentration of protein at equilibrium, surface tension is also minimised at the isoelectric point (Ostermaier and Dobias (1984)). At pH values distant from the isoelectric point the occurrence of negative charges inhibits molecular association and thus impairs foam formation and stabilisation. This behaviour is in agreement with reports by Poole et al. (1984) where foam stability of BSA solutions was maximum at its isoelectric point.

At strongly acidic pH conditions, namely pH < 4.0, experimental difficulties continually arose. Protein solutions were characterised by hazy appearances due to reduced protein solubility, and an indistinct liquid-foam interface at the onset of foam collapse during HRV determinations. During conductivity measurements of foam at pH 3.8, blocks of very dry foam tended to adhere to the conductivity probe, thus interfering with the recorded foam drainage profile. Under such conditions, BSA molecules are subjected to a partial denaturation which was considered responsible for the above observations. Adherent behaviour was particularly obvious at bulk concentrations higher that 3 mg $cm^{-3}$. Head retention measurements were performed in quadruplicate, where necessary, to meet the prerequisite two second difference between two valid readings. As a result, the decrease in foam stability observed at pH

values below 4.8 might also be partially associated with the fact that a proportion of the protein was insolubilised. Comparisons between FP values obtained at various pH conditions is not fruitful since the starting conductivities of the foaming solutions vary with pH.

In heterogeneous solutions of BSA and lysozyme at pH 6.0 (Figure 3.2 and Table 3.1) the observed enhancement in foam stability (with respect to the control) must be attributed to electrostatic interactions between the oppositely charged proteins (Poole et al. (1984)). Increase in the foaming power of heterogeneous solutions (Table 3.1) must be associated with the fact that lysozyme addition overcomes the charge barrier which retards the adsorption of BSA at the gas-liquid interface.

Interacting molecules form complexes at the gas-liquid interface and promote synergistic enhancement of foam stability. Lysozyme was added at concentrations (1 mg $cm^{-3}$) which in homogeneous solutions failed to generate foam able to register in HRV analyses. Lysozyme exhibited very poor foaming behaviour in homogeneous solutions and gave measurable HRV only at concentrations greater than 5 mg $cm^{-3}$ (Velissariou (1988)). This characteristic behaviour may be attributed to molecular rigidity associated with disulphide inter-chain linkages in the protein conformation (Townsend and Nakai (1983); Kim and Kinsella (1987)). Synergy due to electrostatic interactions between BSA and lysozyme was also observed (Velissariou (1988)) when a series of BSA and lysozyme mixtures of decreasing respective concentrations were foamed. The mixture yielded high foam stability, even at protein concentrations which failed to produce measurable foam (HRV) in homogeneous solutions.

It has been suggested (Poole et al. (1984); Clark et al. (1989)) that during foaming, BSA and lysozyme molecules migrate to the gas-liquid interface as individual molecules and/or small aggregates whereupon BSA molecules partially unfold. In contrast, lysozyme molecules mostly retain

their native structure (Graham and Phillips (1979c)). Driven by predominantly electrostatic forces, the oppositely charged protein molecules rearrange themselves in a network of BSA cross-linked to lysozyme. Such formation fortifies film strength, thus enhancing foam stability. Yagisawa (1975) studied such protein interactions and stated that complex formation under such circumstances is an equilibrium process. Studies conducted by Poole et al. (1984) indicated the importance of mixture composition upon molecular interactions and foam stability, and concluded that best foaming properties were obtained when the BSA: lysozyme molar ratio was unity. Such composition effects were not observed in the conditions applied to obtain the results presented in Figure 3.2 and Table 3.1, but their importance is highlighted by results presented in Figures 3.3 and 3.6, and Chapter 4.

The use of cytochrome-*c* as an alternative basic protein (Figure 3.3), characterised by similar molecular mass and isoelectric point to that of lysozyme, clearly indicated the significance of stoichiometry of molecular interactions in foam stability. Observation of synergy could therefore only be observed within a critical range of BSA concentrations for a given cytochrome-*c* concentration (BSA: cytochrome-*c* molar ratio $\leq$ 7.5). However, studies by Velissariou (1988) on cytochrome-*c* and BSA revealed that although stoichiometric ratios might be within the appropriate range, synergy cannot be observed unless the concentration of individual proteins fulfills certain conditions. Unlike lysozyme, cytochrome-*c* was readily soluble and acted as a very good foaming agent in homogeneous solutions (1 to 3 mg $cm^{-3}$). Addition of 1 mg $cm^{-3}$ cytochrome-*c* in BSA solutions (1 to 3 mg $cm^{-3}$) at pH 6.0 (50 mM citrate buffer) resulted in a slight linear increase in foam stability from the HRV of a 1 mg $cm^{-3}$ cytochrome-*c* but no synergy was observed.

It has been shown that electrostatic interactions between basic and

acidic proteins, beneficial to foam stability, do not exclusively apply to BSA and lysozyme. They can include a variety of proteins such as cytochrome-c. Indeed, clupeine was found more effective than lysozyme (Poole et al. (1984)). It is however essential that individual pairs of acidic-basic systems should be fully characterised with respect to their influence upon foam stability.

Addition of salt in homogeneous BSA and heterogeneous BSA-lysozyme solutions (Figure 3.4) suppressed electrostatic interactions between BSA and lysozyme. Such interference appears to exhibit a negative effect upon foam stability up to certain concentration of salt (0.5 M). The observed increase in foam stability at higher salt concentrations to a magnitude previously seen with 4 mg $cm^{-3}$ BSA mixed 1 mg $cm^{-3}$ lysozyme (see Figure 3.2) may be attributed to promotion of hydrophobic forces between molecules. It is also important to mention that foam stability of the heterogeneous solutions remained higher than that of the control throughout the salt concentration applied. This implies that the presence of NaCl did not compromise complex formation as has has been stated in other reports (Poole et al. (1984)). However, increase in ionic interference by increasing buffer molarity had a negative effect upon foam stability expressed as conductivity half-life (see Figure 3.11). Such conflicting evidence draws attention to likely effects associated with the combination of 50 mM citrate buffer (pH 6.0) and NaCl, which cannot be identified with the current evidence. Confirmation of such presumption would include repetition of the experiment of Figure 3.4 with all protein solutions prepared in distilled water and appropriately adjusted in pH. The importance of salt type and the extent of its effects upon foam quality of proteins has been discussed by Bumbullis et al. (1981). In the presence of salts, the ability of a protein solution to generate foam is enhanced but foam stability is decreased.

Enhancement in foam stability of homogeneous BSA solutions with increasing salt concentration (see control in Figure 3.4) must be implicated in part with the promotion of intermolecular association between non-polar residues on the surface of the protein (Nakai (1983)). Such phenomena strengthen the interfacial film as a result of increased rheological properties. These data are in agreement with similar studies by Velissariou (1988), where a 2 mg $cm^{-3}$ BSA solution in citrate buffer (pH 4.8) containing 2 % v $v^{-1}$ ethanol exhibited improved foam stability at higher buffer molarity. Further studies on the role of salt in BSA-lysozyme electrostatic interactions and foam quality are presented in Chapter 5.

The benefits from the presence of lysozyme in BSA foaming solutions are clearly eliminated (Figures 3.5 and 3.10) at the isoelectric point of BSA where electrostatic interactions between BSA and lysozyme are absent. This behaviour is certainly consistent throughout a wide range of BSA concentrations as Figure 3.6 indicates. Enhancement in foam stability at pH > 4.8 via electrostatic attractions between BSA and lysozyme has already been discussed. However, the distinct enhancement in foam stability observed at pH < 4.8 (Figure 3.5) in the presence of lysozyme, implies the existence of positive effects associated with other types of interactions between the two proteins of hydrophobic nature. At pH < 4.8 both proteins carry positive charges and are partially unfolded. It is therefore expected that molecular associations between like and unlike proteins may take place, which appear to impose stabilising effects upon foam. It is noteworthy that foam stability enhancement is gradually increased at pH values distant from the isoelectric point of BSA. Further experimentation (see Figure 3.7), which strongly confirmed such observations, also indicated that the positive influence of the addition of lysozyme is eliminated at and above equimolar conditions (ie

BSA: lysozyme molar ratio ≥ 1). This emphasises the importance of the protein content of the foaming solution with respect to the stoichiometry of the interactions taking place. Other reports (Poole et al. (1984)) concluded that the presence of lysozyme at pH values below the isoelectric point of BSA provides negligible improvement in foam stability. However, these data were obtained with mixtures of equimolar BSA-lysozyme solutions, and therefore cannot account for positive phenomena at BSA: lysozyme molar ratios < 1.

In conclusion, foam stability of a heterogeneous protein solution appears to be enhanced when pH conditions favour electrostatic interactions between acidic and basic proteins. However, suppression of electrostatic attractions and/or expression of interactions of hydrophobic nature in conjunction with the appropriate solution composition can additionally improve foam stability.

### 3.3.2 Quantitative Analysis of Foam from Homogeneous and Heterogeneous Feedstocks Generated During Foam Assessment by Conductivity Methods

Analysis of foams, produced during foam stability assessments by conductivity measurements, was a preliminary vehicle to investigate the relationship between foam stability and quantitative characteristics of foam, such as protein enrichment (e), protein recovery (R) and fractionation $Fr_{i,j}$, where applicable. Protein enrichment e, can be defined as the ratio of protein concentration in the foam relative to the initial concentration in the feedstock as described by Equation 3.1:

$$e_i = c_{iF}/c_{iO} \qquad \text{(Equation 3.1)}$$

where : $e_i$ is the enrichment of protein i

$c_{iF}$ is the concentration of protein i in the foam

$c_{i0}$ is the concentration of protein i in the feedstock

In the case of a heterogeneous solution of n components total protein enrichment can be described by Equation 3.2:

$$e = (\sum_{i=1}^{n} c_{iF})/(\sum_{i=1}^{n} c_{i0}) \qquad \text{(Equation 3.2)}$$

Protein recovery ($R_i$) expresses the mass of a protein collected in the foam as a percentage of its initial mass in the feedstock, and can be described by Equation 3.3:

$$R_i = (c_{iF}V_F)/(c_{i0}V_0) = e(V_F/V_0) \qquad \text{(Equation 3.3)}$$

where : $R_i$ is the recovery of protein i

$c_{iF}$, $c_{i0}$ and $e_i$ as in equation 3.1

$V_F$ and $V_0$ are the volumes of foam and feedstock respectively.

In the case of a heterogeneous solution of n, components then recovery (R) can be defined by Equation 3.4:

$$R = \sum_{i=1}^{n} R_i = e(V_F/V_0) \qquad \text{(Equation 3.4)}$$

Replacement of $c_{i0}$ in Equation 3.1 by $c_{iB}$, ie the concentration of protein i in the residual liquid phase (liquid pool), gives the separation ratio $s_i$, which quantifies the difference in protein concentration between the top (foam) and the bottom product (residual liquid). The separation ratio is described by Equation 3.5:

$$s_i = c_{iF}/c_{iB} \qquad \text{(Equation 3.5)}$$

From material balances (see Equation 2.2, Chapter 2) it can be seen that $c_{iB}$ depends upon both protein concentration in the foam and foam volume, ie protein recovery, and therefore $s_i$ is dependent upon the amount of

protein removed into the foam.

Fractionation is applicable to heterogeneous solutions and can be expressed as a fractionation index ($Fr_{i,j}$) given by Equation 3.6 for components i and j. Any departure from unity will indicate unequal partition of i and j from the bulk to the foam phase. In the case of BSA and lysozyme, low $Fr_{BSA,lysozyme}$ values indicate effective partition of lysozyme into the foam due most probably to effective electrostatic binding with BSA.

$$Fr_{i,j} = (c_{iF}c_{jF}^{-1})/(c_{iO}c_{jO}^{-1}) = e_i e_j^{-1} \qquad \text{(Equation 3.6)}$$

The effects upon enrichment and recovery of increasing BSA feedstock concentration in homogeneous solutions at a constant pH 6.0 are given in Table 3.2. It can be seen that there was a gradual decline in BSA enrichment and simultaneous increase in the volume of collected foam at higher protein concentration in the initial solution. The resultant protein recovery was therefore favoured under such conditions. It should be mentioned that for 0.5 mg $cm^{-3}$ BSA concentration it was not possible to collect the foam due to its rapid and complete decay. At defined concentrations of homogeneous feedstocks, the dependence of enrichment and recovery upon system pH are illustrated in Tables 3.3(a-b) for 0.5 and 2 mg $cm^{-3}$ BSA concentration respectively. Table 3.3a shows that, unlike pH 6.0, enhancement in foam stability at pH 4.8 and 3.8 enabled foam collection and further assay. The determined enrichment and recovery figures were maximal at pH 3.8 where the most stable foam was also observed. In Table 3.3b it can be seen that enrichment figures did not vary significantly with pH, although there was a shallow minimum at the isoelectric point (pH 4.8) where maximal foam stability occurred. In both

**Table 3.2: Dependence of Quantitative Characteristics of BSA Foams upon Feedstock Concentration**

Effects of BSA feedstock concentration upon enrichment (e), foam volume ($V_F$) and recovery (R) in foams formed by BSA solutions (0.5 to 3.0 mg $cm^{-3}$) in 50 mM citrate buffer containing 4 % ethanol; pH 6.0. Results are mean values of three determinations, and standard deviations of data points are denoted by subscripts. Collection and protein analysis of foam from 0.5 mg $cm^{-3}$ BSA solution was impossible due to rapid and complete destruction of the produced foam.

| BSA Feedstock Concentration (mg $cm^{-3}$) | BSA Enrichment ($e_{BSA}$) | Foam Volume ($V_F$) ($cm^3$) | BSA Recovery ($R_{BSA}$) (%) |
|---|---|---|---|
| 1.0 | $2.98_{0.30}$ | $0.50_{0.03}$ | $2.48_{0.12}$ |
| 2.0 | $2.57_{0.20}$ | $0.56_{0.03}$ | $2.38_{0.07}$ |
| 3.0 | $2.48_{0.24}$ | $0.61_{0.08}$ | $2.48_{0.12}$ |

**Table 3.3: Effects of pH upon Quantitative Characteristics of Foams from Homogeneous BSA Solutions**

Effects of pH upon enrichment (e), foam volume ($V_F$) and recovery (R) in foams formed by **(a)** 0.5 mg $cm^{-3}$ and **(b)** 2 mg $cm^{-3}$ BSA solutions. Results are mean values of two or three determinations, and standard deviations of data points are denoted by subscripts. Collection and protein analysis of foam from 0.5 mg $cm^{-3}$ BSA solution at pH 6.0 was impossible due to rapid and complete destruction of the produced foam.

(a)

| pH† | BSA Enrichment ($e_{BSA}$) | Foam Volume ($V_F$) ($cm^3$) | BSA Recovery ($R_{BSA}$) (%) |
|---|---|---|---|
| $3.8^2$ | $4.61_{0.55}$ | $1.49_{0.11}$ | $11.35_{0.55}$ |
| $4.8^3$ | $3.28_{0.35}$ | $0.96_{0.25}$ | $5.13_{1.10}$ |

(b)

| pH† | BSA Enrichment ($e_{BSA}$) | Foam Volume ($V_F$) ($cm^3$) | BSA Recovery ($R_{BSA}$) (%) |
|---|---|---|---|
| $3.8^2$ | $2.59_{0.19}$ | $1.30_{0.22}$ | $5.61_{0.52}$ |
| $4.8^3$ | $2.41_{0.19}$ | $0.84_{0.12}$ | $3.36_{0.25}$ |
| $6.0^2$ | $2.89_{0.23}$ | $0.57_{0.08}$ | $2.65_{0.10}$ |

†-Superscripts indicate the exact number of determinations for each result.

cases the best recovery was achieved at pH 3.8 and coincided with the highest collection foam volume.

In the heterogeneous solutions studied, the lysozyme concentration was 1 mg $cm^{-3}$ and BSA concentrations were set at 0.5 and 2 mg $cm^{-3}$. The partition of BSA and lysozyme into foam at various operating pH values is presented in Table 3.4(a-b) for 0.5 and 2 mg $cm^{-3}$ BSA respectively. At the lowest BSA concentration (see Table 3.4a) the presence of lysozyme at pH 6.0 enabled the generation of readily collectable foam (foam collection was impossible in the absence of lysozyme at equivalent conditions). At pH 6.0 the enrichment of lysozyme was maximal at both BSA concentrations although the highest lysozyme recoveries were observed at the lowest pH value and coincided with maximal foam volumes. Improvement in BSA enrichment and recovery was also achieved at pH 6.0 (compare with Table 3.3) with more pronounced effects seen at the lowest BSA feedstock concentration. In contrast, it is clear that the addition of lysozyme at pH $\leq$ 4.8 did not significantly affect the enrichment and recovery of BSA when compared with values observed in the control (Table 3.3). As in homogeneous BSA solutions, a minimum in enrichment at the isoelectric point was also observed. Variations in partition patterns into foam between BSA and lysozyme are described by the fractionation index $Fr_{BSA,lysozyme}$ (Table 3.4). It can be seen that the lowest $Fr_{BSA,lysozyme}$ was obtained at pH 6.0 (this trend was more pronounced at the lowest BSA feedstock concentration) and coincided with the highest lysozyme enrichment. Under conditions of varied buffer ionic strength and constant pH 6.0 (see Table 3.5) foams generated from solutions of 2 mg $cm^{-3}$ BSA mixed with 1 mg $cm^{-3}$ lysozyme exhibited maximal protein enrichment and recovery for both components at 25 mM buffer. Such maxima coincided with the highest volume of collected foam and lowest fractionation index.

It appears that in homogeneous BSA solutions at constant pH,

**Table 3.4 : Effects of pH upon Quantitative Characteristics of Foams from BSA-Lysozyme Solutions**

Effects of pH on protein enrichment (e), foam volume ($V_F$), recovery (R) and fractionation index ($Fr_{BSA,lysozyme}$) in foams generated from **( a )** 0.5 mg $cm^{-3}$ BSA mixed with 1 mg $cm^{-3}$ lysozyme and **( b )** 2 mg $cm^{-3}$ BSA mixed with 1 mg $cm^{-3}$ lysozyme solutions. Results are the mean of three determinations and subscript values are standard deviations.

**(a)**

| pH | Enrichment | | Foam Volume | Recovery ( % ) | | $(Fr_{BSA,lysozyme})$ |
|---|---|---|---|---|---|---|
| | $e_{BSA}$ | $e_{lysozyme}$ | $(V_F)$ $(cm^3)$ | $R_{BSA}$ | $R_{lysozyme}$ | |
| 3.8 | $5.08_{0.23}$ | $1.23_{0.09}$ | $1.41_{0.12}$ | $11.93_{0.70}$ | $2.91_{0.37}$ | $4.15_{0.33}$ |
| 4.8 | $4.05_{0.10}$ | $1.05_{0.04}$ | $0.75_{0.05}$ | $4.91_{0.28}$ | $1.27_{0.10}$ | $4.48_{0.16}$ |
| 6.0 | $4.58_{0.46}$ | $2.05_{0.16}$ | $0.40_{0.03}$ | $3.04_{0.07}$ | $1.38_{0.22}$ | $2.27_{0.04}$ |

**(b)**

| pH | Enrichment | | Foam Volume | Recovery ( % ) | | $(Fr_{BSA,lysozyme})$ |
|---|---|---|---|---|---|---|
| | $e_{BSA}$ | $e_{lysozyme}$ | $(V_F)$ $(cm^3)$ | $R_{BSA}$ | $R_{lysozyme}$ | |
| 3.8 | $2.70_{0.22}$ | $1.33_{0.11}$ | $1.26_{0.11}$ | $5.19_{0.27}$ | $2.77_{0.22}$ | $1.95_{0.06}$ |
| 4.8 | $2.40_{0.10}$ | $1.23_{0.04}$ | $0.92_{0.06}$ | $3.86_{0.13}$ | $1.87_{0.13}$ | $2.05_{0.13}$ |
| 6.0 | $3.45_{0.39}$ | $1.96_{0.11}$ | $0.69_{0.13}$ | $3.86_{0.30}$ | $2.26_{0.58}$ | $1.78_{0.31}$ |

**Table 3.5 : Effects of Ionic Strength upon Quantitative Characteristics of Foams from BSA-Lysozyme Solutions**

Effects of increase in buffer molarity upon protein enrichment (e), foam volume ($V_F$), recovery (R) and fractionation index ($Fr_{BSA,lysozyme}$) in foams generated from feedstocks of 2 mg $cm^{-3}$ BSA mixed with 1 mg $cm^{-3}$ lysozyme at pH 6.0. Results are the average of three determinations and values in subscript are standard deviations.

| **Buffer Molarity (mM)** | **Enrichment** $e_{BSA}$ | $e_{lysozyme}$ | **Foam Volume** $(V_F)$ $(cm^3)$ | **Recovery (%)** $R_{BSA}$ | $R_{lysozyme}$ | $(Fr_{BSA,lysozyme})$ |
|---|---|---|---|---|---|---|
| 5 | $2.38_{.20}$ | $1.13_{.07}$ | $0.92_{.10}$ | $3.61_{.21}$ | $1.74_{.28}$ | $2.12_{.27}$ |
| 25 | $3.20_{.62}$ | $2.30_{.53}$ | $1.00_{.05}$ | $5.30_{.76}$ | $3.53_{.69}$ | $1.52_{.10}$ |
| 50 | $2.55_{.41}$ | $1.27_{.17}$ | $0.87_{.04}$ | $3.67_{.46}$ | $1.83_{.18}$ | $2.00_{.06}$ |
| 100 | $2.42_{.18}$ | $1.24_{.09}$ | $0.83_{.12}$ | $3.30_{.29}$ | $1.68_{.29}$ | $1.99_{.29}$ |

increase in bulk concentration decreases protein enrichment and yields higher quantities of collected foam. The resultant BSA recovery did not seem to be affected by the feedstock concentration in the applied range. At comparable BSA concentrations and varied pH conditions, a minimal in enrichment appears to occur at the isoelectric point but recovery is highest at pH < 4.8. In the presence of lysozyme, a significant improvement in BSA enrichment and recovery occurs at pH 6.0 when compared with the control. These effects are insignificant at pH values at and below the isoelectric point of BSA. The observed increase in BSA recovery coincides with an increase in foam volume. At pH 6.0 the highest enrichment of lysozyme also occurs and coincides with the lowest values in the respective fractionation index. Such effects are more pronounced at the most dilute BSA conditions. As Table 3.5 indicated, protein partition into foam at varied molarities of citrate buffer (pH 6.0) is favoured at an optimal ionic concentration (25 mM) which appears to promote maximum BSA and lysozyme enrichment and recovery. This is in spite of expected reduction in the attractive forces between BSA and lysozyme in the presence of ionic competition. Such behaviour minimises protein fractionation in foam.

The observed decrease in BSA enrichment with increasing feedstock concentration (Table 3.2) is associated with adsorption kinetics and foam drainage at various bulk concentrations. The observed increase in enrichment at dilute feedstocks agrees with the prediction of Gibb's equation (Equation 1.3, Chapter 1). Increase in the slope, ie $d\sigma/d\ln c$, results in greater protein surface excess $\Gamma$ and higher enrichment. At high BSA concentrations, the amphiphilic nature of BSA, resulting from the presence of both polar and non-polar groups, induces formation of stable aggregates (micelles) in the bulk phase. Thus the effective concentration of BSA molecules at the gas-liquid interface is reduced (CMC region in

$\sigma$-ln c diagram, see Figure III1b in Appendix III). Increase in BSA enrichment must also be related to more stable foam obtained from concentrated feedstocks as shown by Figures 3.1 and 3.9. Enhanced foam stability reduces drainage and coalescence and therefore a higher volume of foam can be collected under comparable operating protocols. Variations in protein recovery are therefore interrelated to opposite trends in enrichment and foam volume (see Equation 3.3). The independence of protein recovery from bulk concentration observed herein indicates that the magnitudes of change in enrichment and foam volume were compensatory.

Observed variations in enrichment with pH at comparable BSA concentrations draw attention to the fact that minimum enrichment at the isoelectric point coincides with maximum foam stability as shown in Figures 3.11b and 3.5. However, the collected foam volumes were highest at pH 3.8 resulting in highest protein recovery. Such behaviour agrees with findings elsewhere (Brown et al. (1990)) where foam was generated continuously, but disagree with some others (Schnepf and Gaden (1959; Ahmad (1975)). The latter report maximal enrichment at the isoelectric point of BSA which became more pronounced with decreasing feedstock concentrations (Schnepf and Gaden (1959)). Such behaviour is in agreement with both the fact that BSA molecules at pH 4.8 are expected to show the greatest tendency to adsorb at the gas-liquid interface, and those experimental results showing that the greatest slope of the $\sigma$-ln c curve is at the pI of BSA (Schnepf and Gaden (1959)). However, it should be emphasised that Schnepf's and Ahmad's definition of enrichment differs from that used in the present work, but coincides with what was herein defined as separation ratio (Equation 3.5). In this case, increase in foam concentration observed in Schnepf and Gaden (1959) and Ahmad (1975) is associated with both protein concentration in the foam and the volume of the collected foam. Hence any direct comparison is difficult. It is likely

that there are additional pH effects upon variables such as foam volume (directly associated with foam stability) which may mask impacts upon protein enrichment.

The high BSA recoveries observed at pH 3.8 are associated with the significantly higher foam volumes recorded under such conditions for both BSA bulk concentrations studied. At pH < 4.8 partial protein denaturation was observed in the form of foam solution turbidity, and it was also clear that foam texture at pH 3.8 approximated to that of solid foams. Such foam was highly adhesive to the walls of the glass vessel and the conductivity electrodes. It is therefore likely that the calculated foam volumes and resultant recoveries are overestimations.

In heterogeneous BSA-lysozyme solutions (Table 3.4(a-b)), the highest lysozyme enrichment ratios at pH 6.0 must be attributed to the electrostatic interactions between BSA and lysozyme which act as a driving force for the partition of lysozyme into the foam. Such interactions have been identified as the synergistic factor enhancing foam stability (see Figure 3.2 and Table 3.1). The production of more stable foam from 0.5 mg $cm^{-3}$ BSA in the presence of lysozyme enabled its collection and analysis as opposed to that produced from the control (lysozyme free). Enhancement in foam stability is also the reason for improvement in BSA recovery with respect to that in the control. Simultaneous increase in BSA enrichment, although under conditions of reduced drainage, is likely to be the consequence of partition kinetics of the complex BSA-lysozyme in more stable foams. In contrast, the lack of any significant effects upon the enrichment and recovery of BSA in the presence of lysozyme at pH ≤ 4.8 reflects the absence of great changes in foam stability at these pH conditions (see Figure 3.10). The observed minimum in lysozyme enrichment at the isoelectric point of BSA is also in line with the absence of any cooperative interactions between the two molecules. However, a slight

increase at pH 3.8 is possibly indicative of the beneficial effects of hydrophobic attractions between the two molecules (see Figure 3.7). Maximum lysozyme and BSA recoveries at pH 3.8 must be simply attributed to high foam volumes recorded in both homogeneous and heterogeneous solutions as previously discussed. The foregoing partition behaviour of the two proteins is best described by the fractionation index which clearly demonstrates that best fractionation occurs at the isoelectric point of BSA (minimal interactions). In contrast, the best lysozyme partition into foam at pH 6.0 occurs under the synergistic effects of electrostatic forces.

A practical understanding of the effects of pH upon protein enrichment and recovery, and their relation to foam stability, must employ an experimental series where pH is studied in association with protein concentration in the foaming solution, and the overall buffer ionic strength. In heterogeneous solutions, understanding of the nature of molecular interactions, and their relation to foam stability and partition should involve experimentation of mixed solutions of varied composition at pH values below and/or above the isoelectric points of both proteins. Experimental evidence should be supplemented with the appropriate $\sigma$-ln c diagrams of BSA in the presence and absence of lysozyme. Batch and/or continuous foam production in the foam tower depicted in Figure 2.3 (see Chapter 2) would enable ready foam collection and estimation of protein precipitated in foam.

The observed composition of foams from BSA-lysozyme solutions in citrate buffer (pH 6.0) of increasing molarity (see Table 3.5), is contrary to the expectation that the highest incorporation of lysozyme into the foam should occur at the lowest ionic strength, where electrostatic attractions are expected to be maximal. This finding is similar to that reported by Clark et al. (1988), where study was made of

the effects of solution conditions upon the composition of foams generated from BSA and lysozyme prepared in double-distilled water dosed with NaCl and adjusted to pH 7.0. They found that at 25 mM NaCl, incorporation of lysozyme in foam was the highest in the range of 0-50 mM NaCl concentration. They (Clark et al. (1989) proposed an explanation for such a behaviour based on the hypothesis that at low ionic strength the formation of large aggregates, not readily adsorbed at the gas-liquid interface, may be detrimental to film strength. They found that suspended thin films were destabilised in the presence of large aggregates at low ionic strength with subsequent negative effects on foam stability and lysozyme incorporation. Film destabilisation may take place by physical disruption of films and/or reduced levels of soluble protein. In contrast, in the presence of 25 mM salt, the presence and size of aggregates was reduced, due to limitations in electrostatic interactions, and film drainage was uniform with formation of the thinnest and most stable aggregate free films. At high salt concentration, it was found that aggregation of BSA molecules promoted stable films having a non-uniform thickness.

In the present study, conductivity measurements of NaCl solutions in double-distilled water and citrate buffer (temperature effects were overcome by use of the ATC conductivity probe) revealed that (see Figure II10 in Appendix II) the conductivity of 25 mM saline lay between the equivalent conductivity readings of 10-25 mM citrate buffer. Conductivity of 5 mM NaCl was lower than that of 5 mM citrate buffer. It is therefore possible that the mechanism of film destabilisation suggested by Clark et al. (1989) determines the foam composition at various buffer ionic strength studied herein. However, such trends are not implied by the negative response of foam stability to elevating buffer molarity (see Figure 3.11). It should also be mentioned that results obtained at 0 mM

citrate buffer (ie distilled water adjusted to pH 6.0 with 1 M NaOH) were not included in Table 3.5 due to the limited solubility of BSA in the foaming solutions. Under such conditions, calculated enrichment and recovery would be inflated and would not fulfill the prerequisite conditions for equivalent feedstock composition throughout the range of buffer molarity applied. The role of the solution conditions upon the extent of the BSA-lysozyme electrostatic interactions and their effects upon foaming is further studied in following Chapter 5.

## 3.4 Concluding Summary

Foam stability measurements in model systems, achieved by the Rudin method and conductivity measurements, revealed good agreement in their description of the effects of various parameters upon foam quality.

It was found that in homogeneous BSA systems, foam stability was directly related to bulk concentration at constant pH while maximal foam stability was observed at the isoelectric point for a given feedstock concentration. In heterogeneous solutions, the presence of lysozyme enhanced foam stability at pH conditions where both proteins carry opposite charges and can interact electrostatically. At the isoelectric point of BSA, there was negligible enhancement in foam stability in the presence of lysozyme, while at pH values below 4.8 it appeared that hydrophobic interactions might occur between the two proteins with beneficial effect upon foam stability. In the current study, enhancement in foam stability associated with electrostatic interactions between BSA and lysozyme did not appear to be limited by solution composition as opposed to finite improvement in stability of foams generated by solutions of comparable composition at pH 3.8. Replacement of lysozyme with cytochrome-*c* at pH 6.0 also highlighted the importance of solution composition upon various degrees of enhancement in foam stability.

Quantitative analysis of collected foams, whose stability was assessed by conductivity measurements, indicated that stable foams from homogeneous solutions are likely to be characterised by low protein enrichment and improved recovery due to reduced liquid drainage and subsequent higher foam volume. It also showed that enhancement in foam stability in the presence of lysozyme at pH 6.0 was associated with maximal lysozyme enrichment and partitioning to foam. However the above experiments did not address the importance of the protein composition of heterogeneous solutions upon foam quality. At pH conditions at and below the isoelectric point of BSA, lysozyme addition did not significantly alter the quantitative characteristics of foam. The work indicated a scope for further investigation of the role of pH upon foam stability and foam composition.

It was decided that further experimentation would study BSA-lysozyme electrostatic interactions under various conditions of feedstock composition and ionic strength in order to better understand their influence upon foaming and exploit synergism in the design of foam fractionation. The experience of achieving reproducible values of foaming power indicated an application for conductivity measurements of foams to monitor batch and continuous operations. Thus further foam production was undertaken with continuous monitoring of foam conductivity as an integral part of process evaluation and control.

# *CHAPTER 4*

## *STUDY OF THE MOLECULAR INTERACTIONS BETWEEN BSA AND LYSOZYME: COMPOSITION EFFECTS UPON PROCESS PERFORMANCE IN BATCH FOAMING OPERATIONS*

### 4.1 Preface

The efficiency of foam separation/fractionation depends upon both the operational and column design, and the equilibrium characteristics of proteins partitioned between the liquid and foam phases. The adsorption of amphipathic proteins at interfaces plays a major role in foam stabilisation, and adsorption characteristics of isolated proteins of various molecular structures have been systematically studied (Graham and Phillips (1979a-c)). However, it has been shown that in complex protein systems adsorption at interfaces is related to bulk phase concentration, type of surface and the composition of the feed mixtures. The latter may advance competition between solutes to attach at interfaces (preferential adsorption) and/or complex formation between molecules with subsequent influence upon adsorption. Effects of complex formation upon adsorption may be synergistic. Synergy is associated with the fact that the surface activity of the mixed surfactant is greater than that expected in the absence of mutual interaction between constituent molecules (Shih Nan Hsu and Jer Ru Maa (1985)).

Preliminary quantitative analysis presented in Chapter 3 highlighted particular trends in the variation of foam composition where stability was remarkably improved by the addition of lysozyme in BSA solutions at pH 6.0. Such trends were characterised by increase in the recoveries of both proteins in the foam together with maximal lysozyme enrichment. The importance of solution composition upon foam stability was apparent in

BSA-cytochrome-c systems at pH 6.0, although it was not observed in BSA-lysozyme solutions under equivalent buffer conditions. However, improvement in foam stability of BSA solutions in the presence of lysozyme at pH 3.8 was determined by the stoichiometric presence of the two proteins.

The current chapter addresses the importance of feedstock composition upon electrostatic interactions between BSA and lysozyme at basic pH conditions (pH 8.0), with particular emphasis on their influence upon foam quality. Thus preparative foam experiments, conducted batchwise, explored the influence of varying concentrations of BSA and lysozyme in heterogeneous solutions upon foaming properties and subsequent separation efficacy.

The experimental design variables included the BSA concentration and the molar ratio of BSA to lysozyme. The selection of experimental BSA concentration was based upon the surface tension - concentration diagram for BSA (see Figure III1(a-b) in Appendix III) and adsorption isotherms in Graham and Phillips (1979b). Concentrations of lysozyme were adjusted accordingly to fulfill the predetermined molar ratios. Experimentation involved equimolar conditions as well as ratios above and below unity, i.e in the presence and absence of excess of lysozyme respectively. Table 4.1 illustrates the solution compositions for each pair of BSA concentration and BSA to lysozyme ratio applied.

## 4.2 Experimental Description

Foam was produced in the batch mode (see Chapter 2 (2.3.2)) and experiments were conducted in the 1,600 $cm^3$ foaming tower illustrated in

**Table 4.1 : Protein Composition of Defined Feedstocks in Batch Foam Production**

Protein composition of **(a)** heterogeneous BSA-lysozyme and **(b)** homogeneous BSA feedstocks, foamed batchwise. Values express protein composition as determined by HPLC gel filtration. Values in parentheses describe the protein composition based on dry weight per volume. Respective BSA to lysozyme molar ratios are rounded to the nearest integral.

**(a) Heterogeneous Feedstocks**

| **Sample Code Number** | **BSA Concentration (mg $cm^{-3}$)** | **Lysozyme Concentration (mg $cm^{-3}$)** | **BSA to Lysozyme Molar Ratio** |
|---|---|---|---|
| 1a | 0.98 (1.000) | 0.98 (1.000) | 0.21 (0.2) |
| 1b | 0.49 (0.500) | 0.48 (0.500) | 0.22 (0.2) |
| 1c | 0.25 (0.250) | 0.28 (0.250) | 0.19 (0.2) |
| 2a | 1.03 (1.000) | 0.19 (0.200) | 1.16 (1.0) |
| 2b | 0.48 (0.500) | 0.10 (0.100) | 1.02 (1.0) |
| 2c | 0.24 (0.250) | 0.06 (0.050) | 0.85 (1.0) |
| 3a | 0.92 (1.000) | 0.09 (0.100) | 2.20 (2.0) |
| 3b | 0.48 (0.500) | 0.05 (0.050) | 2.05 (2.0) |
| 3c | 0.24 (0.250) | 0.03 (0.025) | 1.71 (2.0) |

**(b) Homogeneous Feedstocks**

| **Sample Code Number** | **BSA Concentration (mg $cm^{-3}$)** |
|---|---|
| 1* | 0.99 (1.00) |
| 2* | 0.48 (0.50) |
| 3* | 0.24 (0.25) |

Figure 2.3 (Chapter 2). Foaming sample (400 $cm^3$) was loaded, and foam was generated by sparging nitrogen at a rate of 80 $cm^3$ $min^{-1}$. Nitrogen was preferred to $CO_2$ because it is chemically inert and ensures pH maintenance. Temperature was kept constant (20 °C) and foam conductivity was continuously monitored. Throughout experimentation the operational time of foaming was maintained at 30 min so that results obtained under various conditions could be compared. It was assumed that adsorption equilibrium had been attained under such conditions.

Protein solutions were prepared separately in 20 mM sodium phosphate buffer pH 8.0, ie approximately the mid-point between the pI values of protein solutes. Under such pH conditions, Poole et al. (1984) observed a maximum in foam stability of aqueous BSA-lysozyme solutions of equimolar composition. Solutions were continuously stirred for approximately 2 hours at room temperature. Under these conditions, the solubility of lysozyme was satisfactory (minimal haze) and centrifugal clarification was not necessary. The homogeneous solutions were mixed 15 minutes prior to foaming to yield the required protein concentrations defined by the experimentation. The pH and the temperature of the solutions were checked after mixing to ensure experimental accuracy and adjusted accordingly where necessary.

Protein composition was determined by HPLC size-exclusion chromatography as described in Chapter 2 (2.4.2). Calibration curves are shown in Figures II3(a-b) and II4(a-b) in Appendix II.

## 4.3 Results and Discussion

The present section describes and discusses the effects of feedstock composition upon protein partition in foam (Subsection 4.3.1) and dynamic changes in the bulk phase (Subsection 4.3.2). Protein partition was

assessed in terms of enrichment ($e_i$; Equation 3.1), fractionation index ($Fr_{i,j}$; Equation 3.6), foam volume ($V_F$), and recovery ($R_i$; Equation 3.3). Dynamic changes in the bulk phase are expressed in terms of volume and protein reduction with time of operation. Such changes also enabled determination of the heat of desorption ($\lambda$; Equation 2.8).

### 4.3.1 Effects of Feedstock Composition upon BSA and Lysozyme Partition in Batch Foams

Figure 4.1(a-b) shows the dependence of BSA and lysozyme enrichment ($e_{BSA}$ and $e_{lysozyme}$ respectively) upon BSA feedstock concentration (0.25 to 1 mg $cm^{-3}$) at various BSA:lysozyme molar ratios. It can be seen that BSA enrichment increases at low bulk concentrations. This behaviour is consistent throughout the range of BSA to lysozyme molar ratios applied, but in heterogeneous solutions enrichment values were constantly lower when compared to those achieved in the absence of lysozyme (control). Under such solutions a gradual decline in $e_{BSA}$ with increasing BSA:lysozyme molar ratio was observed, and a minimum was reached under equimolar conditions. The experimental results indicated that excess of BSA, ie at molar ratios above 1, the observed effects were approximately equivalent to those at equimolar concentrations. Changes in lysozyme enrichment with BSA feedstock concentration (Figure 4.1b) showed that the observed $e_{lysozyme}$ values were lower than 1.5 and did not vary in a specific manner with BSA concentration or BSA:lysozyme molar ratio. When $e_{lysozyme}$ values were assessed with respect to lysozyme concentration in the feedstock (see Table 4.2), lysozyme enrichment was not found to be related to its respective concentration in the feedstock in a manner

**Figure 4.1: Effects of BSA Concentration and Feedstock Composition upon BSA Enrichment in Batch Foam Production**

Variations in **(a)** BSA enrichment ($e_{BSA}$) and **(b)** lysozyme enrichment ($e_{lysozyme}$) are expressed in relation to BSA feedstock concentration and BSA: lysozyme molar ratio in heterogeneous solutions, for foams produced in batch operations.

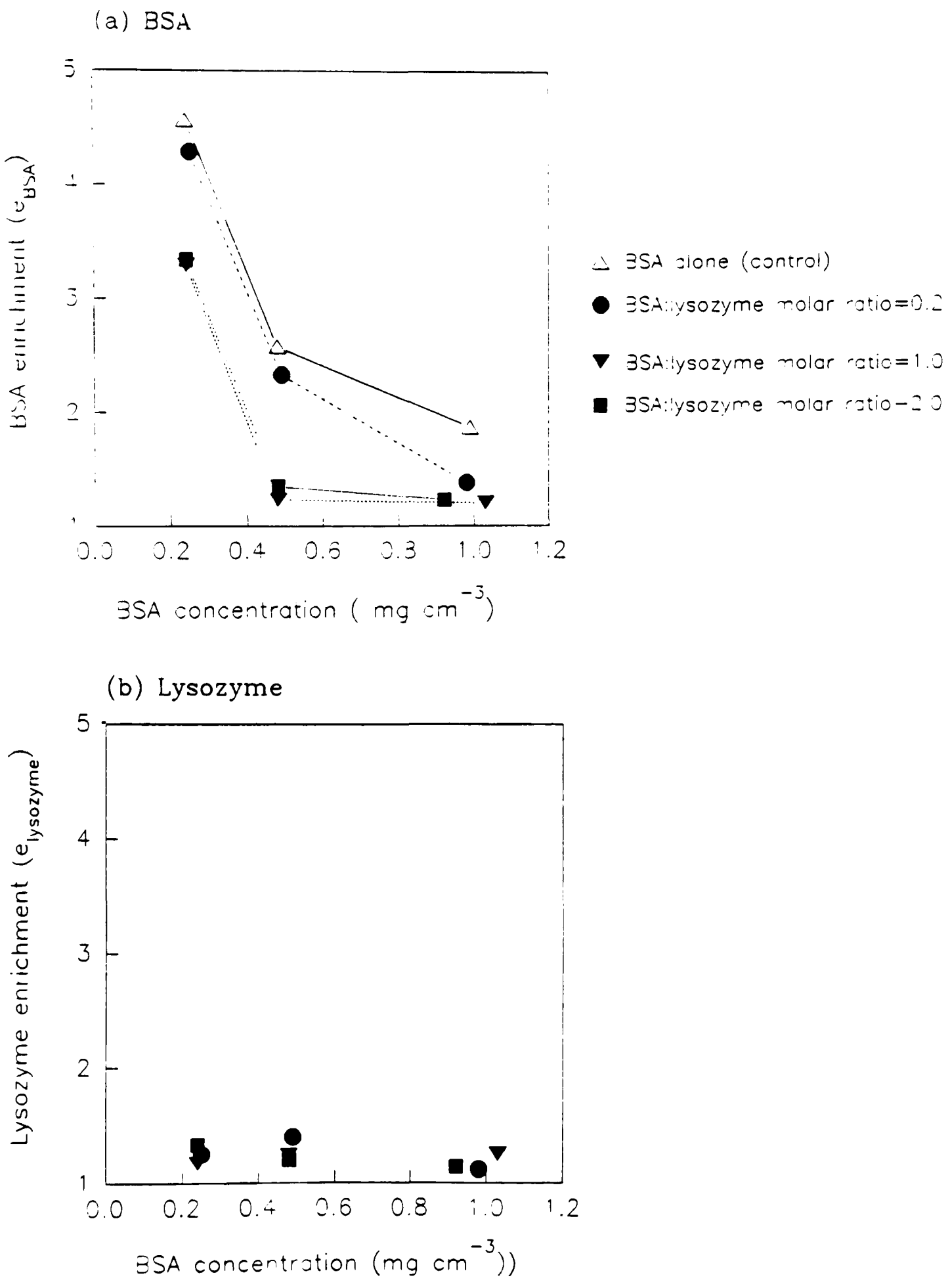

**Table 4.2: Lysozyme Enrichment in Batch Foam Production**

Lysozyme enrichment ($e_{lysozyme}$) in foam generated batchwise from heterogeneous solutions, with reference to the concentration of lysozyme in the bulk phase of the solutions of origin. Lysozyme concentration was determined by HPLC analysis.

| **Sample Code Number** | **Lysozyme Concentration (mg $cm^{-3}$)** | **Enrichment ($e_{lysozyme}$)** |
|---|---|---|
| 1a | 0.98 | 1.12 |
| 1b | 0.48 | 1.40 |
| 1c | 0.25 | 1.25 |
| 2a | 0.19 | 1.24 |
| 2b | 0.10 | 1.24 |
| 2c | 0.06 | 1.03 |
| 3a | 0.09 | 1.22 |
| 3b | 0.05 | 1.18 |
| 3c | 0.03 | 1.12 |

comparable to that depicted in Figure 4.1a for BSA. However, examination of the fractionation index ($Fr_{BSA,lysozyme}$) at varied BSA feedstock concentrations (0.25 to 1 mg $cm^{-3}$) and BSA:lysozyme molar ratios (see Figure 4.2(a-c)) revealed certain patterns of lysozyme partition into the foam. Thus, as shown in Figures 4.2(a-b), where BSA concentration was 1 and 0.5 mg $cm^{-3}$ respectively, the fractionation index exhibited a minimum at BSA:lysozyme molar ratios of one. $Fr_{BSA,lysozyme}$ was greater than one in excess of lysozyme (below equimolar conditions). It approached values of one at equimolar composition, and showed a slight increase in excess of BSA (above equimolar conditions). In contrast, for BSA feedstock concentrations of 0.25 mg $cm^{-3}$ (Figure 4.2(c)) the observed $Fr_{BSA,lysozyme}$ values were significantly above unity ($3.0 < Fr_{BSA,lysozyme} < 3.8$) throughout the BSA to lysozyme molar ratios studied. They appeared to continuously decline with increasing BSA:lysozyme molar ratio.

Figure 4.3 describes variations in foam volumes ($V_F$) with BSA feedstock concentration at various BSA:lysozyme molar ratios. It can be seen that, during comparable times of batch operation, the largest quantities of foam were consistently generated from the highest BSA concentrations in the feed for all the BSA:lysozyme molar ratios applied. The addition of lysozyme to BSA solutions increased the volume of collected foam and, at comparable BSA concentrations, a maximum in $V_F$ occurred at equimolar conditions. The observed volume enhancement was more pronounced at BSA concentrations of 0.5 and 1 mg $cm^{-3}$. Table 4.3 shows that solution composition appeared to exert similar effects upon the reduced foam conductivity ($H_r$, see Equation 1.6). At comparable BSA:lysozyme molar ratios, $H_r$ increased with BSA feedstock concentration, while at equivalent BSA concentrations $H_r$ was highest under equimolar

**Figure 4.2: Dependence of Fractionation Index upon Feedstock Composition in Batch Foam Production**

Comparative illustration of the effects of feedstock composition, ie BSA: lysozyme molar ratio in heterogeneous solutions, upon the fractionation index ($Fr_{BSA,lysozyme}$) at BSA feedstock concentrations of **(a)** 1 mg $cm^{-3}$, **(b)** 0.5 mg $cm^{-3}$ and **(c)** 0.25 mg $cm^{-3}$.

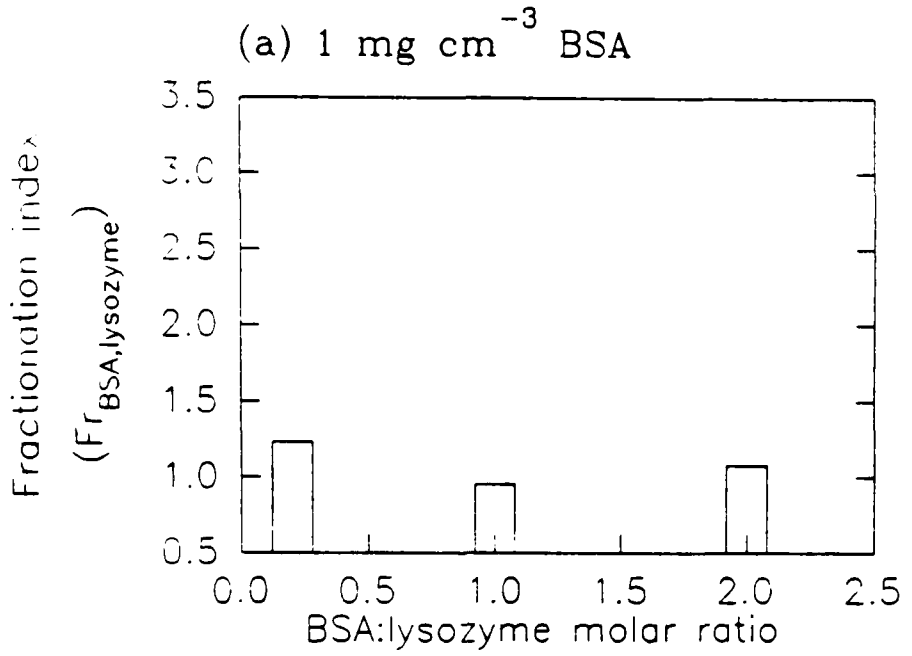

**Figure 4.3: Volumes of Collected Foams in Batch Operations at Varied BSA Concentrations and Feedstock Compositions**

Variations in collected volumes of foam ($V_F$) are expressed in relation to BSA feedstock concentration and BSA: lysozyme molar ratio in heterogeneous solutions. Foams were collected at comparable times of batch operation (30 minutes). $V_F$ values of heterogeneous foams are compared with those of homogeneous BSA solutions (control).

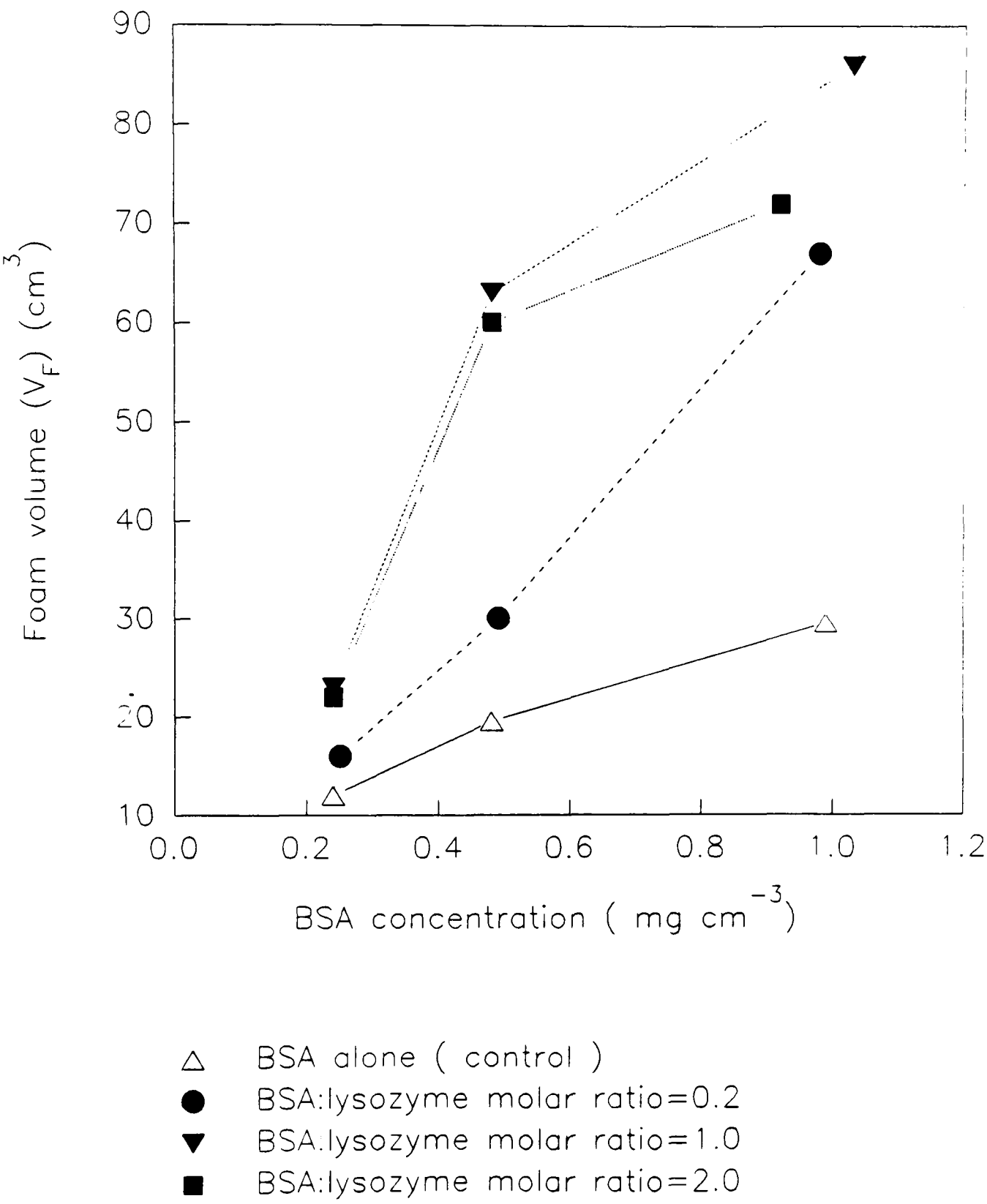

**Table 4.3: Reduced Conductivity of Foams Formed Batchwise by Heterogeneous and Homogeneous Feedstocks**

Reduced foam conductivities ($H_r$), namely the conductivity of foam as a fraction of that of the feedstock (see Equation 1.6 in Chapter 1), are expressed in relation to protein composition in the feedstock. Values in superscripts describe the volumes of foam collected under such conditions.

**(a)**

| Sample Code Number | Feedstock Concentration (mg $cm^{-3}$) BSA | Lysozyme | Reduced Foam Conductivity ($H_r$) (x $10^{-2}$) |
|---|---|---|---|
| 1a | 0.98 | 0.98 | $2.75^{(67)}$ |
| 1b | 0.49 | 0.48 | $2.40^{(30)}$ |
| 1c | 0.25 | 0.28 | $1.60^{(16)}$ |
| 2a | 1.03 | 0.19 | $3.65^{(86)}$ |
| 2b | 0.48 | 0.10 | $2.77^{(63)}$ |
| 2c | 0.24 | 0.06 | $1.88^{(23)}$ |
| 3a | 0.92 | 0.09 | $3.32^{(72)}$ |
| 3b | 0.48 | 0.05 | $2.48^{(60)}$ |
| 3c | 0.24 | 0.03 | $2.10^{(22)}$ |

**(b)**

| Sample Code Number | BSA Feedstock Concentration (mg $cm^{-3}$) | Reduced Foam Conductivity ($H_r$)(x $10^{-2}$) |
|---|---|---|
| 1* | 0.99 | $2.33^{(29.5)}$ |
| 2* | 0.48 | $1.87^{(19.5)}$ |
| 3* | 0.24 | $1.43^{(15.0)}$ |

**Table 4.4: Volumetric Foam Capacity of Defined Feedstocks in Batch Foam Production**

Foam volumes ($V_F$) collected batchwise are expressed in relation to the total protein concentration in the feedstocks : **(a)** heterogeneous BSA-lysozyme solutions **(b)** homogeneous BSA solutions. In heterogeneous solutions the total protein concentration is the sum of the individual solute concentrations whilst in homogeneous solutions the total protein concentration coincides with the BSA concentration. Protein concentrations were determined by HPLC analysis.

**(a)**

| **Sample Code Number** | **Total Protein Concentration (mg $cm^{-3}$)** | **Foam Volume ($V_F$) ($cm^3$)** |
|---|---|---|
| 1a | 1.96 | 67.0 |
| 1b | 0.97 | 30.0 |
| 1c | 0.53 | 16.0 |
| 2a | 1.22 | 86.0 |
| 2b | 0.58 | 63.0 |
| 2c | 0.30 | 23.0 |
| 3a | 1.01 | 71.0 |
| 3b | 0.53 | 60.0 |
| 3c | 0.27 | 22.0 |

**(b)**

| **Sample Code Number** | **Total Protein Concentration (mg $cm^{-3}$)** | **Foam Volume ($V_F$) ($cm^3$)** |
|---|---|---|
| 1* | 0.99 | 29.5 |
| 2* | 0.48 | 19.5 |
| 3* | 0.24 | 15.0 |

conditions. Table 4.3 is supplemented with $V_F$ values in superscript form for immediate comparison between trends in foam conductivity and volume. In relation to total protein concentration in heterogeneous solutions, collection of the highest foam volumes did not correspond to the solutions with the highest total protein content (see Table 4.4).

Variations in BSA and lysozyme recoveries in respect of BSA: lysozyme molar ratio are illustrated in Figures 4.4(a-c) for BSA feedstock concentrations of 1, 0.5 and 0.25 mg $cm^{-3}$ respectively. At equivalent BSA: lysozyme molar ratios BSA recovery was highest at the most concentrated feedstock (compare Figures 4.4(a-c)). For BSA concentrations of 1 and 0.5 mg $cm^{-3}$ (Figures 4.4(a-b) respectively) the presence of lysozyme in mixed solutions improved the recovery of BSA with slightly higher values at and above equimolar conditions. At equivalent BSA concentrations in the feed, the recovery of lysozyme depended upon feedstock composition and showed a maximum at equimolar conditions. Under such conditions, $R_{lysozyme}$ values were similar to those of BSA. In contrast, at dilute conditions ie 0.25 mg $cm^{-3}$ (Figure 4.4c), the recovery of lysozyme was significantly lower than that of BSA at all BSA: lysozyme molar ratios. $R_{lysozyme}$ values followed an upward trend with increasing BSA: lysozyme molar ratio.

It is therefore evident that the concentration of both proteins is increased in the foam, relative to the bulk, although not in an equivalent manner. BSA enrichment is significantly greater than that of lysozyme and definitely follows a certain profile with respect to feedstock composition, namely BSA enrichment declines in foams formed by solutions of increasing BSA concentration. Such behaviour is common in both homogeneous and heterogeneous solutions. At comparable BSA concentrations,

**Figure 4.4: Dependence of Protein Recovery upon Feedstock Composition in Batch Foams**

Effects of feedstock composition upon the recovery of BSA ($R_{BSA}$) and lysozyme ($R_{lysozyme}$) in batch foams from heterogeneous solutions for BSA concentrations of **(a)** 1 mg $cm^{-3}$, **(b)** 0.5 mg $cm^{-3}$ and **(c)** 0.25 mg $cm^{-3}$. BSA recoveries in heterogeneous solutions are illustrated in direct comparison with those of the control.

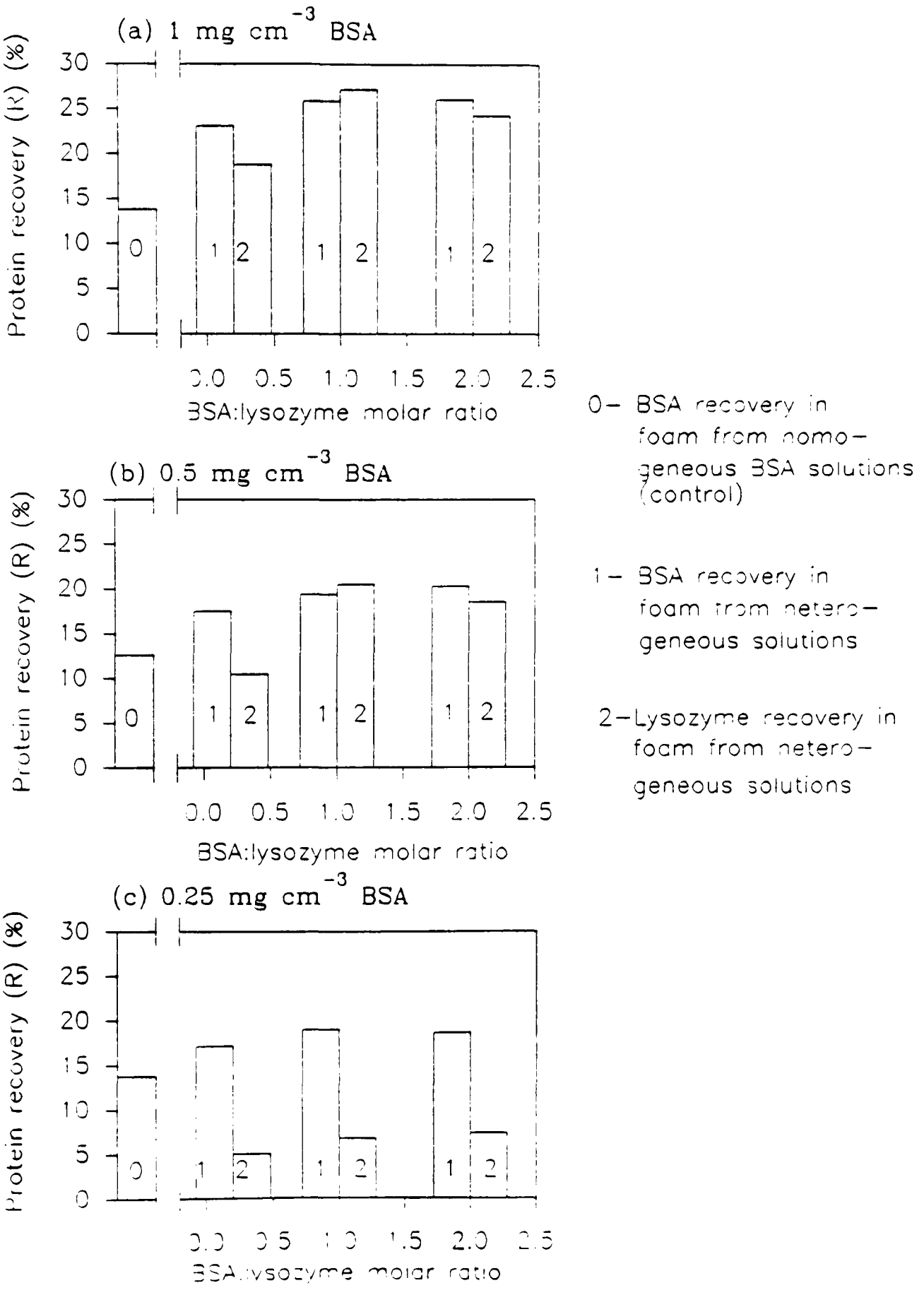

the lowest enrichment appears to occur at equimolar conditions. Lysozyme enrichment seems to be independent from its feedstock concentration, but its partition into foam is maximised at BSA: lysozyme molar ratios > 1 for 1 and 0.5 mg $cm^{-3}$ BSA concentration in the feed. At more dilute feedstocks it appears that lysozyme partition is favoured by increasing BSA: lysozyme molar ratios. This indicates that the enrichment of lysozyme depends upon the molar ratio of the two proteins in solution, but in dilute feedstocks, BSA concentration seems to play an important role. Contrary to trends in BSA enrichment, foam volume and BSA recovery are enhanced in the presence of lysozyme, with maxima at and above equimolar conditions. In the most concentrated feedstocks, the recovery of lysozyme appears to be maximal at equimolar conditions. In dilute feedstocks, the recovery of lysozyme seems to increase with increasing BSA: lysozyme molar ratio in a manner similar to that of fractionation index.

The decline in BSA enrichment in foams from concentrated bulk solutions must be associated with predictions from the Gibbs's equation and adsorption kinetics, which have already been discussed in Chapter 3, as well as the dynamics of liquid drainage in the rising foam. At low protein concentrations, the adsorption of protein at the gas-liquid interface, which is responsible for foam stabilisation, is low and foams are less stable (see Figures 3.1 and 3.9 in Chapter 3). Therefore the extent of bubble coalescence is greater, promoting the formation of larger bubbles and lower foam volumes. Reduction in the liquid load of foam is reflected in the observed trends in reduced foam conductivity (Table 4.3). Coalescence acts in practice as internal reflux which increases the concentration of protein in the rising bubbles as well as the residual bulk phase. The role of coalescence upon bubble dynamics and protein partition into foam will be discussed in more detail in Chapter 7.

The independence of $e_{lysozyme}$ from feedstock concentration must be associated with its poor foaming properties, discussed in Chapter 3. Therefore any presence of lysozyme in foams from heterogeneous solutions must be attributed to entrainment of mother liquors in the plateau borders and surface excess in the form of BSA-lysozyme complexes. These foams are stabilised by BSA molecules and BSA-lysozyme complexes formed by BSA-lysozyme electrostatic interactions. Such interactions have been previously noted (Chapter 3) as a crucial factor in the synergistic enhancement of foam stability in BSA solutions fortified by lysozyme (see Figure 3.2 and Table 3.1 in Chapter 3). Stable foams from BSA-lysozyme solutions are expected to incorporate increased amounts of lysozyme (ie low $Fr_{BSA,lysozyme}$) and to yield higher foam volumes and $H_r$ values but reduced BSA enrichment. The extend of this phenomenon is clearly related to the feedstock composition, particularly at BSA feedstock concentrations of 1 and 0.5 mg $cm^{-3}$. $Fr_{BSA,lysozyme}$ values near unity, minimal $e_{BSA}$, and maximal $V_F$ at equimolar conditions indicate that such effects are maximal when proteins are present in quantities demanded by molecular stoichiometry. This behaviour is in accordance with results reported by Poole et al. (1984) which indicated that maximal enhancement in foam stability was achieved when BSA and lysozyme were present in equimolar concentrations.

Foam fractionation involving the use of a collector (Rose and Sebba (1969); Lee and Ryu (1979); Gehle and Schügerl (1984a)) was found to be most efficient at an optimal collector:colligend ratio. Such behaviour was attributed to the fact that in collector excess, adsorption of collector-colligend complexes is difficult as colligend is crowded with collector. If the collector exceeds the critical micelle concentration (CMC), flotation may be impaired because colligend ions are adsorbed on

the micelles, which are themselves unable to float because of their hydrophobic surfaces. In the present case of foams from mixtures of BSA (collector) and lysozyme (colligend), it appears that there is a tendency to inhibit lysozyme partition in foam at BSA:lysozyme molar ratios of approximately two. This tendency must be attributed to excess of BSA and not to impairment of flotation due to bulk concentrations higher than CMC, since the range of BSA concentrations applied was below such values (see Figure III1b in Appendix III).

At dilute BSA conditions (Figure 4.2c) it appears that the predominant factor for protein partition is the bulk concentration of BSA and not the BSA:lysozyme molar ratio. The BSA:lysozyme molar ratio still exerts the same effect as in more concentrated feedstocks, but to a reduced degree. It is very likely that foams generated from dilute solutions can accommodate BSA-lysozyme dimers as well as single BSA molecules existing in free state (Yasisawa (1975)). It is also possible that there is some competition between BSA monomers and BSA-lysozyme dimers analogous to competition between small and large surfactant molecules in emulsions, where the latter can be displaced by the former (Dickinson and Woskett (1989)).

The reduction of BSA enrichment in foams generated in the presence of lysozyme could also involve the concept of surface occupancy. The preferential adsorption of BSA-lysozyme dimer molecules would be expected to reduce the space available to single BSA molecules to attach to the gas-liquid interface. If lysozyme were more foam positive, and the operating conditions (ie pH and/or ionic strength) were adjusted to suppress electrostatic interactions between protein molecules, then competitive rather than synergistic adsorption would require consideration to explain discrepancies in the behaviour of heterogeneous and homogeneous

solutions.

The influence of feedstock composition on total protein concentration is highlighted in Table 4.4, where there is not any obvious correlation between total protein concentration and the quantities of collected foam. This phenomenon is in complete disagreement with observed increases in foam volume with elevating protein concentration in homogeneous systems (see Table 4.4b, and Table 3.2 in Chapter 3). It is therefore evident that laws governing foam performance in single component systems cannot always be applicable in multi-component ones. Realistic designs of foam fractionation processes should first investigate the role of component protein composition upon foaming.

Protein recovery is by definition related to enrichment and foam volume and therefore is directly dependent upon all such factors. Increase in BSA recovery from heterogeneous solutions, as compared with that of the control, implies that recovery is primarily governed by the same mechanisms which influence coalescence and drainage. At comparable BSA to lysozyme ratios, decline in BSA recovery with decreasing feedstock concentration is associated with the formation of less stable foam at dilute conditions. At BSA feedstock concentrations of 1 and 0.5 mg $cm^{-3}$, maxima in lysozyme recovery at equimolar conditions must be attributed to the highest representation of lysozyme in foam (see Figure 4.2(a-b)) due to maximisation of BSA-lysozyme complex formation. At 0.25 mg $cm^{-3}$ BSA feedstock concentration, the predominant factor affecting protein recovery appears to be dilute feedstock conditions rather than solution composition. It is noteworthy to mention that the patterns of BSA and lysozyme recoveries reflects tendencies in their partition into foam as shown in Figure 4.2(a-c).

The foregoing trends in protein partition into foams from systems

such as BSA and lysozyme indicate that judicious selection of feedstock composition can promote either fractionation of solutes which synergistically interact and enhance foaming, or induce the collection of a poor foaming agent, such as lysozyme, by the use of a collector such as BSA. Correlation between trends in foam volumes and reduced foam conductivity confirms the importance of conductivity measurements of foam as a tool of foam density assessment and process monitoring.

### 4.3.2 Dynamic Changes in the Bulk Phase

Dynamic changes in the bulk phase during batch foaming refer to volume and protein reduction. As mentioned in Chapter 2 (2.3.2), experiments were performed whilst noting changes in the volume and protein concentration of the bulk phase at timed intervals during the 30 minute operation. Time-dependent changes in protein concentration of the bulk phase are expressed in terms of a stripping factor $s_{t,i}$ defined by equation 4.1:

$$s_{t,i} = c_{iB}/c_{iO} \qquad \text{(Equation 4.1)}$$

where: $s_{t,i}$ is the stripping factor of protein i

$c_{iB}$ and $c_{iO}$ are the concentrations of protein i in the liquid pool (bulk phase) and feedstock respectively.

Protein stripping factor quantifies protein depletion from the bulk phase due to protein enrichment in the foam and is always $\leq 1$. Stripping factors are expected to continuously decrease during the time of batch operation but to remain constant in continuous foaming once steady-state conditions have been attained.

Systematic characterisation of the reduction in volume and protein concentration in the bulk phase enabled the determination of the residual

protein ratio (r). The parameter r describes the mass of protein left in the bulk phase at any time during foaming operation as a fraction of the mass of the same protein species in the feedstock, and is denoted by Equation 4.2:

$$r_i = r_{i0}\exp(\kappa t) \Leftrightarrow \ln r_i = \ln r_{i0} + \kappa t \qquad \text{(Equation 4.2)}$$

where: $r_i$ is the residual protein ratio for protein i

$r_{i0}$ is the intercept on the ln r axis

$\kappa$ is the slope of the straight line ($\kappa \leq 0$), $\kappa$ [=] $min^{-1}$

t is the time of operation, t[=]min.

The residual protein ratio (r) and protein recovery (R) constitute the criteria of foam separation efficiency. For low $\kappa$ values, Equation 4.2 yields low residual protein ratios which imply high foam separation efficiency.

Increase in the volume of collected foam (see Figure 4.3) coincided with lower residual liquid volumes at the end of operation (30 minutes) as Figure 4.5 shows. A gradual reduction in the residual volume was observed at increasing BSA concentrations. There was also a decline in volume with increasing BSA: lysozyme molar ratio at comparable BSA concentrations, with lowest bulk volumes observed at equimolar conditions. This phenomenon was more pronounced at higher BSA content. Figure 4.6 illustrates the reduction in bulk volume with time for heterogeneous solutions of different BSA concentrations and a BSA: lysozyme molar ratio of 0.2. It can be seen that concentrated feedstocks exhibited greater volume reduction rates when compared with dilute samples. This behaviour was identical at and above equimolar conditions. Figure 4.7(a-c) describes the reduction rates of bulk volumes in heterogeneous solutions of varied BSA: lysozyme molar ratio and BSA feedstock concentrations of 1, 0.5 and 0.25 mg

**Figure 4.5: Dependence of Residual Bulk Volume upon BSA Feedstock Concentration in Batch Foam Production**

Variations in the residual volumes of the bulk phase are expressed in relation to BSA concentration in the feed at various BSA: lysozyme molar ratios (heterogeneous solutions). Results refer to values at the end of the foaming process (30 minutes) and are compared with those of the control.

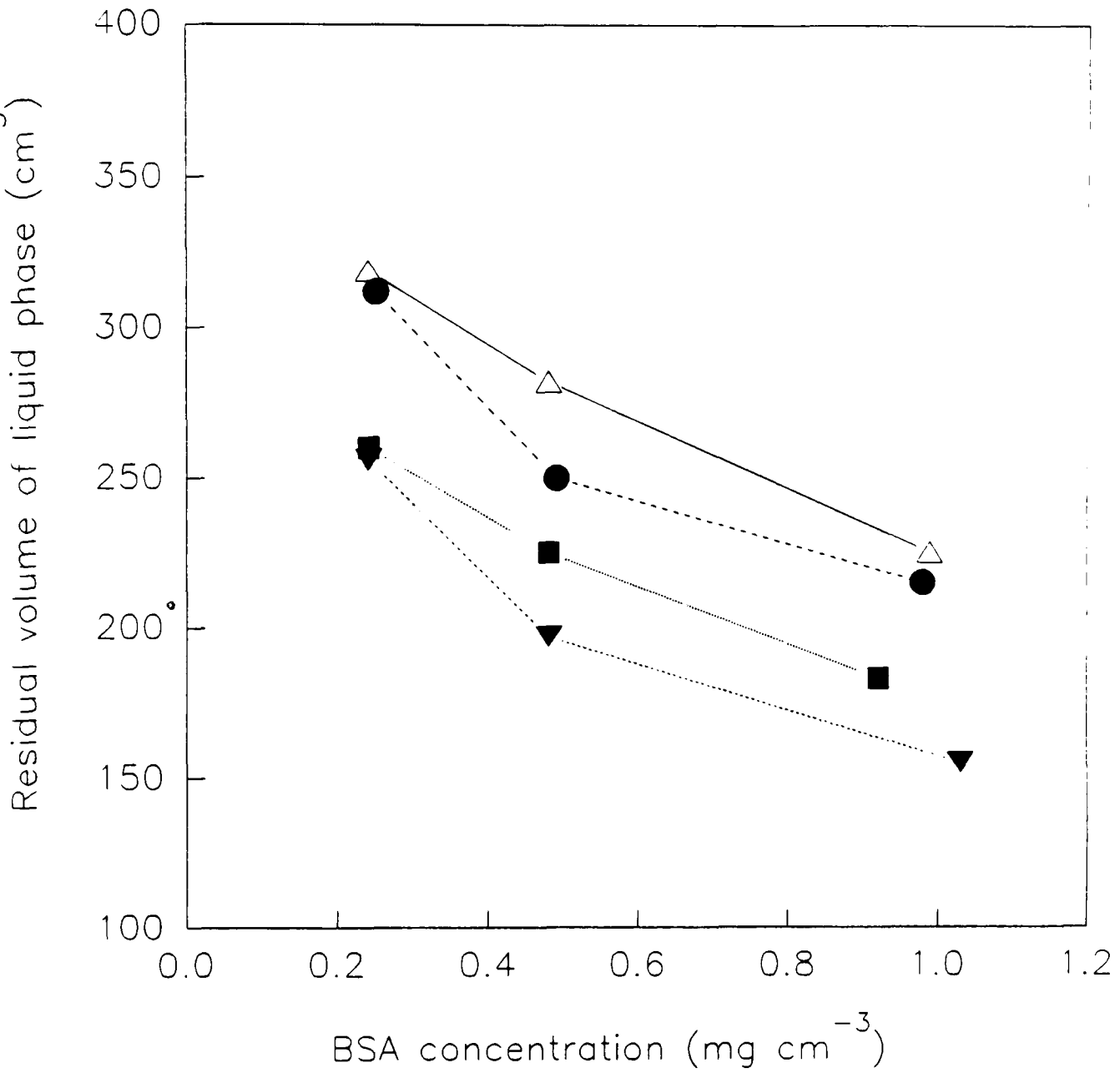

**Figure 4.6: Effects of BSA Feedstock Concentration upon Reduction in Bulk Phase Volume**

Description of the rate and magnitude of reduction in the volume of the bulk phase during batch foaming at varied BSA concentrations in heterogeneous feedstocks (1, 0.5 and 0.25 mg $cm^{-3}$). The BSA: lysozyme molar ratio was constant at 0.2.

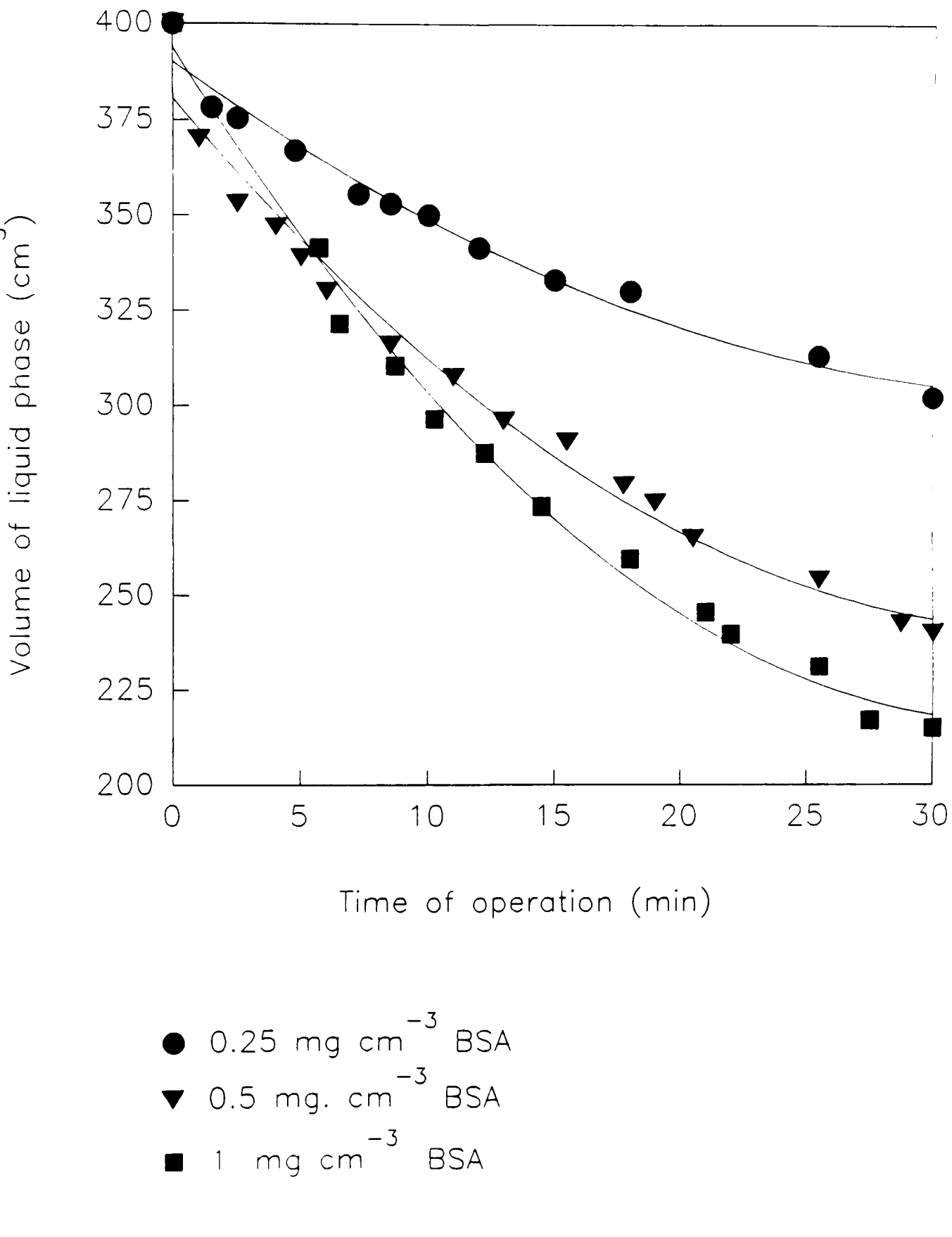

$cm^{-3}$ respectively. In each case, results are compared with the control. It can be observed that the addition of lysozyme to BSA solutions of equivalent concentrations resulted in increased reduction rates of bulk volumes when compared with those of the control solution (lysozyme free). The observed reductions were greatest at equimolar conditions for 1 and 0.5 mg $cm^{-3}$ BSA concentrations, whilst there was a gradual decline in volume reduction with BSA: lysozyme molar ratio in experiments at 0.25 mg $cm^{-3}$ BSA.

Figure 4.8(a-b) describes the rate of reduction in stripping factors of BSA and lysozyme respectively for various BSA concentrations and a constant BSA: lysozyme ratio of 0.2. It can be seen that the greatest reduction in $s_{t,i}$ for both BSA and lysozyme was achieved at the most dilute BSA conditions. These changes were less pronounced in the case of lysozyme. Figure 4.9(a-b) describes the effects of feedstock composition upon $s_{t,BSA}$ and $s_{t,lysozyme}$ respectively, at comparable BSA concentration in the feed (0.5 mg $cm^{-3}$). It can be seen that the addition of lysozyme in BSA solutions resulted in increased depletion of BSA from the bulk phase when compared with that of the control. This depletion was most effective when the BSA: lysozyme ratio was equal to 1. Equivalent plots for lysozyme in Figure 4.9b show a similar trend although in a less pronounced manner.

Table 4.5(a-b) presents the experimentally determined values of $r_{i0}$ and $\kappa$ for BSA and lysozyme respectively, by application of Equation 4.2. The values of $r_{i0}$ and $\kappa$ for BSA indicate that at comparable time-scales of operation, $r_i$ decreased with increasing BSA: lysozyme ratio for 0.25 mg $cm^{-3}$ BSA concentration, but reached a minimum at equimolar conditions for more concentrated feedstocks (ie 1 and 0.5 mg $cm^{-3}$ BSA). However, such values are clearly below the $r_i$ value of the control (Table 4.5b). The values of $r_{i0}$ and $\kappa$ for lysozyme indicate that, at comparable times of

**Figure 4.7: Effects of Feedstock Composition upon Reduction in Bulk Phase Volume**

Effects of BSA:lysozyme molar ratio (heterogeneous feedstocks) upon the rate and magnitude of reduction in the volume of the bulk phase during batch foaming. Such effects are studied at varied BSA feedstock concentrations, namely **(a)** 1 mg $cm^{-3}$, **(b)** 0.5 mg $cm^{-3}$ and **(c)** 0.25 mg $cm^{-3}$.

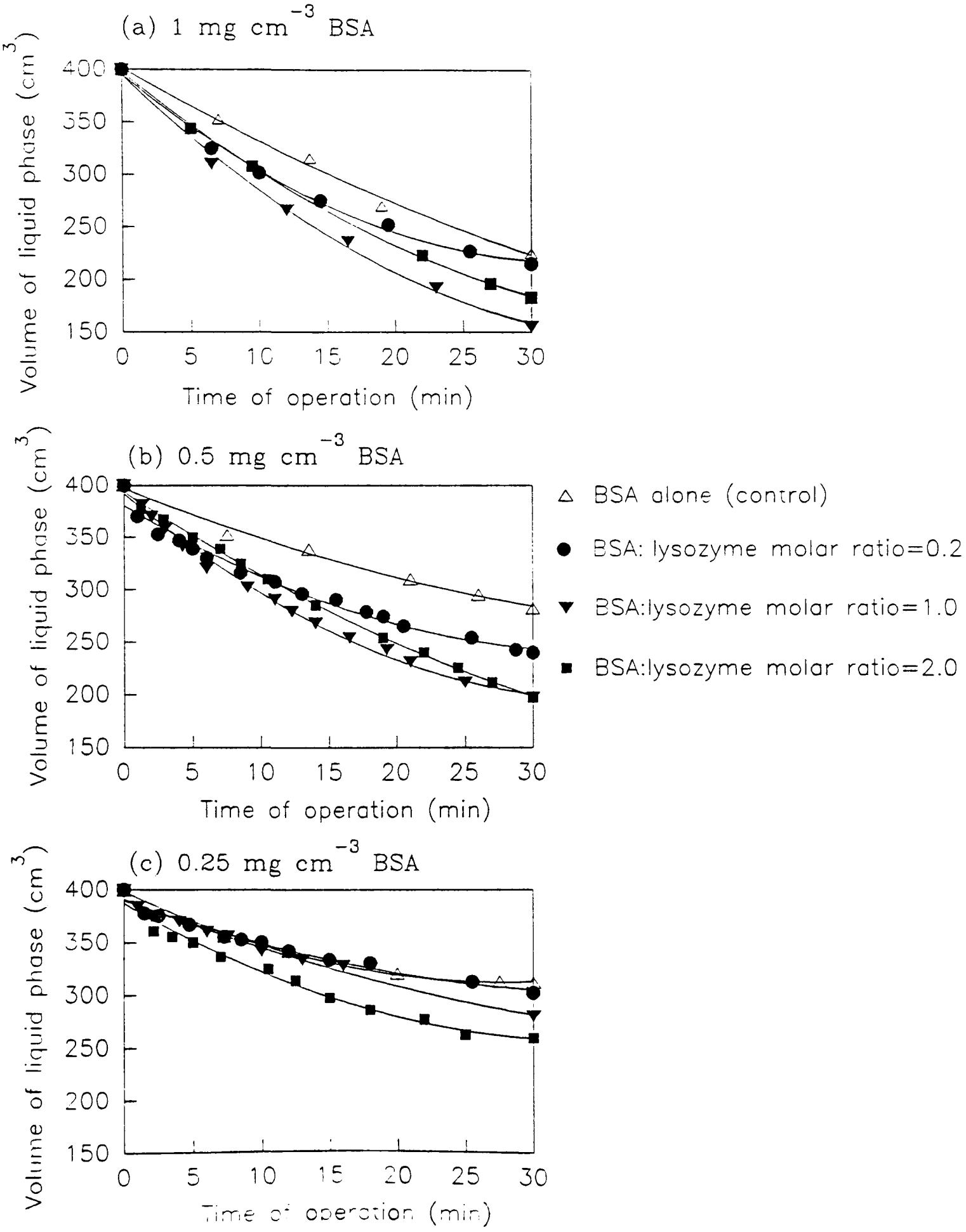

**Figure 4.8: Effects of BSA Concentration upon Variations of Stripping Factor with Time of Batch Foaming**

Effects of BSA concentration in heterogeneous feedstocks upon the rate and magnitude of reduction in the stripping factor ($s_{t,i}$) of **(a)** BSA and **(b)** lysozyme during batch foam production. Results refer to comparable feedstock compositions where the BSA: lysozyme molar ratio was constant at 0.2.

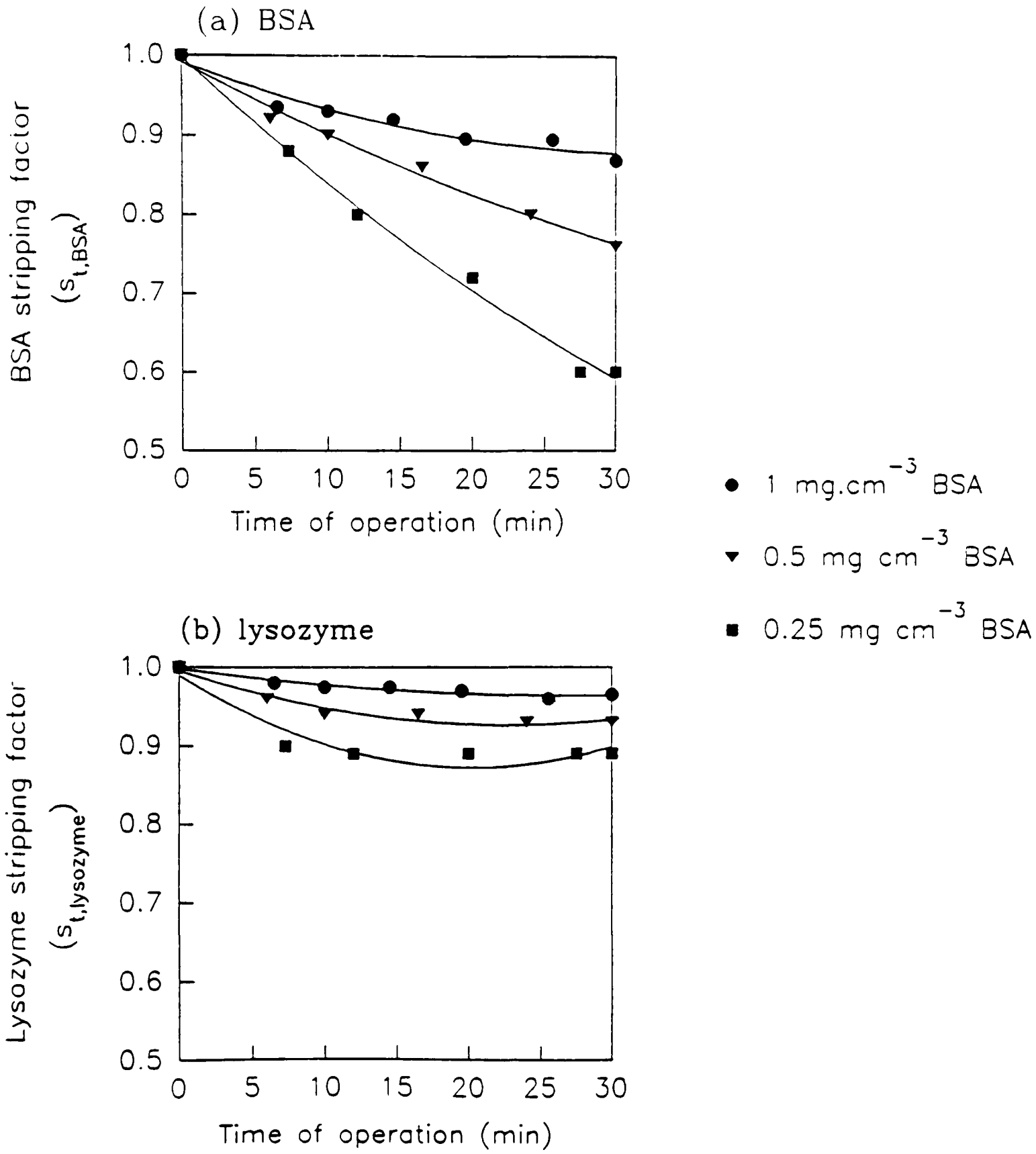

**Figure 4.9: Effects of Feedstock Composition upon the Rate of Reduction in Stripping Factor**

Effects of BSA: lysozyme molar ratio (heterogeneous feedstocks) upon the rate and magnitude of reduction of stripping factor of **(a)** BSA and **(b)** lysozyme during batch foaming. The BSA feedstock concentration was 0.5 mg $cm^{-3}$ and $s_{t,BSA}$ values in heterogeneous solutions are compared with those of the control.

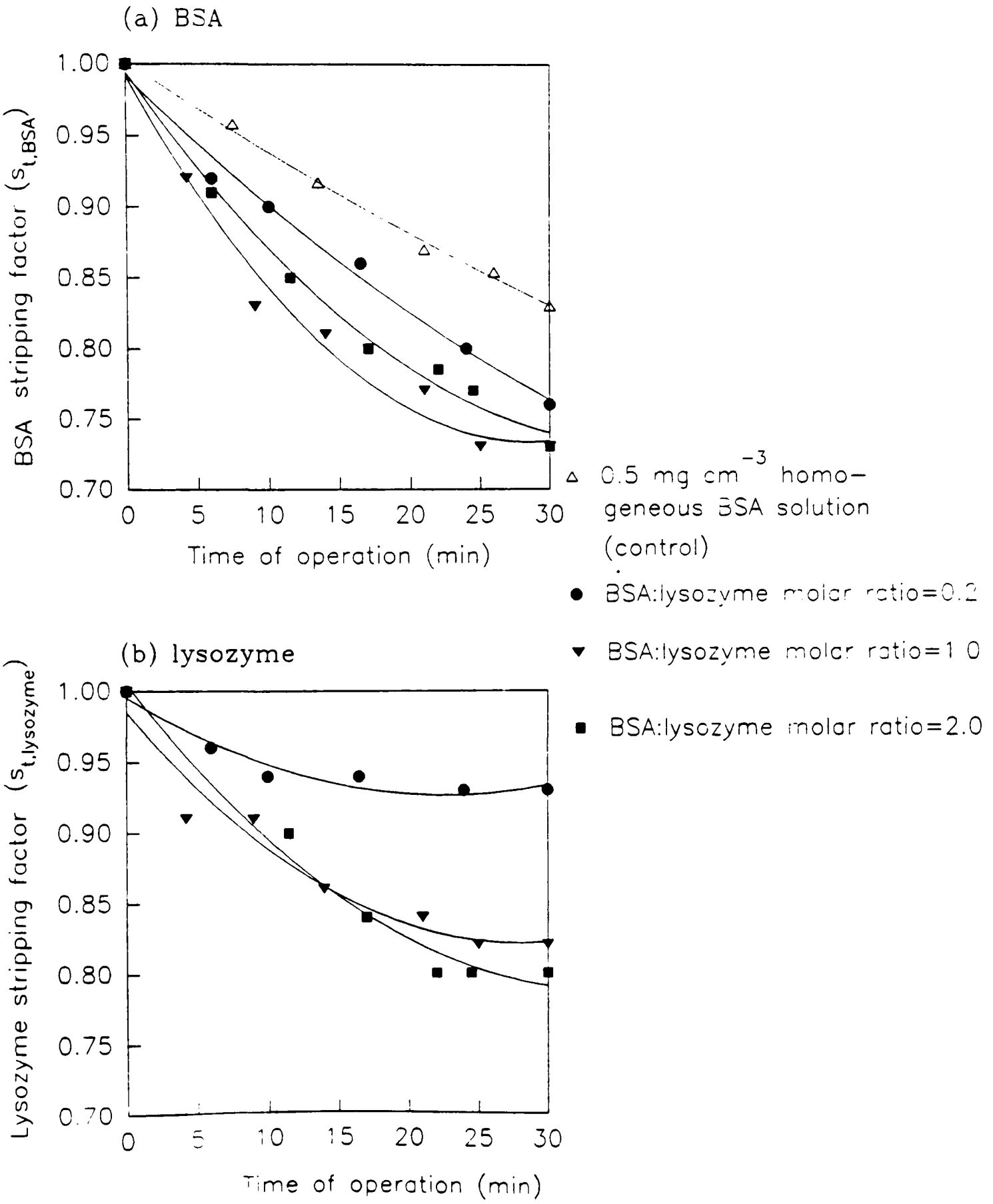

**Table 4.5: Description of Residual Protein Ratio for BSA and Lysozyme**

Experimental determination of coefficients $r_{i0}$ and $\kappa$ in Equation 4.2 for (a) heterogeneous BSA-lysozyme solutions and (b) homogeneous BSA solutions. Regression coefficients refer to straight line plots of ln(r) against time (t) of operation.

**(a)**

| Sample Code | $r_{i0}$ | | $\kappa$ | | Regression Coefficient (%) | |
|---|---|---|---|---|---|---|
| **Number** | **BSA** | **lysozyme** | **BSA** | **lysozyme** | **BSA** | **lysozyme** |
| 1a | 0.860 | 0.885 | -0.021 | -0.018 | 99.80 | 99.68 |
| 1b | 0.861 | 0.834 | -0.220 | -0.013 | 99.95 | 98.79 |
| 1c | 0.914 | 0.819 | -0.023 | -0.006 | 99.56 | 97.41 |
| 2a | 0.863 | 0.901 | -0.034 | -0.034 | 99.80 | 99.80 |
| 2b | 0.869 | 0.888 | -0.031 | -0.028 | 99.13 | 98.58 |
| 2c | 1.018 | 0.994 | -0.030 | -0.017 | 99.80 | 96.95 |
| 3a | 0.900 | 0.932 | -0.029 | -0.030 | 99.80 | 98.92 |
| 3b | 1.060 | 1.053 | -0.036 | -0.034 | 99.79 | 98.33 |
| 3c | 0.940 | 0.890 | -0.032 | -0.027 | 99.29 | 90.64 |

**(b)**

| Sample Code Number | $r_{i0}$ | $\kappa$ | Regression Coefficient (%) |
|---|---|---|---|
| 1* | 0.982 | -0.021 | 99.90 |
| 2* | 0.963 | -0.017 | 99.46 |
| 3* | 0.988 | -0.019 | 99.74 |

operation, most efficient reduction in $r_i$ occurred at equimolar conditions for feedstocks of 1 and 0.5 mg $cm^{-3}$ BSA but there was a continuous decline in r at the most dilute feedstocks (0.25 mg $cm^{-3}$).

The determined values of the heat of desorption ($\lambda$) for BSA are shown in Table 4.6(a-b) for heterogeneous and homogeneous feedstocks respectively. Selected $\lambda$ values for lysozyme are also shown in Table 4.6a. It can be seen that $\lambda_{BSA}$ increases with decreasing feedstock concentration. Comparison of the $\lambda$ values of BSA at equivalent BSA concentrations, in both homogeneous and heterogeneous feedstocks, does not suggest that the presence of lysozyme affected the heat of desorption in any identifiable manner. Determination of the heat of desorption of lysozyme for some feedstocks seems to agree with the trend of increased $\lambda$ at low bulk concentrations. However, comparison between $\lambda_{BSA}$ and $\lambda_{lysozyme}$, at similar respective concentrations, shows that the heat of desorption of lysozyme found to be significantly lower than that of BSA.

The foregoing experimental evidence shows that, during batch operation, dynamic changes in volume, protein concentration and residual protein mass in the bulk phase strongly depend upon the factors influencing protein enrichment and recovery. Higher foam volumes are associated with greatest reductions in bulk volume. Efficient protein removal in foam promotes steeper reductions in $s_{t,BSA}$ and $s_{t,lysozyme}$, and $r_{BSA}$ and $r_{lysozyme}$. Efficient protein removal may involve high enrichment, high recovery and low fractionation index. At comparable BSA concentrations in the feed above 0.25 mg $cm^{-3}$, a peak in such effects is likely to be observed at equimolar conditions. However, for dilute feedstocks (0.25 mg $cm^{-3}$ BSA), increase in the BSA:lysozyme molar ratio seems to gradually increase these effects.

Collection of the lowest bulk volumes at the end of operation at the

**Table 4.6: Heat of Desorption λ**

Experimental determination of the heat of desorption, λ, of **(a)** BSA and lysozyme in heterogeneous and **(b)** BSA in homogeneous solutions. Determination of λ was based on Equation 2.8 (Chapter 2).

**(a)**

| **Sample Code Number** | **Feedstock Concentration (mg $cm^{-3}$) BSA** | **Lysozyme** | $\lambda_{BSA}$ **(cal $mole^{-1}$)** | $\lambda_{lysozyme}$ **(cal $mole^{-1}$)** |
|---|---|---|---|---|
| 1a | 0.98 | 0.98 | 136 | 16 |
| 1b | 0.49 | 0.48 | 223 | 33 |
| 1c | 0.25 | 0.28 | 517 | 234 |
| 2a | 1.03 | 0.19 | 154 | 139 |
| 2b | 0.48 | 0.10 | 230 | - |
| 2c | 0.24 | 0.06 | 456 | - |
| 3a | 0.92 | 0.09 | 165 | - |
| 3b | 0.48 | 0.05 | 203 | - |
| 3c | 0.24 | 0.03 | 480 | - |

**(b)**

| **Sample Code Number** | **BSA Feedstock Concentration (mg $cm^{-3}$)** | $\lambda_{BSA}$ **(cal $mole^{-1}$)** |
|---|---|---|
| 1* | 0.99 | 136 |
| 2* | 0.48 | 216 |
| 3* | 0.24 | 422 |

highest BSA concentration (equivalent composition) and at equimolar conditions (equivalent BSA feedstock concentration) is in accordance with trends in foam volume under respective conditions (see Figure 4.3). Such effects have been attributed to maximisation in foam stability and therefore higher liquid uptake in foam. The effects of BSA-lysozyme interactions upon foam stability and drainage dynamics are also reflected in the observed rates of bulk volume reduction (Figures 4.6 and 4.7(a-b)). There is a direct correlation between the rates of bulk volume reduction (Figure 4.7(a-c)), $H_r$ (see Table 4.3) and lysozyme partition described by the fractionation index (Figure 4.2). Thus 0.5 and 1 mg $cm^{-3}$ BSA, the steepest reduction of bulk volume at equimolar conditions coincides with highest $H_r$ and $Fr_{BSA,lysozyme}$ values. Similarly, for feedstocks of 0.25 mg $cm^{-3}$ BSA highest $H_r$ and $Fr_{BSA,lysozyme}$ values at BSA:lysozyme molar ratios > 1 appear to yield the greatest reduction in bulk volume.

The stripping behaviour of BSA and lysozyme described in Figure 2.8 is in line with the enrichment profiles of the two proteins (Figures 4.1(a-b)). Low stripping factors for BSA coincide with high enrichment ratios. In contrast, poor lysozyme enrichment appears to yield high stripping factors. Trends in stripping factors presented in Figure 4.9(a-b) do not seem to fulfill such a correspondence between $e_i$ and $s_{t,i}$. In this latter Figure (4.9), a correlation between protein recovery (Figure 4.4) and stripping factor appears to exist, and indicates that efficient protein recovery causes steeper decreases in stripping factor. Thus, for a 0.5 mg $cm^{-3}$ BSA feedstock, maximisation in BSA and lysozyme recovery at and above equimolar conditions coincide with greatest reductions in $s_{t,BSA}$ and $s_{t,lysozyme}$ respectively. Observations in protein recovery at various BSA feedstock concentrations and BSA:lysozyme molar ratios appear to account for the values of residual protein ratio (r) (see

Table 4.5 and Equation 4.2). At low lysozyme concentrations some regression coefficients fall below 97% due to limitations in the analytical methods utilised, which could not detect concentration differences of 0-10 $\mu g\ cm^{-3}$ (Figure II4b, Appendix II).

The observed reductions in residual protein ratio would seem to obey first order kinetics (logarithmic reduction), although Equation 4.2 appears to yield $r_i < 1$ for $t = 0$. This latter implies that protein adsorption and removal from the liquid phase might be rapid in the first minutes of batch operation before it becomes logarithmic. Such an hypothesis could be confirmed by very frequent sampling from the liquid pool within the first 5 minutes of operation. Reduction of stripping factor and bulk volume also seem to follow a logarithmic decline. Such findings agree with studies by Bushell (1966); Grieves and Wang (1966); Rudin (1968); Sarkar et al. (1987), where the reduction in the mass of surfactant in the bulk phase is described by an equation equivalent to Equation 4.2. Grieves and Wang (1966) and Rudin (1968) stated that the coefficient $\kappa$ may depend upon factors such as surfactant concentration and gas flowrate. The present study has also shown that, in cases of mixed feedstocks characterised by protein-protein interactions, the composition of the feed plays an important role. It appears that in the case of a collector, such as BSA, the value of $\kappa$ is primarily determined by its concentration. However at comparable collector concentrations, feedstock composition becomes important. In contrast, in the case of a colligend, such as lysozyme, the value of $\kappa$ is likely to be determined by the stoichiometry of the mixture, ie collector:colligend ratio, and not its feedstock concentration.

High $\lambda$ values, observed at dilute solutions, imply large chemical potential difference which is the driving force for component transferring

between phases, and applies to other processes such as precipitation (Melander and Horvath (1977)). Significantly higher $\lambda_{BSA}$ values in comparison with $\lambda_{lysozyme}$ at similar bulk concentrations must be attributed to the poor foaming qualities of lysozyme. However, both proteins used in the current experiments exhibited very low $\lambda$ values when compared with those of other proteins such as LDH in chicken heart homogenate ($\lambda$=5530 cal $mol^{-1}$) (Charm (1973)) and 2% placental extract ($\lambda$=1890 cal $mol^{-1}$) (Sarkar et al (1987)). It is noteworthy however that the latter foaming mixtures comprise a complex multitude of proteins, characterised by high foamability and subsequent high $\lambda$ values. Investigation of the role that BSA-lysozyme interactions may play in determining the heat of desorption should involve very frequent sampling from the bulk phase during operation and the study of a wider spectrum of compositions. Limitations in the existing assay of lysozyme might be overcome by increasing the volume of loaded sample during HPLC analysis.

## 4.4 Concluding Summary

The addition of lysozyme in BSA solutions at pH 8.0 results in increase in the foam volume and BSA recovery, but reduction in BSA enrichment with respect to the control. Such phenomena are attributed to enhancement in foam stability due to complex formation between BSA and lysozyme under the buffer conditions applied, and appear to be maximal at equimolar conditions. In the presence of lysozyme variations in BSA enrichment and recovery appear to be primarily governed by the same factors as in homogeneous solutions. In contrast, lysozyme partition in the foam, described by the fractionation index and lysozyme recovery, is most likely to be dictated by the BSA: lysozyme molar ratio in the foaming solution with maximal effects seen at equimolar conditions. However, at

dilute feedstocks (0.25 mg $cm^{-3}$ BSA) it appears that the predominant factor is BSA concentration in the feed and not feedstock composition, with maximal effects seen above equimolar composition.

The observed variations in enrichment, foam volume and recovery in the foam are directly reflected in the quality of the residual bulk phase. Dynamic changes in the bulk phase during batch foaming can be described by first order kinetics. Maximal volume reduction and protein depletion in the bulk phase occur at the most concentrated feedstocks for comparable compositions, and at equimolar conditions for comparable BSA concentrations with the exception of dilute feedstocks. As in the case of foam, dynamic changes in the bulk phase of dilute feedstocks appear to be most profound at BSA: lysozyme molar ratios > 1.

The above findings suggest that protein recovery in foams, generated by the synergistic action of two components, is optimal at solution conditions where protein-protein association is maximal. In contrast, foam fractionation of a solute from a solution, where solutes generate foam synergistically, should be undertaken at dilute conditions, where the concentration of the most foaming active component is the driving force for partition.

# *CHAPTER 5*

## *BSA-LYSOZYME INTERACTIONS DURING CONTINUOUS FOAM PRODUCTION*

### 5.1 P r e f a c e

Chapters 3 and 4 have well established the importance of electrostatic interactions between BSA and lysozyme upon foam stability and protein recovery. They have also demonstrated that such interactions are dependent upon interactive stoichiometry and ionic concentration. The present chapter aims both to characterise the dynamic effects of such interactions in continuous foaming and exploit the notion of foam components as mobile ion-exchange media.

As in the case of fermentation, where the ability of a process to overcome a disturbance is studied with respect to its dynamic recovery from an external pulse, a study was undertaken to examine the deviation from steady-state foam production from BSA solutions when lysozyme is introduced as a unit impulse. The subsequent disturbance inflicted upon foam production and quality was indicative of the impact the presence of lysozyme had upon the foaming capacity of the system. This impact was studied with respect to ionic strength, protein composition and liquid residence time. The ability of the system to recover and return to initial levels of steady-state operation was assessed by recording the dynamic return of foam characteristics to levels prior to the pulse of lysozyme.

Study of the efficiency of BSA as a carrier for lysozyme into the foam under various operating conditions enabled comparison with analogous phenomena in ion-exchange. As a result, this chapter introduces the concept of foam positive proteins acting as mobile ion-exchange carriers when challenged by proteins of opposite charge and poor foaming qualities, during steady-state foam production.

## 5.2 Experimental Description

Steady-state foam production from homogeneous BSA feedstocks was conducted in the 1,600 $cm^3$ foam tower illustrated in Figure 2.3 (Chapter 2). Feed was introduced into the liquid pool with the feed element through the top of the tower. Continuous foam production from 0.5 mg $cm^{-3}$ BSA solutions, prepared in sodium phosphate buffer, pH 8.0 (see Section 4.2 in Chapter 4), was allowed to attain steady-state conditions by following the start-up procedure described in Chapter 2 (Subsection 2.3.3). It was found that an average time of 90 minutes was required to reach steady-state operation. The inlet volumetric flowrate was 10 $cm^3$ $min^{-1}$, unless stated otherwise, and the volume of the liquid pool was kept constant at 400 $cm^3$. Thus a liquid residence time was maintained constant at 40 min (unless the inlet flowrate was varied) and the height of the foam bed was always 47-48 cm. Nitrogen was sparged at a rate of 100 $cm^3$ $min^{-1}$. The combination of feed input and gas sparging enabled perfect mixing in the pool, regularly checked by comparing the protein composition of simultaneous samples from the pool and the bottom effluent. The operating temperature was maintained at 20 $^{\circ}C$, and foam conductivity was continuously monitored.

Steady-state foam production was interrupted by a pulse of concentrated lysozyme solution forcefully introduced into the liquid pool through the sampling port situated 2.5 cm above the foam-liquid interface (SP 1 in Figure 2.3). Prior to this, an identical volume of BSA solution was removed from the pool in order to maintain a constant volume of the liquid pool. Lysozyme solutions were prepared in identical buffer conditions as those of BSA at a constant concentration of 5 mg $cm^{-3}$(dry w $v^{-1}$). The preparation procedure followed is described in Chapter 4 (Section 4.2). The volume of the pulse was determined by experimental design such that a predetermined BSA: lysozyme molar ratio at the moment of the pulse introduction was achieved. Calculations were based on the dry w

$v^{-1}$ BSA concentration in the feed and the lysozyme preparation.

Changes in foam quality and performance, caused by the imposed pulse of lysozyme were studied with respect to buffer ionic strength, BSA: lysozyme molar ratio and liquid residence time. Under conditions of varied ionic strength, the BSA: lysozyme molar ratio was maintained constant, while at constant ionic strength it was set at values above and below unity. Variations in the liquid residence time were conducted by varying the feed flowrate under comparable conditions of buffer molarity and lysozyme load.

Continuous monitoring of foam conductivity enabled determination of changes in foam density associated with the pulse of lysozyme. Experiments also involved the accurate detection of changes in the volumetric flowrate of foam and its protein composition. Foaming continued until the recorded conductivity, foam volumetric flowrate and BSA concentration in foam levelled off and asymptotically reached the steady-state values observed prior to lysozyme injection.

In tandem with foam sampling, simultaneous collection of samples from the pool and the bottom effluent was undertaken at selected time intervals. These intervals were more frequent during the first hour following the lysozyme pulse. The protein content of these samples was determined. Samples taken from the bottom effluent also enabled determination of variations in the bottoms flowrate due to the addition of lysozyme.

Foam and bottoms collections were operated in three stages. These comprised the 40 min of steady-state operation prior to lysozyme addition (Stage 1), a period after lysozyme injection (Stage 2) which was 10 minutes longer than the residence time, and the final stage of system recovery (Stage 3). Collection was followed by volume and protein content determination. In the case of foam, foam fractions collected during these

three stages were pooled and the total volumes and protein concentrations were determined. Protein concentrations were determined by HPLC analysis (see Chapter 2) and based on calibrations presented in Figures II3(a-b) and II4(a-b) in Appendix II.

## 5.3 Results and Discussion

Changes in foam quality and process performance caused by a pulse of lysozyme are described in terms of reduced foam conductivity ($H_r$; Equation 1.6), BSA concentration in foam, foam volumetric flowrate ($Q_F$), BSA mass flowrate ($m_{BSA}$; Equation 5.1), lysozyme enrichment ($e_{lysozyme}$; Equation 3.1), fractionation index ($Fr_{BSA,\ lysozyme}$; Equation 3.6) and BSA and lysozyme recovery in foam ($R_{BSA}$ and $R_{lysozyme}$ respectively). At steady-state conditions $R_{BSA}$ is described by Equation 3.3, whilst at continuous unsteady-state foaming $R_{BSA}$ is denoted by Equation 5.2. Lysozyme recovery describes the mass recovered in foam as a percentage of the applied pulse.

The mass flowrate of protein i ($m_i$) is defined by Equation 5.1:

$$m_{i,J} = c_{i,J}\, Q_J \qquad \text{(Equation 5.1)}$$

where: $m_{i,J}$ is mass flowrate of protein i in stream J; $m_i$[=] mg $min^{-1}$

$c_{i,J}$ is concentration of protein i in stream J; $c_{iJ}$[=] mg $cm^{-3}$

$Q_J$ is volumetric flowrate of stream J (J=O,F,B for feed, foam and bottoms respectively); $Q_J$[=] $cm^3$ $min^{-1}$

Mass flowrate trends are representative of trends in protein recovery for equivalent feeds. At non steady-state operations collection of volume $V_J$ during a period of time t gives the average volumetric flowrate $\bar{Q}_J$. Equation 5.1 then yields an average mass flowrate $\bar{m}_{i,J}$.

In continuous steady-state operations protein recovery in foam can be described by Equation 3.3 where $V_F$ and $V_0$ may be replaced by $Q_F$ and $Q_0$

respectively. In non-steady-state operations average protein recovery during a certain period of time t is described by Equation 5.2:

$$\bar{R}_i(\%) = \bar{m}_{i,F}/\bar{m}_{i,0}(\%) \qquad \text{(Equation 5.2)}$$

The dynamic response of BSA foam to a 10 $cm^{-3}$ pulse of lysozyme under varied ionic strength (5 to 40 mM phosphate buffer) and constant liquid residence time ($r_D$=40 min) are described in Figures 5.1(a-d)-5.5. Figure 5.1(a-d) describes the observed variations in reduced foam conductivity ($H_r$) with time, prior and after the pulse of lysozyme, at varied ionic strengths. The $H_r$ profile can be divided into three distinct stages. Stage 1 illustrates the constant conductivity readings at steady-state foam production from a BSA feedstock. Stage 2 describes the conductivity response to the addition of lysozyme for a period of 60 minutes following the pulse. Thus, a stepwise increase in foam conductivity occurred within two minutes of the pulse and was followed by a shallow arcing in values for approximately 40 min (the duration being equal to liquid residence time). In Stage 3, which corresponds to the recovery of the system from the disturbance and a return to its initial state, conductivity readings proceeded to decline in an exponential-like manner. The magnitude of the observed changes in foam conductivity depended upon the ionic strength of the solution, and was pronounced at low ionic concentrations (5, 10 and 25 mM phosphate buffer). Buffer molarities in excess of 25 mM effectively minimised the phenomena observed. Fluctuations in BSA concentration in foam due to the pulse of lysozyme (Figure 5.2(a-d)) can be divided into three stages equivalent to those in Figure 5.1(a-d). BSA concentration was constant during steady state foaming (Stage 1), but rapidly decreased following the addition of lysozyme and remained low for approximately 40 min (Stage 2). In Stage 3, BSA concentration progressively increased and approached the levels

observed in Stage 1. Such effects were more pronounced at low ionic strength and there was only a shallow decrease at 40 mM. It seems that concentration "recovery" following the pulse of lysozyme was more sluggish where the effects of the imposed disturbance were more profound (low buffer molarity). Contrary to concentration, BSA mass flowrate in foam ($m_{BSA,F}$) benefited from the addition of lysozyme as Figure 5.3(a-d) indicates, and this was more pronounced at low ionic strength. The pattern and stages of the observed changes in $m_{BSA,F}$ are equivalent to those of $H_r$ in Figure 5.1(a-d). The importance of ionic strength in BSA partition into foam, during periods of operation prior to and during the presence of lysozyme is depicted in Figures 5.4(a-b). It can be seen (Figure 5.4a) that at steady-state foaming (Stage 1), increasing buffer molarity corresponded with a decrease in BSA concentration in foam, but favoured increased foam volumetric flowrates. As a result, BSA mass flowrate in the foam was greater at high ionic strength as illustrated by the lower plot in Figure 5.4b. The presence of lysozyme in the liquid pool of BSA (Stage 2), resulted in a considerable increase in BSA average mass flowrate at low ionic strength, but effects gradually weakened at higher buffer molarity (upper plot in Figure 5.4b). Lysozyme recovery in Stage 2 was favoured at low ionic strength, as shown in Figure 5.5, but increase in buffer molarity appeared to be detrimental. Lysozyme recoveries were similar in both 5 and 10 mM buffers.

Variations in the volume of the pulse of lysozyme applied in BSA liquid pools at equivalent buffer molarity (10 mM) and residence time ($r_D$ = 40 min) resulted in different compositions of the liquid pool at the moment of the addition as Table 5.1 shows. Thus BSA: lysozyme molar ratios included values above and below unity. The observed dynamic changes in foam, namely $H_r$, $c_{BSA,F}$ and $m_{BSA,F}$, were in line with those described in Figures 5.1b, 5.2b and 5.3b. Table 5.2(a-b) describes the recovery of

**Figure 5.1: Profile of the Conductivity of Foam Prior to and Post Lysozyme Addition**

Variations in reduced foam conductivity ($H_r$) with time at Stages 1, 2 and 3 due to the imposed pulse of lysozyme. A constant amount of lysozyme was added (48 mg) at varied concentrations of sodium phosphate buffer, namely **(a)** 5 mM, **(b)** 10 mM, **(c)** 25 mM and **(d)** 40 mM. The liquid residence time was 40 minutes.

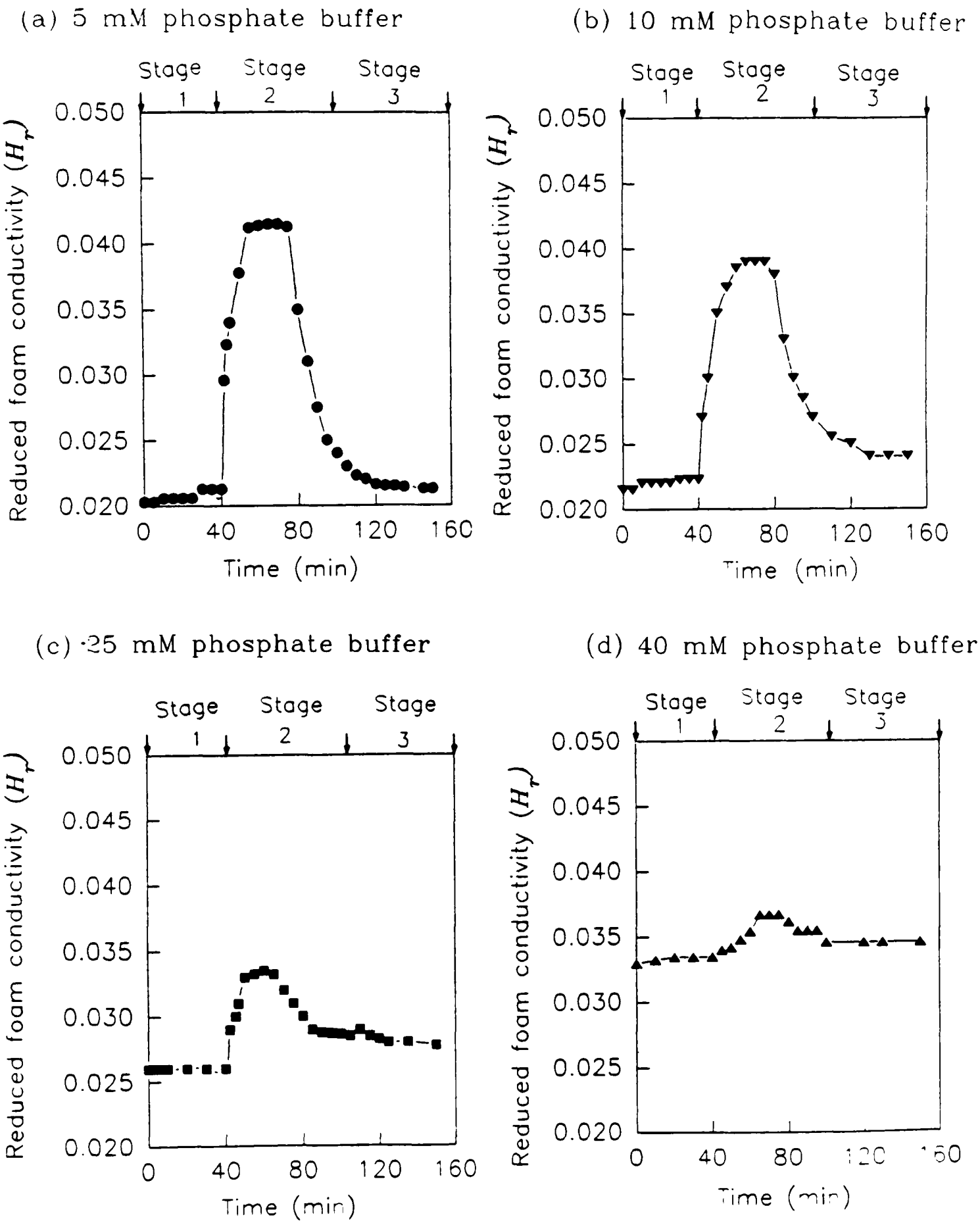

**Figure 5.2: BSA Concentration in Foam Prior to and Post Lysozyme Addition**

Variations in BSA concentration in foam ($c_{BSA,F}$) with time at Stages 1, 2 and 3 due to the imposed pulse of lysozyme. A constant amount of lysozyme was added (48 mg) at varied concentrations of sodium phosphate buffer, namely **(a)** 5 mM, **(b)** 10 mM, **(c)** 25 mM and **(d)** 40 mM. The liquid residence time was 40 minutes.

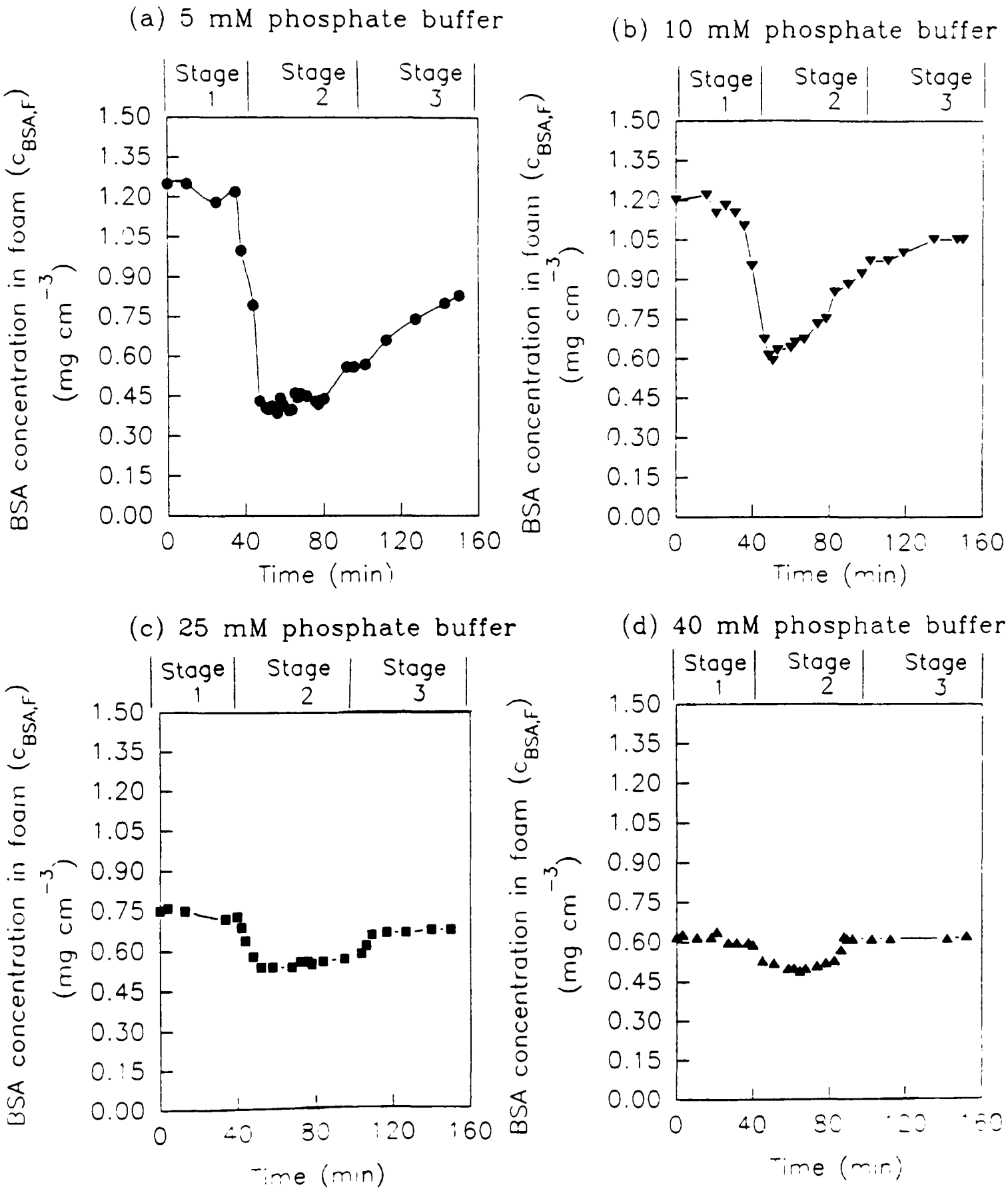

**Figure 5.3: BSA Mass Flowrate in Foam Prior to and Post Lysozyme Addition**

Variations BSA mass flowrate in foam ($m_{BSA,F}$) with time at Stages 1, 2 and 3 due to the imposed pulse of lysozyme. A constant amount of lysozyme was added (48 mg) at varied concentrations of sodium phosphate buffer, namely **(a)** 5 mM, **(b)** 10 mM, **(c)** 25 mM and **(d)** 40 mM. The liquid residence time was 40 minutes.

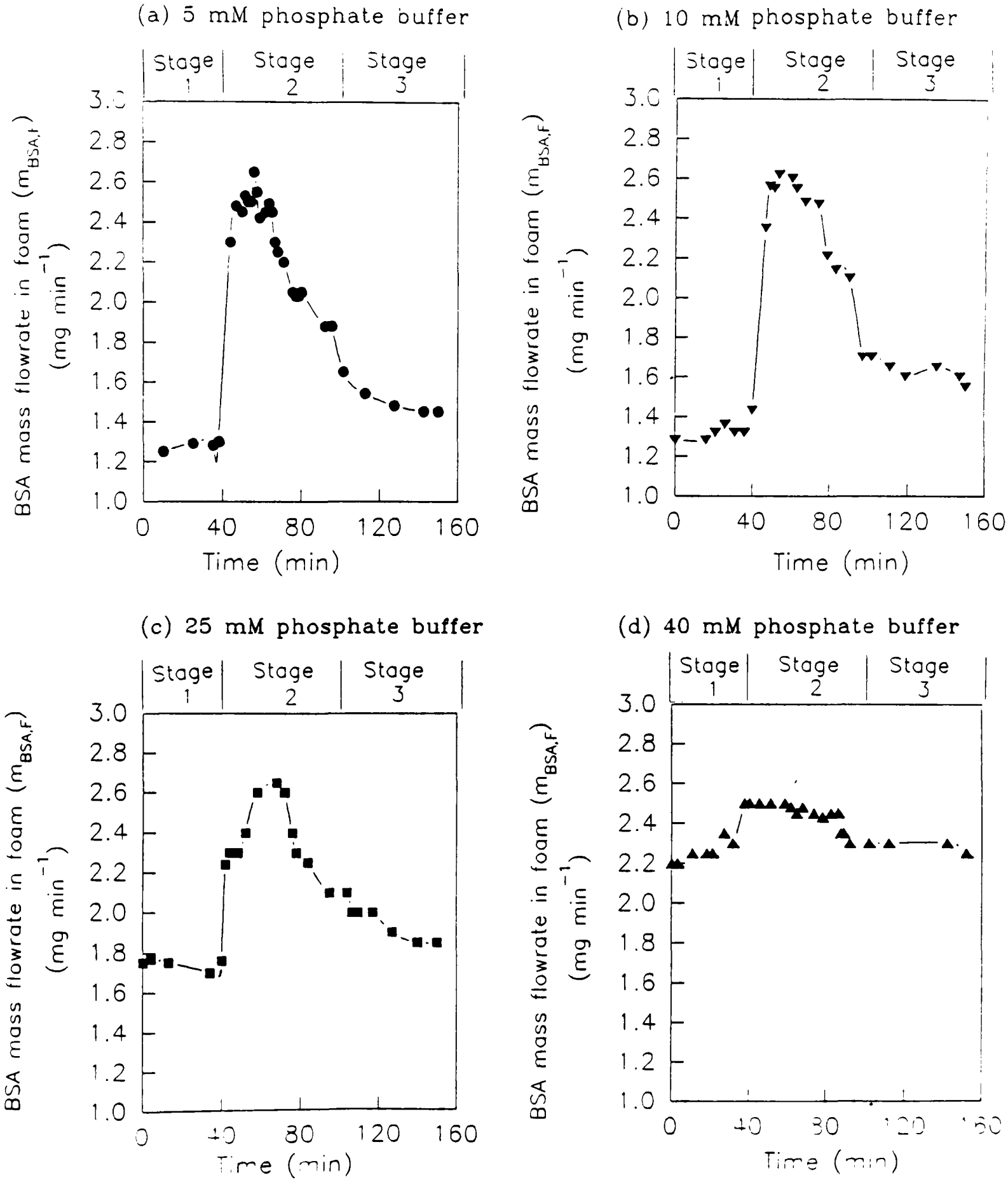

**Figure 5.4: Effects of Buffer Molarity upon BSA Partition in Foam**

Description of the effects of buffer molarity upon **(a)** BSA concentration in foam ($c_{BSA,F}$) and foam volumetric flowrate ($Q_F$) during steady-state operation at Stage 1, and **(b)** increase in average BSA mass flowrate in foam ($\bar{c}_{BSA,F}$) during Stage 2 (upper plot) when compared with $m_{BSA,F}$ at Stage 1 (lower plot). A constant amount of lysozyme was added (48 mg) at varied concentrations of sodium phosphate buffer, namely 5 mM, 10 mM, 25 mM and 40 mM. The liquid residence time was 40 minutes.

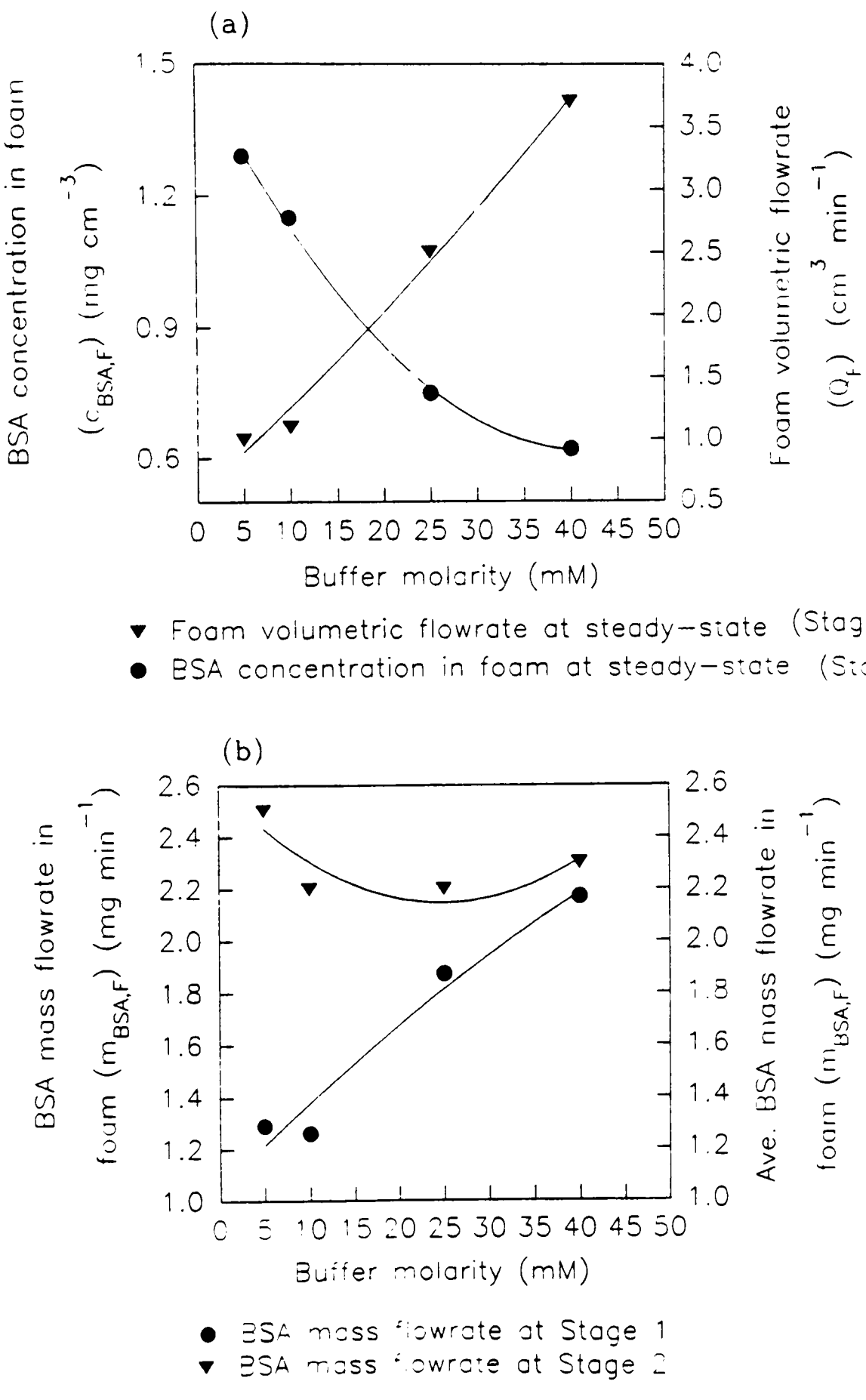

**Figure 5.5: Effects of Ionic Strength upon Lysozyme Recovery in Foam**

Dependence of lysozyme recovery at Stage 2, namely the mass of lysozyme recovered in foam expressed as a percentage of the injected load, upon the sodium phosphate buffer molarity for comparable pulses of lysozyme of 10 $cm^3$ (48 mg) and liquid residence time of 40 minutes.

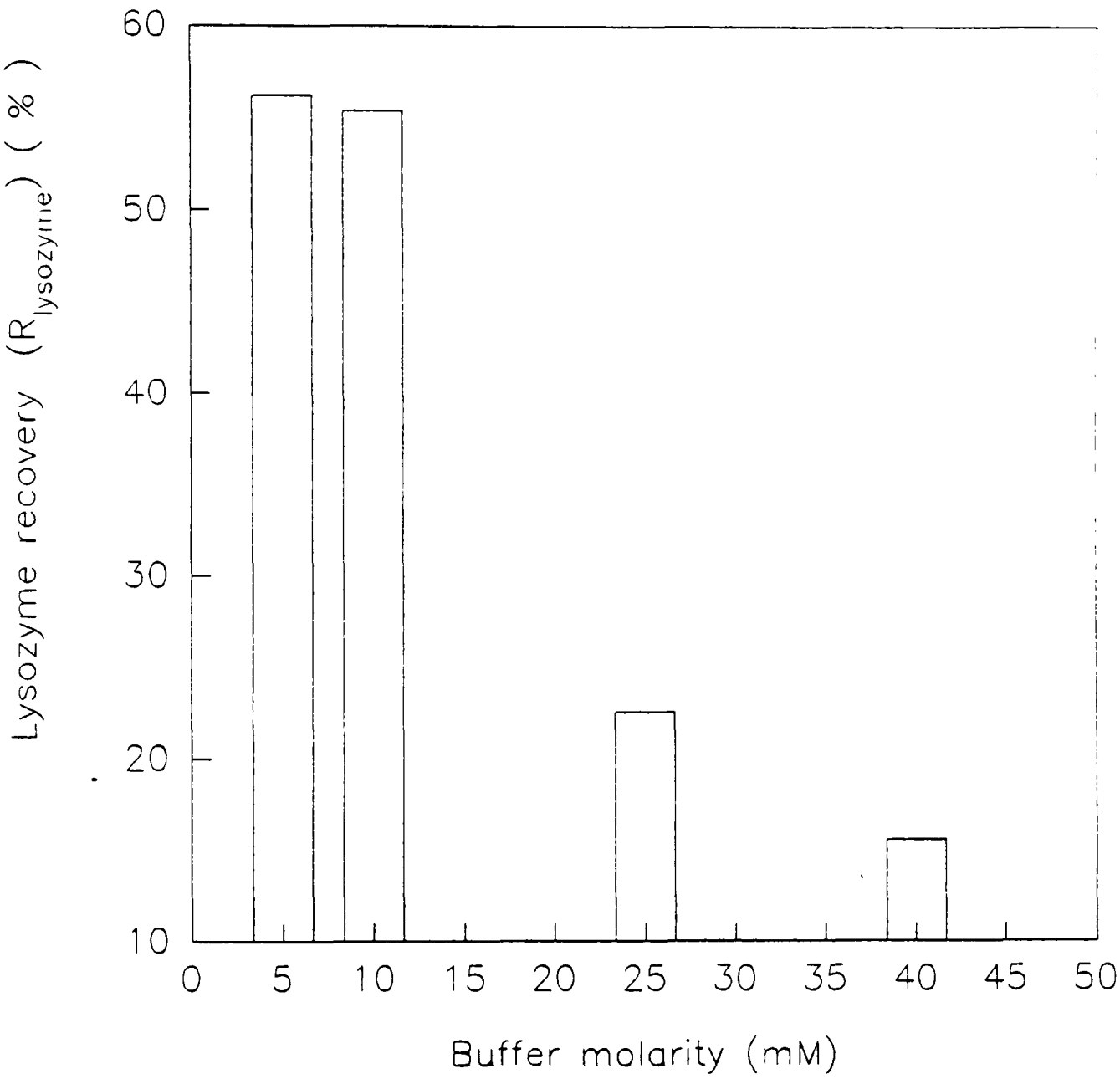

lysozyme in the foam at Stages 2 and 3 respectively with varied pulses of lysozyme. It appears that maximal lysozyme recovery in the foam during Stage 2 (Table 5.2a) occurred when 48 mg lysozyme were injected, and marginally lower recovery was observed for half of this quantity (ie 24 mg lysozyme). In both cases recoveries were higher than 50%. However lysozyme recovery was significantly limited (approximately 25%) when 96 mg of lysozyme were injected. Maximal lysozyme recoveries in foam coincided with minimal losses in the bottoms. Table 5.2b shows that the amount of lysozyme present in the foam at Stage 3 was higher at the greatest lysozyme pulse. Figure 5.6 describes the time course of lysozyme enrichment and fractionation index in foam at Stages 2 and 3, for 24 and 96 mg of lysozyme pulse. Lysozyme enrichment and fractionation index refer to protein concentration in the pool immediately after the lysozyme pulse. In both cases, it can be seen that the peak of lysozyme enrichment occurred at Stage 2, and maximal $e_{lysozyme}$ values were achieved with 24 mg lysozyme. Stage 2 was also characterised by reduction in fractionation index for both lysozyme pulses. However, the difference between the observed $Fr_{BSA,lysozyme}$ for the two lysozyme loads was not as profound as that in the case of $e_{lysozyme}$. In Stage 3 increase in the values of fractionation index occurred. Such increase was faster for the lowest load of lysozyme. Figure 5.7 describes the rate of decline in lysozyme concentration in the liquid pool during Stage 2 for pulses of lysozyme of 24 and 96 mg. The decline is described by the fraction of lysozyme concentration in the pool at selected time intervals relative to that at the pulse injection. The rate of reduction was faster at the lowest lysozyme pulse, and it appears that lysozyme was virtually all removed within 40 min, ie within time equal to $r_D$.

The influence of the residence time ($r_D$) upon BSA and lysozyme recovery is described in Table 5.3, for comparable pulses of lysozyme (10

**Table 5.1: Protein Concentration in the Liquid Pool at Varied Lysozyme Pulse Volumes**

A description of the experimental conditions immediately after the injection of various volumes of lysozyme in the liquid pool of BSA solutions in 10 mM sodium phosphate bubber. The concentration of the stock lysozyme solution was 4.8 mg $cm^{-3}$. The feed volumetric flowrate was 10 mg $cm^{-3}$. All protein concentrations were determined with HPLC analysis.

| Pulse Volume Molar ($cm^3$) | Pulse mass (mg) | Liquid Pool Concentration at Start of Stage 2 (mg $cm^{-3}$) | | BSA:Lysozyme Ratio |
|---|---|---|---|---|
| | | BSA | lysozyme | |
| 5 | 22.4 | 0.40 | 0.06 | 1.42 |
| 10 | 48.0 | 0.37 | 0.12 | 0.66 |
| 20 | 96.0 | 0.37 | 0.24 | 0.33 |

**Table 5.2 : Lysozyme Distribution at Top and Bottom Products at Varied Lysozyme Pulse Volumes**

Effects of the size of the pulse of lysozyme upon the recovery of lysozyme in foam at **(a)** Stage 2 and **(b)** Stage 3 of operation. The amount of lysozyme in the bottom stream is refered to as a loss. Both lysozyme recovery and loss are expressed as percentages of the original load. The buffer molarity was 10 mM and the inlet flowrate was 10 $cm^3$ $min^{-1}$.

**(a) Stage 2**

| Pulse Mass (mg) | Lysozyme Recovery† (%) | Lysozyme Losses (%) |
|---|---|---|
| 22.4 | 53.75 ( 12.10 ) | 45.35 |
| 48.0 | 57.40 ( 27.55 ) | 30.85 |
| 96.0 | 24.50 ( 24.01 ) | 53.10 |

**(b) Stage 3**

| Pulse Mass (mg) | Lysozyme Recovery (%) | Lysozyme Losses (%) |
|---|---|---|
| 22.4 | - | - |
| 48.0 | 10.0 | - |
| 98.0 | 17.9 | 6.5 |

† Values in parentheses represent the total mass (mg) of lysozyme in foam.

**Figure 5.6: Effects of the Size of Lysozyme Pulse upon its Time-Course Partition in Foam**

The time-course (Stages 2 and 3) variations in lysozyme enrichment and fractionation from BSA are described for lysozyme pulses of 5 $cm^3$ (24 mg) and 20 $cm^3$ (96 mg). Lysozyme enrichment and fractionation refer to lysozyme and BSA concentration in the pool at the moment of pulse application. The experimental conditions were the same as in Table 5.2(a-b).

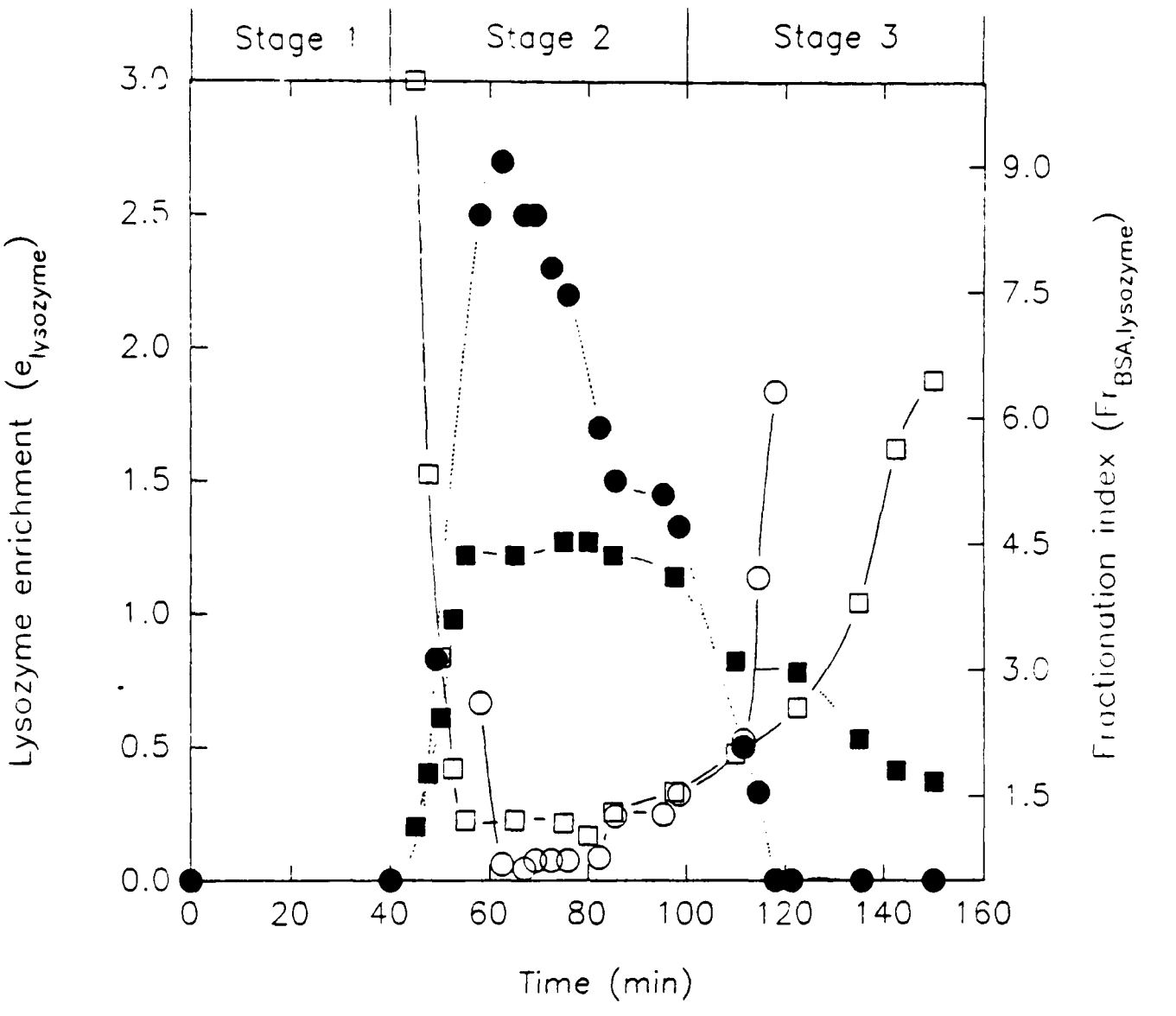

**Figure 5.7: Effects of the Size of Lysozyme Pulse upon the Rate of Decline of Lysozyme Concentration in the Liquid Pool.**

The rate of decline in lysozyme concentration in the liquid pool at Stages 2 is described for lysozyme pulses of 5 $cm^3$ (24 mg) and 20 $cm^3$ (96 mg). The experimental conditions were the same as in Table 5.2(a-b).

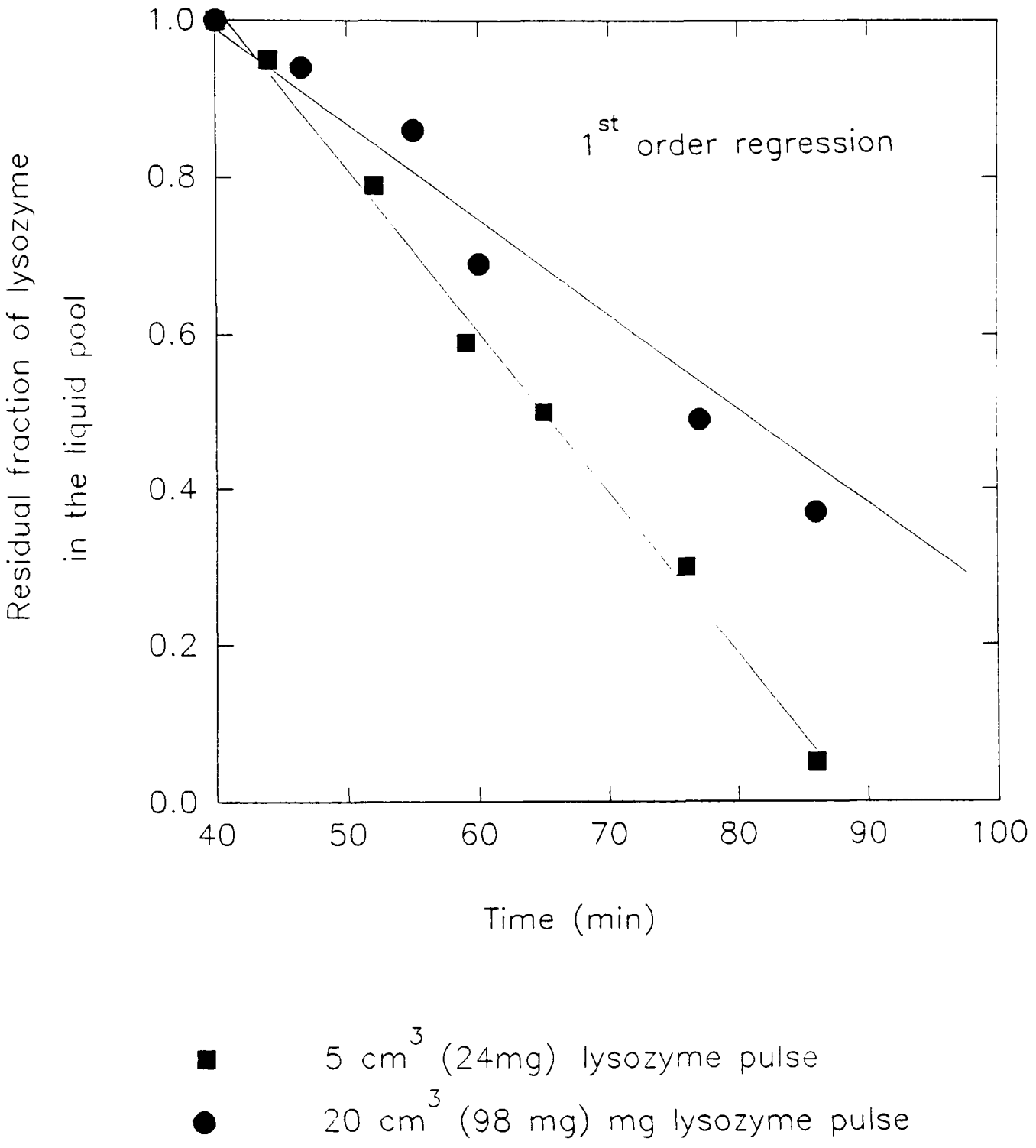

$cm^{-3}$) and 10 mM buffer. The feed flowrates were 10 and 4.5 $cm^3$ $min^{-1}$ for $r_D$ values of 40 and 90 minutes respectively. It can be seen that at all the stages of operation, the recovery of BSA was highest at the longest residence time. Under the same conditions the recovery of lysozyme was significantly improved at Stage 2 and only traces of the protein were detected in the foam at Stage 3.

In conclusion, disruption of the steady-state foam production from homogeneous BSA solutions by a pulse of lysozyme results in changes in foam quality. It appears that, during a period of time approximately equal to the liquid residence time, foam density (measured as conductivity) and BSA mass flowrate increase while BSA concentration in foam decreases. Such changes are likely to be more pronounced at low buffer molarity for comparable lysozyme pulses. It is also clear that lysozyme recovery in foam is favoured by low ionic strength. For the same buffer molarity and residence time, the stoichiometrical representation of BSA and lysozyme in the liquid pool at the moment of the pulse appears to be very important in lysozyme partition into the foam. Lysozyme recovery is enhanced at BSA: lysozyme molar ratios in the proximity of unity. Comparable pulses of lysozyme and buffer molarities appear to yield more efficient lysozyme recovery at longer residence times.

The observed variations in foam conductivity following the injection of lysozyme (Figure 5.1(a-d)) clearly express changes in both foam stability and density. The presence of lysozyme in the liquid pool of BSA triggers co-operative electrostatic interactions between the two proteins which enhance foam stability and reduce drainage and coalescence. This effect is observed in Stage 2 where the pool concentration of lysozyme gradually decreases due to its synergistic partition into the foam and the continuous feed which renews the content of the liquid pool. These effects cease when lysozyme is washed out of the pool in a period of time

**Table 5.3: Effects of Residence Time upon BSA and Lysozyme Recovery in Foam**

Influence of the residence time ($r_D$) upon the recovery of BSA and lysozyme in the foam at Stages 1,2 and 3 for a pulse of 10 $cm^3$ (48 mg) lysozyme at 10 mM sodium phosphate buffer. At Stage 1, $R_{BSA}$ is described by Equation 3.3, while at Stages 2 and 3 $\bar{R}_{BSA}$ is described by Equation 5.2. The recovery of lysozyme refers to the mass of lysozyme collected in the foam and expressed as a fraction of the initial load.

| Stages | BSA Recovery (%) | | Lysozyme Recovery (%) | |
|---|---|---|---|---|
| | $r_D$=40 min | $r_D$=90 min | $r_D$=40 min | $r_D$=90 min |
| 1 | 27.4 | 49.8 | - | - |
| 2 | 44.0 | 67.3 | 57.4 | 77.4 |
| 3 | 24.6 | 51.0 | 10.0 | 2.5 |

approximating to the liquid residence time, and foam production becomes dependent upon BSA alone again (Stage 3). The magnitude of such electrostatic interactions appears to be inevitably impaired by ionic competition at high buffer molarities. The observed increase in foam conductivity appeared to coincide with a physical transition from large to smaller bubbles in Stage 2 and a subsequent gradual return to larger bubbles in Stage 3. In Stage 2 foam was thick and resistant to mechanical breakage. These changes in bubble size were pronounced at 5 and 10 mM, less so at 25 mM and indistinct at 40 mM. Changes in foam conductivity were directly reflected in fluctuations in the volumetric flowrate of collected foam. Stage 2 was characterised by an increase in the volume of foam fractions collected at identical time intervals. The magnitude of this increase was greatest at the highest ionic strengths. At Stage 3 fraction volumes gradually declined to approach values observed prior to the injection of lysozyme.

The observed decrease in BSA concentration in foam following the pulse of lysozyme (Figure 5.2(a-d)) is associated with increased foam stability in the presence of lysozyme as Figure 5.1(a-d) indicates. It could also be attributed to reduced availability of space for single BSA molecules to attach at the gas-liquid interface because of competition with BSA-lysozyme complexes. The profile of BSA foam concentration at Stages 1,2 and 3 is also representative of that of BSA enrichment since the feed concentrations were equivalent (see Equation 3.1). Gradual reduction in the magnitude of such changes at higher ionic strength due to ionic interference parallels respective changes in foam conductivity. The resultant behaviour of protein concentration and foam volumetric flowrate is responsible for the observed trend in BSA mass flowrate in foam (see Figure 5.3(a-d)). This response is representative of that of BSA recovery since equivalent feed mass flowrates were applied throughout

experimentation. At low ionic strength, the improved BSA recovery at Stage 2, contrary to reduction in enrichment, must be attributed to the increased volumes of foam produced under conditions of enhanced foam stability influenced BSA-lysozyme electrostatic interactions. The results imply that changes in foam volume dominate those observed for BSA enrichment, and ultimately determine the recovery of the process.

The observed trend in BSA concentration and mass flowrate in foam, and foam volumetric flowrate at Stage 1 (see Figure 5.4(a-b)) must be attributed to bubble dynamics and drainage at varied ionic strengths. At low ionic strength, foam bubbles tend to be larger and less uniform in size. This behaviour was clearly observed during experimentation. Large bubbles are associated with faster drainage and lower liquid hold-up, and therefore lead to higher protein enrichment in foam. The size of a gas bubble produced through a porous frit is proportional to the square root of the surface tension of the foaming solution (Leonard and Lemlich (1965)). Any decrease in the ionic strength of the foaming sample results in an increase in its surface tension, and the subsequent formation of large bubbles. The trend observed herein is in agreement with reports of other workers (Brown et al. (1990)). In the presence of lysozyme at Stage 2, the considerable increase in $\bar{m}_{BSA,F}$ at low ionic strength (see upper plot in Figure 5.4b) must be associated with the formation of more stable foam due to strong association between BSA and lysozyme molecules.

Minimisation of interference in the formation of BSA-lysozyme complexes at low buffer molarity is also the reason for the observed high lysozyme recovery at Stage 2 for 5 and 10 mM phosphate buffer (Figure 5.5). Such behaviour highlights analogies with ionic exchange adsorption, since it appears that BSA acts as the mobile carrier for lysozyme. Collection is therefore based on electrostatic interactions, which may be severely limited in the presence of ionic competition.

The range of buffer molarities applied in these experiments did not confirm the existence of an intermediate ionic concentration where maximal lysozyme recovery occurs, as suggested in Table 3.5 in Chapter 3. Conductivity measurements of the phosphate buffer solutions applied in the present set of experiments were found to lie below that of 25 mM citrate buffer, pH 6.0 (see Figure II10(a-c)). However, further experimentation in the range of 0-5 and 10-25 mM sodium phosphate buffer, pH 8.0 might reveal that there is an optimal ionic environment for the collection of lysozyme in the foam.

The importance of stoichiometry in lysozyme recovery at Stage 2 is highlighted by maximal lysozyme recoveries (approximately 54-58%, see Table 5.2a)) observed at bulk phase compositions close to equimolar conditions at the introduction of lysozyme (see Table 5.1). The importance of equimolar representation of BSA and lysozyme in maximisation of lysozyme partition and recovery in foam is in line with findings presented in Chapter 4 for batch operations. As in Chapter 4, the efficient recovery of lysozyme in the foam was handicapped by an excess of lysozyme in the bulk phase created by a 20 $cm^3$ (96 mg) pulse. Under such conditions, the presence of lysozyme in both the foam and bottoms at Stage 3 (Table 5.2b), where the protein would be expected to be eliminated from the bulk phase, is likely to be associated with occurrence of internal reflux enriched in lysozyme. Liquid containing lysozyme, which did not interact with BSA due to the lack of stoichiometric demand, drains back into the liquid pool. This prolongs the presence of lysozyme in the system and its effects upon foam formation.

Higher enrichment ratios at the lowest lysozyme load in Stage 2 (Figure 5.6) must be associated with high lysozyme recovery in the foam as shown in Table 5.2a. The latter can also explain the lowest values in fractionation index obtained under the same conditions. Slow increase with

time in the fractionation index at Stage 3, for the highest lysozyme load (96 mg), is attributed to prolonged lysozyme activity at Stage 3 (see Table 5.2b). Faster rates of reduction in the bulk concentration of lysozyme for the smallest lysozyme pulse (Figure 5.7) must also be attributed to differences in its uptake in the foam since the residence time was the same for both experiments.

The foregoing evidence indicates that, at constant buffer molarity (10 mM) and residence time ($r_D$ = 40 min) the capacity of BSA to act as carrier for lysozyme in foam reaches a maximum limit. Further increase in the amount of injected lysozyme is not reflected in an increase in foam recovery. Thus, the maximal capacity of 0.4 mg $cm^{-1}$ BSA solution (the concentration in the pool at steady-state conditions) is 25 mg extracted lysozyme. This observation is in line with similar capacity profiles of ion exchangers for specific proteins.

The beneficial effects of prolonged residence time upon the recovery of BSA in the foam and together with the extraction of added lysozyme (Table 5.3), are likely to be associated with prolonged contact of the liquid pool with sparged gas. Analogies between the present process and protein recovery by ion-exchange draw attention to the importance of contact time in reaching equilibrium in protein binding onto the matrix. In continuous ion-exchange processes such equilibrium is achieved by regulating the flowrate for a fixed bed of constant cross-sectional area. The importance of residence time in protein enrichment and recovery are discussed in more detail in Chapter 6.

## 5.4 Concluding Summary

The disruption of steady-state production of BSA foam at pH 8.0 by application of a unit impulse of lysozyme is associated with the stabilising action of BSA-lysozyme complexes promoted by electrostatic

interactions. The magnitude of such a disruption appears to be greatest at low ionic strength (minimal ionic interference), equimolar protein representation, and prolonged residence time in the liquid pool.

Deviation from steady-state conditions is characterised by a rapid increase in foam volumetric flowrate and BSA recovery, which coincides with reduction in BSA enrichment. During these changes a percentage of the injected lysozyme was recovered in the foam, and this was highest at low ionic strength, equimolar conditions and prolonged residence time. The duration of these phenomena was dictated by the liquid residence time, which determines the wash-out time of lysozyme. A period of system recovery followed, during which foam quality and performance returned to levels prior to lysozyme pulse. Such a return was slower under conditions of strong BSA-lysozyme binding.

During the presence of lysozyme in the liquid pool, BSA behaved as a carrier for lysozyme analogous to a mobile ion-exchanger. Thus, as in the case of protein recovery by ion-exchange adsorption, buffer molarity, contact time and composition were important operational features. Maximal recovery was favoured at low ionic presence and prolonged residence time, and was related to the saturation capacity of BSA.

# CHAPTER 6

## CONTINUOUS FOAM PRODUCTION FROM CLARIFIED BREWER'S YEAST EXTRACT

### 6.1 Preface

Most feasibility studies of the development of foam fractionation for protein recovery from dilute feedstocks have used model systems (commonly BSA) to empirically determine the laws of foam formation and fractionation. Such studies have also included research towards optimisation and modelling of operation (see Section 1.3 in Chapter 1). However it is important to recognise that single protein systems cannot account for the complexity of factors associated with the presence of a number of other components. Additionally, optimisation of foam fractionation of non-biological surfactants cannot necessarily be applicable to protein systems because of the unique nature of proteins and their sensitivity to gas-liquid interfaces.

The present study has clearly shown (see Chapters 4 and 5) that the presence of lysozyme in BSA solutions significantly altered foam performance under appropriate conditions as a result of intermolecular interactions. It also highlighted the influence of feedstock composition upon the recovery of lysozyme, and demonstrated the role of BSA as an ion-exchange carrier for lysozyme to the foam phase.

Experience with BSA-lysozyme binary systems inspired the study of a complex feedstock. Disrupted and clarified waste brewer's yeast was selected for continuous foaming studies. Such extracts have been shown to possess foaming and whipping properties of interest to the food processing industries. Foam fractionation was considered to be a possible selective means of isolating proteins which would improve on more conventional methods of adsorption by liquid-liquid extraction (Flanagan and Lyddiatt

(1991)). Experimental design focused on the investigation of operating conditions which would promote bulk protein enrichment and recovery in continuous foams whilst achieving maximal fractionation from contained RNA. The elimination of the latter is of particular importance in subsequent use of the protein product as a food additive.

Continuous foaming was undertaken at various feedstock concentrations, pH conditions, gas flowrates and liquid residence times. Bottoms recycle was applied to exploit further protein stripping from the bulk solution. Experimental results highlighted the importance of each parameter in terms of protein enrichment and fractionation from RNA, but also quantified degrees of protein precipitation under selected operating conditions. In this preliminary study, preferential fractionation of individual enzymes and maintenance of biological activity was not studied. However, gel electrophoresis was used to illustrate the protein composition of foam in comparison with feedstock and bottoms, and to indicate preferential partition of individual or groups of polypeptides in foam. Foam quality was assessed in terms of content of total protein, RNA, carbohydrates and proteases, together with its foamability. All analyses were comparative and included respective feedstocks and bottoms. Comparative evaluation of the benefits of foam separation as a first crude step exploited further fractionation of foam, feedstock and bottoms by ion-exchange adsorption, where results were expressed in terms of protein fractionation from RNA.

## 6.2 Experimental Description

Foaming of brewer's yeast extract was undertaken in the simple continuous mode (see Figure 1.6b), as described in Chapter 2 (2.3.3) to study the effects of operating conditions upon foam performance. Foam was produced by sparging humidified nitrogen into a liquid pool of 400 $cm^3$.

The gas outlet was adjusted to 1.5 bar. The gas flow indicator was calibrated for air and conversion to nitrogen flowrate was achieved by multiplying with a factor of 1.017. Since the volume of the pool was constant, the height of the foam column was fixed to 47 cm. The tower was thermostated at 20 °C. Exhaustive protein stripping was attempted by recycling the bottom stream (see Figure 2.8b). The recycle ratio $R/Q_B$ and fresh feed $Q_0$ were varied so that $Q_0^*$ and liquid residence times remained constant throughout experimentation.

Brewer's yeast extract was prepared by milling a suspension of 400 g of brewer's yeast cake in 1 l of 20 mM potassium phosphate buffer; pH 8.0 (unless stated otherwise) in a 600 $cm^3$ KDL Dynomill. The feed flowrate was 15,000 $cm^3$ $hr^{-1}$, the tip (64 mm $\phi$) speed was 10.5 m $sec^{-1}$, and the agitator shaft was driven at 3,200 rpm. Cell debris was removed by centrifugation in a Beckman centrifuge for 90 minutes at 30,000 g force. The supernatant, the volume of which was 90% of the volume of the cell suspension prior to cell disruption, was aliquoted and frozen at -20 °C. The choice of buffer molarity and pH enabled further anion-exchange treatment, which was optimised at pH 8.0 (Flanagan and Lyddiatt (1991)). Prior to foaming, stock aliquots were thawed overnight at 4 °C and appropriately diluted in the phosphate buffer to meet the required protein concentration. The pH was adjusted as necessary with 2 M NaOH, and the temperature of feedstocks was equilibrated to 20 °C.

Biochemical analysis of feed and products at steady-state conditions involved determination of protein and RNA concentrations by application of the respective colourimetric assays described in Chapter 2 (2.4.3 and 2.4.4). It also included SDS-PAGE and IEF electrophoresis to study polypeptide composition in terms of molecular weight and isoelectric point respectively; see Chapter 2 (2.4.7).

Product quality assessment involved determination of protein, RNA,

carbohydrate and acidic proteases content for equivalent amounts of freeze-dried samples from the feedstock, foam and bottom product. These studies were complemented by testing the foamability of these solutions. The criteria for conditions of foam production included high protein enrichment and limited dryness to prevent extended denaturation and allow collection of a sufficient quantity of product for further treatment. The selection of production conditions was based on experimental evidence assembled from the present chapter. Thus foams were generated by feedstocks containing 0.45 mg $cm^{-3}$ protein at a feed flowrate of 5 $cm^3$ $min^{-1}$ and gas rate of 60 $cm^3$ $min^{-1}$. Phosphate buffer (20 mM) at pH values of 7.0, 7.6 and 8.0 was used. Turbid foam samples were centrifuged at 30,000 g for 90 minutes. The precipitate was resolubilised in 2 M NaOH. Feedstock, bottoms, foam supernatant and foam precipitate (in 2 M NaOH) were exhaustively dialysed against 2.5 mM potassium phosphate, pH 7.6 in 10 kDaltons molecular weight rejection membranes. Source samples were subsequently shell-frozen and lyophilised. Solutions of freeze-dried material (1 mg $cm^{-3}$) were prepared in 40 mM potassium phosphate buffer, pH 7.6. Biochemical analysis employed the assays as described in Chapter 2 (2.4.3, 2.4.4, 2.4.5, 2.4.6). The foam stability of these solutions was determined by application of the Rudin method using the miniature apparatus as described in Chapter 2 (2.2.1). HRV tests were undertaken in the presence of 4% ethanol.

Secondary treatment of yeast extract involved foam processing through a fixed bed of DEAE-52 cellulose. Matrix (5 $cm^3$) was packed into a column of ID=1 cm and 8 cm in height, and was equilibrated with 20 mM potassium phosphate pH 8.0. The flowrate was 1 $cm^3$ $min^{-1}$ and the sample volume was 6 $cm^3$. Prior to loading, foam samples were clarified free of protein precipitate by centrifugation in a microfuge at 16,000 g for 2 minutes. Step elution of adsorbed compounds was achieved with 0.2 and 0.8

M NaCl in 20 mM phosphate buffer, pH 8.0. Elution profiles of foam, feedstock and bottoms were compared under equivalent conditions in order to investigate variations in protein and RNA composition associated with molecular partition during foaming. Samples were selected on the basis of their foam quality, and originated from continuous foaming of feedstocks containing 0.45 mg $cm^3$ protein in 20 mM phosphate buffer, pH 8.0. The inlet flowrate was 5 $cm^3\ min^{-1}$ and the gas flowrate was 60 $cm^3\ min^{-1}$.

## 6.3 Results and Discussion

The mass balances for the following experiments are described by Equations 2.9-2.12 and are depicted in Figure 2.8(a-b) in Chapter 2. Results are expressed in terms of quantitative characteristics of foam, namely enrichment ($e_i$); see Equations 3.1 and 3.2, separation ($s_i$) see Equation 3.5, stripping factor ($s_{ti}$); see Equation 4.1, fractionation index ($Fr_{i,j}$); see Equation 3.6, foam volumetric flowrate ($Q_F$), reduced foam conductivity ($H_r$); see Equation 1.6, and recovery in foam ($R_i$); see Equations 3.3 and 3.4. Protein losses in the precipitate of collected foam ($R_d$), expressed as a percentage of recovered protein are described by Equation 6.1:

$$R_d = \{(c_{iF,real} - c_{iF,app})Q_F\}/c_{iF,real}Q_F = 1 - e_{i,app}/e_{i,real} \quad \text{(Equation 6.1)}$$

where: $c_{iF,app}$ is apparent concentration of protein i in foam, readily detected in solution

$c_{iF,real}$ is the real concentration of protein i in foam, ie total amount of protein i in solution and precipitate

$e_{i,app}$ and $e_{i,real}$ are enrichment ratios corresponding to $c_{iF,app}$ and $c_{iF,real}$ respectively.

$Q_F$ is foam volumetric flowrate

### 6.3.1 Effects of Operating Conditions upon Protein and RNA Partition into Foam

Table 6.1 describes the protein/RNA ratio in feedstocks of varied concentrations and it can be seen that it practically remains constant throughout the range of dilutions applied. Figure 6.1(a-b) illustrates the dependence of protein and RNA enrichment ($e_{protein}$ and $e_{RNA}$ respectively), and fractionation index ($Fr_{protein,RNA}$) upon feedstock concentration ($c_{protein,0}$ = 0.26 to 1 mg $cm^{-3}$). The feed flowrate was 10 $cm^3$ $min^{-1}$ and nitrogen was sparged at a rate of 80 $cm^3$ $min^{-1}$. The calculation of $Fr_{protein,RNA}$ was based upon $e_{protein,real}$. It can be seen that high $e_{protein,real}$ were achieved at dilute feedstock conditions, where protein losses were also highest as shown by the dotted plot corresponding to $e_{protein,app}$ values. The variation of $e_{RNA}$ is similar to that of protein enrichment although significantly lower values were observed compared with protein. The observed differences in the response of protein and RNA enrichment to feedstock concentration are directly reflected in variation of protein fractionation (Figure 6.1b), where fractionation was highest at the most dilute feedstock conditions. Figure 6.2 describes the influence of feedstock protein concentration upon foam volumetric flowrate ($Q_F$) and reduced foam conductivity recorded at steady-state conditions, and shows that concentrated feedstocks generated foams of highest liquid content. It appears that (see Figure 6.3) reduction in feedstock protein concentration had detrimental effects upon protein recovery ($R_{protein,real}$). As in the case of protein enrichment, $R_{protein,real}$ refers to total protein detected in collapsed foam solutions and the recovered precipitate. It can also be seen that precipitated protein ($R_d$), expressed as a percentage of $R_{protein,real}$ (see Equation 6.1), was highest at low feedstock concentrations.

Table 6.2 describes the effects of three distinct pH values of the

**Table 6.1 : Composition of Protein and RNA of Various Feedstocks of Brewer's Yeast in Continuous Foaming**

Protein and RNA content of feedstocks made up in 20 mM potassium phosphate buffer, pH 8.0 and foamed continuously by sparging nitrogen at a rate of 80 $cm^3$ $min^{-1}$. The inlet flowrate was 10 $cm^3$ $min^{-1}$ and the volume of the liquid pool was 400 $cm^3$.

| **Protein Concentration** ($c_{protein,0}$) **(mg** $cm^{-3}$**)** | **RNA Concentration** ($c_{RNA,0}$) **(mg** $cm^{-3}$**)** | $c_{protein,0}/c_{RNA,0}$ |
|---|---|---|
| 0.260 | 0.100 | 2.60 |
| 0.350 | 0.130 | 2.69 |
| 0.500 | 0.200 | 2.50 |
| 0.625 | 0.240 | 2.60 |
| 0.975 | 0.330 | 2.95 |

**Figure 6.1: Effects of Feedstock Concentration upon Foam Composition in Continuous Foam Production from Brewer's Yeast Extracts**

Effects of feedstock concentration upon **(a)** protein and RNA enrichment ($e_{protein}$ and $e_{RNA}$ respectively) protein and **(b)** fractionation from RNA ($Fr_{protein,RNA}$) in continuous foaming of brewer's yeast extract. Preparations were made in 20 mM potassium phosphate buffer pH 8.0. Feed flowrate was 10 $cm^3 min^{-1}$ and gas flowrate was 80 $cm^3$ $min^{-1}$. The volume of the liquid pool was 400 $cm^3$.

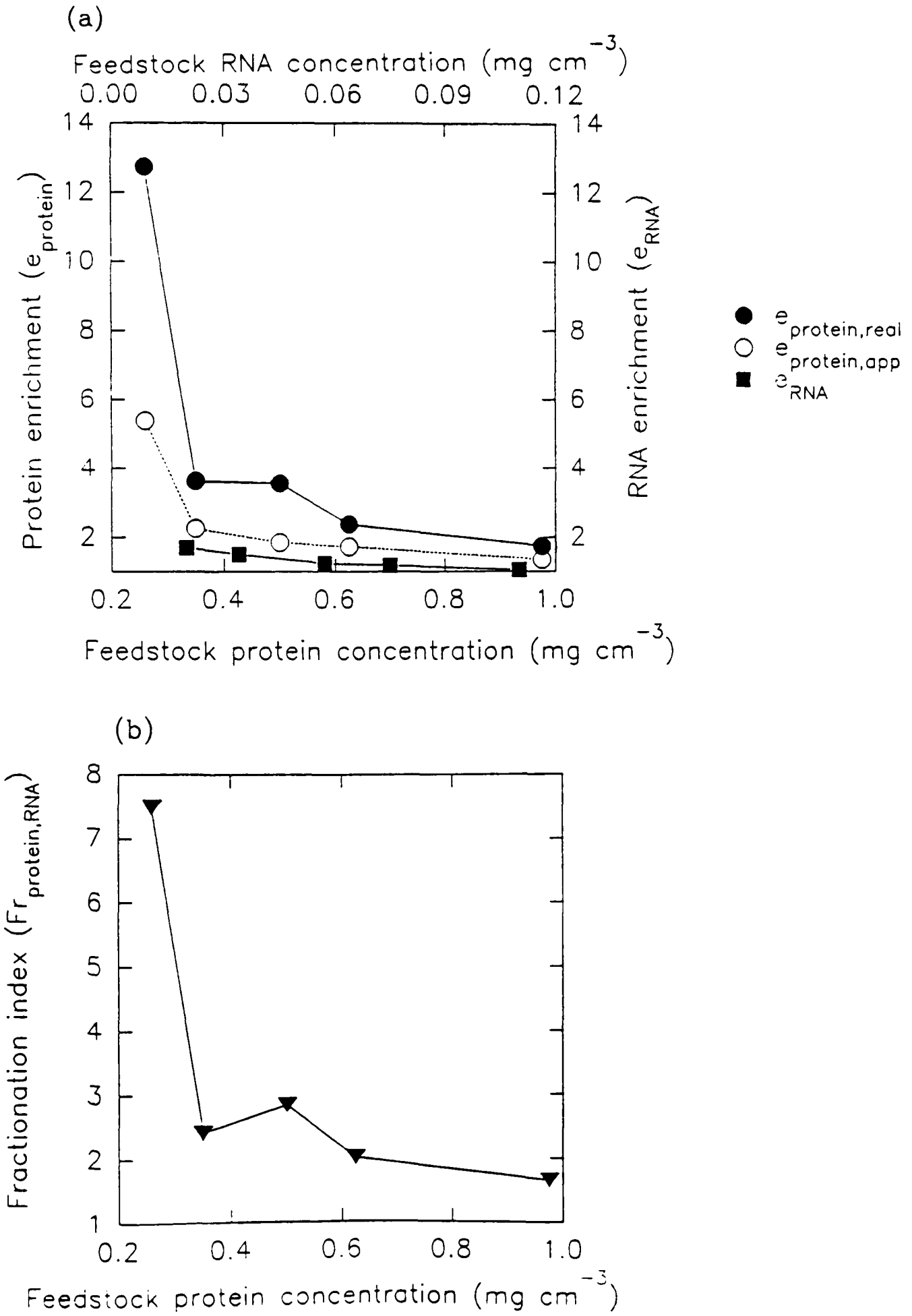

**Figure 6.2 Effects of Feedstock Concentration upon the Liquid Content of Foam Continuously Produced from Brewer's Yeast Extracts**

Effects of feedstock concentration upon foam volumetric flowrate ($Q_F$) and reduced foam conductivity ($H_r$) in foam continuously produced from brewer's yeast extracts. The experimental conditions were the same as in Figure 6.1.

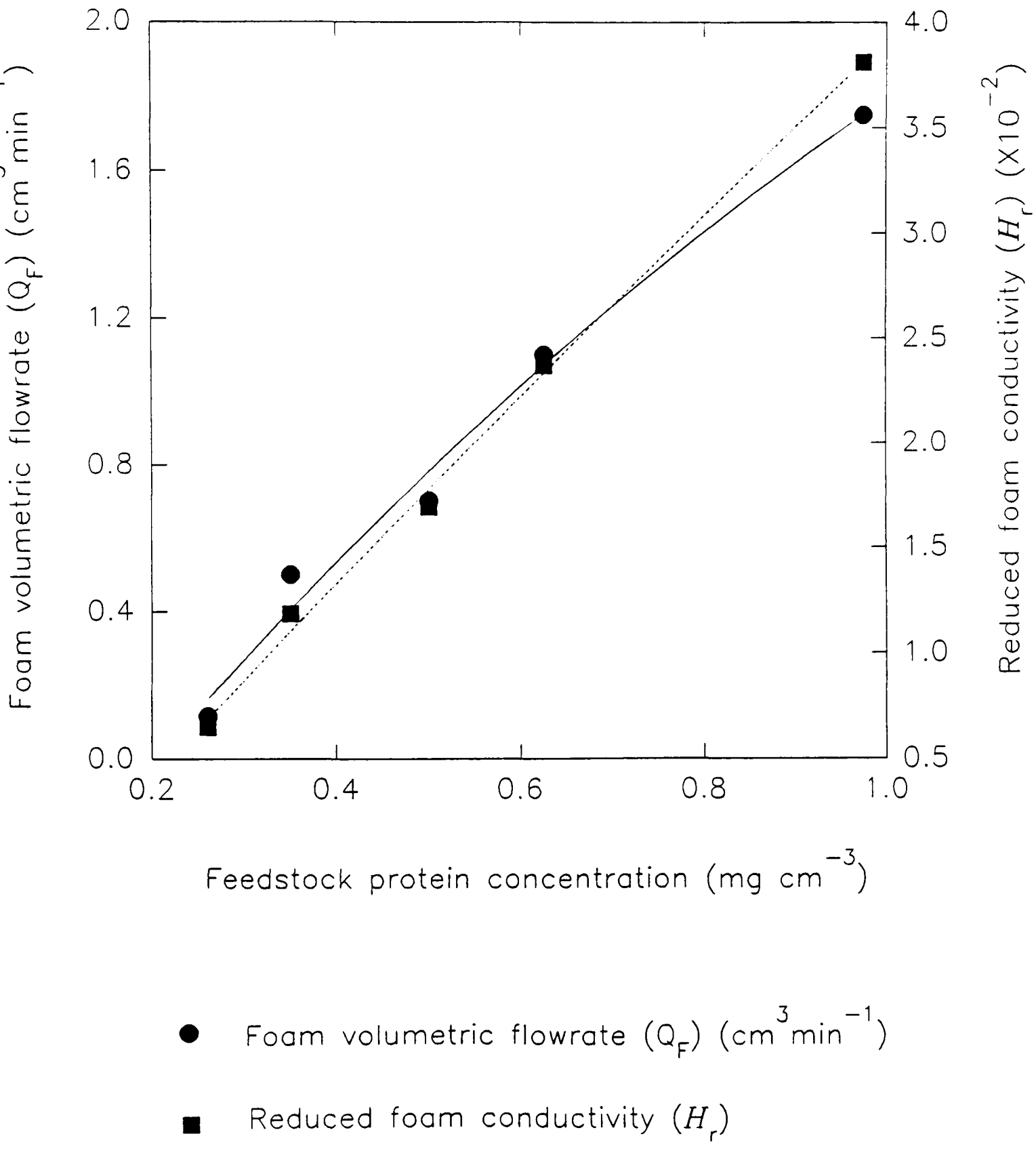

**Figure 6.3: Effects of Feedstock Concentration upon Protein Recovery in Foam Continuously Produced from Brewer's Yeast Extracts**

Effects of feedstock concentration upon protein recovery (R%) and precipitated protein $R_d$ (see Equation 4.1), expressed as a percentage of R, in foam continuously produced from brewer's yeast extract. The experimental conditions are the same as in Figure 6.1.

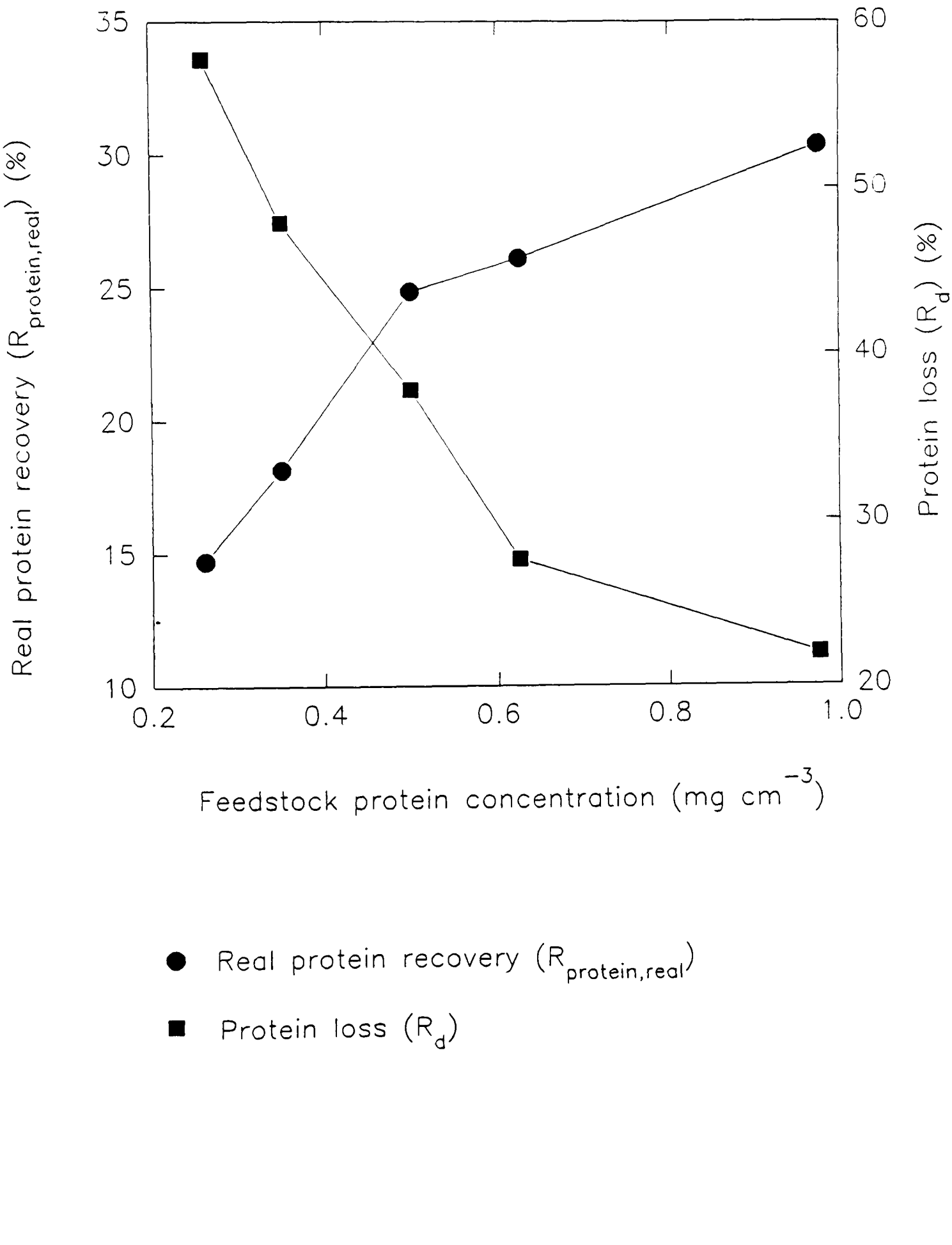

**Table 6.2: Effects of pH upon Characteristics of Foam Generated from Brewer's Yeast Extracts in Continuous Operations**

The effects of three distinct feedstock pH values are shown for protein and RNA enrichment ($e_{protein}$ and $e_{RNA}$ respectively), protein fractionation from RNA ($Fr_{protein,RNA}$), foam volumetric flowrate ($Q_F$) and protein recovery ($R_{protein,real}$). The $Fr_{protein,RNA}$ refers to the total amount of protein in solution and the precipitate. Foam was continuously produced from a 400 $cm^3$ liquid pool by sparging $N_2$ at a rate of 60 $cm^3$ $min^{-1}$. The feed flowrate was 5 $cm^3$ $min^{-1}$ and its protein concentration was 0.45 mg $cm^{-3}$.

| pH | $e_{protein}$ real | $e_{protein}$ app | $e_{RNA}$ | $Fr_{protein,RNA}$ | $Q_F$ ($cm^3 min^{-1}$) | $R_{protein,real}$ (%) † |
|---|---|---|---|---|---|---|
| 7.0 | 3.82 | 2.24 | 3.15 | 1.21 | 0.45 | 35.0 (41.5) |
| 7.6 | 4.32 | 2.00 | 2.21 | 1.95 | 0.45 | 38.9 (53.7) |
| 8.0 | 3.77 | 2.06 | 1.95 | 1.93 | 0.40 | 41.4 (45.5) |

**Table 6.3: Foam Characteristics of Foam Produced at pH 7.0 from Dilute Brewer's Yeast Extracts**

Characteristics of foam produced at pH 7.0 for a feedstock protein concentration of 0.2 mg $cm^{-3}$. Foam was continuously produced from a 400 $cm^3$ liquid pool by sparging $N_2$ at a rate of 60 $cm^3$ $min^{-1}$. The feed flowrate was 5 $cm^3$ $min^{-1}$.

| $e_{protein}$ real | $e_{protein}$ app | $e_{RNA}$ | $Fr_{protein,RNA}$ | $Q_F$ ($cm^3 min^{-1}$) | $R_{protein,real}$ (%) † |
|---|---|---|---|---|---|
| 13.5 | 7.0 | 13.7 | 0.99 | 0.05 | 13.92 (48.15) |

† Values in parenthesis describe the proportion of precipitated protein in foam ($R_d$); see Equation 6.1 and are expressed as percentages of $R_{protein,real}$.

feed upon quantitative foam characteristics. Feedstock protein concentration was 0.45 mg $cm^{-3}$, gas flowrate 60 $cm^3$ $min^{-1}$ and the feed flowrate was 5 $cm^3$ $min^{-1}$. Results indicate that varied pH conditions did not generally affect protein recovery and foam volumetric flowrate although maximum $e_{protein,real}$ was observed at pH 7.6. However, neutral pH appeared to enhance $e_{RNA}$ with consequent detriment upon protein fractionation from RNA. This behaviour was confirmed by similar findings (see Table 6.3), where foam was produced at pH 7.0 from more dilute solutions ($c_{protein,0}$ = 0.2 mg $cm^{-3}$) but comparable feed and gas rates.

SDS-PAGE analysis (see Plates 6.1(a-c)) illustrates the distinction of molecular weights of yeast polypeptides in feedstock, foam and bottom product at pH 7.0, 7.6 and 8.0. Foam samples were loaded undiluted, or diluted by factors indicated by the respective enrichment ratios in order to achieve quantitative comparison with the original feedstock. Calibrations for separations of LMW and HMW standards are presented in Figure II9(a-b) in Appendix II. It appears that the majority of yeast polypeptide subunits lay in the mass range of 27-70 kDaltons, and no preferential partition to the foam of individual polypeptides could be detected. However, it is clear that bottom products were constantly depleted of polypeptides of molecular weight < 30 kDaltons. Such species were found in foam, produced at the three pH values and appeared in both undiluted and appropriately diluted foam samples (see labelled tracks). A representative range of polypeptides was present in precipitates, but species of approximately 28 kDaltons were predominant (see tracks 6 and 7 in Plates 6.1(b-c) respectively). However, the picture is not very clear due to the severe conditions of alkaline resolubilisation in 2 M NaOH. Positive enrichment of foam with light fractions of molecular weight < 30 kDaltons was also observed at dilute feedstock conditions (0.2 mg $cm^{-3}$ protein) as shown in Plate 6.2. Distribution of the isoelectric points of

**Plate 6.1: Separation by Molecular Weight Using SDS-PAGE of Products from Continuous Foam Fractionation of Brewer's Yeast Extract.**

Comparative illustration of SDS-PAGE analysis (see Chapter 2 (2.4.7)) of products of continuous foam processing of brewer's yeast extract comprising foams, foam precipitates, bottoms and feedstocks at operating pH **(a)** 7.0, **(b)** 7.6 and **(c)** 8.0. The experimental conditions were the same as in Table 6.2. Foam samples were appropriately diluted according to their apparent protein enrichment (see $e_{protein,app}$ values in Table 6.2) to enable comparison with respective feedstocks at comparable protein contents. Foam precipitates were also diluted to protein concentration levels comparable with respective feedstocks.

**(a) pH 7.0**

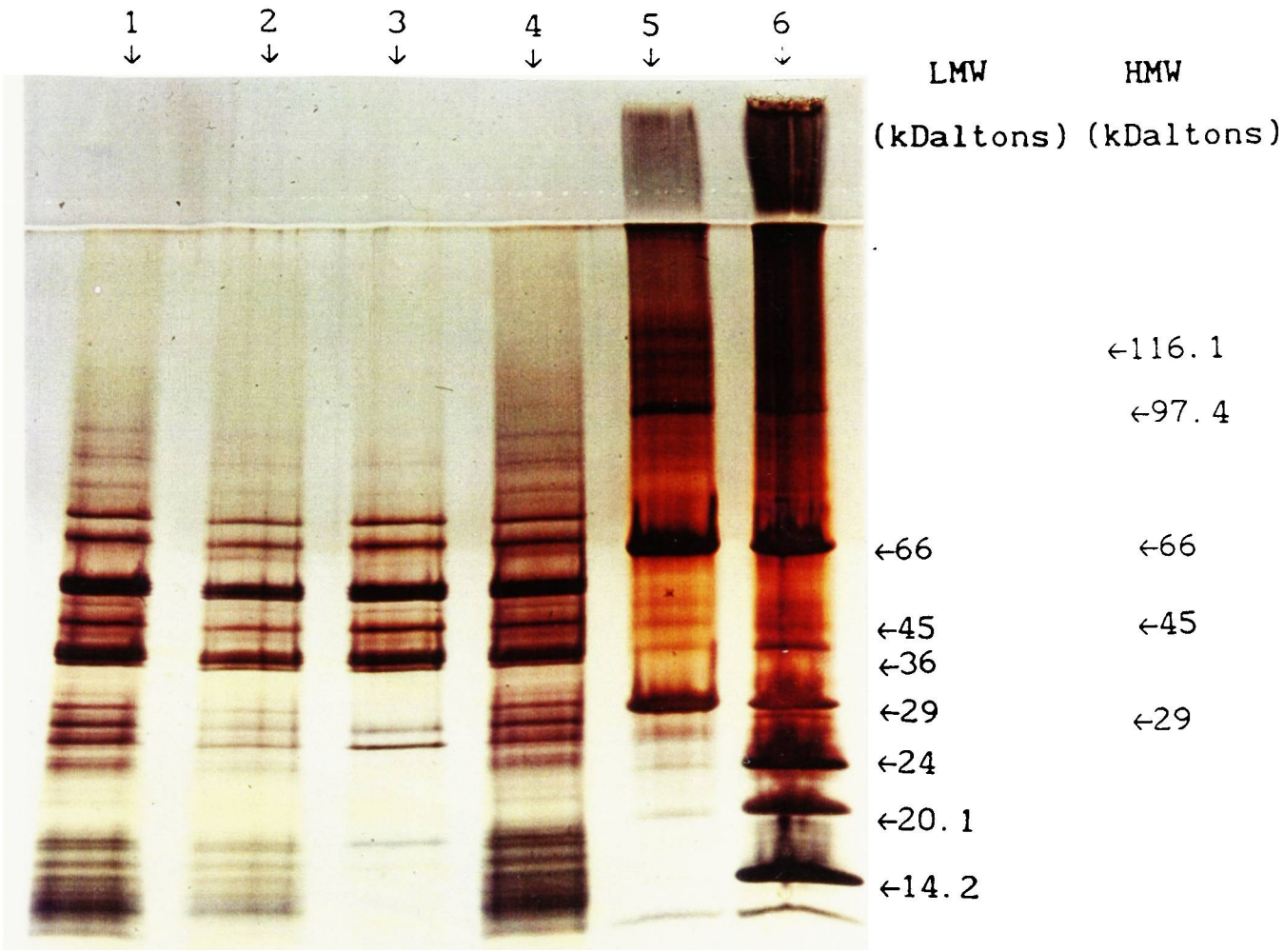


| Track No. | Sample |
|---|---|
| 1 | Foam; pH 7.0 |
| 2 | Foam (diluted); pH 7.0 |
| 3 | Bottoms; pH 7.0 |
| 4 | Feedstock; pH 7.0 |
| 5 | HMW standards |
| 6 | LMW standards |

Plate 6.1 continues

**(b) pH 7.6**

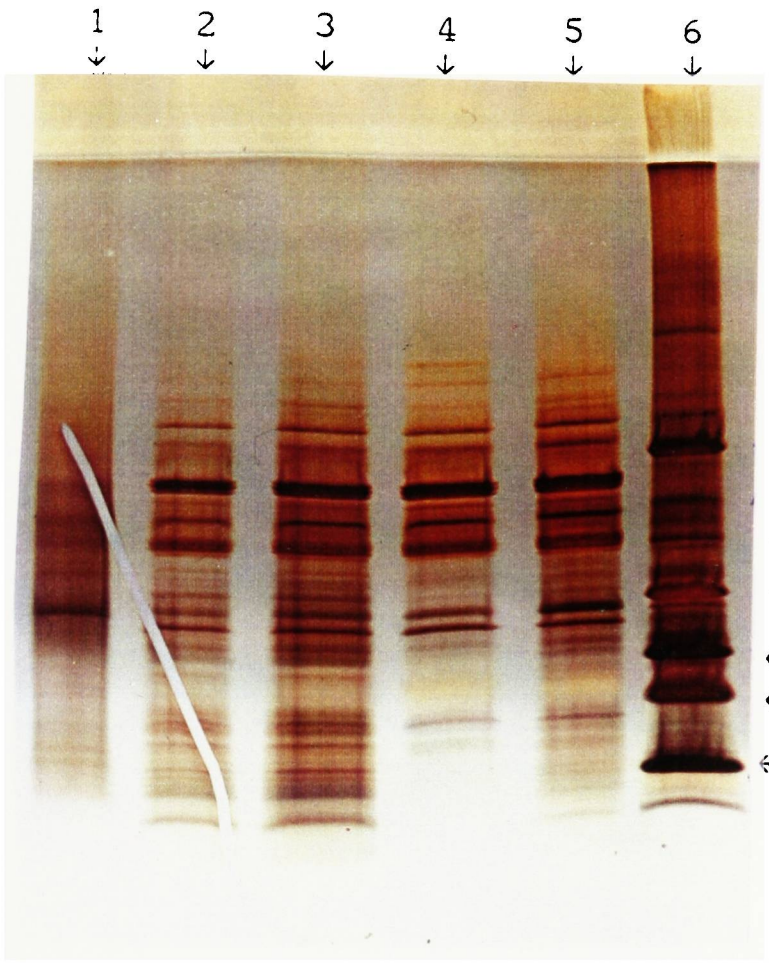


| Track No. | Sample |
|---|---|
| 1 | Foam precipitate; pH 7.6 |
| 2 | Foam (diluted); pH 7.6 |
| 3 | Foam; pH 7.6 |
| 4 | Bottoms; pH 7.6 |
| 5 | Feedstock; pH 7.6 |
| 6 | LMW standards |

Plate 6.1 continues

(c) pH 8.0

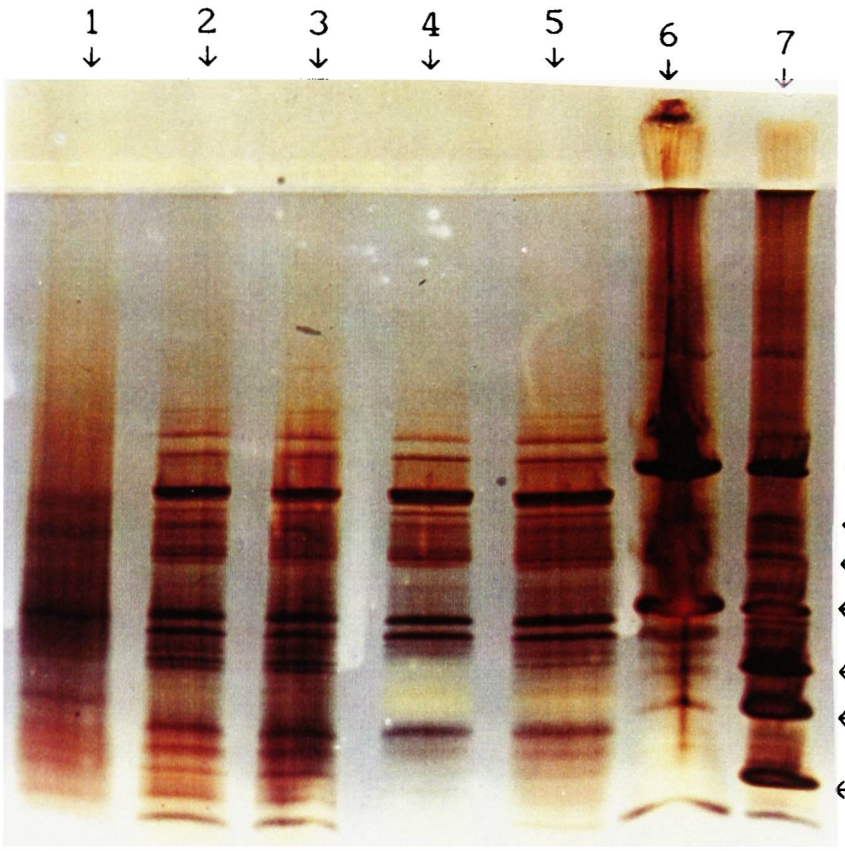


| Track No. | Sample |
|---|---|
| 1 | Foam precipitate; pH 8.0 |
| 2 | Foam (diluted); pH 8.0 |
| 3 | Foam; pH 8.0 |
| 4 | Bottoms; pH 8.0 |
| 5 | Feedstock; pH 8.0 |
| 6 | HMW standards |
| 7 | LMW standards |

**Plate 6.2: Separation by Molecular Weight Using SDS-PAGE of Products from Continuous Foam Fractionation of Dilute Brewer's Yeast Extract at pH 7.0**

Comparative illustration of SDS-PAGE analysis (see Chapter 2 (2.4.7)) of products of continuous foam processing of dilute brewer's yeast extract (0.2 mg $cm^{-3}$ feedstock protein concentration) at pH 7.0. Such samples comprise foam, bottoms and feedstock. The experimental conditions were the same as in Table 6.3. Foam samples were appropriately diluted according to their apparent protein enrichment (see $e_{protein,app}$ values in Table 6.3) to enable comparison with respective feedstocks at comparable protein contents.

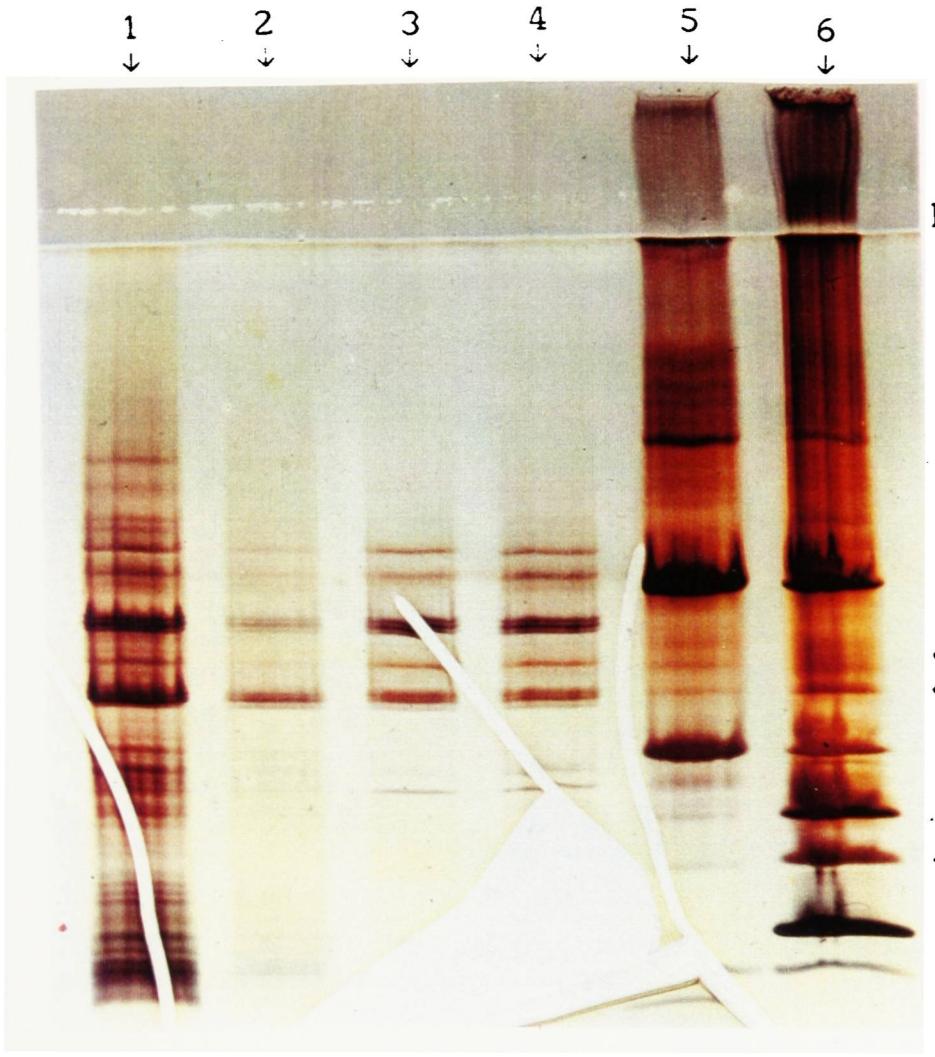


**LMW (kDaltons) HMW (kDaltons)**

| Track No. | Sample |
|---|---|
| 1 | Foam; pH 7.0 |
| 2 | Foam (diluted); pH 7.0 |
| 3 | Bottoms; pH 7.0 |
| 4 | Feedstock; pH 7.0 |
| 5 | HMW standards |
| 6 | LMW standards |

**Plate 6.3: Isoelectring Focusing of Proteins in Products from Continuous Foam Fractionation of Brewer's Yeast Extract Using Page**

Comparative illustration of the protein composition of feedstock and bottoms at pH 8.0, and foams at pH 8.0, 7.6 and 7.0 determined by IEF-PAGE (see Chapter 2 (2.4.7)). The protein contents of samples were comparable. Foam fractionation was undertaken under conditions described in Table 6.2. The sample buffer was 20 mM sodium phosphate buffer, pH 7.6.

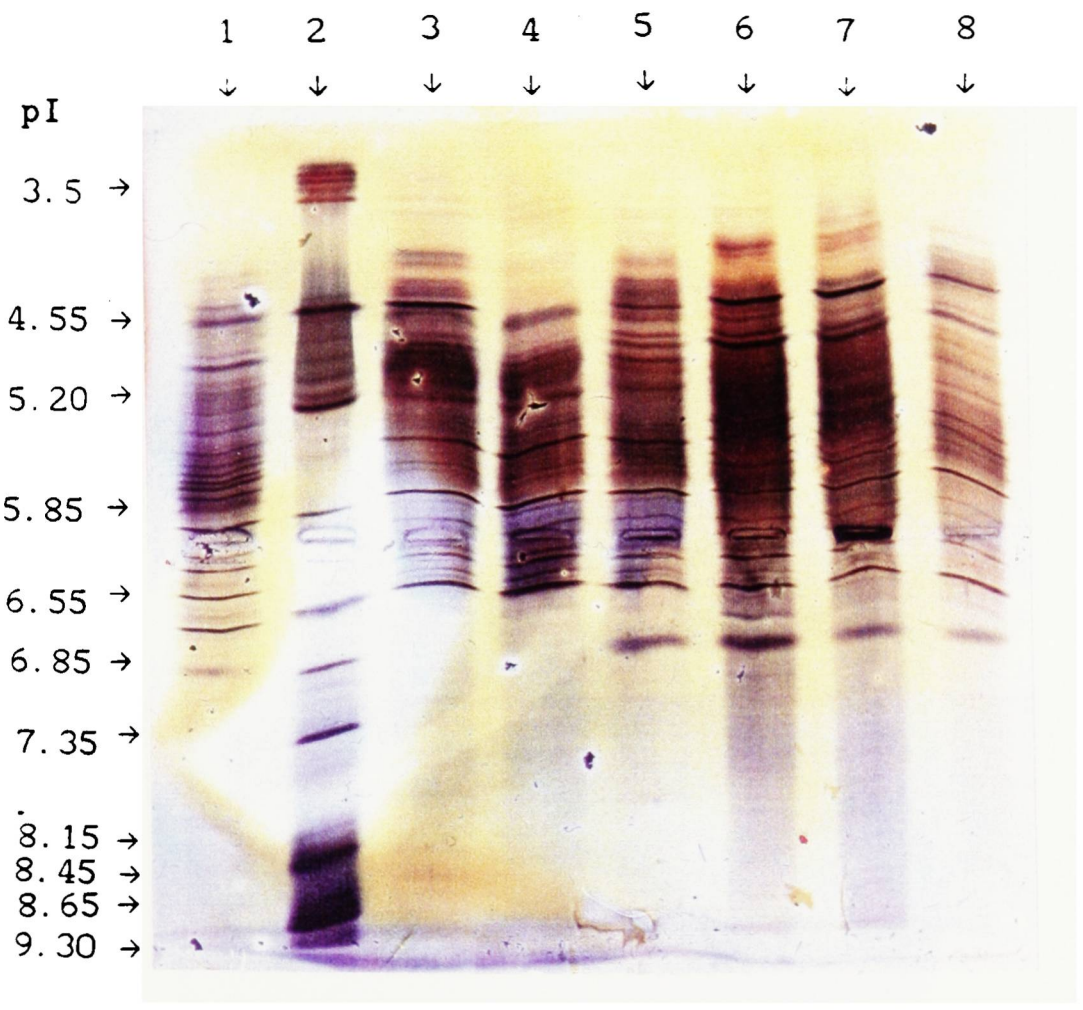


| Track No. | Sample |
|---|---|
| 1 | Freeze-dried foam; pH 8.0 |
| 2 | IEF standards |
| 3 | Feedstock; pH 8.0 |
| 4 | Bottoms; pH 8.0 |
| 5 | Foam (diluted); pH 8.0 |
| 6 | Foam (diluted); pH 7.6 |
| 7 | Foam (diluted); pH 7.0 |
| 8 | Freeze-dried foam; pH 7.6 |

**Plate 6.4: Isoelectring Focusing of Proteins in Products from Continuous Foam Fractionation of Brewer's Yeast Extract at pH 7.6 Using Page**

Comparative illustration of the protein composition of foam, bottoms and feedstock at pH 7.6 determined by IEF-PAGE (see Chapter 2 (2.4.7)). Foam samples were undiluted, and accordingly diluted (see respective $e_{protein,app}$ in Table 6.2). The experimental conditions were the same as in Table 6.2. The sample buffer was 20 mM sodium phosphate buffer, pH 7.6.

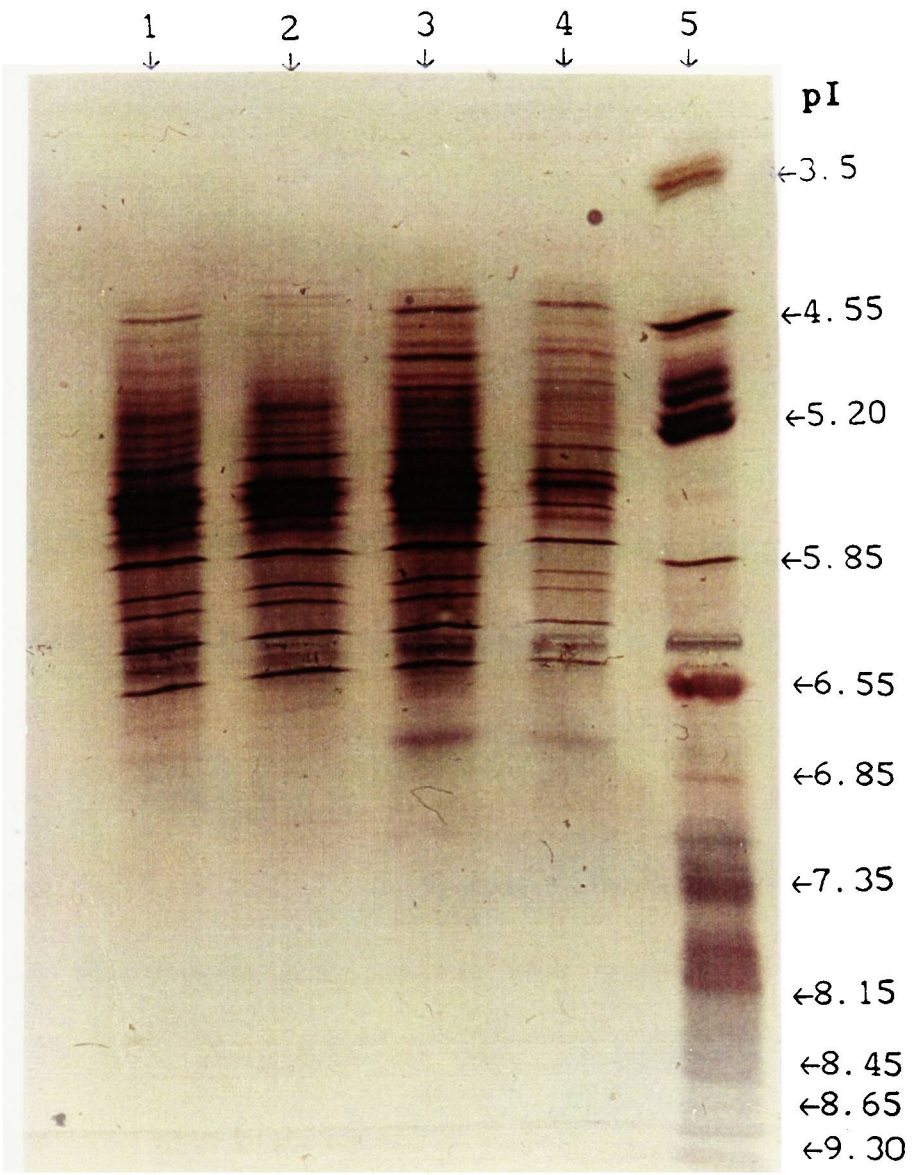


| Track No. | Sample |
|---|---|
| 1 | Feedstock; pH 7.6 |
| 2 | Bottoms; pH 7 |
| 3 | Foam; pH 7.6 |
| 4 | Foam (diluted); pH 7.6 |
| 5 | IEF standards |

constituent polypeptides in feedstock, bottoms and foam were revealed by IEF-PAGE as shown in Plates 6.3 and 6.4. Foam samples were appropriately diluted to give protein concentrations comparable to those of the original feedstocks. It appears that the vast majority of values for polypeptides in all samples lay between pH 4.55 and 6.55. However, a protein or complex of proteins of pI approximately 7.0 consistently and exclusively appeared in foam products generated at all the three pH values applied.

The influence of gas flowrate upon $e_{protein,real}$, $Q_F$ and $R_{protein,real}$ are depicted in Figure 6.4, while Figure 6.5 illustrates the dependence of $e_{RNA}$ and $Fr_{protein,RNA}$ upon gas rate. The response of all these variables can be divided in two zones. In Zone I (G = 15-80 $cm^3$ $min^{-1}$) there was a decrease in $e_{protein,real}$, $e_{RNA}$ and $Fr_{protein,RNA}$ as opposed to a simultaneous increase in $Q_F$ and $R_{protein,real}$. In Zone II (G = 80-320 $cm^3$ $min^{-1}$), transitional increase in $e_{protein,real}$, $e_{RNA}$ and $Fr_{protein,RNA}$ and simultaneous decrease in $Q_F$ were followed by fairly stable values for G > 160 $cm^3$ $min^{-1}$. Protein recovery was characterised by a slight finite decrease in Zone II.

Figures 6.6 and 6.7 depict the influence of liquid residence time ($r_D$) upon the quantitative characteristics of foams produced by feedstocks containing 0.46 mg $cm^{-3}$ protein at a gas flowrate of 30 $cm^3$ $min^{-3}$. Liquid residence time was varied by adjusting the inlet flowrate and maintaining the volume of the liquid pool at 400 $cm^3$. It appears that (see Figure 6.5) prolonged residence times resulted in a moderate improvement in $e_{protein,real}$ and $e_{RNA}$ which coincided with a finite decline in $s_{t,protein}$. The pattern of RNA enrichment was similar to that observed for protein, although with lower values. In the same figure, the response of $Fr_{protein,RNA}$ (based on $e_{protein,real}$) suggests that the fractionation of protein from RNA was relatively constant throughout the range of residence times studied. It appears that $H_r$ and the volumetric flowrate of foam,

**Figure 6.4: Effects of Gas Flowrate upon Protein Enrichment and Recovery in Continuous Foam Production from Brewer's Yeast Extracts**

Effects of gas flowrate upon protein enrichment ($e_{protein,real}$) foam volumetric flowrate ($Q_F$) and protein recovery ($R_{protein,real}$) in continuous foam production from brewer's yeast extract. Preparation was made up in 20 mM potassium phosphate buffer, pH 8.0. Feedstock protein concentration was 0.45 mg $cm^{-3}$, feed flowrate 5 $cm^3$ $min^{-1}$ and the volume of the liquid pool was 400 $cm^3$.

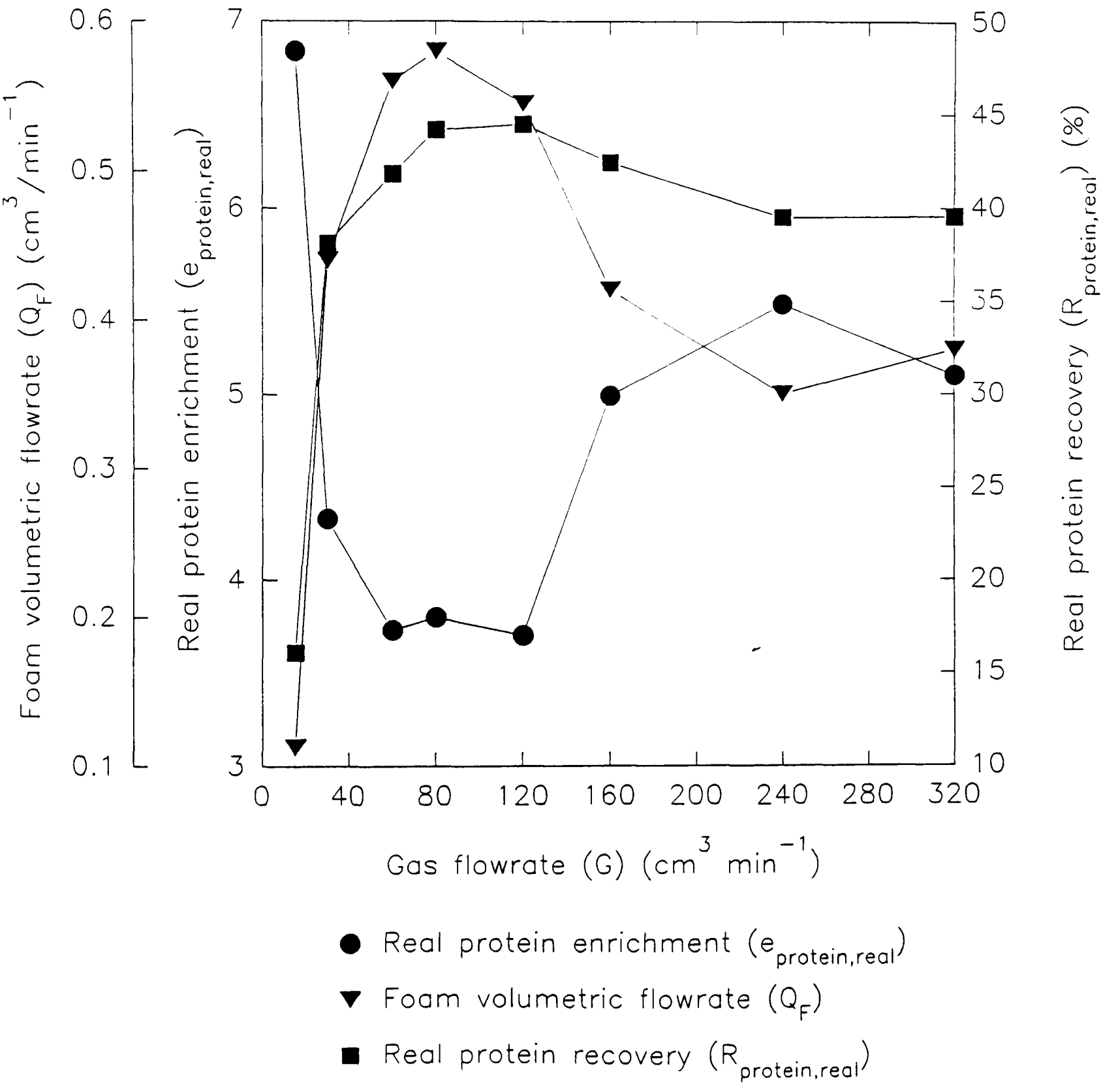

**Figure 6.5: Effects of Gas Flowrate upon RNA Enrichment and Fractionation Index in Continuous Foam Production from Brewer's Yeast Extracts**

Effects of gas flowrate upon RNA enrichment ($e_{RNA}$) and protein fractionation from RNA ($Fr_{protein,RNA}$) in continuous foam production from brewer's yeast extract. Experimental conditions were the same as in Figure 6.4.

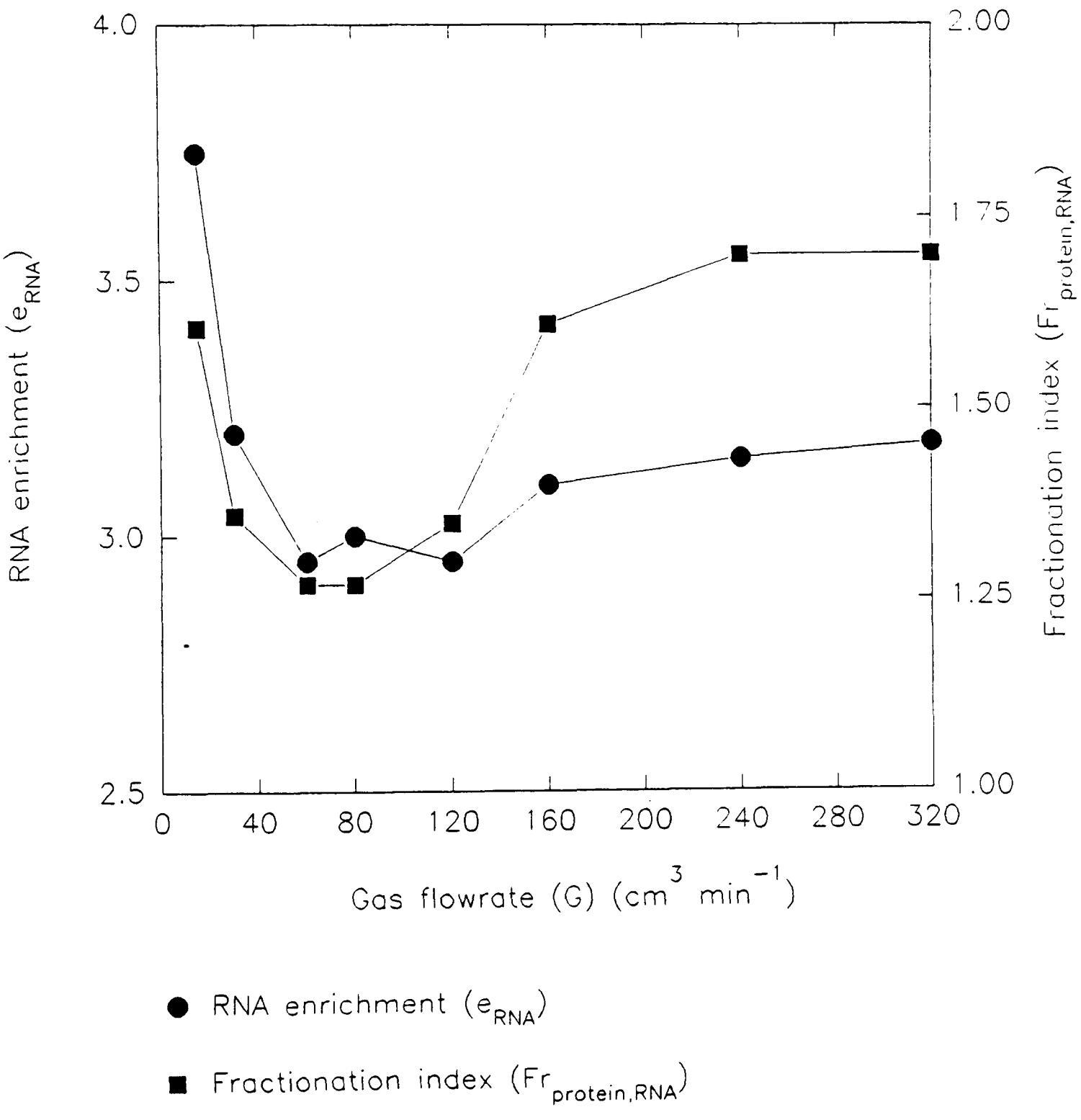

**Figure 6.6: Effects of Liquid Residence Time $r_D$ upon Foam Composition and Protein Stripping Factor in Continuous Foam Production from Brewer's Yeast Extracts**

Effects of liquid residence time ($r_D$) upon protein enrichment ($e_{protein,real}$), RNA enrichment ($e_{RNA}$), protein fractionation from RNA ($Fr_{protein,RNA}$), protein separation ratio ($s_{protein,real}$) and protein stripping factor ($s_{t,protein}$). Solutions were prepared in 20 mM potassium phosphate buffer, pH 8.0. Feedstock protein concentration was 0.45 mg $cm^{-3}$ and the gas flowrate was 30 $cm^3$ $min^{-1}$. The volume of the liquid pool was fixed to 400 $cm^3$.

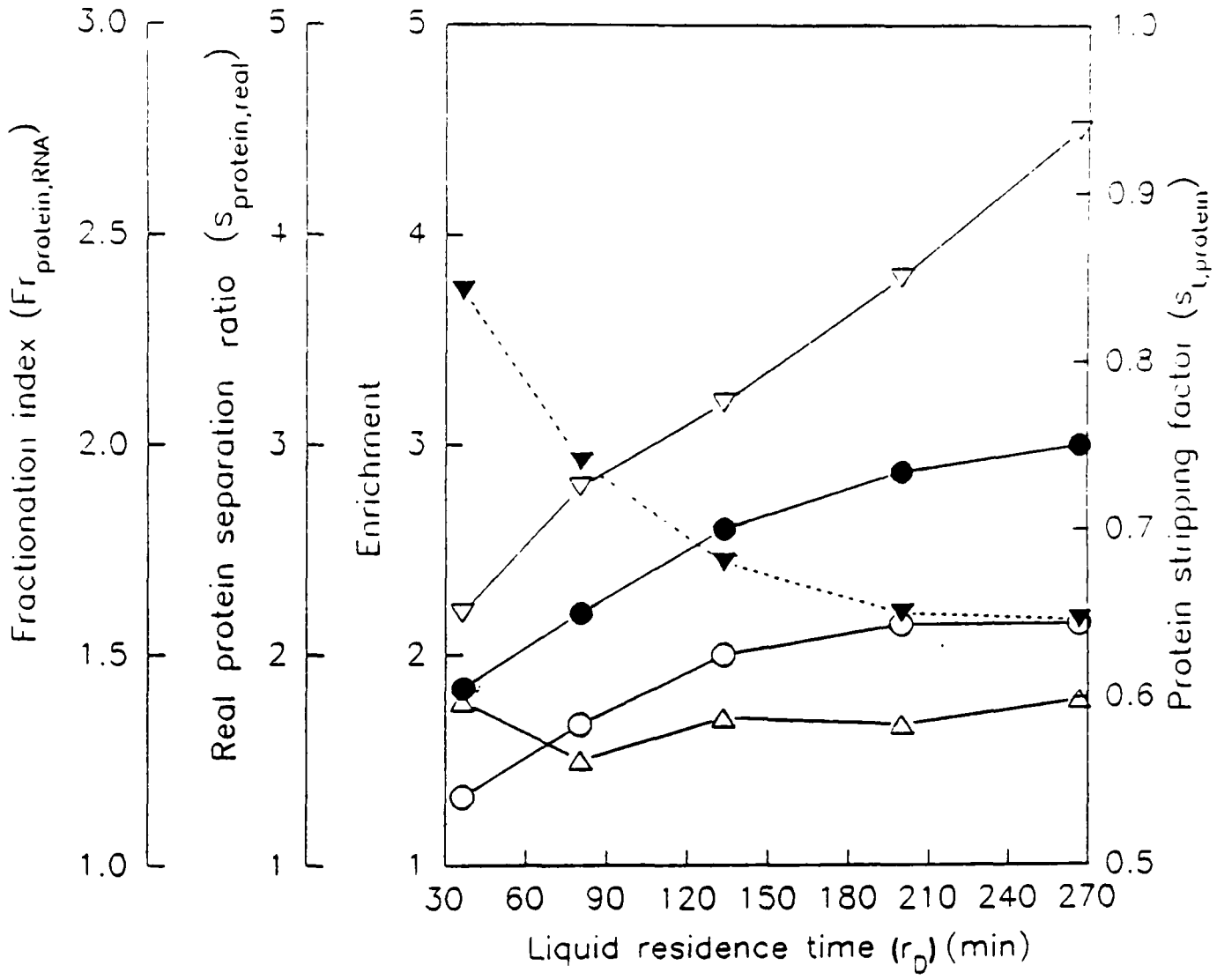

**Figure 6.7 Effects of Liquid Residence Time $r_D$ upon Foam Liquid Content and Protein Recovery in Continuous Foam Production from Brewer's Yeast Extracts**

Effects of liquid residence time $r_D$ upon foam volumetric flowrate ($Q_F$ is expressed as a percentage of the inlet flowrate $Q_0$), reduced foam conductivity ($H_r$) and protein recovery ($R_{protein,real}$). The experimental conditions were the same as in Figure 6.6.

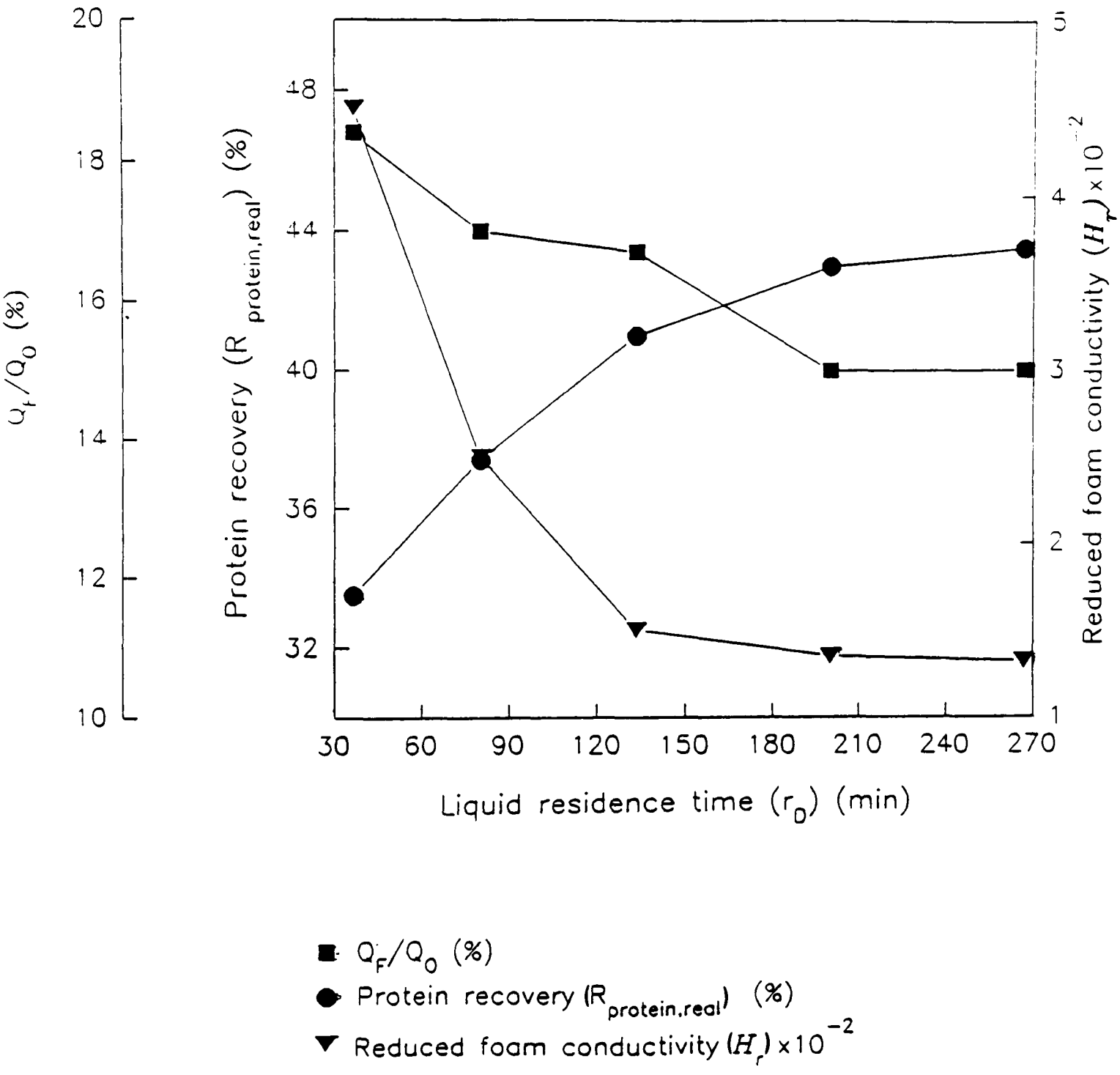

expressed as a percentage of the inlet flowrate ($Q_F/Q_0$ %), declined with prolonged residence times (see Figure 6.7), whilst $R_{protein,real}$ seemed to benefit under under such conditions.

Continuous foam production with bottoms recycle (see Figure 2.8b and Equation 2.12 in Chapter 2) was undertaken at a gas rate of 80 $cm^3\ min^{-1}$, $Q_0^*$ = 5 $cm^3\ min^{-1}$ and 0.45 mg $cm^{-3}$ protein in the fresh feed (ie $Q_0$). Table 6.4 describes variations in protein concentration of the feed at the entrance of the tower (ie $c^*_{protein,0}$), determined both experimentally and theoretically (see Equation 2.12), at varied ratios of bottoms recycle. It can be seen that experimental and theoretical values are in good agreement. The experimental values alone were used in the analysis of results. Figure 6.8(a-b) describes the effects of increasing bottoms recycle ratio ($R/Q_B$) upon $e_{protein,real}$, $e_{RNA}$, $s_{t,protein}$, $s_{t,RNA}$ and $Fr_{protein,RNA}$, and results refer to protein and RNA concentrations in the fresh feed (ie stream $Q_0$). It appears that increased bottoms recycle ratios strongly enhanced protein enrichment and its fractionation from RNA, but RNA enrichment was only marginally improved under such conditions. A significant decline in the stripping factor of protein was observed at increased $R/Q_B$ but the stripping factor of RNA did not appear to be affected by application of bottoms recycle. As with protein enrichment, it can be seen that (see Figure 6.9) protein recovery ($R_{protein,real}$) improved with increasing bottoms recycle ratio, but such increase was also characterised by extensive precipitation ($R_d$). When protein enrichment and recovery were expressed in respect of protein concentration of stream $Q_0^*$, it can be seen that (see Figure 6.10) high bottoms recycle ratios resulted in a pronounced increase in protein enrichment ($e^*_{protein,real}$) and a steep decline in protein recovery ($R^*_{protein,real}$). Figure 6.10 also shows that increased $R/Q_B$ values were associated with a considerable reduction in foam volumetric flowrate.

**Table 6.4: Theoretical and Measured Feed Protein Concentrations at the Entrance of the Tower in Operations with Bottoms Recycle**

Comparison between theoretical and experimentally determined values of the feed concentration ($c^*_{protein,0}$) at the entrance of the tower (stream $Q^*_0$), in continuous foaming of brewer's yeast extract with bottoms recycle. The theoretical values are derived from Equation 2.12 in Chapter 2. The fresh feed concentration $c_{protein,0}$ was 0.45 mg $cm^{-3}$ and the flowrate at the entrance of the tower $Q^*_0$ was 5 $cm^3$ $min^{-1}$. Nitrogen was sparged at a rate of 80 $cm^3$ $min^{-1}$.

| Bottoms Recycle $R/Q_B$ (%) | $R/Q_0$ | $c^*_{protein,0}$ (mg $cm^{-3}$) | |
|---|---|---|---|
| | | Theoretical | Experimental |
| 0.00 | 0.00 | 0.460 | 0.460 |
| 28.87 | 0.35 | 0.405 | 0.387 |
| 53.76 | 0.50 | 0.353 | 0.365 |
| 76.14 | 0.75 | 0.289 | 0.305 |

**Figure 6.8: Effects of Bottoms Recycle upon Foam and Bottoms Composition in Continuous Foam Production from Brewer's Yeast Extracts**

Effects of increasing bottoms recycle ratio ($R/Q_B$) upon **(a)** protein enrichment ($e_{protein,real}$), RNA enrichment ($e_{RNA}$), protein stripping factor ($s_{t,protein}$) and RNA stripping factor ($s_{t,RNA}$) and **(b)** protein fractionation from RNA ($Fr_{protein,RNA}$). Calculations were based on fresh feed $Q_0$ concentrations. The gas flowrate was 80 $cm^3$ $min^{-1}$ and the residence time 80 min.

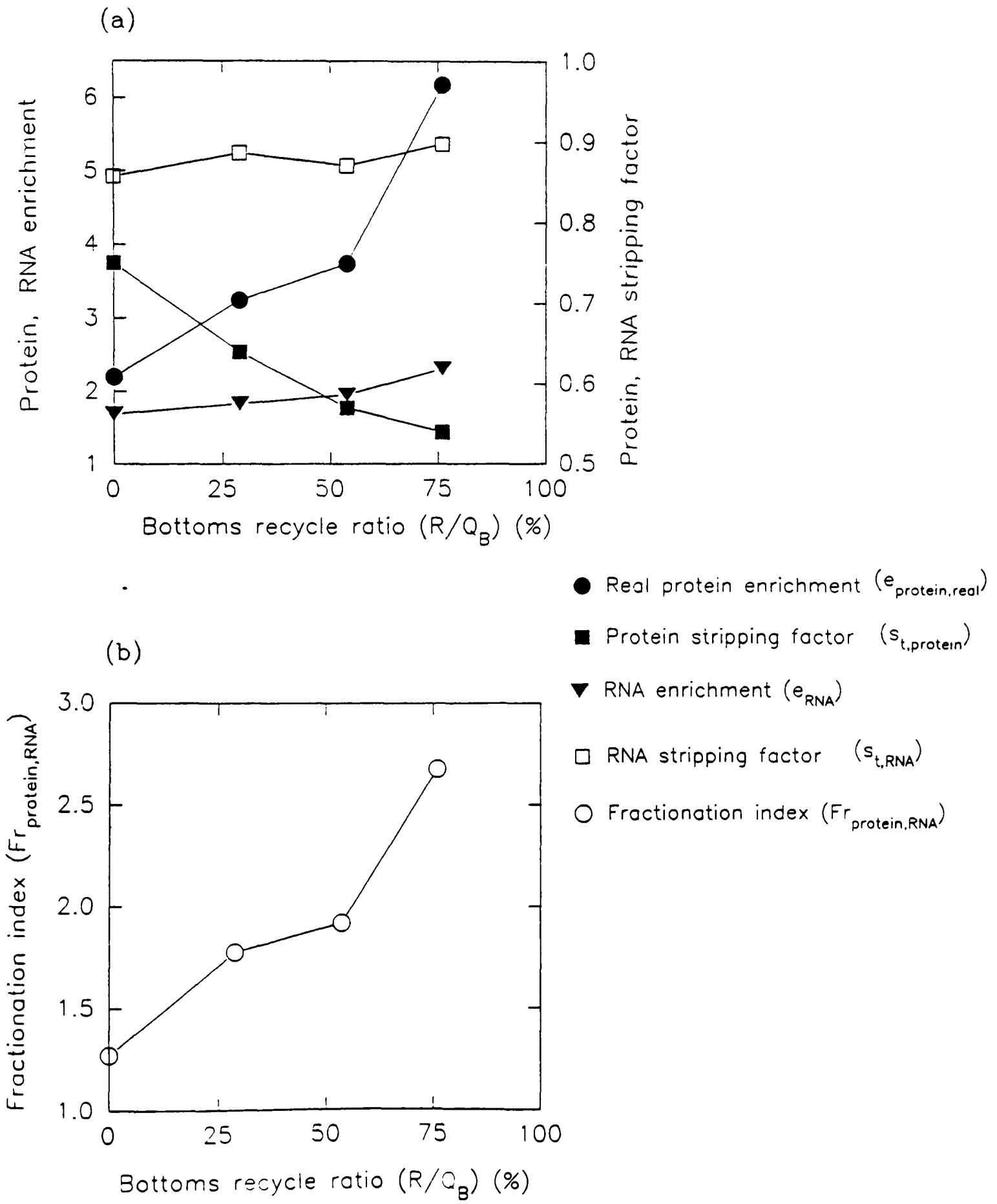

**Figure 6.9: Effects of Bottoms Recycle upon Protein Recovery in Continuous Foam Production from Brewer's Yeast Extracts**

Variations in protein recovery ($R_{protein,real}$) and precipitated protein ($R_d$) with increasing bottoms recycle ratio. Results refer to the mass flowrate of the fresh feed $Q_0$. Experimental conditions were the same as in Figure 6.8.

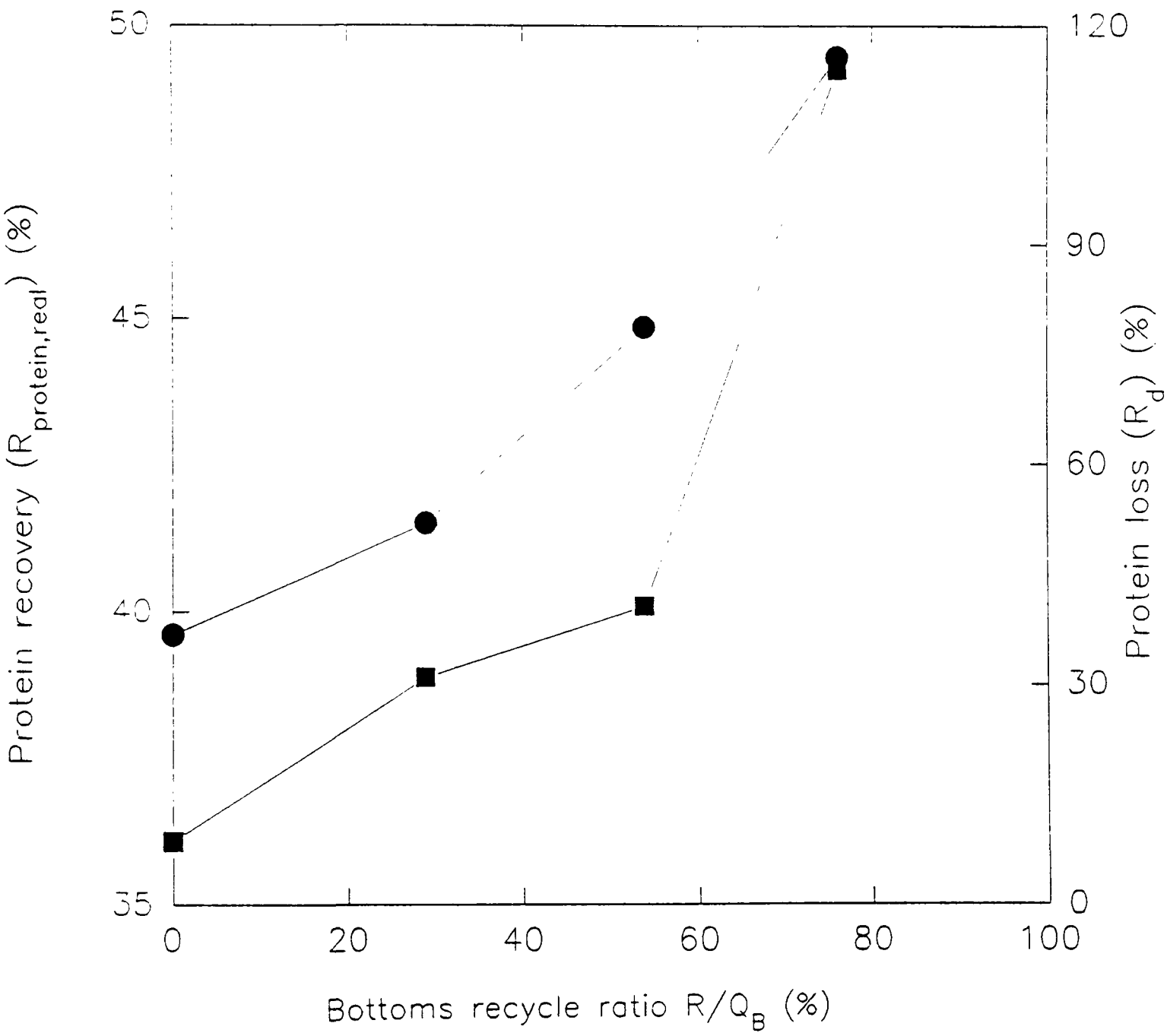

**Figure 6.10: Protein Migration into the Foam Phase with Respect to the Fresh Feed in Operations with Bottoms Recycle**

Description of the effects of bottoms recycle upon protein enrichment ($e^*_{protein,real}$), foam volumetric flowrate ($Q_F$) and protein recovery ($R^*_{protein,real}$) with respect to the feed at the entrance of the tower $Q^*_0$. Its protein concentration is described in Table 6.4 for various bottom recycle ratios. The flowrate of $Q^*_0$ was 5 $cm^3 min^{-1}$, the volume of the liquid pool 400 $cm^3$ and the gas flowrate was 80 $cm^3\ min^{-1}$.

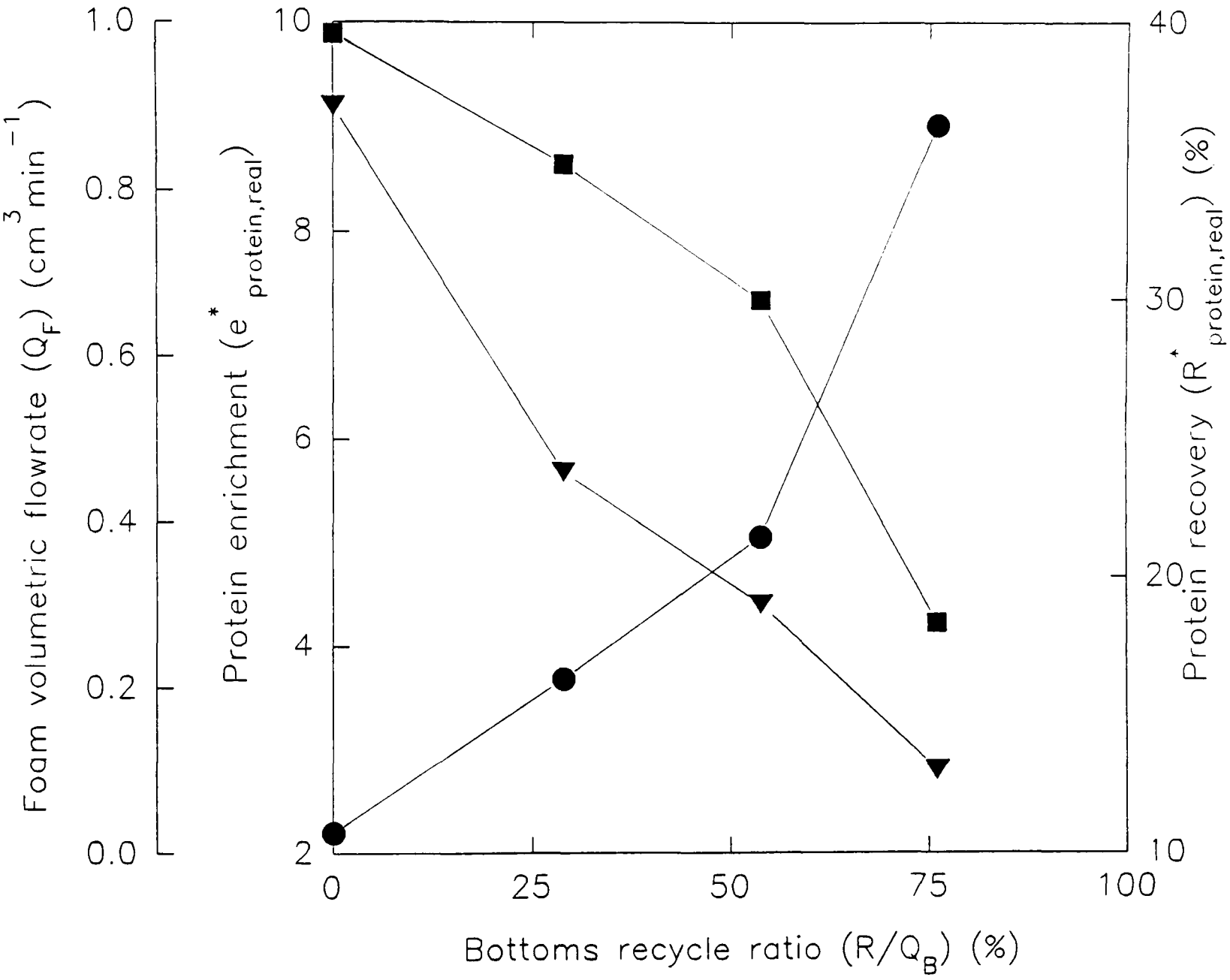


- ● Protein enrichment ($e^*_{protein,real}$) with respect to the feed $Q^*_0$ at the entrance of the tower
- ▼ Foam volumetric flowrate ($Q_F$)
- ■ Protein recovery ($R^*_{protein,real}$) with respect to the feed $Q^*_0$ at the entrance of the tower

The present results indicate that protein and RNA enrichment are enhanced in dry foams, but enhancement in protein enrichment is more pronounced at pH > 7.0. As a result, protein fractionation from RNA is increased under such conditions. Dry foams can be produced under conditions of dilute feedstocks and/or low gas flowrate. However, such foams yield low protein recovery and are compromised by extensive precipitation. The polypeptide composition of foams seems to be similar to that of the original feedstocks, although a species of pI 7.0 clearly concentrates in the foam phase. It also appears that the bottoms are depleted of light polypeptide fractions (MW < 30). In the present study, increase in the liquid residence time appeared to be beneficial to both protein enrichment and recovery, but did not seem to influence fractionation. High bottoms recycle ratios can promote extensive protein stripping from the liquid phase, which coincides with high enrichment, recovery and fractionation. However, such foams are very dry and are likely to exhibit high levels of protein precipitation.

The observed increase in protein enrichment with dilute feedstocks (Figure 6.1a) must be attributed to extensive drainage and coalescence, and enhanced mass transfer due to internal reflux. It is noteworthy that the inverse dependence of $e_{protein}$ on the concentration of feedstocks, comprising large numbers of diverse polypeptides, is consistent with that of a homogeneous BSA solution (see Figure 4.1a). It appears that a steep rise in protein enrichment occurs at those feedstock concentrations which produce a negative slope in the plot of surface tension $\sigma$ versus $\ln(c_{protein})$ as depicted in Figure III3 in Appendix III.

It is clear that the greatest discrepancy between $e_{protein,real}$ and $e_{protein,app}$ was observed at dilute conditions where enhancement in protein enrichment is maximal. This reflects the increased degree of denaturation associated with extensive coalescence taking place at dilute

feedstock conditions and leads to unfolding and precipitation of protein molecules. However, it is likely that the extent of these effects differs for the various polypeptides and enzymes present in brewer's yeast extract.

The limited ability of RNA to concentrate in foam, (compare $e_{RNA}$ with $e_{protein,real}$ in Figure 6.1a), must be associated with reduced surface activity when compared with that of the bulk of proteins. Comparison between various plots in Figure III2 shows that, surface tension measurements of solutions of freeze-dried yeast protein rigorously depleted in RNA by ion-exchange fractionation (see fraction 2 in Figure 6.11c), suggests that the contribution of RNA to bulk surface tension measurements is not important. However, the observed variation in $e_{RNA}$ with feedstock concentration confirms that independent RNA adsorption at the foam phase accounts in part for its concentration in the foam. The presence of RNA will also be influenced by mother liquor in the plateau borders and interactions between protein molecules and RNA at the gas-liquid interface. At pH 8.0, more than 70% of yeast proteins would be expected to be present in their anionic form (Gianazza and Righetti (1980)) whilst the remainder will be close to their isoelectric points or positively charged. Hence interactions of the latter with RNA will be expected. However, the observed decline in RNA enrichment with feedstcok concentration excludes the possibility that RNA surface excesses primarily result from protein-RNA interactions, because such interactions would be expected to result in RNA enrichment ratios unrelated to RNA feedstock concentration. Such behaviour was clearly observed in the partition of lysozyme to the foam phase by means of interactions with BSA (see Table 4.2). RNA losses were not observed in the calculated mass balances, indicating that RNA precipitation did not take place during foaming. This observation was confirmed by the negligible quantities of RNA detected in

resuspended foam precipitates.

The observed differences in the response of protein and RNA enrichment to feedstock concentrations are directly reflected upon the profile of protein fractionation from RNA (Figure 6.1b). Similar observations are reported by Lalchev et al. (1982), where feedstocks of BSA-DNA, lysozyme-DNA and chromatin solutions were foamed in batchwise processes. In these studies, proteins and DNA were equivalently represented in terms of mass in the foaming solutions. It was found that proteins preferentially adsorbed at the gas-liquid interface whilst RNA remained in the bulk phase. Application of negative pressure in the plateau borders (Khristov et al. (1981)) induced foam dryness and led to significant improvement in protein fractionation from DNA through enhancement of protein enrichment. However protein denaturation was a critical disadvantage of improved fractionation by means of "dry" foam production. In the same report, it is also reported that the pH played an important role in the fractionation of lysozyme from DNA, with the best results achieved near the pI of lysozyme. Here, foamability could be expected to be maximal despite the poor foaminess of lysozyme (see Chapters 3 and 4).

Greater foam volumetric flowrates (Figure 6.2) and protein recovery values (Figure 6.3) with increasing protein feedstock concentration are associated with effective stabilisation of foam bubbles in the presence of high concentrations of bulk protein. Under such conditions, bubble coalescence and drainage are significantly reduced. The response of protein recovery to varied feedstock concentrations indicates that the mechanisms controlling foam flowrates predominate over those dictating protein enrichment (see Equations 3.3 and 3.4). High levels of protein loss in the precipitate at dilute conditions reflect the observed discrepancies between real and apparent protein enrichment (see Figure

6.1a) and agree with observations of increased protein denaturation in dry foams reported by Lalchev et al. (1982). The observed trends in $Q_F$ and $R_{protein,real}$ for a continuously operated process with complex feedstocks agree with reports by Brown et al. (1990) and Ahmad (1975) for continuous foam fractionation of BSA model solutions. This implies that the mixture of yeast proteins behaves in a manner similar to that of a single protein system. In contrast, experience from BSA-lysozyme systems has shown that the volume of collected foams (see Table 4.3a) was not related to total bulk protein, but to the solution composition (see Figure 4.3).

Results in Figures 6.1(a-b)-6.3 have highlighted the merits of foam production from dilute solutions, but equally have emphasised the disadvantages associated with diminished protein recovery and protein denaturation/precipitation. It can be concluded that such conditions should be applied where protein denaturation does not compromise product quality. Modified operating conditions should be adopted when protein products must retain their native states and activities.

Significant improvement in RNA enrichment in foam at neutral pH (Tables 6.2 and 6.3) implies that promotion of interactions between protein molecules and RNA is likely to occur. Such interactions do not seem to significantly effect protein partition, but definitely improve that of RNA. This behaviour is more pronounced at dilute feedstock conditions (see Table 6.3). It is interesting to note that, although the achieved protein enrichment ($e_{protein,real}$ = 13.5; Table 6.3) approximated that obtained under similar feedstock concentrations at pH 8.0 ($e_{protein,real}$ = 12.75; Figure 6.1a), the observed RNA enrichment ($e_{RNA}$ = 11.8; Table 6.3) was significantly higher than that shown in Figure 6.1a ($e_{RNA}$ = 1.7) for similar conditions. As a result, the fractionation index at pH 7.0 ($Fr_{protein,RNA}$ = 1.18) was considerably lower that that of $Fr_{protein,RNA}$ = 7.49 at pH 8.0 (see Figure 6.1b). Therefore any foaming

process directed towards protein fractionation from RNA should operate at pH > 7.0.

Foam production under varied pH conditions and subsequent electrophoretic analysis seem to suggest that there is not a significant difference in polypeptide composition between the foam phase and the original feedstock. This tallies with previous suggestions that foam quality is likely to be determined by the total protein content rather than individual polypeptides. Evidence that, the pI values of the vast majority of proteins in all samples lie between 4.55 and 6.55, agrees with other evidence (Gianazza and Righetti (1980)), which draws on a larger number of microorganisms. However, IEF-PAGE offers firm evidence that a species of pI 7.0 (see Plates 6.3 and 6.4) preferentially fractionates into foam. This molecular species is likely to play an important role in foam formation and requires further investigation. Gel scanning was not successful in protein achieving quantitation due to the dark background of the silver stain. Further investigation of the molecular weight of the species of pI 7.0 was not undertaken herein, but such studies would have included 2-dimensional electrophoresis. IEF-PAGE would have enabled the separation of this particular species on the basis of charge. Incubation of the gel band in SDS sample buffer and subsequent SDS-PAGE in the second dimension would have revealed the molecular weight distribution of the SDS dissociated protein or cluster of proteins. Similar evidence for native molecules could be derived by appropriately designed ion-exchange chromatography possibly coupled with high resolution gel filtration on HPLC. It is likely that such experimentation would require a number of steps, and would need verification by gel electrophoresis. Similar combined experimentation applied by Leeson (1989) dealt with identification of beer proteins involved in foam and showed that polypeptides with pI equal to 5.5, 5.7 and 6.7 were heavily involved in

beer foam formation.

Although there is little evidence for the importance of specific polypeptides and molecular interactions in foam formation, it would be expected that during foaming of brewer's yeast extract, a multitude of protein-protein interactions occur and synergistically contribute to foam stabilisation. Such behaviour would inevitably mask the individual role of proteins or polypeptide complexes. However, the complexity of the system poses a great number of difficulties in identifying these interactions and assessing the role of "key" components in foam production. A similar biochemical system, closely related to yeast proteins, is that of beer foam. The role of various beer proteins in foam has been studied in the context of the control of foam behaviour, and has involved immunochemical analysis. Hollemans and Tonies (1989) gave no conclusive evidence as to whether the total amount of protein or a specific protein compound in beer determines foam behaviour. It was shown however, that complete removal of a 40 kDaltons fraction from the beer resulted in some reduction in its stability as compared with no reduction observed when a 15 kDaltons fraction was removed. The importance of the 40 kDaltons fraction in beer foam has been reported by other workers and has been identified with the z protein characteristic of barley malt (Leeson (1989)). However, further evidence (Mohan et al. (1990); Mohan et al. (1992)) based on immunochemical dissection of protein foams suggests that extensive association between many species of polypeptides form strong complexes, which are primarily implicated in foam formation and stabilisation.

The influence of varied gas rates upon continuous foam production was divided into two zones (see Figures 6.4 and 6.5). In Zone I, reduction in protein and RNA enrichment with simultaneous increase in foam volumetric flowrates must be associated with the dynamics of liquid drainage. At higher gas rates the amount of liquid entrained in the foam

is increased and less time is available for liquid drainage through the plateau borders. The increased liquid entrainment suppresses the contribution of adsorbed protein and RNA to respective solute enrichment, but does result in higher foam flowrates. At lower gas flowrates (ie G < 60 $cm^3$ $min^{-1}$) extensive internal reflux occurs due to increased liquid drainage and bubble breakage. The counter-current motion of dripping liquid enriches the rising foam as well as the interstitial liquids, which enhances enrichment ratios. Reduced liquid entrainment and increased drainage account for low foam flowrates at low gas flowrates. The observed recoveries (Figure 6.4) reflect simultaneous changes in protein enrichment and foam volumetric flowrate.

The present findings agree with other work (Brown et al. (1990); Ahmad (1975)) where model systems of BSA were used in continuous foam production. It is also noteworthy to mention that experimental evidence verifies theoretical predictions based on the model of Brown et al. (1990), although this model assumed negligible coalescence along the foam tower with consequent underestimated enrichment ratios and overestimated recoveries. Wace et al. (1969) studied flow patterns of foam at different gas flowrates, in experiments directed towards the design of multi-stage foam columns. Such experiments revealed that at low gas rates a pseudo-rigid foam was formed. Rates of foam rise were decreased because foam was carried downwards by the draining liquid. At higher gas rates coalescence was limited and foam bubbles were strong and distinct. Bubbles were subjected to eddy forces in a regime identical to that in the liquid pool. The influence of gas flowrate upon bubble size and coalescence is presented in Chapter 7.

In Zone II (Figures 6.4 and 6.5) a dramatically different regime was observed in terms of bubble dynamics along the foam column. It was observed that forceful sparging of nitrogen (G > 160 $cm^3$ $min^{-1}$) produced

very unstable bubbles which coalesced severely and delayed the upwards movement of the foam. The flow regime in the liquid pool was highly turbulent and the gas-liquid interface was indistinct. As a result, an increase in protein enrichment with a simultaneous decrease in respective foam flowrates was observed, the combination of which led to a slight decline in protein recovery. Highest protein fractionation from RNA (Figure 6.5) observed at low flowrates in Zone I ($G < 60\ cm^3\ min^{-1}$) and Zone II ($G > 160\ cm^3\ min^{-1}$) must be attributed to the formation of dry foams of high protein content.

It appears that there is a critical gas flowrate which, when exceeded, may upset the equilibrium of solute adsorption at the gas-liquid interface of the rising bubbles. Equilibrium depends on the diffusion of the solute to the gas-liquid interface and is a very slow process, particularly in dilute solutions. Therefore the contact time for the rising bubbles and the liquid medium is very critical for the formation of firmly stabilised bubbles and foam of high liquid content. An increase in gas flowrate, such as that in Zone II, appears to have shortened the contact time to such an extent that it became detrimental to foam stability and mass transfer. Wace et al. (1969) found that there is a critical gas velocity above which the foam column floods, ie the foam-liquid interface becomes indistinguishable. Ahmad (1975) studied the effects of different liquid column heights for a constant gas flowrate upon BSA enrichment and found that values continuously increased with increasing liquid height. This suggested that increase in contact time between bubbles and liquid allowed more time for the albumin to diffuse onto the surface of the rising bubbles.

Improved protein enrichment and separation with prolonged residence times (Figure 6.6) must be associated with the observed more efficient protein stripping from the liquid phase. The latter is associated with

improved transfer of protein molecules from the liquid to the foam phase under such conditions. The observed improvement in RNA enrichment must be attributed to the same mechanism as protein enrichment. The dependence of protein enrichment and separation ratio are similar to those observed by Grieves and Wood (1964) and Ahmad (1975), but are at variance with published BSA enrichment profiles by Brown et al.(1990). According to the latter, there is a distinct residence time, above which enrichment tends to decrease due to decrease in the concentration of the entrained liquid.

The observed reductions in $Q_F/Q_0$ and $H_r$ with increasing residence time (Figure 6.7) must be associated with higher enrichment and lower stripping factors. Intense protein stripping from the bulk solution reduced its capacity to produce strong foams having a high liquid content. Expression of the foam flowrate as a percentage of the inlet compensates for variations in the inlet flowrate ($Q_0$), as dictated by the experimental design.

The beneficial effects of prolonged residence time upon protein recovery (Figure 6.7) imply that, under the applied experimental conditions, the factors influencing protein enrichment predominated those affecting foam volumetric flowrate. This trend agrees with experimental evidence in Table 5.3; Chapter 5, which shows that increased residence times improved the recovery of BSA in the foam. The results also agree with those of Brown et al. (1990), where BSA recovery benefited from long residence times despite a decrease in protein enrichment.

Residence time could also be adjusted by maintaining a constant flowrate and varying the volume of the liquid pool. This would lead to variations in the height of the foam column (a dependent variable) and would affect the mass transfer of solutes from the bulk to the foam phase. Ahmad (1975) reported that the separation ratio of albumin was improved with increasing height of the liquid pool, due to extended times for

diffusion of albumin molecules to the interface. Similarly, the effects of varied varied gas flowrates upon foam characteristics (Figures 6.4 and 6.5) highlighted the importance of the contact time between bubbles and solutes to the quality of foam.

In the light of the above evidence, it is evident that there is a combined effect of rates of sparged gas and inlet feed, upon the determination of foam characteristics. It is suggested that experimentation be undertaken at various gas to liquid feed ratios ($G/Q_0$), in order to observe the behaviour of protein enrichment and recovery. Ahmad (1975) reported that increasing $G/Q_0$ ratios increase the mass of albumin in the foam expressed as a fraction of that in the bottom stream. Critical $G/Q_0$ values were found above which no further increase occurred. However, in this latter report, there is description of the dependence of albumin enrichment and recovery upon $G/Q_0$.

Additional experimentation with brewer's yeast extract should also study the response of protein enrichment, fractionation and recovery to a fixed critical $G/Q_0$ ratio , derived from appropriately varied G and $Q_0$ values. The results would demonstrate the importance of these individual parameters when imposed simultaneously in nominated proportions.

In conclusion, the above results showed that prolonged residence times for foams from yeast extracts can be beneficial to protein enrichment and recovery. However no improvement in protein fractionation from RNA was observed under experimental conditions. The eventual attainment of steady values for both enrichment and recovery suggested that further experimentation at higher residence times was not necessary. However, in the light of the existence of Zone II in Figure 6.3, it could be argued that further increase in residence time would lead to a further increase in protein enrichment and fractionation, but a reduction in recovery. The benefits of such a process would have to be weighed against

the serious drawback of slow inlet flowrates resulting in long processing times and diminished throughput.

The improved protein enrichment at higher bottoms recycle ratios (Figure 6.8) is irrefutably related to simultaneous reduction in protein stripping factors. Application of bottoms recycle leads to further removal of that protein in the liquid pool which was not extracted in the foam during the original residence time. This, in conjunction with the fact that at higher recycle R the fresh feed $Q_o$ is reduced in volume, creates conditions of increasingly dilute feed streams $Q_o^*$ at the entrance of the tower (see Table 6.4). As a result enrichment ratios are enhanced with increased $R/Q_B$ ratios, where the feed protein concentration is expected to be most diluted (compare Figure 6.10 with Figure 6.1a).

The effects of bottoms recycle upon RNA enrichment are not as pronounced as in the case of protein, due to its limited partition into the foam phase. As previously mentioned (see Figure 6.1a), RNA enrichment ratios are not extensively improved at dilute conditions. Therefore, bottoms recycle cannot significantly increase the RNA transfer from liquid to foam phase. Such behaviour, in association with promotion of protein enrichment at high bottoms recycle ratios, results in the pronounced improvement in protein fractionation from RNA. This behaviour is in line with previous findings (see Figure 6.1b) that protein is separated more efficiently from RNA at dilute feedstock conditions.

At high bottoms recycle ratios, the observed enhancement in protein recovery in respect of protein mass in the fresh feed (see Figure 6.9) must be attributed to pronounced increases in protein enrichment (Figure 6.8a). However, extensive denaturation, associated with dilute liquid pool conditions, leads to parallel increase in the precipitated protein ($R_d$). Reduction in protein recovery, referring to mass throughput in stream $Q_o^*$ at the entrance of the tower, with increasing bottoms recycle ratio (see

Figure 6.10) is clearly associated with dilute feedstock conditions (compare with Figure 6.3).

The above experiments clearly described the positive effects of continuous recycle upon protein enrichment, recovery and fractionation from RNA. However, the experimental design, based on a fixed feed at the entrance of the tower and standard liquid residence time, did not describe the benefits of bottoms recycle when a fixed fresh feed $Q_0$ is applied to achieve a target protein recovery in a defined period of time. In such operations, the liquid residence time would necessarily vary. Prediction of the effects of these variations could rely upon previous experience from studies on the effects of liquid residence time upon foam performance (see Figures 6.6 and 6.7).

### 6.3.2 Product Quality Assessment

The composition of 1 mg $cm^{-3}$ freeze-dried matter (in 40 mM phosphate buffer) in terms of protein, RNA, carbohydrate and acidic protease is presented in Table 6.5(a-e), and includes samples from feedstock, bottoms, foam and foam precipitate at pH 7.0, 7.6 and 8.0. All samples formed clear solutions and solubility tests were not considered necessary. Protein concentrations (Table 6.5a) in bottoms were routinely lower than those of respective feedstocks. The highest protein content in feedstock samples coincided with pH 7.6. Protein concentration in foam samples was only marginally higher than that of the respective feedstocks. In contrast, the highest protein concentration was consistently observed in foam precipitates. Foam samples were significantly enriched in RNA (Table 6.5b) when compared with respective feedstocks, and coincided with a slight decrease in the RNA content of bottoms. Foam precipitates were practically RNA free at all pH values. Carbohydrate analysis showed that (Table 6.5c) there was a slight increase in the amount of carbohydrate in foam samples,

**Table 6.5: Freeze-dried Feedstock and Products Composition in Continuous Foam Processing of Brewer's Yeast Extract**

Comparative description of the content of freeze-dried feedstock, bottoms, foam and foam precipitate in respect of **(a)** protein, **(b)** RNA, **(c)** carbohydrate, **(d)** acidic proteases and **(e)** protein/RNA ratio in 1 mg $cm^{-3}$ preparations of freeze-dried matter. Feedstocks and products correspond to continuous operations at pH 7.0, 7.6 and 8.0. Feedstock protein concentration was approximately 0.45 mg $cm^{-3}$. The inlet flowrate was 5 $cm^3$ $min^{-1}$ and nitrogen was sparged at a rate of 60 $cm^3$ $min^{-1}$.

**(a)**

| pH | Protein Concentration (mg $cm^{-3}$) | | | |
|---|---|---|---|---|
| | Feedstock | Bottoms | Foam | Foam Precipitate |
| 7.0 | 0.250 | 0.140 | 0.262 | 0.680 |
| 7.6 | 0.300 | 0.175 | 0.340 | 0.750 |
| 8.0 | 0.240 | 0.150 | 0.250 | 0.725 |

**(b)**

| pH | RNA Concentration (mg $cm^{-3}$) | | | |
|---|---|---|---|---|
| | Feedstock | Bottoms | Foam | Foam Precipitate |
| 7.0 | 0.050 | 0.035 | 0.135 | 0.010 |
| 7.6 | 0.065 | 0.045 | 0.110 | 0.015 |
| 8.0 | 0.045 | 0.035 | 0.080 | 0.010 |

**(c)**

| pH | Carbohydrate Concentration (mg $cm^{-3}$) | | | |
|---|---|---|---|---|
| | Feedstock | Bottoms | Foam | Foam Precipitate |
| 7.0 | 0.200 | 0.185 | 0.260 | 0.110 |
| 7.6 | 0.280 | 0.260 | 0.350 | 0.150 |
| 8.0 | 0.240 | 0.200 | 0.280 | 0.170 |

**(d)**

| pH | Acidic Proteases Concentration ($\mu$g $cm^{-3}$) | | | |
|---|---|---|---|---|
| | Feedstock | Bottoms | Foam | Foam Precipitate |
| 7.0 | 7.0 | 2.0 | 30 | - |
| 7.6 | 6.0 | 2.0 | 35 | - |
| 8.0 | 5.0 | 2.0 | 25 | - |

**(e)**

| pH | Protein/RNA Ratio | | | |
|---|---|---|---|---|
| | Feedstock | Bottoms | Foam | Foam Precipitate |
| 7.0 | 5.00 | 4.00 | 1.94 | 68.00 |
| 7.6 | 4.61 | 3.89 | 3.09 | 62.50 |
| 8.0 | 5.33 | 4.28 | 3.13 | 72.50 |

**Table 6.6: Foam Stability of Feedstock and Products Recovered from Continuous Foam Processing of Brewer's Yeast Extracts**

Head retention values (HRV) were determined for solutions of freeze-dried feedstock, bottoms, foam and foam precipitate produced in continuous foaming of Brewer's yeast extract. Foaming solutions of 1 mg $cm^{-3}$ freeze-dried matter were prepared in 40 mM potassium phosphate buffer, pH 7.6, in the presence of 4% ethanol. A description of the content of the foaming samples in protein, RNA, carbohydrates and acidic proteases and the conditions of continuous foam production is described in Table 6.5.

| pH | Head Retention Values (HRV) (sec) | | | |
|---|---|---|---|---|
| | Feedstock | Bottoms | Foam | Foam Precipitate |
| 7.0 | 202 | 177 | 70 | 450 |
| 7.6 | 210 | 200 | 122 | 480 |
| 8.0 | 180 | 136 | 65 | 447 |

while foam precipitates also contained a significant amount of carbohydrate. Acidic proteases (Table 6.5d) appeared to concentrate in foam by a factor of 4.5-6 fold, while bottoms were considerably depleted of protease activity. There was no detectable protease activity in foam precipitates. Table 6.5e describes variations in the protein/RNA ratio in feedstocks, bottoms, foams and foam precipitates. It appears that foams were enriched in RNA when compared with respective feedstocks and bottoms, and this behaviour was significantly pronounced at neutral pH. In contrast, foam precipitates demonstrated remarkably high protein/RNA ratios at all pH values applied.

Table 6.6 gives a comparative account of the foam stability (HRV) of the protein solutions described in Table 6.5. It can be seen that there was a significant drop in foam stability (as compared with the original feedstock) of solutions corresponding to foams, throughout the pH range applied. Foam stability from bottom products was routinely lower than that of feedstocks. On the contrary, stable creamy foams, generated from foam precipitates, exhibited head retention values more than double those of original feedstocks.

These results indicate that, although a decrease in protein content characterised all bottoms, foam samples did not seem to be enriched in protein. However, foam precipitates exhibited highest protein content, were practically RNA free and yielded the most stable foam. It is noteworthy that foam samples, although containing comparable amounts of protein with respective feedstocks, gave less stable foams than feedstocks and bottoms.

It can be seen that feedstock, bottoms and foam samples suffered a decrease in protein content associated with the process of dialysis and freeze-drying, when compared with pre-dialysis values presented in Table 6.2. Reductions in protein content in bottoms agree with previous

observations of protein depletion and appear to approximate stripping factors reported in Table 6.2. However, the low protein content in freeze-dried foams is at variance with the respective enrichment factors presented in Table 6.2. In the latter table, it is also shown that the amount of precipitated protein during foaming does not tally with the high protein content in foam precipitates detected in freeze-dried samples. It is possible that, prolonged centrifugation prior to freeze-drying precipitated a further significant amount of protein not sedimented, when bench centrifugation was applied to remove the denatured protein prior to the Bradford assay. IEF electrophoresis (see Plate 6.4) showed no evidence of selective removal of certain protein components by centrifugation.

The RNA content (Table 6.5b) reflects the pattern observed in Table 6.2, namely depletion of RNA from the bottom product, increase in foam, and virtual absence in foam precipitates. The observed depletion of RNA in the bottoms is less than for protein at equivalent conditions. The amount of RNA in foam samples appears to be higher than that in the feedstock by a factor in the proximity of $e_{RNA}$ values shown in Table 6.2. Centrifugation does not appear to affect RNA content, and the fact that only traces were found in the precipitate confirms previous evidence that RNA is not structurally sensitive at interfaces. Freeze-dried foam samples are therefore enriched in RNA, in comparison with respective feedstocks (Table 6.5e) due to loss of protein only during centrifugation. In contrast foam precipitates are virtually RNA free, and the observed protein/RNA ratios are higher than the acceptable limit of 10 (Emery et al. (1977)).

The presence of carbohydrates in foam and precipitates is expected since they have been involved in foam formation and stability in systems such as beer foams (Bamforth (1985)), or were found to improve foam

stability when added at various concentrations in protein solutions (Velissariou (1988); Leeson et. al. (1991)). Enrichment in protease activity by a factor of 4.5-6, which is 2-3 times higher than the $e_{protein,app}$ (see Table 6.2), implies that protease specific activity was 2-3 times higher in the foam than the feedstock. Fukal et al. (1986) have studied the properties of yeast proteases and found that, unlike plant proteases, they retain their activity at pH 3.0 and are thermostable. Other types of protease, such as basic protease, was found (Sarkar et al. (1987)), to exhibit 2-4 fold increase in specific activity in foam, during its crude purification by foam fractionation from raw materials, such as hospital waste tissues.

The foaming capacity of all these solutions of freeze-dried matter is significant given that their protein content is less than the minimal BSA concentration, which would yield measurable foam in homogeneous solutions (see Figure 3.1). Reduction in the foam stability of solutions containing lyophilised bottoms (Table 6.6) is consistent with the observed reduction in protein content (Table 6.5a). In contrast, a dramatic decrease in HRV for freeze-dried foam samples (Table 6.6), where protein content is comparable to respective feedstocks, suggests that "key" components or complexes might have been precipitated during the centrifugation employed in sample preparation. This finding is in contrast with results reported by Leeson (1989), where freeze-dried beer foam, produced by foaming beer, gave a higher protein content and HRV compared with the starting material. However, in this latter report, there is no mention of centrifugation prior to dialysis. The significant HRV for foam precipitates (see Table 6.6) may therefore be attributed to high protein content and the possible presence of "foam positive" molecules. It should also be noted that the treatment of protein precipitates with strong alkali, as a means of solubilisation, might have played an important role

in this foaming behaviour. In addition, the foaming process itself may have contributed to a conditioning of proteins to promote increased surface activity evidenced in enhanced HRV. However, whatever the reasons might be, freeze-dried foam precipitates, having a very high protein/RNA ratio (see Table 6.5) and good solubility, exhibited excellent foaming properties.

Further investigation of these phenomena should recover protein precipitates in foams by short duration slow speed centrifugation. It should also include alkali treatments of feedstock, bottoms, foam supernatant and foam precipitates prior to dialysis. The possibility of alkali conditioning of protein for enhanced surface activity could also be investigated with homogeneous preparations of BSA. Gel electrophoresis of yeast samples and products, where concentration factors have been meticulously calculated, would facilitate coomassie or silver staining and subsequent gel scanning. The latter would give an estimate of likely losses of specific polypeptides during centrifugal recovery of foam denatured protein.

### 6.3.3: Secondary Foam Treatment by Ion-exchange Adsorption

Figure 6.11(a-c) shows the elution profiles for foam, bottoms and feedstock respectively. It can be seen that basic and weakly acidic proteins with proportion of RNA were collected in the breakthrough (fraction 1), and represent species unable to bind DEAE-52 cellulose in 20 mM phosphate buffer, pH 8.0. The first elution step, involving 0.2 M NaCl, desorbed those proteins whose pI values are below pH 8.0 (fraction 2). The second step with 0.8 M NaCl eluted the strongly bound RNA (fraction 3). Table 6.7(a-c) describes the protein and RNA distribution in fractions 1, 2 and 3 as percentages of the respective loaded amounts for all the samples studied. It can be seen that, the percentage of acidic proteins

**Table 6.7: Protein and RNA contents in Fractions of Foam, Bottoms and Feedstock Eluted from a Fixed Bed of DEAE-52 Cellulose**

Quantitative description of the collected **(a)** protein and **(b)** RNA, expressed as percentages of the load, present in each fraction eluted from a DEAE-52 column loaded with foam, bottoms and feedstock. The protein/RNA ratio in each fraction is shown in **(c)**. The operating conditions were the same as in Figure 6.11.

**(a)**

| | Protein Load (mg) | Protein (%) | | |
|---|---|---|---|---|
| | | Fraction 1 | Fraction 2 | Fraction 3 |
| **Foam** | 5.40 | 43.98 | 44.44 | 1.00 |
| **Bottoms** | 1.92 | 58.59 | 21.67 | 3.91 |
| **Feedstock** | 2.70 | 55.55 | 30.21 | 2.22 |

**(b)**

| | RNA Load (mg) | RNA (%) | | |
|---|---|---|---|---|
| | | Fraction 1 | Fraction 2 | Fraction 3 |
| **Foam** | 1.42 | 35.21 | 16.90 | 42.25 |
| **Bottoms** | 0.73 | 58.22 | 19.18 | 13.70 |
| **Feedstock** | 0.84 | 47.62 | 23.81 | 16.77 |

**(c)**

| | Protein/RNA Ratios | | | |
|---|---|---|---|---|
| | Load | Fraction 1 | Fraction 2 | Fraction 3 |
| **Foam** | 3.81 | 4.75 | 10.00 | 0.10 |
| **Bottoms** | 2.63 | 2.65 | 4.16 | 0.75 |
| **Feedstock** | 3.21 | 3.75 | 4.50 | 0.32 |

**Figure 6.11: Elution Profile of Foam, Bottoms and Feedstock Fractionated on a Fixed Bed of DEAE-52 Cellulose.**

Elution profile of (a) foam, (b) bottoms and (c) feedstock from a DEAE-52 fixed bed equilibrated at pH 8.0 by 20 mM potassium phosphate buffer. Elution involved 0.2 and 0.8 M NaCl two-step gradient in equilibration buffer. 6 $cm^3$ of sample were loaded at a rate of 1 $cm^3$ $min^{-1}$. The volume of the bed was 5 $cm^3$and the ID of the column was 1 $cm^2$.

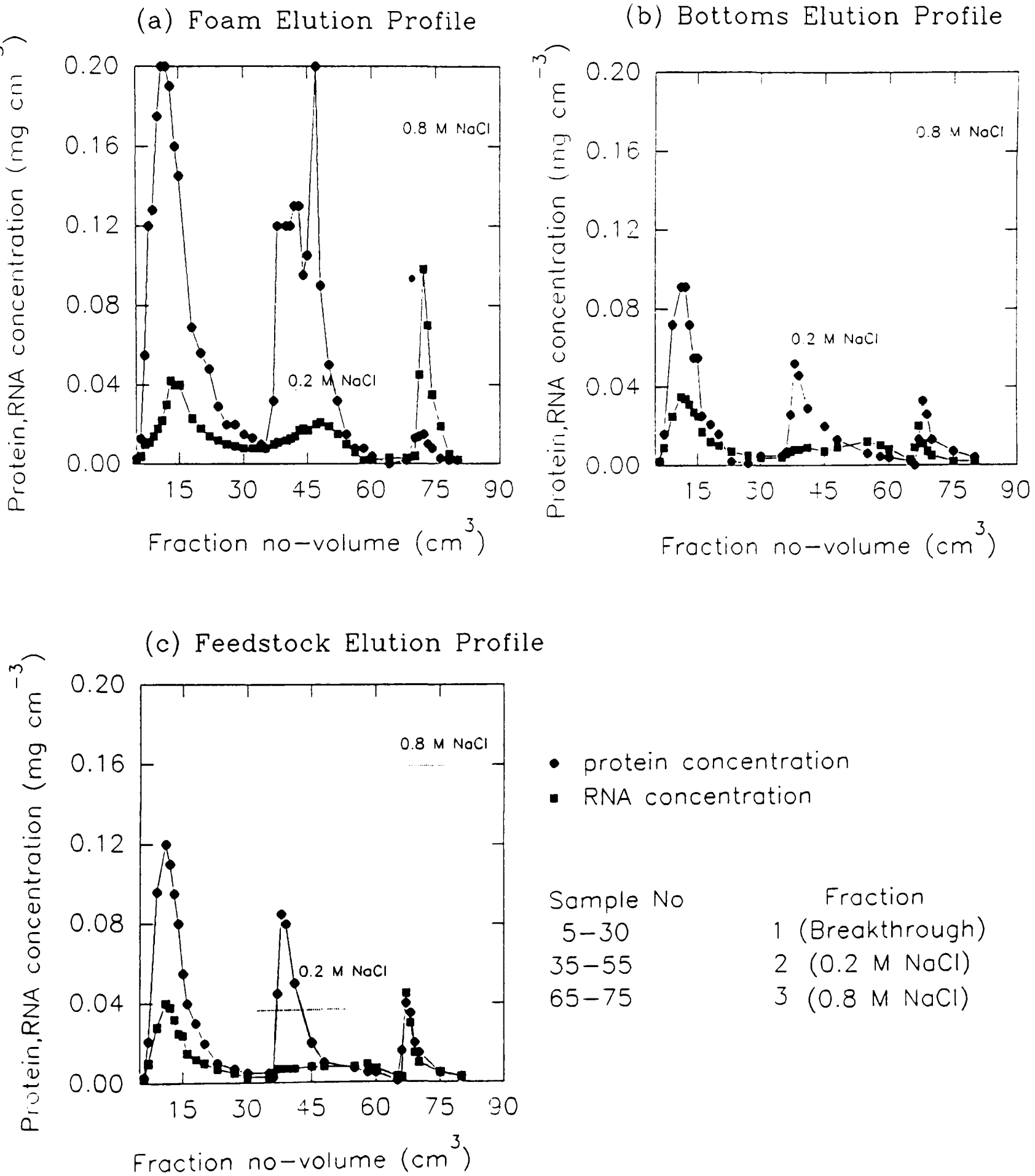

separated in fraction 2 for the foam load was higher than that of the feedstock and the bottoms. In the same fraction the achieved protein/RNA ratio was 10 as opposed to significantly lower ratios for the feedstock and the bottoms. In contrast, the lowest percentage of collected protein in fraction 2 corresponded to the bottom product.

These results suggest acidic proteins tend to concentrate in the foam leading to depletion in the bottom product. This evidence is in line with previous observations based on IEF gel electrophoresis (see Plates 6.3 and 6.4). Comparison of the ratios of protein in fractions 1 and 2, gives values of 0.99, 2.70 and 1.84 for foam, bottoms and feedstock respectively. Breakthrough (fraction 1) from DEAE-52 would be expected to contain a large proportion of basic and weakly acidic proteins. The basic:acidic mass balance, as indicated by fraction 1:fraction 2, is closest to unity for the foam, and may indicate the importance of electrostatic interactions in foam partition. Close parallels can be drawn with the BSA-lysozyme systems exhaustively discussed in Chapters 3 to 5. Such behaviour also results in high levels of protein fractionation from RNA, and the observed value (ie protein/RNA = 10) is comparable to protein/RNA ratios achieved by extraction of proteins from heated cells and RNA removal from disrupted cell suspensions by incubation in NaCl at 50 $^{o}$C (Emery et al. (1977)). It is however, less than values obtained from precipitated material recovered from foams (see Table 6.5). In retrospect it is regrettable that DEAE-52 analysis was not applied to alkaline solubilised and dialysed precipitates.

The above experiment has underlined the qualitative and quantitative importance of foam processing, as a crude step prior to further treatment by ion-exchange. Thus protein concentration by foaming processes may accelerate further treatment by reducing the volume of feedstocks. Since the foam sample was selected on the basis of its moderate protein

enrichment in the foam ($e_{protein,app}$=2.0) and fractionation index ($Fr_{protein,RNA}$=1.19), such behaviour is expected to be representative of both wet and dry foams. Further work could focus on the performance of ion-exchange with samples with high protein enrichment ratios and it would be essential for electrophoretic and IEF analysis to be undertaken to identify differences in protein patterns in fractions 1 and 2 for foams, bottoms and feedstocks.

## 6.4 Concluding Summary

Continuous foaming of brewer's yeast extract showed that protein enrichment was favoured under conditions which promoted foam of low liquid content. Such conditions required dilute feedstocks, low gas flowrate and prolonged residence times. In experiments with various feedstock concentrations, bulk protein behaved much as a single protein in a model solution. This suggested that in such complex systems, it is the overall contribution of proteins or polypetide complexes that determine foam characteristics. Such behaviour is in contrast with the predominance of composition over total protein concentration, observed in BSA-lysozyme systems (see Chapter 4). Under conditions of enhanced protein enrichment, overall recovery was low due to the low liquid load of the foam, whilst the extent of denaturation was higher.

RNA enrichment showed a similar but less pronounced trend. Under conditions of slow foam production (ie dry foam), protein enrichment was found to be significantly higher than that of RNA. Therefore, protein fractionation from RNA was maximal under such conditions. It was also found that RNA partition in foam was best at pH 7.0 and as a result fractionation was minimal even at dilute conditions. Therefore any operations designed to fractionate protein from RNA should take place at pH values greater than pH 7.0.

Extensive protein stripping from the liquid phase was achieved by recycling the bottom effluent. This resulted in enhanced protein enrichment and fractionation, but extensive denaturation. The experimental evidence suggests that the achievement of high quality foams is routinely compromised by low recovery and increased precipitation. Therefore, where the latter does not constitute a serious problem, such operations should be applied.

SDS-PAGE analysis of foam, feedstock and bottoms showed that those proteins which partition to foam are generally representative of the original feedstocks. However, IEF highlighted that acidic proteins are depleted from the bottoms and a protein or proteins of pI approximately 7.0 appears to selectively fractionate in foam. Further analysis by 2-dimensional electrophoresis could provide more information about the molecular characteristics of these species.

Product quality assessment showed that the precipitated protein in foam exhibited good solubility, minimal RNA content and maximal foam stability. Such qualities may recommend applications as a food additive. Low protein content and foamability of foam supernatant draw attention to the centrifugation procedure applied to remove the precipitated protein. The fact that the protein content of freeze-dried foam supernatant was equivalent to that of the feedstock (in comparable mass quantities) but of inferior foaming qualities suggests that "foam positive" proteins were precipitated during centrifugation. It would be therefore interesting to investigate the role of these proteins in conjunction with the effects of alkali (used to resolubilise the precipitate). Ion-exchange treatment of foam on a DEAE-52 fixed bed indicated that the eluted foam yielded product of higher purity in terms of RNA content. This indicates a scope for further evaluation of foam separation prior to ion-exchange purification.

Foam reflux was not applied at this stage due to the observed

precipitation. However, it would be interesting to see the benefits of combined reflux and bottoms recycle under conditions of limited denaturation. Such studies would facilitate assessment of the effects of precipitate upon the stability of rising foam bubbles. Concentration by the achievement of small foam volumes having high protein content might generate interesting products, but would certainly benefit other downstream processes of molecular fractionation (selective adsorption, gel permeation, preparative electrophoresis).

# CHAPTER 7

## DYNAMIC CHANGES IN FOAM BUBBLES AND EFFECTS UPON PROTEIN PARTITION

### 7.1 Preface

Quantitative studies of foams from model and realistic protein feedstocks presented in the previous chapters (Chapters 3-6) indicated a scope for a study of bubble dynamics in foams and their relation to protein partition. Thus, a study was undertaken to investigate the relation between bubble size and foam quality. It also dealt with prediction of process performance by application of the model by Brown et al. (1990), which describes the hydrodynamics of protein stabilised foam beds. As opposed to other studies based on model systems, the present work included foams generated from brewer's yeast feedstocks in order to investigate those characteristics associated with the complexity of the system. The presence of a great number of proteins and other molecules, such as RNA, might pose limitations in the adoption of those simplifying assumptions acceptable in simple homogeneous model systems.

As pointed out in Chapter 1, various studies have been carried out on liquid hold-up in mostly semi-batch foams. Various expressions have been developed (Desai and Kumar (1983)) to predict liquid hold-up based on bubble size and physical properties of the solution and operating parameters. Similarly various predictive expressions have been presented, which model foam fractionation. Most of them have focused on small surfactants molecules (Fanlo and Lemlich (1965)). Some studies however have dealt with protein stabilised foams in semi-batch (Narsimhan and Ruckenstein (1986a-b)) and continuous operations (Brown et al. (1990)) using BSA as a model protein, and have highlighted the peculiarities of protein foams. The proposed models generally predict protein enrichment

and foam volumetric flowrate. Such variables are related to the dynamics of foam which determine the liquid load of foam and the equilibrium isotherm for the foaming agents.

In the current study, the application of the model by Narsimhan and Ruckenstein (1986a), which was adapted for continuous operations by Brown et al. (1990) (for a detailed description see Appendix IV), has assumed constant bubble size with height, namely zero coalescence. Such an assumption necessitated the application of small foam beds, to ensure limited drainage and coalescence. Under such conditions similar values of bubble size at the bottom and the top of the tower can be achieved. Bubble size was measured at the foam-liquid interface for various feedstock concentrations and gas flowrates. However, changes in bubble size with height were also studied for certain operating conditions.

Variation of foam coalescence with the height of the foam bed, and its effects upon foam partition, were examined at extended foam beds. A preliminary study involved measurements of bubble size, liquid hold-up and quantitative characteristics of foam. This study was undertaken with a view to determine the rates of bubble coalescence and mass transfer of protein to the foam phase, and to indicate a possible experimental procedure which would yield an empirical correlation of bubble coalescence with height. An empirical expression of bubble size and liquid hold-up as functions of the physical properties of the solution and operating conditions would improve the aforementioned model by inclusion of the coalescence factor in performance prediction.

## 7.2 Experimental Description

Continuous foaming of brewer's yeast extract was conducted in a manner described in Chapter 2 (2.3.3) in the foam tower illustrated in Figure 2.5. The protocol of feedstock preparation was identical to that

described in Chapter 6 (6.2). Solutions were prepared in 20 mM phosphate buffer, pH 8.0. Bubble photographs and bubble size measurements were performed as outlined in Chapter 2 (2.5.2).

Liquid hold-up at various heights of the foam bed was measured by slowly pumping foam through the sampling ports at a fixed volumetric flowrate for 1 minute. The collected foam was weighed to enable determination of the flowrate. The liquid hold-up was determined as a fraction of the liquid content of foam relative to the volumetric pump rate. Similarly, the volumetric flowrate of foam was determined from the mass of freely collected foam from each sampling port. In both cases, sampling started from the top of the foam bed, where the liquid hold-up was reduced, in order to eliminate disturbance of the foam bed. Both duplicate sampling, and the determination of the liquid hold-up and foam volumetric flowrate, were separated by sufficient time to maintain the foam bed in steady-state conditions.

Foam studies of small foam beds (5 cm) were carried out in the bottom section of the two-section tower of Figure 2.5. Both sections were used, which yielded an extended foam tower of 40 cm in height, for studies of height effects upon foam.

## 7.3 Results and Discussion

Results are expressed in terms of the following variables:

-Protein enrichment, $e_{protein,real}$, (Equation 3.1 and/or 3.2)

-Protein separation, $s_{protein}$ (Equation 3.5)

-Protein recovery, $R_{protein,real}$(%), (Equation 3.3 and/or 3.4)

-Protein mass flowrate, $m_{protein,F}$, (Equation 5.1); for comparable feedstocks variations in mass flowrate reflect variations in recovery

-Average bubble diameter, $\bar{d}_b$, (arithmetic average); $\bar{d}_b$[=]mm unless otherwise specified.

-Liquid and gas hold-up ($\varepsilon_l$ and $\varepsilon_g$ respectively), interrelated by Equation 7.1; $\varepsilon_l$ and $\varepsilon_g$ are dimensionless:

$$\varepsilon_g = 1-\varepsilon_l \qquad \text{(Equation 7.1)}$$

-Number of bubbles per unit volume of the foam bed ($N_b$) given by Equation 7.2:

$$N_b = 6\varepsilon_g/(\pi\bar{d}_b^{\,3}) \qquad \text{(Equation 7.2)}$$

-Interfacial transfer area per unit volume of foam bed ($f_{sp}$) which is defined by Equation 7.3; $f_{sp}[=]cm^{-1}$

$$f_{sp} = \pi(\bar{d}_b)^2 N_b = 6\varepsilon_g/\bar{d}_b \qquad \text{(Equation 7.3)}$$

-coalescence frequency ($\omega$), ie percentage of $N_b$ collapsing per unit time, described by Equation 7.4 (Brown et al. (1990)); the right-hand side i divided by a factor of 2 to avoid double counting:

$$dn/dh_f = -\omega N_b/2 \qquad \text{(Equation 7.4)}$$

where: n is the number of bubbles passing through a cross-sectional area of the foam column per unit time.

$h_f$ is the height of foam bed from the foam-liquid interface

Equation 7.5 relates n to the superficial gas velocity $u_g$ and the volume of a single bubble (Brown et al. (1990)):

$$n = 6u_g/\pi(\bar{d}_b)^3 \qquad \text{(Equation 7.5)}$$

Combination of Equations 7.4 and 7.5 yield Equation 7.6:

$$\omega = 36u_g(d\bar{d}_b/dh_f)/\{\pi N_b(\bar{d}_b)^4\} \qquad \text{(Equation 7.6)}$$

The differential $d\bar{d}_b/dh_f$ can be expressed as a function of $h_f$ by experimental determination of $\bar{d}_b$ as a function of $h_f$.

$-m^*_{protein,F}$, namely the mass flowrate of protein in the foam per interfacial transfer area per unit volume of the foam bed; $m^*_{protein,F}$[=]mg cm $min^{-1}$.

$-k_{N2}$ is the mass transfer coefficient for the adsorption of nitrogen into the liquid phase, and described by the following empirical equation (Maminov and Mutriskov (1969)):

$$k = 5.35x10^3\{2Du_{rel}/(\bar{d}_b h_f)\}^{0.7}(1+\mu_d/\mu_c)^{-1/2} \qquad \text{(Equation 7.7)}$$

where: $k$ is the mass transfer coefficient of the gas into the liquid phase; $k$[=]cm $sec^{-1}$

$D$ is the molecular diffusivity of the gas; $D$[=]$cm^2$ $sec^{-1}$

$u_{rel}$ is the relative phase velocity described in Appendix V; $u_{rel}$[=]cm $sec^{-1}$

$h_f$ is the height of the foam bed; $h_f$[=]cm

$\bar{d}_b$ is average bubble diameter; $\bar{d}_b$[=]cm

$\mu_d$ and $\mu_c$ are the viscosities of the dispersed and continued phase respectively; $\mu_d$ and $\mu_c$[=]dyn sec $cm^{-2}$.

Equation 7.7 is applicable for $1< N_{Re} < 300$, which is in the general range of Reynolds numbers (based on bubble diameter) in foams. Because the feedstock viscosity was very close to that of the water (see Table 7.1) the diffusivity of nitrogen in water at 25 °C ($D_L x\ 10^{-5}$=1.9 $cm^2$ $sec^{-1}$), found in Perry and Green (1984), was used in Equation 7.4. The value of $\mu_d$ was found to be $1.75x10^{-4}$ dyn sec $cm^{-2}$ (Perry and Green (1984)). Both diffusivity and viscosity values correspond to 22.5°C. The physical properties of the foaming feedstocks are presented in Table 7.1. It can be seen that the viscosity and density of all feedstocks is very close to that of the water.

### 7.3.1 Bubble Size and Protein Partition to Foam at Small Foam Bed Heights

Figures 7.1(a-b) to 7.5 describe variations in bubble size and protein partition into foam with the operating conditions; namely feedstock protein concentration ($c_{protein,0}$) and gas flowrate (G), at low heights of foam bed ($h_f$ = 0-5 cm). The effects of gas flowrate and feedstock protein concentration upon average bubble diameter at the gas-liquid interface ($\bar{d}_{b0}$) are illustrated in Figure 7.1(a-b) respectively. At equivalent feedstock concentrations, higher gas flowrates resulted in the formation of smaller bubbles (Figure 7.1a). This trend was consistent at both feedstock concentrations applied and it can be seen that at comparable gas flowrates larger bubbles were formed at the lowest feedstock concentration (0.25 mg $cm^{-3}$). This behaviour is more pronounced in Figure 7.1b where a sharp increase in $\bar{d}_{b0}$ can be observed at very dilute conditions for foams produced at a fixed gas flowrate of 40 $cm^3$ $min^{-1}$. The distribution of bubble diameter at the foam-liquid interface for foams produced from feedstocks of varied protein concentration at a fixed gas flowrate of 40 $cm^3$ $min^{-1}$ is shown in Figure 7.2(a-c). It can be seen that the distribution of bubble diameter became broader with decreasing feedstock protein concentration, and coincided with the formation of larger bubbles (see Figure 7.1b). Increase in average bubble diameter $\bar{d}_b$ with height, is described in Figure 7.3(a-b) for (a) various feedstock protein concentrations and fixed gas flowrate (G=40 $cm^3$ $min^{-1}$) and (b) varied gas flowrate and equivalent feedstock protein concentration ($c_{protein,0}$ = 0.25 mg $cm^{-3}$). Some photographs of foam bubbles at various heights of the foam bed are presented in Appendix IV. In Figure 7.3a it can be seen that $\bar{d}_b$ increased with height. Such increase was more pronounced at low $c_{protein,0}$. Figure 7.3b shows that, at comparable heights of the foam bed, $\bar{d}_b$ was highest at the lowest gas flowrate

**Table 7.1: Physical Properties of Foaming Feedstocks form Brewer's Yeast Extract**

Physical properties for various concentrations of brewer's yeast extract. Preparations were made in 20 mM phosphate buffer pH 8.0. Measurements were undertaken at room temperature (22.5-22.8 °C).

| Feedstock Protein Concentration (mg $cm^{-3}$) | Surface Tension (dyn $cm^{-1}$) | Viscosity (g $cm^{-1}$ $sec^{-1}$) | Density (g $cm^{-3}$) |
|---|---|---|---|
| 0.45 | 52.25 | $1.19 \times 10^{-2}$ | 1.015 |
| 0.25 | 53.15 | $1.15 \times 10^{-2}$ | 1.008 |
| 0.17 | 54.50 | $1.10 \times 10^{-2}$ | 1.002 |
| 0.10 | 57.25 | $1.05 \times 10^{-2}$ | 1.002 |

**Figure 7.1: Effects of Operating Conditions upon Bubble Size at the Origin of Foam Bed**

Dependence of bubble diameter at the foam liquid interface ($\bar{d}_{bO}$) upon **(a)** gas flowrate and **(b)** feedstock protein concentration. The total height of the foam bed was 5 cm and foam was produced continuously from brewer's yeast extract at an inlet flowrate of 5 $cm^3$ $min^{-1}$.

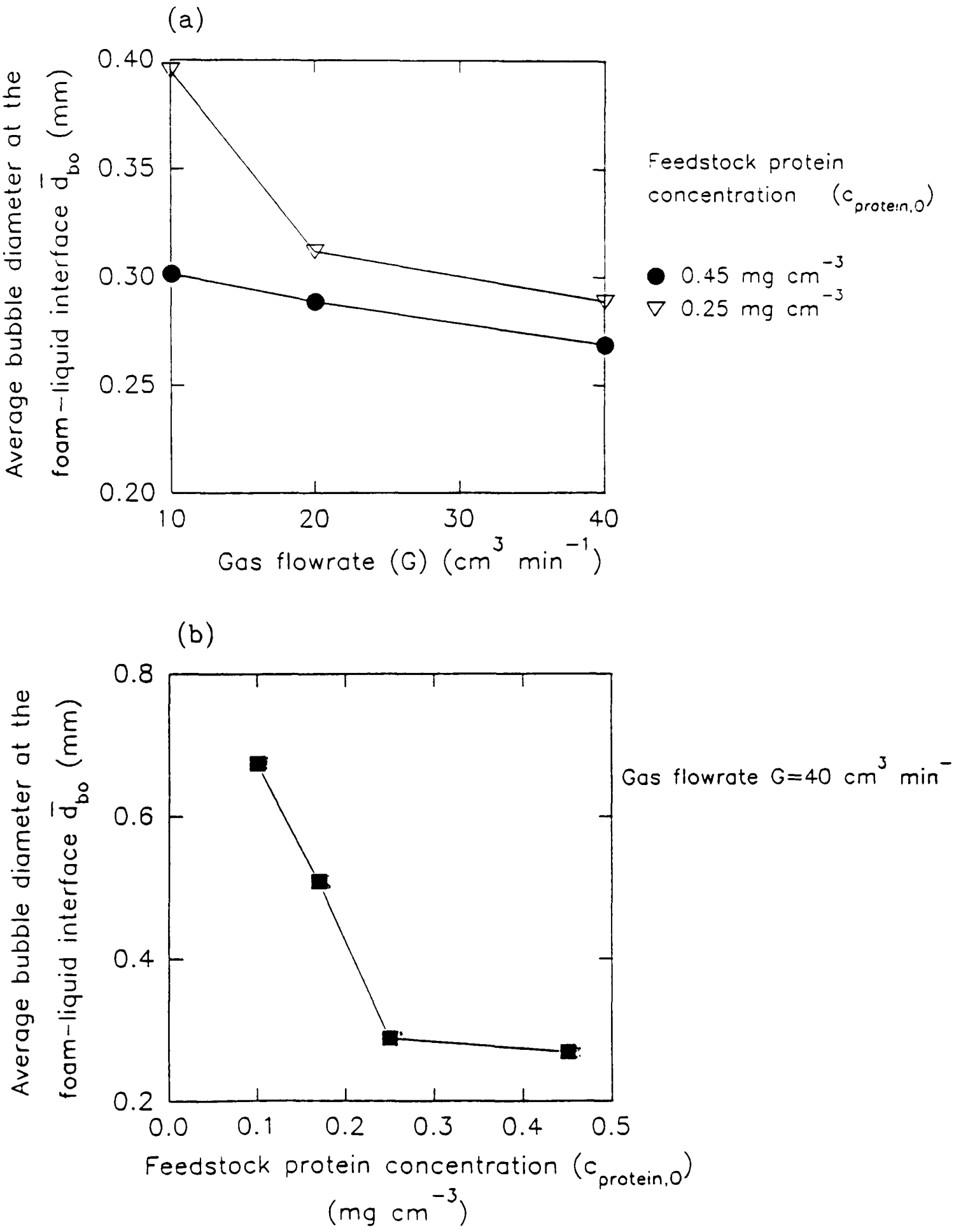

**Figure 7.2: Normalised Bubble Size Distribution at the Origin of Foam Bed**

Normalised bubble size distribution (Gaussian distribution) of measured bubble diameters at the foam liquid interface ($\bar{d}_{b0}$) for feedstocks of **(a)** 0.45 mg $cm^{-3}$ protein, **(b)** 0.25 mg $cm^{-3}$ protein and **(c)** 0.1 mg $cm^{-3}$ protein. Foam was produced continuously from brewer's yeast extract at an inlet flowrate of 5 $cm^3$ $min^{-1}$ and a gas flowrate of 40 $cm^3$ $min^{-1}$.

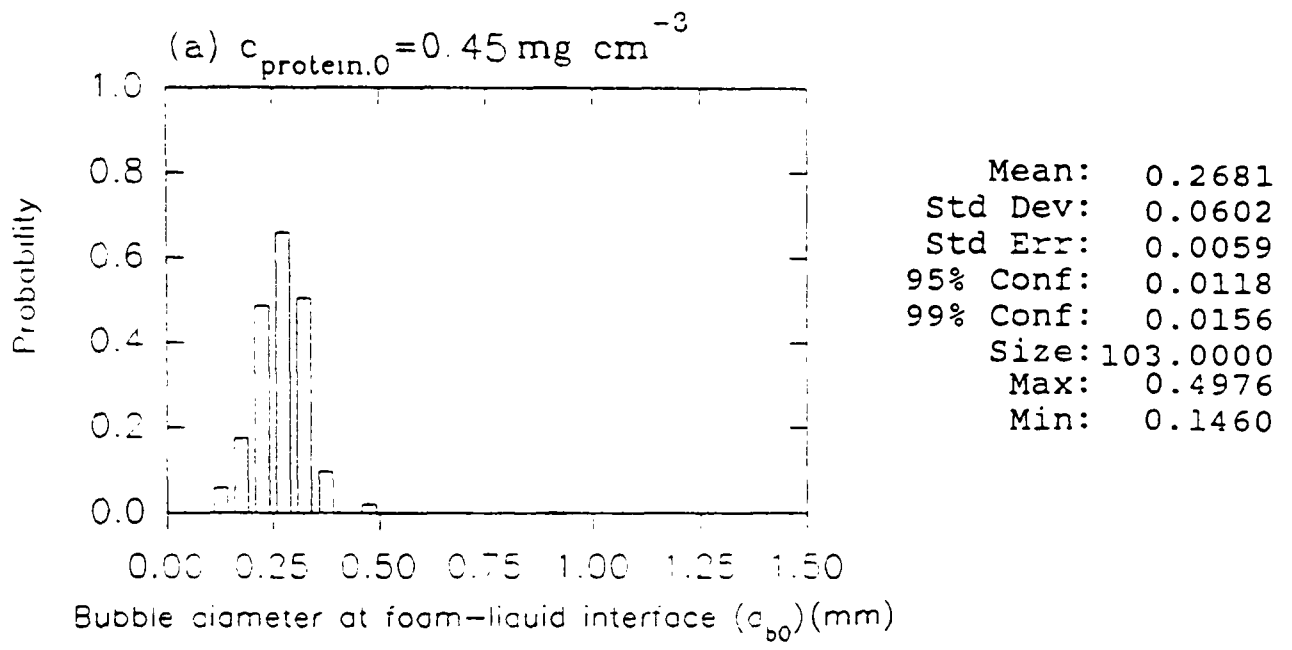

**Figure 7.3: Variations in Bubble Size with Height for Foam Beds of 5 cm in Height**

Changes in bubble diameter ($\bar{d}_b$) with foam height at small foam beds (5 cm) for various operating parameters; **(a)** varied feedstock concentration and fixed gas flowrate (G=40 $cm^3$ $min^{-1}$) and **(b)** fixed feedstcok concentration ($c_{protein,0}$=0.25 mg $cm^{-3}$) and varied gas flowrate.

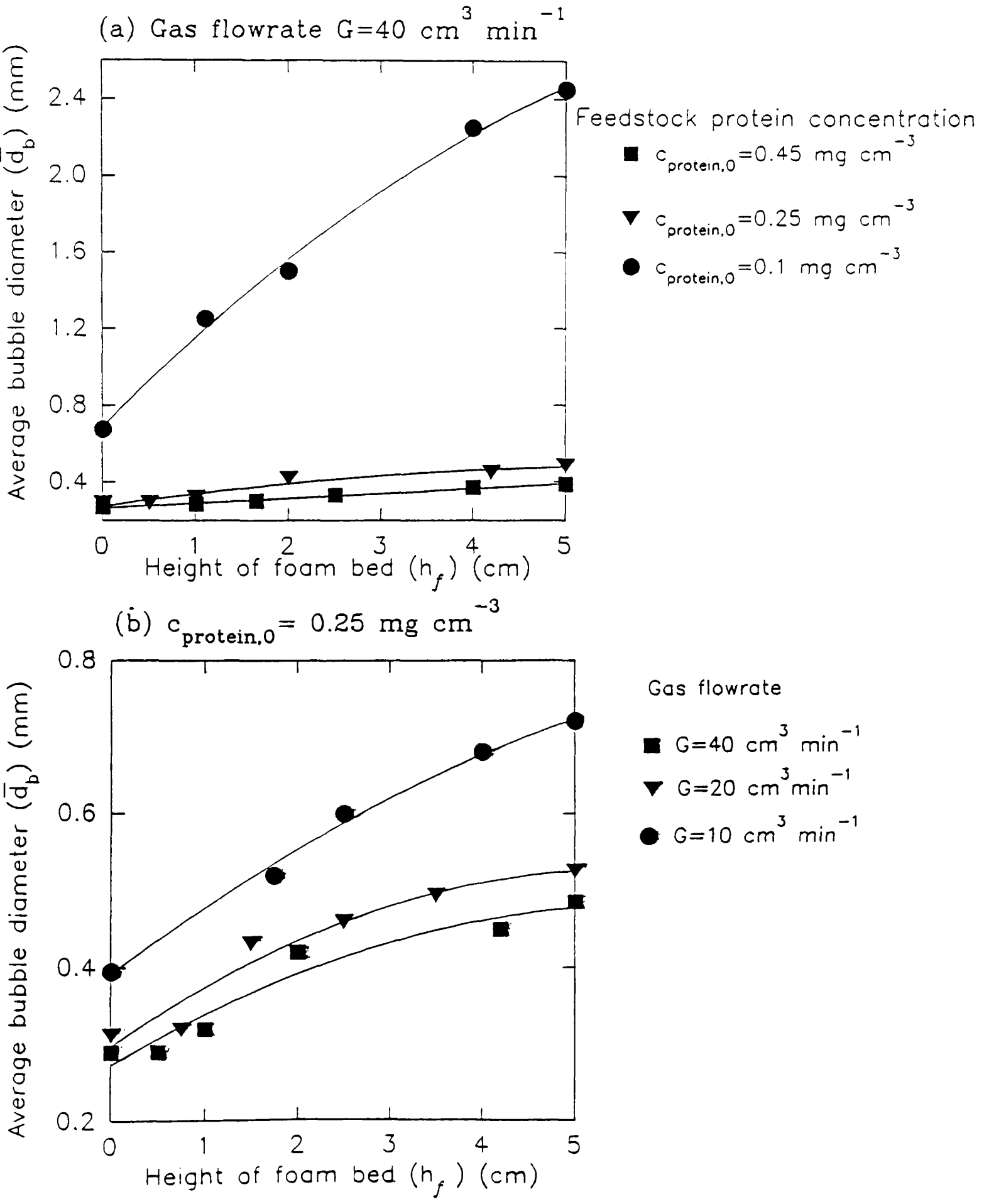

applied, and it appears that increase in $\bar{d}_b$ was most pronounced at G=10 $cm^3\ min^{-1}$. In contrast, increase in $\bar{d}_b$ with height was broadly similar for G= 20 and 40 $cm^3\ min^{-1}$. In all plots however it appears that the observed increase in $\bar{d}_b$ with foam height approached plateau values at the top of the foam bed.

Figure 7.4(a-b) describes the effect of gas flowrate upon protein enrichment ($e_{protein,real}$), gas volumetric flowrate ($Q_F$) and protein recovery ($R_{protein,real}$) for feedstock protein concentrations of 0.45 and 0.25 mg $cm^{-3}$ respectively. Protein enrichment and separation was favoured at low gas flowrates whilst foam flowrate and protein recovery increased at higher gas flowrates. It can also be seen that at $c_{protein,0}$ = 0.25 mg $cm^{-3}$, protein enrichment and separation were consistently higher and foam volumetric flowrates were below respective values at $c_{protein,0}$ = 0.45 mg $cm^{-3}$. At constant gas flowrate (G=40 $cm^3\ min^{-1}$) protein enrichment and separation sharply increased at low feedstock concentrations (Figure 7.5a), while foam volumetric flowrate and protein recovery were enhanced at concentrated feedstocks (Figure 7.5b).

The results suggest that dilute feedstock are associated with the formation at the foam-liquid interface of larger bubbles of broad size distribution. This narrows as the bubble size decreases at more concentrated solutions. At comparable feedstock concentrations, reduction in gas volumetric flowrate leads to the formation of larger bubbles. It seems that increase in bubble size with height is more pronounced at dilute conditions. Variations in gas flowrate for solutions of equivalent concentration seem to result in an approximately parallel increase in bubble size throughout the height of the foam bed. It is evident that there is a consistent correlation between bubble size and quantitative characteristics of foam. Hence, high enrichment and separation ratios, associated with dilute feedstocks and low gas flowrates, coincide with

**Figure 7.4: Effects of Gas Flowrate upon Protein Partition for Foam Beds of 5 cm in Height**

Effects of gas flowrate upon real protein enrichment ($e_{protein,real}$) and separation ($s_{protein,real}$), foam volumetric flowrate ($Q_F$) and real protein recovery ($R_{protein,real}$) for varied feedstock protein concentrations; **(a)** $c_{protein,0}$=0.45 mg $cm^{-3}$ and **(b)** $c_{protein,0}$=0.25 mg $cm^{-3}$.

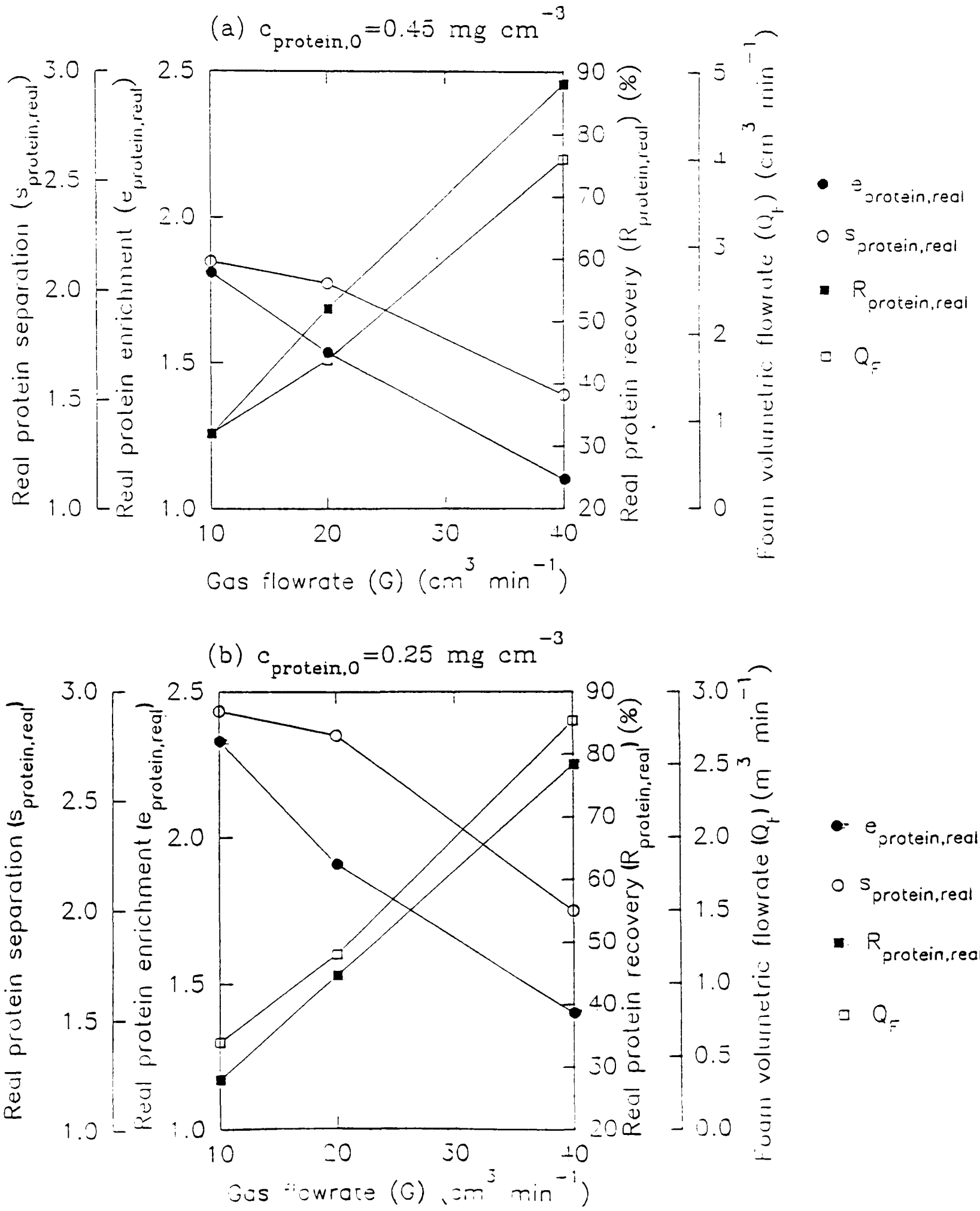

**Figure 7.5: Effects of Feedstock Concentration upon Protein Partition in Foams of 5 cm in Height**

Effects of feedstock protein concentration upon **(a)** real protein enrichment ($e_{protein,real}$) and separation ($s_{protein,real}$) and **(b)** foam volumetric flowrate ($Q_F$) and real protein recovery ($R_{protein,real}$) for foams produced continuously at a fixed gas flowrate (G=40 $cm^3$ $min^{-1}$).

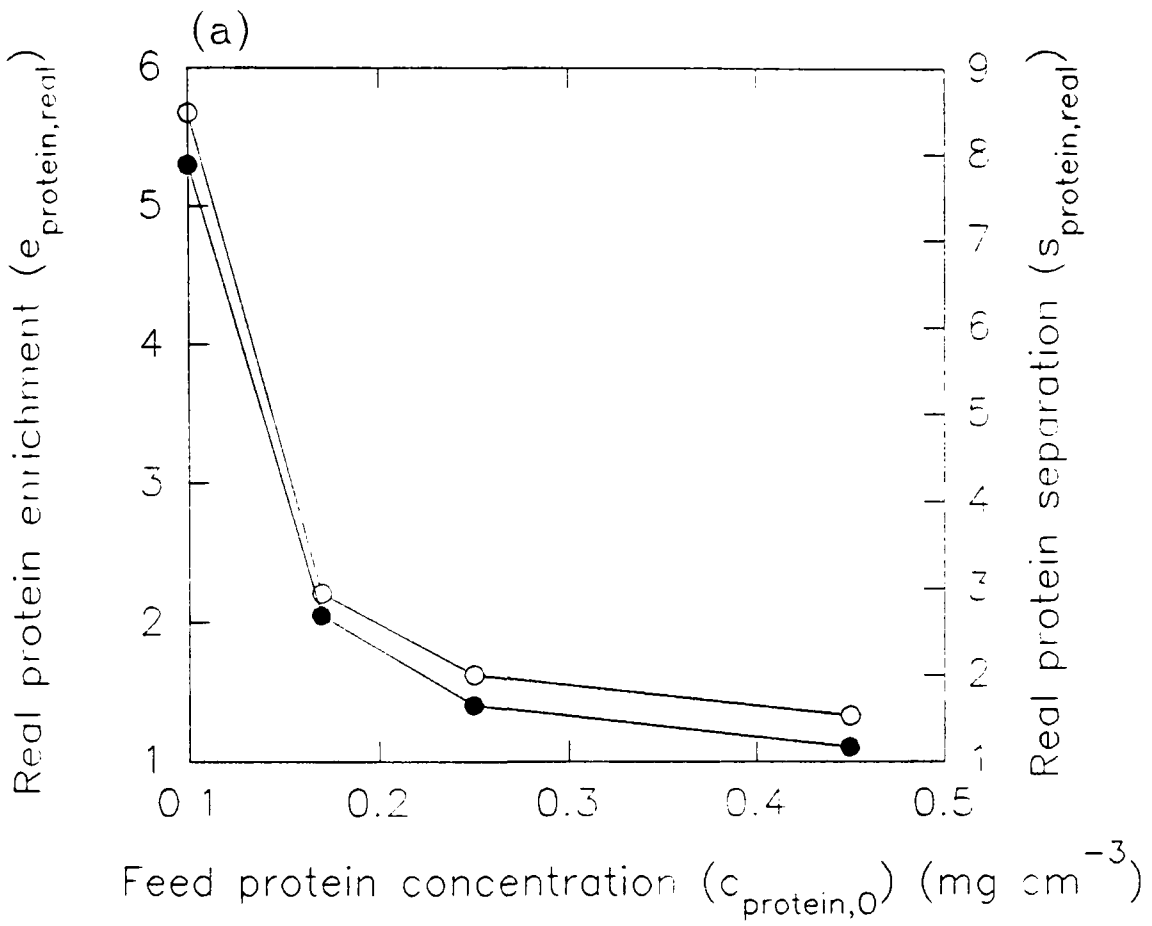


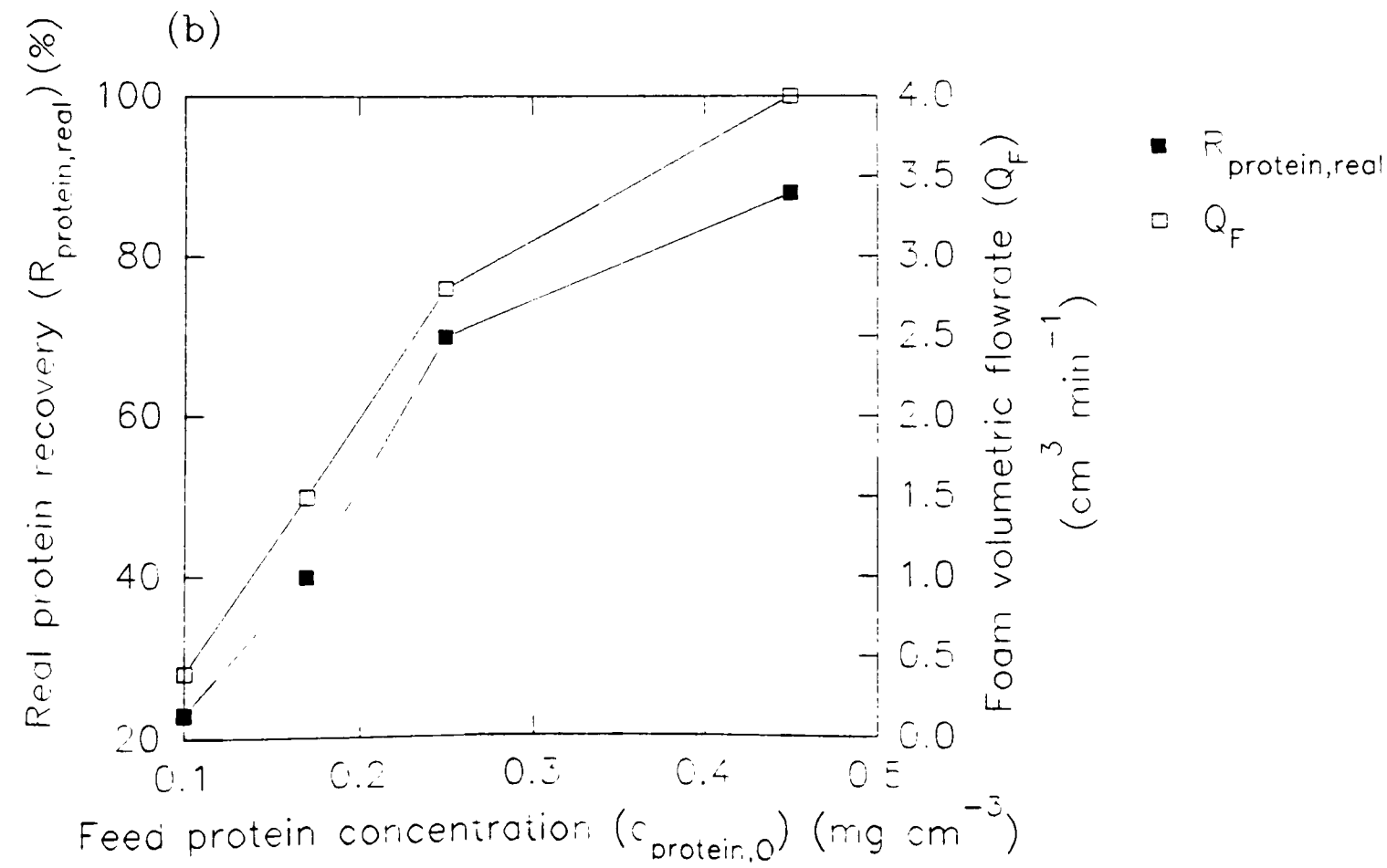

large bubble diameters at the foam-liquid interface and pronounced increase in bubble size with foam height. In contrast, under similar conditions the observed values of volumetric flowrate and protein recovery declined. It is therefore indicated that the liquid hold-up of foams, characterised by large bubbles and sharp increase in bubble size with height, is expected to be reduced.

The observed dependence of bubble size at the foam-liquid interface ($\bar{d}_{b0}$) upon feedstock concentration (Figure 7.1b) is in accordance with studies on bubble formation by gas flow through static spargers (Bonakdarpour (1990)). Bubbles produced by static spargers are influenced by the following parameters:

-surface tension (ie surfactant concentration, buffer molarity and pH, temperature and pressure)

-viscosity

-hole diameter

-gas velocity (orifice gas phase Reynolds number)

-coalescence promoting/inhibiting property of the solution

-liquid phase turbulence

Bubble formation by porous plate spargers, of the type used in this study, is claimed to produce the smallest bubble sizes (Perry and Green (1984)) although the pore size and the pressure drop across the sparger, which is proportional to the air inlet (Bird et al. (1960)), may play an adverse role in small bubble formation. In surfactant solutions, such as protein feedstocks, bubble coalescence in the liquid pool is inhibited and bubbles produced at the sparger tend to maintain their size up to the foam-liquid interface (Koide et al. (1968)). However, pressure drop along high liquid pools, such as the one in the present study, is expected to result in some bubble growth. Such behaviour is common in carbonated beverages, where, once a bubble is nucleated, it will grow by diffusion of

carbon dioxide during its ascension to the top of the container (Hansen and Derderian (1975)). The correlation, which quantifies the effects of various parameters on bubble size in porous plate spargers is described by the following equation (Koide et al. (1968)), and applies to coalescence inhibiting solutions:

$$d_b^* = 6.1 \times 10^{-3} (u_g d_o)^{0.1} d_o^{0.08} (\sigma/\sigma_w)^{0.38} \qquad \text{(Equation 7.8)}$$

where: $d_b^*$ is bubble diameter in the liquid pool; $d_b^*$ [=] cm

$d_o$ is the average porous plate diameter; $d_o$ [=]cm

$u_g$ superficial gas velocity; $u_g$ [=]cm $sec^{-1}$

$\sigma$ and $\sigma_w$ surface tension of the medium and pure water respectively; $\sigma$, $\sigma_w$ [=] dynes $cm^{-1}$

In the present study the same sinter was used throughout experimentation and thus the influence of sinter pore size (ie $d_o$) can be eliminated. At equivalent gas flowrates, the size of bubbles created by the sinter depended on the surface tension of the solution, $\sigma$, to the power of 0.38, and it appears that surface tension influences bubble size at the gas-liquid interface in a similar manner. Subsequently, $\bar{d}_{b0}$ was larger at low feedstock concentrations where $\sigma$ increased (see Figure III2, Appendix III). Increase in $\bar{d}_{b0}$ at dilute solutions is in agreement with results reported elsewhere (Brown et al. (1990)) for foams produced from BSA solutions.

Contrary to predictions from Equation 7.8, $\bar{d}_{b0}$ slightly increased with decreasing $u_g$ for foams produced from feedstocks of comparable protein concentrations at various gas flowrates (Figure 7.1a). Such behaviour agrees with results by Brown et al. (1990). Disagreement between the observed results and predictions from Equation 7.8 may be associated with possible extensive changes in bubble size in the liquid pool at low gas flowrates, and fast drainage and coalescence at the foam-liquid

interface. Such phenomena are therefore likely to mask the formation of smaller bubbles near the surface of the sparger at lower gas flowrates, as predicted by Equation 7.8.

Broad bubble size distribution, associated with the bubbles of largest diameter (Figure 7.2(a-c)), must be associated with extensive coalescence and drainage. This promotes the formation of larger bubbles due to pressure differences between large and small ones. Bubble rupture also occurs due to film thinning, but is more likely to be extensively observed at a distance from the foam-liquid interface. However small variations in bubble diameter may also reflect differences in the size of sparger pores. The observed variations in bubble size raise the question of the suitability of the arithmetic average as a representative bubble diameter as opposed to the sauter average. For narrow size distributions these two averages will differ only slightly. Previous reports (Narsimhan and Ruckenstein (1986b)) have shown that the former should be used in material balances for liquid in the plateau borders whilst the latter is more appropriate in material balances for liquid in bubble films. For broad size distributions, the sauter diameter, will be much larger than the arithmetic average, and one single appropriate average size will not exist. It was therefore considered that the arithmetic average would be the most appropriate form of description of bubble sizes in the present study.

Sharp increases in bubble size with foam height at dilute conditions (Figure 7.3a) are associated with extensive coalescence and film rupture in the absence of excess surfactant molecules to stabilise the bubble films. At decreasing gas flowrates and comparable concentrations increase in $\bar{d}_b$ is steeper due to extensive drainage and coalescence whilst increase in gas flowrate can sustain a more stable foam. Extensive coalescence led to the formation of polyhedral bubbles as illustrated by Plate IV1 in

Appendix IV. Consistently similar $\bar{d}_b$ values along the foam bed for G = 20 and 40 $cm^3$ $min^{-1}$ indicate that the effects of gas flowrate upon bubble size reach a plateau, as previously discussed in Chapter 6 with reference to Figure 6.3. At this stage, further increase in gas flowrate, which would be expected to lead to unstable foam as demonstrated in Chapter 6 (Figure 6.3), was not applied. This behaviour is similar to observations by Rotentalp et al. (1991) for beer foams of various degrees of wetness.

The results obtained on bubble size and distribution only refer to bubbles at the glass wall, but were considered to be representative of all bubbles in a cross-section of the foam column of the same height. Such approaches ignore wall effects and distortion due to the cylindrical shape of the glass column. However, Ho and Prince (1971) showed that bubbles adjacent to the wall are fairly representative of those in the interior, but they might give a slightly overestimated average bubble diameter. Improved experimentation would involve bubble photography with the use of an endoscope submerged in the foam column (avoiding disruption of the foam structure and flow) and, where appropriate (ie broad bubble size distribution), the distribution of bubbles should be accounted for. It would also be interesting to statistically manipulate two-dimensional bubble size distribution to obtain information in three dimensions (Ronteltap and Prins (1989)).

Steep increase in protein enrichment occurred at feedstock concentrations below the CMC region in Figure III3 in Appendix III, where a negative slope in the $\sigma$ versus $\ln(c_{protein})$ was obtained. Foams highly enriched in protein were also characterised by low volumetric flowrate and protein recovery. This behaviour is in complete agreement with previous results based on BSA and brewer's yeast extract systems and discussed extensively in Chapters 4 and 6. Comparison between the patterns of variation in bubble size and protein enrichment clearly demonstrates a

direct dependence of the latter upon both bubble size at the foam-liquid interface and the extent of coalescence. In contrast, bubble size and coalescence exert an inverse effect upon foam volumetric flowrate and generally upon recovery. Similar association between bubble size and protein enrichment/recovery can be observed at various gas flowrates. Lower enrichment ratios and higher recoveries with increasing gas flowrates must be associated with enhanced liquid uptake and limited drainage under such conditions. Similar results have been reported by Narsimhan (1987) and Brown et al. (1990) respectively for semi-batch and continuous foams from BSA solutions.

Performance prediction of the current process by application of the model by Brown et al. (1990); see Appendix IV, was hampered by certain unacceptable boundary conditions. These included negative values for film thickness ($x_f$) at the foam-liquid interface as described by Equations IV23-IV26 (see Table IV1, Appendix IV). Calculations were based on the assumption that the surface viscosity of the bulk of proteins was infinite. Therefore the parameter $c_v$ (the ratio of average velocity with finite surface viscosity to the average velocity through the plateau border for infinite surface viscosity; see Equation IV14) was considered to be equal to one. This assumption is valid (Graham and Phillips (1980); Davies and Rideal (1961)) for relatively high concentrations of solutions of globular proteins, such as BSA, because their surface viscosity is much higher than other proteins and low molecular weight surfactants. For example, the surface viscosity of BSA is 60 dyn sec $cm^{-1}$ at concentrations greater than $10^{-2}$ mg $cm^{-3}$ (Brown et al. (1990)). However, in a complex protein system, such as brewer's yeast extract, this assumption may be invalid, and therefore the values of $c_v$ would be higher than one. Further study should therefore involve determination of the surface viscosity of brewer's yeast extract as described by Desai and Kumar (1983).

Consideration should also be given to the validity in the present study of another assumption, which presupposes that, with high foam beds where the liquid hold up remains practically constant; Desai and Kumar (1983), the rate of liquid uptake is approximately equal to the rate of drainage at the foam-liquid interface (see Equations IV21-IV22). It is likely that such assumption contrasts the reality with small foam beds and wet foams, such as these formed by a solution of $c_{protein,0}$ = 0.45 mg $cm^{-3}$ and G = 40 $cm^3$ $min^{-1}$. Under such conditions, the declining liquid hold-up with increasing distance from the foam-liquid interface, may not have reached a plateau region.

### 7.3.2 Bubble Dynamics and Protein Partition to Foam with Height in a High Foam Bed

Dynamic changes in foam characteristics with foam bed height are described in Figures 7.6 to 7.11. The quantitative characteristics of the collected foam at the top of the tower are described in Table 7.2. Average bubble diameter ($\bar{d}_b$) was found to initially increase with height and gradually level off as shown in Figure 7.6. The observed changes in bubble diameter with foam height can be described by a first order differential equation, generally described by the following notation:

$$\bar{d}_b = \alpha(1-e^{(-\beta h_f)}) + \bar{d}_{b0} \qquad \text{(Equation 7.9)}$$

The experimentally determined coefficients $\alpha$ and $\beta$ for $\bar{d}_b$ are shown in the legend to Figure 7.6.

The effects of foam height upon liquid and gas hold-up ($\varepsilon_l$ and $\varepsilon_g$ respectively) are illustrated in Figure 7.7. A logarithmic decrease in liquid hold-up with increasing distance from the gas-liquid interface was observed, which can be described by Equation 7.10:

$$\varepsilon_l = \alpha e^{(-\beta h_f)} \qquad \text{(Equation 7.10)}$$

Conversely, the gas hold-up increased with foam height, as expected by definition (see Equation 7.1), and this trend can be described by a first order differential equation. Both $\varepsilon_l$ and $\varepsilon_g$ are described by the equations presented in the legend to Figure 7.7.

The foregoing data enabled determination of the effects of foam height upon the number of bubbles per unit volume of the foam bed ($N_b$), coalescence frequency ($\omega$), and interfacial transfer area ($f_{sp}$). A dramatic reduction in $N_b$ (Figure 7.8a) was observed in the first 5 cm from the foam-liquid interface followed by a slower decline and a tendency to level off at the top of the foaming tower. Figure 7.8b shows that bubble coalescence was extensive at a small distance from the bottom of the foam column ($\omega$=53.7% at $h_f$=0.5 cm) and logarithmically declined to values approximating zero ($\omega$=2.6% at $h_f$=37.5%) at the top of the foam tower. Similarly, the interfacial transfer area (Figure 7.8c) was found to decrease with foam height and approached a stable value at the top part of the tower. .

Simultaneous changes in protein concentration ($c_{protein,F}$), foam volumetric flowrate ($Q_F$) and protein mass flowrate ($m_{protein,F}$) along the foam column are described in Figure 7.9. It can be seen that protein concentration increased with height in a manner described by a first order differential equation, while a logarithmic reduction in foam volumetric flowrate with height was observed. Both foam protein concentration and volumetric flowrate are described by respective equations, shown in the legend to Figure 7.9 and are based on curves fitted to the experimental data. The resultant mass flowrate appeared to decrease with height in a linear manner. Variations in protein mass flowrate per unit transfer area ($m^*_{protein,F}$) with foam height are described by Figure 7.10. It seems that

**Table 7.2: Quantitative Characteristics of Top Foam for a 40 cm Foam Bed**

Quantitative characteristics of foam at the top of a 40 cm foam bed (see Figure 2.5), produced from brewer's yeast extract. The protein concentration of the feedstock was 0.40 mg $cm^{-3}$ and the inlet flowrate 5 $cm^3$ $min^{-1}$.

| | |
|---|---|
| **Real Protein Enrichment ($e_{protein,real}$)** | 2.02 |
| **Apparent protein Enrichment ($e_{protein,app}$)** | 1.60 |
| **Real Protein Separation ($s_{protein,real}$)** | 2.65 |
| **RNA Enrichment ($e_{RNA}$)** | 1.33 |
| **Fractionation Index ($Fr_{protein,RNA}$)** | 1.52 |
| **Foam Volumetric Flowrate ($Q_F$) ($cm^{-1}$ $min^{-1}$)** | 0.85 |
| **Protein Recovery (R) (%)** | 34.33 |

**Figure 7.6: Variations in Bubble Size with Foam Height at Extended Foam Beds**

Effects of foam height upon average bubble diameter ($\bar{d}_b$) in extended foam beds of total height of 40 cm. Foam was produced continuously at an inlet flowrate of 5 $cm^3$ $min^{-1}$. The feedstock protein concentration was 0.4 mg $cm^{-3}$ and the gas flowrate 20 $cm^3$ $min^{-1}$.

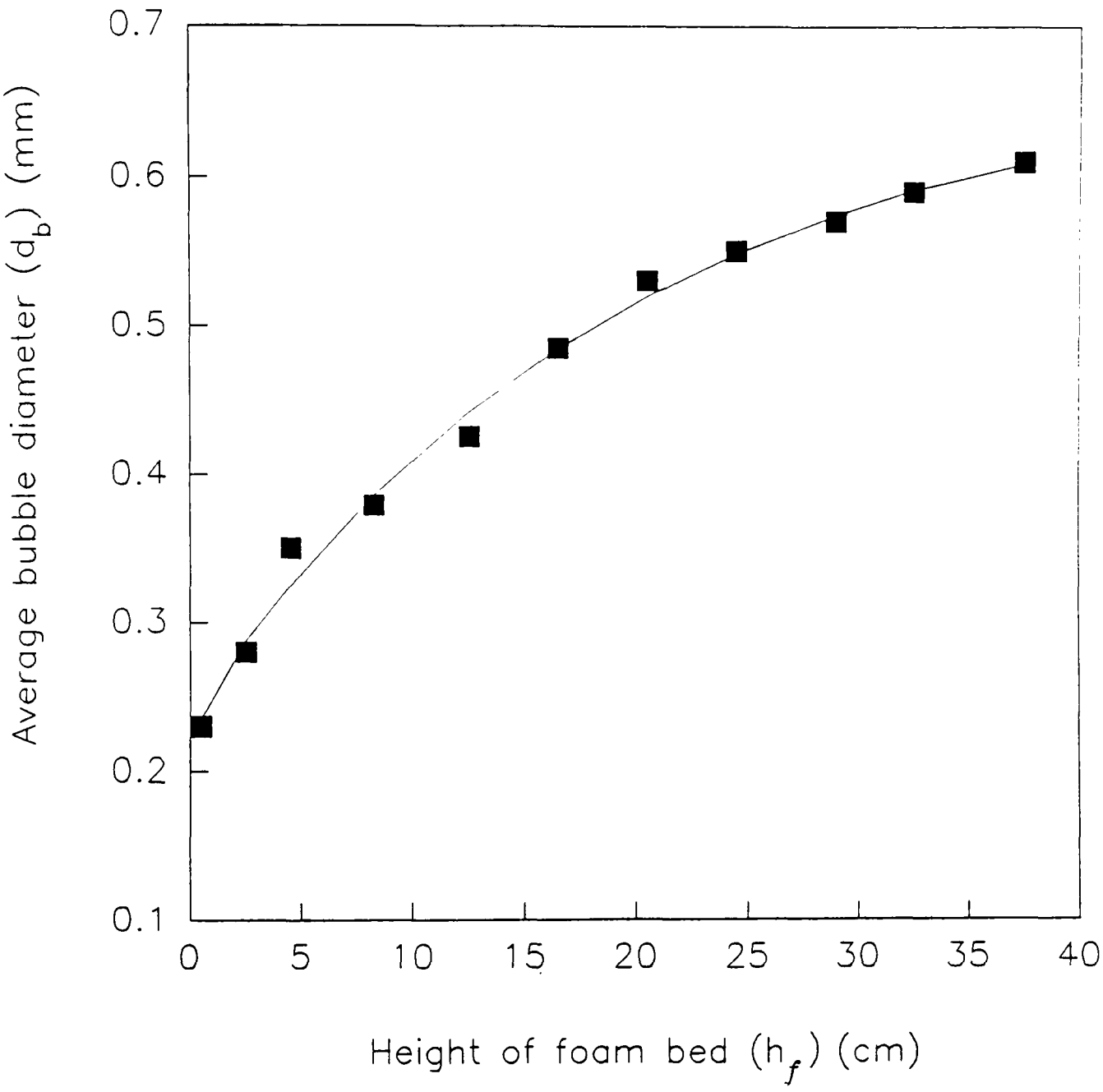


■ Experimental values for $\bar{d}_b$

—— Fitted curve to equation $\bar{d}_b = 0.4427*(1-\exp(-0.05023h_f))+0.2349$ for ■ experimental values

**Figure 7.7: Variations in Gas and Liquid Hold-up with Foam Height at Extended Foam Beds**

Variations in liquid and gas hold-up ($\varepsilon_l$ and $\varepsilon_g$ respectively) with with foam height in extended foam beds of total height of 40 cm. The experimental conditions are the same as in Figure 7.6.

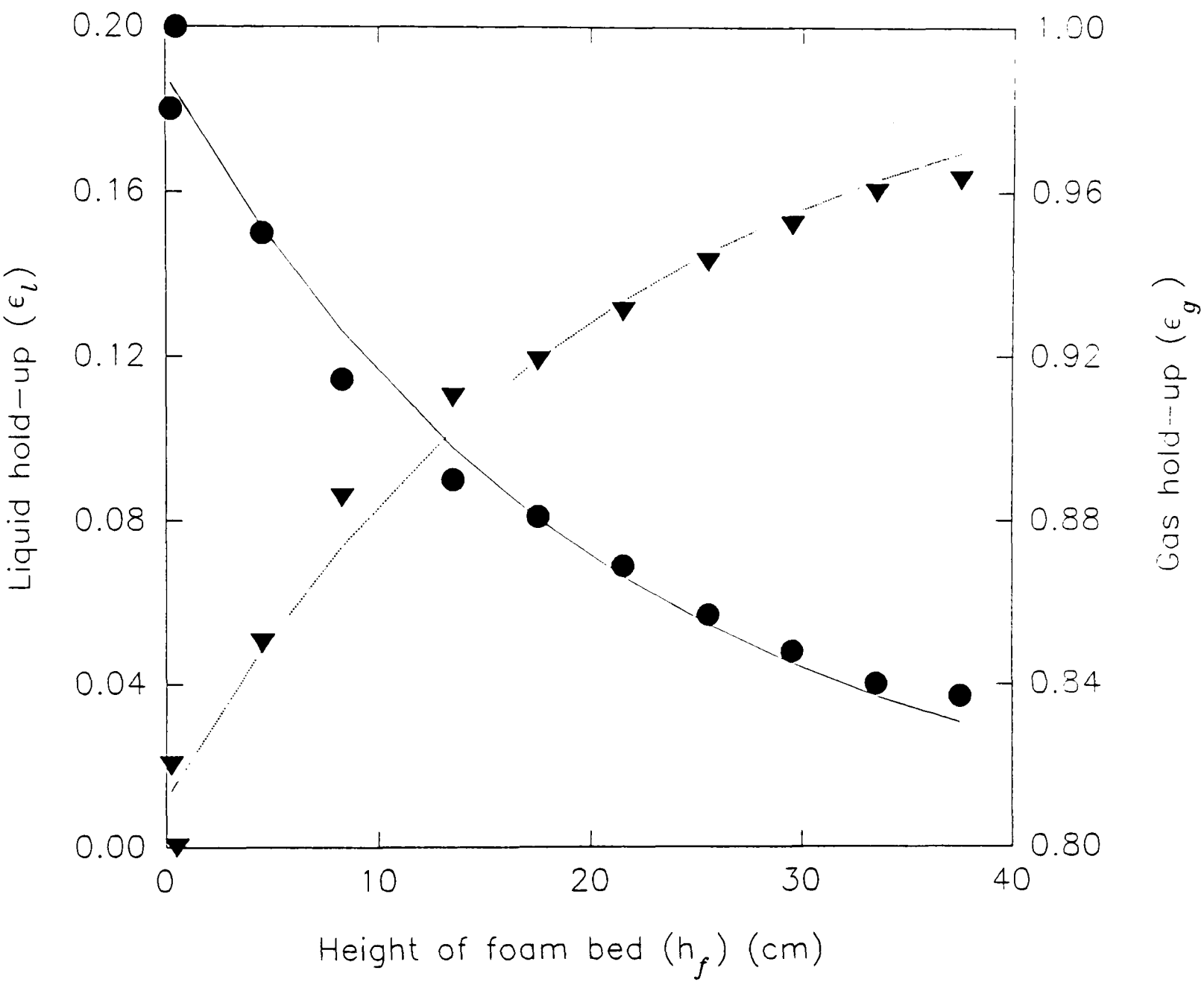

**Figure 7.8: Variations in Bubble Coalescence and Interfacial Transfer Area with Foam Height**

Effects of height of foam bed upon **(a)** number of bubbles per unit volume of the foam bed ($N_b$), **(b)** coalescence frequency ($\omega$) and **(c)** interfacial transfer area ($f_{sp}$) in foam beds of a total height of 40 cm. The experimental conditions are the same as in Figure 7.6.

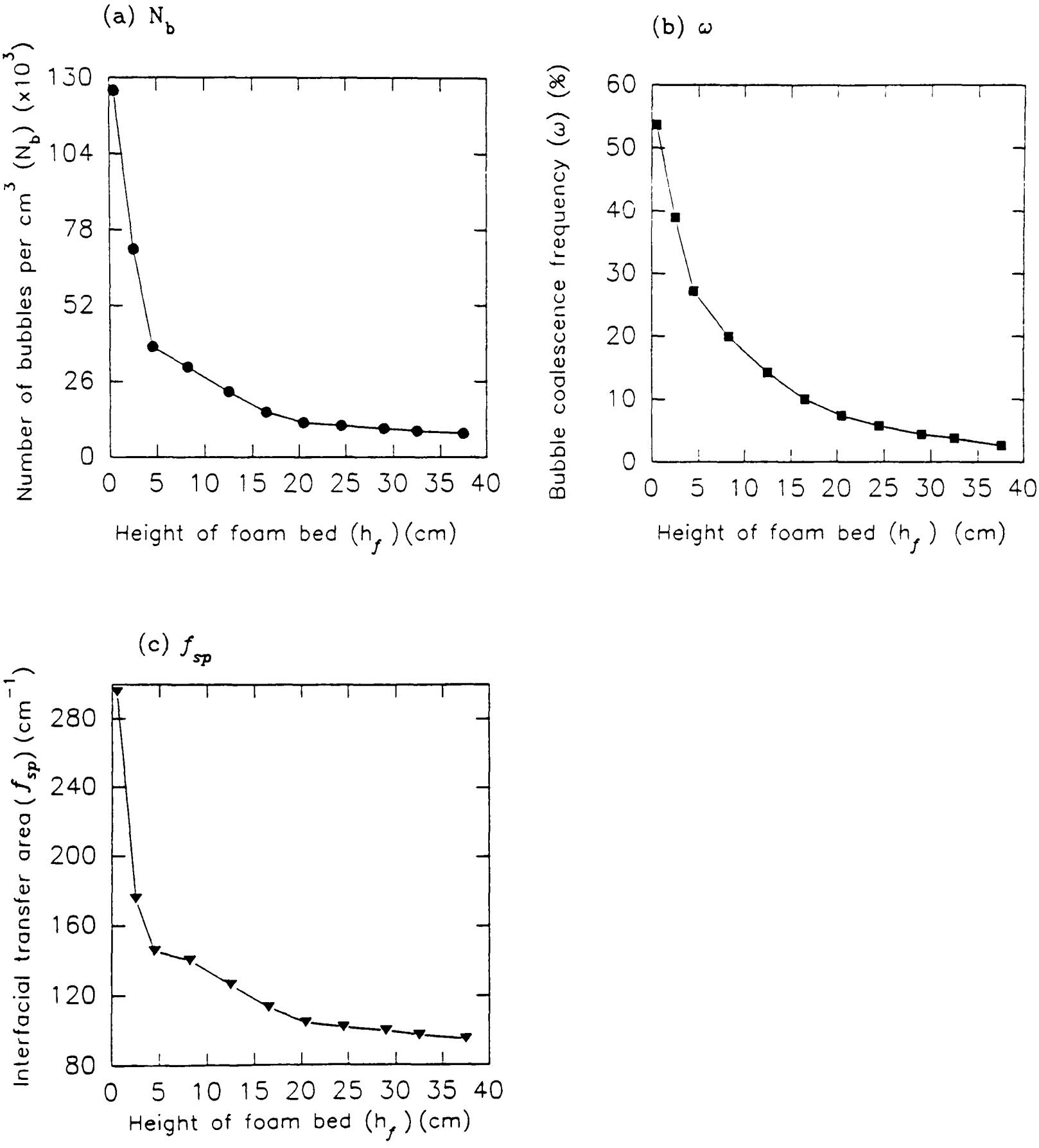

**Figure 7.9: Variations in Quantitative Characteristics of Foam with Foam Height**

Effects of foam height upon protein concentration in foam ($c_{protein,F}$), foam volumetric flowrate ($Q_F$) and protein mass flowrate ($m_{protein,F}$) in extended foam beds of a total height of 40 cm. The experimental conditions are the same as in Figure 7.6.

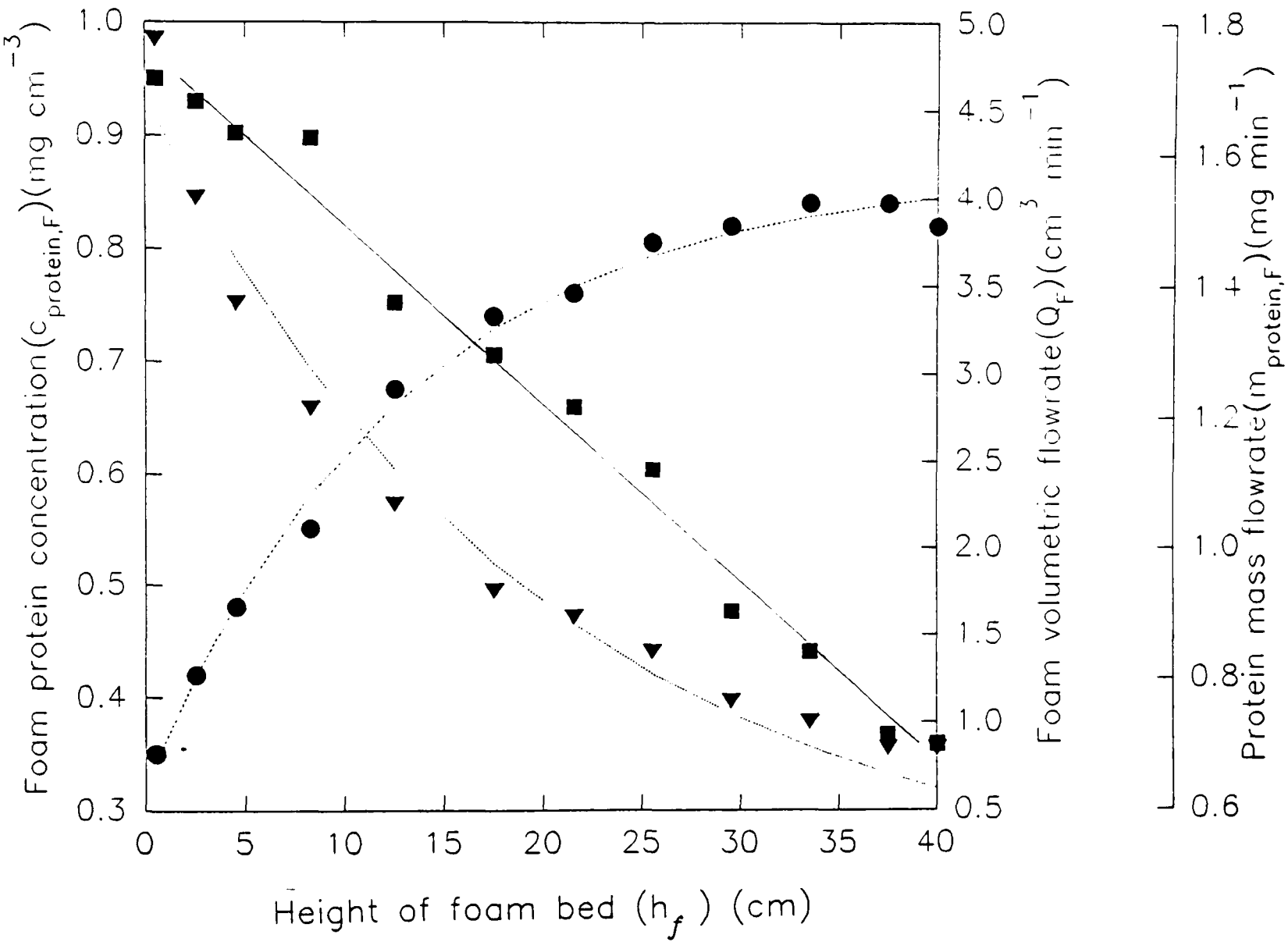


● Real protein concentration in foam $c_{protein,F}$

····· Curve fitted to $c_{protein,F}$ experimental values ( ● )

$c_{protein,F}=0.548(1-\exp(-0.078h_f))+0.32$

▼ Foam volumetric flowrate $Q_F$

—— Curve fitted to $Q_F$ experimental values ( ▼ )

$Q_F=4.58\exp(-0.05h_f)$

■ Mass flowrate of protein in foam $m_{protein,F}$

mass transfer was maximal toward the middle of the foam bed.

The mass transfer coefficient of nitrogen $k_{N2}$ was found to decrease with height of the foam bed as Figure 7.11 shows. A rapid decrease in $k_{N2}$ was observed in the first 5 cm from the foam-liquid interface followed by a slower reduction and virtual stabilisation at the top of the foam bed.

The above results indicate that finite increases in bubble size with height are directly associated with simultaneous increase in gas hold-up (or equivalently a logarithmic decrease in liquid hold-up), decrease in interfacial transfer area, and the number of bubbles per unit volume. Gradual increase in bubble size and decrease in liquid hold-up correspond to finite increase in protein enrichment and decline in protein mass flowrate. Mass transfer of protein per unit interfacial area however appears to approach a maximum at a certain height of the foam bed. Simultaneous increase in bubble size and gas hold-up with height were also found to be associated with decrease in the mass transfer coefficient of nitrogen from gaseous to liquid phase.

Increase in average bubble size (Figure 7.6) and decrease in liquid hold-up (Figure 7.7) with height can be attributed to coalescence and drainage. Results presented in Figure 7.3(a-b) for small foam bed heights indicated the influence of bulk concentration and gas flowrate upon increase in $\bar{d}_b$ with foam height. As foam moves upwards, the liquid in the films drains into the neighbouring plateau borders under the sucking action of plateau borders and disjoining pressure. The liquid in the plateau borders trickles down by force of gravity (Bickerman (1973)). Drainage causes film thinning which reaches an equilibrium state (Khristov et al. (1984)). Capillary pressure differences between large and small bubbles causes diffusion of the inert gas through thin liquid films from the smaller to the larger bubbles. Thus small bubbles coalesce to form larger ones. Adsorption of protein molecules at the gas-liquid interface

**Figure 7.10: Variations in Mass Transfer of Protein at Various Heights of Foam Bed**

Variations in protein mass transfer per unit interfacial transfer area ($m^*_{protein}$) with increasing height of foam bed. The experimental conditions are the same as in Figure 7.6. The curve fitted to the experimental points was based on 2$^{nd}$ order regression.

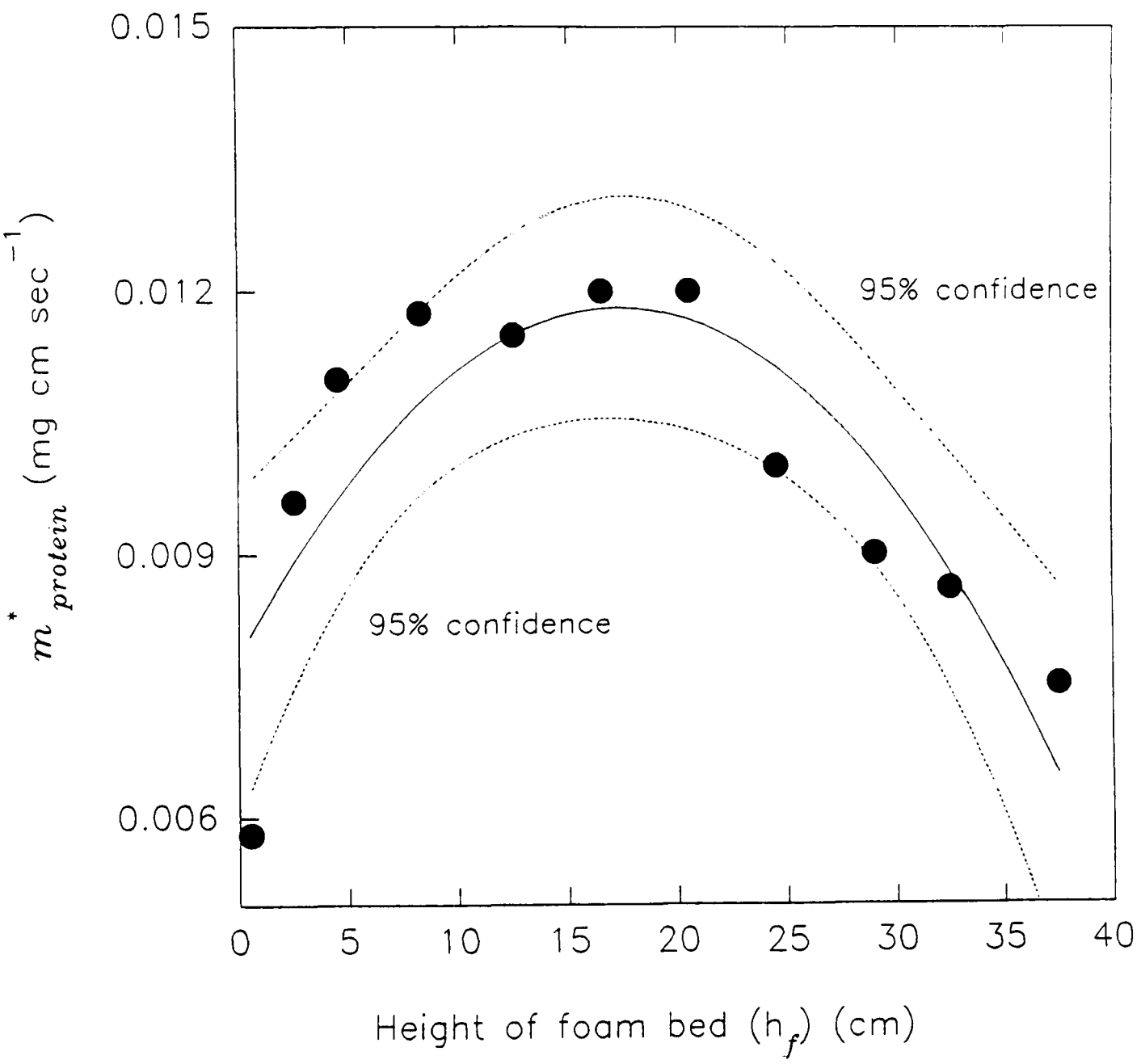

**Figure 7.11: Variations in the Mass Transfer Coefficient of Gas with Foam Height**

Variations in the mass transfer coefficient of $N_2$ ($k_{N2}$) with increasing height of the foam bed. The experimental conditions are the same as in Figure 7.6.

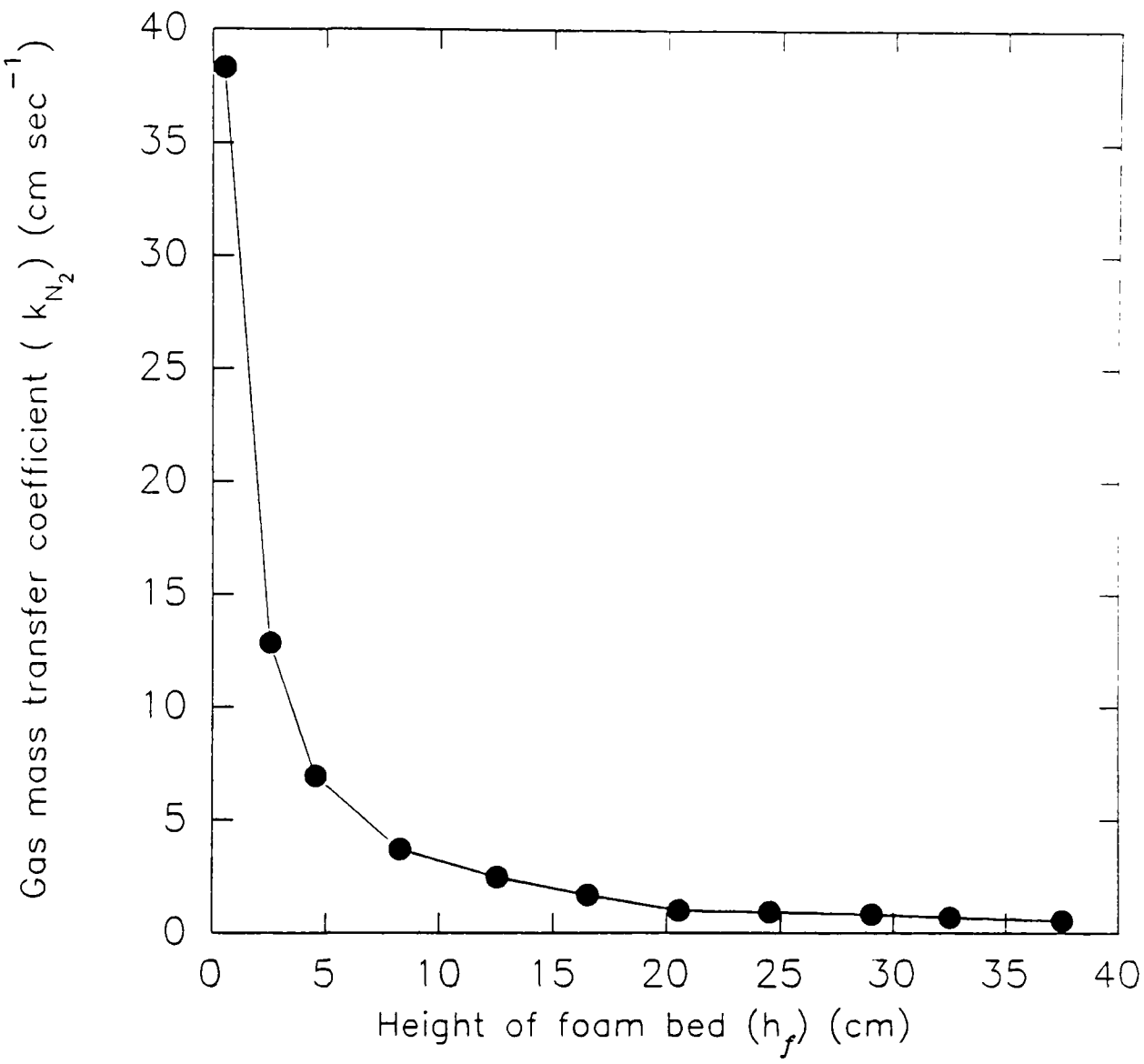

charges the interface, and the net charge depends on the pH of the solution and the isoelectric points of the constituents proteins. Such charge leads to double layer repulsion between adjacent films, which, in conjunction with van der Waals attraction, may counterbalance capillary pressure and plateau border suction (for film thickness smaller than 1 μm) and cause film rupture if the film fails to reach a new state of balance. Such balance depends on film stability to thermal and mechanical perturbations. Film rupture is followed by coalescence and may lead to eventual collapse of the foam bed. This phenomenon is commonly observed in foams from very dilute solutions and foam decay during foam stability studies.

The rate of drainage is influenced by the initial distribution of liquid between films and plateau borders. Near the foam-liquid interface gravitational drainage from the plateau borders is predominant while faster drainage from the film occurs at the higher sections of the foam column as bubbles glow larger and a larger proportion of liquid is redistributed in the films. In contrast, increase in bubble size tends to accelerate drainage and decrease bubble number and interfacial transfer area per unit volume. The observed decrease in $f_{sp}$ is in agreement with the literature with the exception of Maminov and Mutriskov (1969), where $f_{sp}$ is claimed to increase with height due to increase in $\varepsilon_g$. However, this report omits discussion of variations in bubble size with foam height, and the comparison of the magnitude of their changes with respective changes in $\varepsilon_g$. The sharp decline in coalescence frequency at the lower section of the foam bed (see Figure 7.8b) must be associated with the rapid rise in bubble size, due to drainage and coalescence, observed in this section of the foam bed (see Equation 7.6).

A direct result of the dynamic changes in bubble size is the observed decrease in liquid hold-up (Figure 7.7). The latter comprises

liquid in the films and vertical and horizontal plateau borders (Desai and Kumar (1983)), and contributes to the foam volumetric flowrate. Practically constant values of $\varepsilon_l$ at the top of the tower suggest that the rate of liquid uptake is equal to the rate of drainage. The observed trends in $\varepsilon_l$ are in agreement with theoretical predictions of liquid hold-up by Narsimhan and Ruckenstein (1986a) and Desai and Kumar (1983), and experimental values of $\varepsilon_l$ (Narsimhan (1987); Desai and Kumar (1983)). In these reports theoretical and experimental values of $\varepsilon_l$ refer to semi-batch foams formed by BSA, and non-biological surfactants (sodium lauryl sulphate, lauryl alcohol and Teepol with or without glycerol). The observed value of $\varepsilon_l$ at the foam-liquid interface (0.21) is close to the theoretical value of 0.26 estimated from the void volume of closely packed spheres.

Protein concentration in foam is expected to increase with increasing $f_{sp}$ and surface excess, and decreasing $\varepsilon_l$. However, experimentation has shown that $c_{protein,F}$ increases with height although $f_{sp}$ decreases. It can therefore be concluded that the predominant factor in protein concentration in foam is the liquid hold-up, which is directly dictated by bubble size and all the factors influencing initial bubble size and the rate of drainage and coalescence. Protein mass flowrate would be favoured by high $f_{sp}$, $\Gamma$ and $\varepsilon_l$. Experimental evidence (Figure 7.9) shows that $m_{protein,F}$ is indeed high at low heights of the foam column. Brown et al. (1990) demonstrated that decline in protein recovery with foam height reflects the detrimental effect of a broad size distribution. In contrast, they claim that coalescence is the predominant factor in protein enrichment.

The existence of a peak in $m^*_{protein}$ suggests that there is an optimal bubble size where simultaneous changes in drainage and coalescence (affecting $c_{protein,F}$, $\varepsilon_l$ and $f_{sp}$) lead to optimal mass transfer. It

should be mentioned that the calculated $m^*_{protein}$ represents protein in the continuous phase of foam, ie plateau borders and films, and protein molecules adsorbed at the gas-liquid interface. Hence it does not coincide with surface excess of protein and cannot reflect variations in protein concentration in the liquid entrained in the foam. This behaviour is closely analogous with reports elsewhere (Wace et al. (1969)) that an optimal bubble diameter can be defined to maximise the solute throughput (adsorbed on the bubble surfaces) per unit transfer area. Also, results by Narsimhan (1987) showed that maximal protein enrichment in semi-batch foams was associated with an optimal bubble diameter, and this was particularly pronounced at low gas flowrates.

Reduction in the $k_{N2}$ with height suggests that increase in $\varepsilon_g$ and decrease in $f_{sp}$ result in a decline of $k_{N2}$. The adopted empirical model for $k_{N2}$ (Equation 7.7) accounted for mass transfer by means of molecular and convective diffusion, and the observed trend is in agreement with results by Maminov and Mutriskov (1969). Calculation of the mass transfer of gas in liquid foams can be useful in cases where gas absorption with chemical reaction occur in the liquid phase of aqueous foams.

Determination of an empirical equation to describe and predict the effects of operating parameters upon variations in bubble size and distribution with foam height should involve experimentation at various values of gas flowrate, surface tension (feedstock concentration, buffer pH and ionic strength, temperature), bulk viscosity, sinter porosity, height of foam bed, and foam tower diameter. The diameter of foam tower has been shown to be of importance in bubble columns for diameters <0.3 m (Shah et al. (1982)). A correlation between the coefficients $\alpha$ and $\beta$ and various operating conditions would describe the effects of these conditions upon bubble size and distribution at various foam heights. The dependence of $\varepsilon_l$ and $c_{protein,F}$ upon bubble size could be described by

correlating their $\alpha$ and $\beta$ coefficients with respective ones for bubble size.

## 7.4 Concluding Summary

The current studies have clearly shown a strong relation between bubble size and protein partition. Large bubbles are associated with enhanced protein enrichment but reduced recovery due to the low liquid hold-up. This results in low foam volumetric flowrates. Coalescence was identified as the predominant factor affecting protein enrichment. Variations in the bubble size at the foam-liquid interface with different solution conditions were found to determine respective variation in protein partition. Large bubbles coincided with dilute feedstocks and low gas flowrate. Under such conditions, these bubbles are likely to coalesce faster and more severely with height of foam bed.

Results indicated that increase in bubble size and protein concentration with height are likely to be governed by kinetics of a first order differential equation, as opposed to liquid-hold-up, which appears to decline in a logarithmic manner. Dynamic changes in foam appeared to result in a maximum in protein mass transfer per unit of interfacial transfer area. Reduction in interfacial transfer area in a logarithmic manner appears to coincide with a similar trend in reduction of the mass transfer coefficient of gas from gaseous to liquid phases.

Difficulties encountered in the application of mathematical modelling for foam performance prediction have indicated the importance of differences between homogeneous model systems of globular proteins and complex biological feedstocks. Design of foam fractionation for real biological systems therefore requires an initial complete characterisation of their physical properties. It would also be beneficial to the accuracy of the theoretical prediction to include a study of bubble coalescence

amongst the factors influencing liquid hold-up and plateau border geometry. The present study has shown that a set of empirical expressions can correlate bubble and liquid hold-up with foam bed height and has suggested further experimentation to include a factor which would account for physical properties and operating conditions in the determination of these empirical correlations. Since present application of the aforementioned theoretical prediction was not successful, attempts to improve the model by introducing a term for coalescence frequency was not pursued. However this would be a very promising subject for future research in foam fractionation of proteins from real biological systems.

# *CHAPTER 8*

## *CONCLUSIONS AND RECOMMENDATIONS*

Foam stability studies of model homogeneous (BSA) and heterogeneous (BSA-lysozyme, BSA-cytochrome-c ) protein solutions clearly highlighted the importance of electrostatic interactions between basic and acidic proteins in foamability and foam stability. Such effects were synergistic, and there was evidence that they might be influenced by the overall composition of the foaming solution. It was also observed that under appropriate buffer and compositional conditions, predominantly hydrophobic interactions between molecules of different type could also enhance the foaming properties of mixed solutions. In homogeneous preparations (BSA solutions) it was demonstrated that foam stability increased with protein concentration and was maximal at the isoelectric point of the protein. Foam stability studies, undertaken by application of the Rudin method (Rudin (1957)) and conductivity measurements of foam, showed good agreement in describing the observed phenomena. Foam stability and a preliminary assessment of protein content of foam in respect to original feedstocks, constituted the basis for further research with model systems (BSA-lysozyme).

Batch foam operations with BSA-lysozyme solutions at basic pH values (ie pH 8) strongly demonstrated the importance of molecular stoichiometry in foam quality and protein recovery in foam. Maximal lysozyme recovery was achieved at equimolar conditions, which coincided with the most efficient formation of BSA-lysozyme complexes responsible for enhancement in foam stability. Under such conditions, BSA fractionation from lysozyme was minimal. However, at dilute feedstock conditions, it appeared that an understanding of these reaction kinetics is insufficient. Under such

conditions, competition between single BSA molecules and complexes to adsorb at non-saturated gas-liquid interfaces is a predominant factor in protein partition. In homogeneous systems, the partition of BSA molecules to the foam phase depends upon feedstock concentration. Similar behaviour also occurs in heterogeneous solutions. Protein enrichment is therefore enhanced in dilute conditions, whereas recovery is favoured by concentrated solutions which yield higher foam volumes. However, the current study assembled important evidence which casts serious doubt upon such generalities of behaviour in mixed systems. This evidence is associated with the fact that the highest volumes of collected foam did not correspond to the highest total protein content in heterogeneous systems. In addition, the enrichment of lysozyme was not related to its feedstock concentration in a manner similar to that of BSA. In contrast, such maxima occurred at BSA:lysozyme molar ratios of one. Therefore direct analogies between model systems and real biological feedstocks must be made with care.

Proteins can function as mobile ion-exchangers, where the protein-collector can carry the protein-colligend into the foam phase under appropriate conditions. As in conventional ion-exchange adsorption, this behaviour can be optimised at low buffer molarity, stoichiometrical conditions dictated by the specific molecules, and low residence times. In processes where the presence of protein-colligend may be a serious disturbance to the steady-state foam fractionation of protein-collectors (in terms of variations in protein enrichment and recovery), experience has shown that the process can be efficiently controlled by a rapid increase in the feed flowrate or a dose of salt to suppress electrostatic interactions.

Complex biological feedstocks, such as brewer's yeast extract and muscle protein, appear to behave like single protein solutions in terms of

the effects of feedstock concentration upon foam performance. Electrophoretic analysis indicated that foams are likely to be stabilised by a broad combination and association of polypeptide components rather by specific individual species. However, more research is needed to understand the role of "foam positive" components. As in batch model systems, protein enrichment is significantly improved at dilute feedstock conditions, low gas flowrates and prolonged residence times. Such behaviour appears to result in enhanced fractionation of protein from RNA which is less surface active. However, "dry foams" are detrimental to protein recovery and lead to severe protein precipitation. The selection of operating conditions is therefore dependent upon the specifications of the desired product. In the current study for example, foam precipitates exhibited excellent food functional properties, and therefore it would be beneficial to operate recovery processes under conditions promoting very "dry" foams. Secondary treatment of foam demonstrated the benefits of foam fractionation prior to further conventional treatment. Such benefits are associated with the achievement of protein fractionation from RNA during foaming.

Dynamic studies of bubbles showed that enriched "dry" foams coincide with bubble coalescence and drainage. Application of long foam beds can finitely promote this behaviour, but it appears that there is an optimal height for mass transfer of protein to the foam phase. The failure of the proposed model of Brown et al. (1990), when applied to the experimental systems herein, suggests that there are limitations in predictive studies derived from model systems for use with realistic biological solutions.

Although protein denaturation may limit the applicability of foam fractionation for the recovery of biologically active proteins and enzymes, it appears that it could be advantageous in processes designed to produce food functional protein. In this instance, the increased potential

of partially denatured proteins to generate very stable foams is a process advantage. Experience in the present study, concerned with waste brewer's yeast extract, has also shown that foam products can be attractive for food use in terms of their reduced nucleic acid content.

The present study has highlighted various areas of interest for future research concerned with both model systems and real biological solutions. More study is required to determine the kinetics of synergistic interactions between acidic and basic proteins under conditions promoting either electrostatic or hydrophobic molecular associations. The mechanisms of adsorption at the gas-liquid interface of both single molecules and molecular complexes must be elucidated in order to understand competitive mass transfer of collector and colligend molecules in dilute and concentrated solutions. The behaviour of biochemical solutes as mobile ion-exchangers must be studied within a wide spectrum of operating parameters and component of colligend-collector molecules in order to maximise performance. Improvement in the colligend recovery in the foam phase could benefit from application of the colligend load at the top of the foam bed. Such studies could utilise well characterised proteins of relevance to the food and pharmaceutical industry and exploit engineering aspects of foam separation.

Further research with brewer's yeast extract, or similar systems, should exploit advanced continuous operations, such as stripping processes with controlled reflux and bottoms recycle or multi-stage foam towers. These processes would yield small quantities of foam enriched in protein and depleted of nucleic acids. As a result, further downstream treatments would benefit from scale-down in equipment and process time. Although foam processing did not appear to profoundly fractionate specific polypeptides, expect for a species of pI approximately 7.0, it is important to undertake research directed to identify "foam positive" species and those molecular

interactions essential to foam formation. Such approaches could exploit adsorption studies of individual and bulk proteins. The positive aspects of protein precipitation, namely the excellent food functional properties of foam precipitates, indicate the merits of operations targetted towards dry foam production although compromised with extensive protein precipitation. However, it is necessary to identify the extent to which individual species are affected by surface denaturation and the role of alkali (used in solubilisation of foam precipitate) in the remarkable foaming properties of freeze-dried foam precipitates. In addition the effects of foaming upon the activity of a wide range of enzymes (alcohol dehydrogenase, fumarase, malate dehydrogenase, proteases, synthetases) should be investigated.

Although experience from muscle protein extracts was not fruitful in terms of the fractionation of cytochrome-*c*, there is a great potential in foam treatment of abattoir waste. Such processes can be appropriately designed according to product specifications. For example, concentration of bulk protein for animal food should be undertaken under conditions maximising protein enrichment and reducing foam volume. Selection of appropriate conditions of pH and ionic strength can also lead to simultaneous isolation of a variety of enzymes in the bottom phase. Studies concerned with the surface activity of muscle proteins such as myosin and actin, and their potential use as food additives, indicates a scope for exploitation of foam fractionation for their selective recovery. Successful design could be based upon the optimal operating conditions. Such conditions have been indicated by studies with brewer's yeast extract, and a detailed knowledge of the prerequisite physical properties for novel food manufacturing (O'Neill et al. (1989); Li-Chan et al. (1987); Dickinson et al. (1987); Fretheim et al. (1986)). Another strand of future research should deal with modelling and performance prediction

in order to advance efficient designs, applicable to a variety of biochemical systems. Such an approach could benefit from relevant experience with model systems (eg BSA), but it is essential to understand other important factors associated with the complexity of real biological feedstocks. In such systems, adsorption competition between molecules, molecular interactions, and the presence of foam destibilising agents are crucial factors requiring detailed investigation prior to design. Adsorption and surface activity studies, coupled with foamability and foam stability, can constitute engineering indicators upon which design can be based. Empirical correlations need to be established between variables (eg. bubble size, coalescence frequency, mass transfer, fundamental physical properties, and operating conditions. Such correlations would enable realistic performance predictions by application of semi-empirical models. Physical properties of fundamental importance are solute hydrophobicity, molecular weight, charge and conformation, and bulk and surface viscosity and surface activity of solutions. In foam fractionation with synergy (eg BSA and lysozyme solutions), it is also important to establish the kinetics of complex formation in respect of stoichiometry and the nature of aqueous environment, together with relevant effects upon the hydrodynamics of the foam bed. Assessment of the extent of protein denaturation must be an integral part of foam fractionation, since it directly affects product quality and may impede further treatments.

The current study has demonstrated that there is a great potential in exploiting the diverse knowledge of protein surface chemistry and fundamentals of foam separation in order to adapt design of foam fractionation to the particular needs of protein molecules. Hitherto, research has almost exclusively exploited model protein systems comprising one protein only, but it is essential to understand the behaviour of real biological systems when subjected to foaming. In addition there is a need

to reassess the role of protein precipitation in respect of its effects upon product quality. Thus precipitation might be a desired feature of foam processing in the manufacturing of food functional protein. Finally, feasibility studies require support by process performance prediction. Development of semi-empirical models applicable to complex protein systems in continuous foam operations is a real challenge and the next mandatory step forward in the establishment of foam fractionation as an alternative unit operation in downstream processing.

# *APPENDICES*

# *APPENDIX I*

## *THE EFFICIENCY AND SUITABILITY OF FUNDAFOM-00 FOR FOAM DISRUPTION IN FOAM FRACTIONATION PROCESSES*

The use of the Fundafom-00 for foam disruption (see Figure 2.4(a-b) and Plate 2.1) was found less efficient when compared with the spinning perforated basket. This difference is associated with the manner in which foam was introduced into the system (see Figure 2.4b) and overheating problems experienced by the Fundafom during long and continuous operations.

The Fundafom was designed to be mounted on the top of reaction vessels, such as fermenters, and be activated by an appropriate control system to disrupt foam when needed (Roy (1989)). In the present study, foam was introduced through the side wall of the glass collector at very low flowrates, thus utilising one layer of rotating disks only. In order to exploit the full capacity of the Fundafom the glass collector was modified by reducing its volume and flattening its bottom so that a "head" of partially broken foam could eventually rise and hit all the layers of the rotating disks leading to complete disruption. However small foam volumetric flowrates did not appear to significantly improve foam breakage while overheating of the metal and glass surfaces were detrimental to foam quality when in prolonged contact.

Continuous operation of the Fundafom for more than 60 minutes resulted in serious overheating of the shaft, the rotating disks and eventually the glass foam collector. Such overheating led to extensive protein denaturation and increased protein losses when compared with those observed in foams, which were disrupted by the rotating perforated basket (see Figure 2.3 and Plate 2.1). The nearly flat bottom of the foam collector (see Figure 2.4b), especially designed to retard foam flow to the fraction collector, prolonged the contact of broken or partially broken foam with the warm glass surface, thus causing further protein precipitation. An experiment was undertaken to assess the effects of overheated surfaces upon the temperature of water flowing through the foam route at various flowrates. The water inlet temperature ($\theta_{in}$) was maintained at 19 $^{o}$C. The outlet temperature ($\theta_{out}$) was continuously measured for 15 minutes for each inlet flowrate applied. It was found that (see Table I1) at low inlet flowrates the effects of overheated surfaces upon the temperature of the water were greater as indicated by the

difference between the water temperature at the outlet and inlet ($\Delta\theta_{out-in}$). At higher inlet flowrates, these effects were reduced but not eliminated. However, the applied water flowrates were significantly higher than those of foam output observed in the present work. Therefore, thermal effects upon protein in the collected foam are inevitable.

**Table I1: Effects of Overheated Surfaces upon the Temperature of Passing Water at Various Flowrates During Continuous Operation of the Fundafom-00.**

| **Inlet Flowrate ($cm^3\ min^{-1}$)** | $\theta_{in}$ (°C) | $\theta_{out}$ (°C) | $\Delta\theta_{out-in}$ (°C) |
|---|---|---|---|
| 4.50 | 19.0 | 29.5 | 10.5 |
| 7.25 | 19.0 | 27.0 | 8.0 |
| 18.00 | 19.0 | 26.0 | 7.0 |
| 27.50 | 19.0 | 25.0 | 6.0 |
| 36.25 | 19.0 | 24.0 | 5.0 |
| 42.50 | 19.0 | 23.5 | 4.5 |
| 50.00 | 19.0 | 22.8 | 3.8 |

*APPENDIX II*

*CALIBRATION OF BIOCHEMICAL ASSAYS*

**Figure II1: Calibration of TSK-4000 Column for Size-Exclusion Chromatography by HPLC Analysis** (see Chapter 2 (2.4.2))

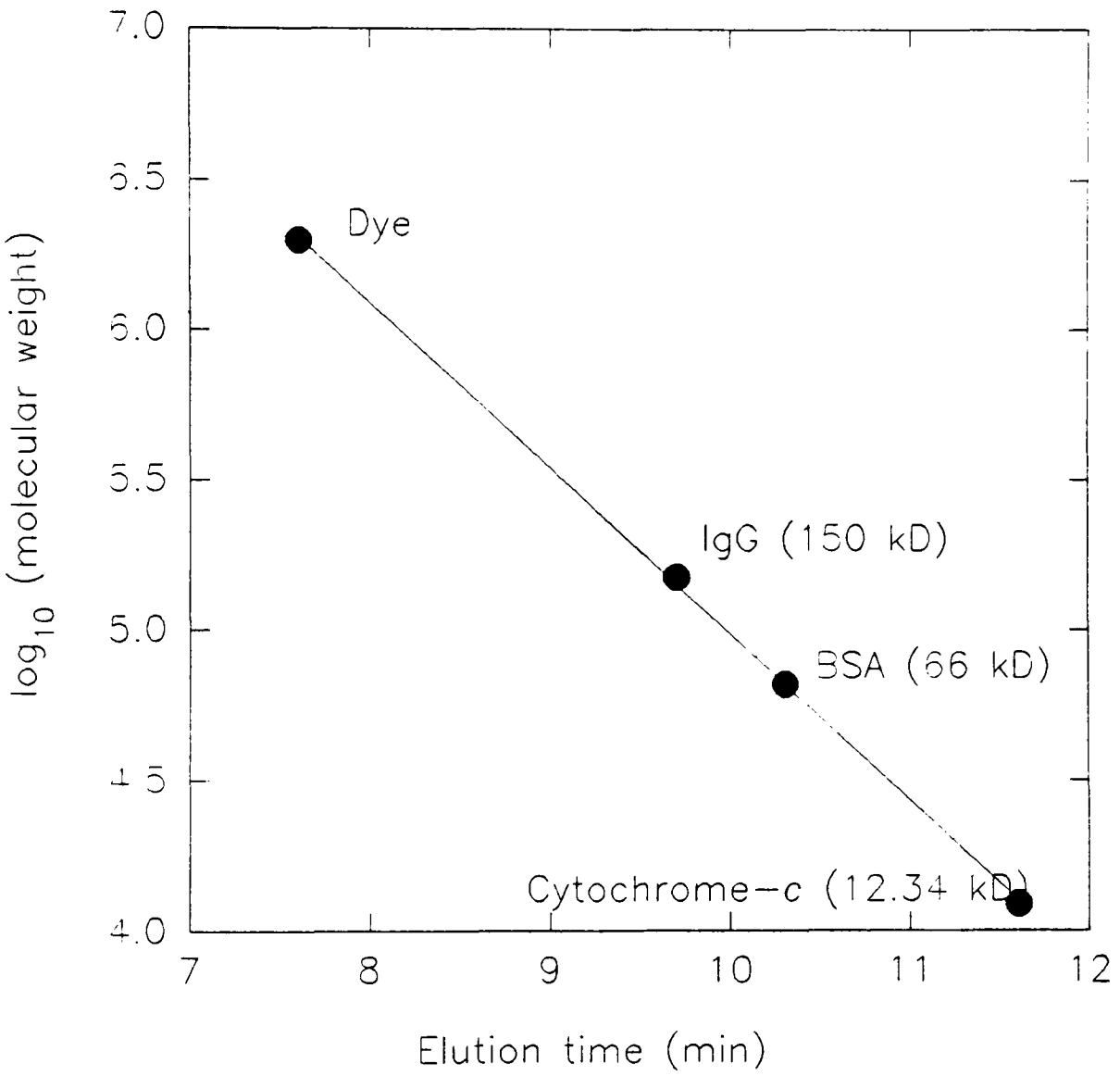

**Figure II2: Calibration Curve for Determination of BSA and Lysozyme Concentrations in Citrate Buffer by HPLC Analysis** (see Chapter 2 (2.4.2))

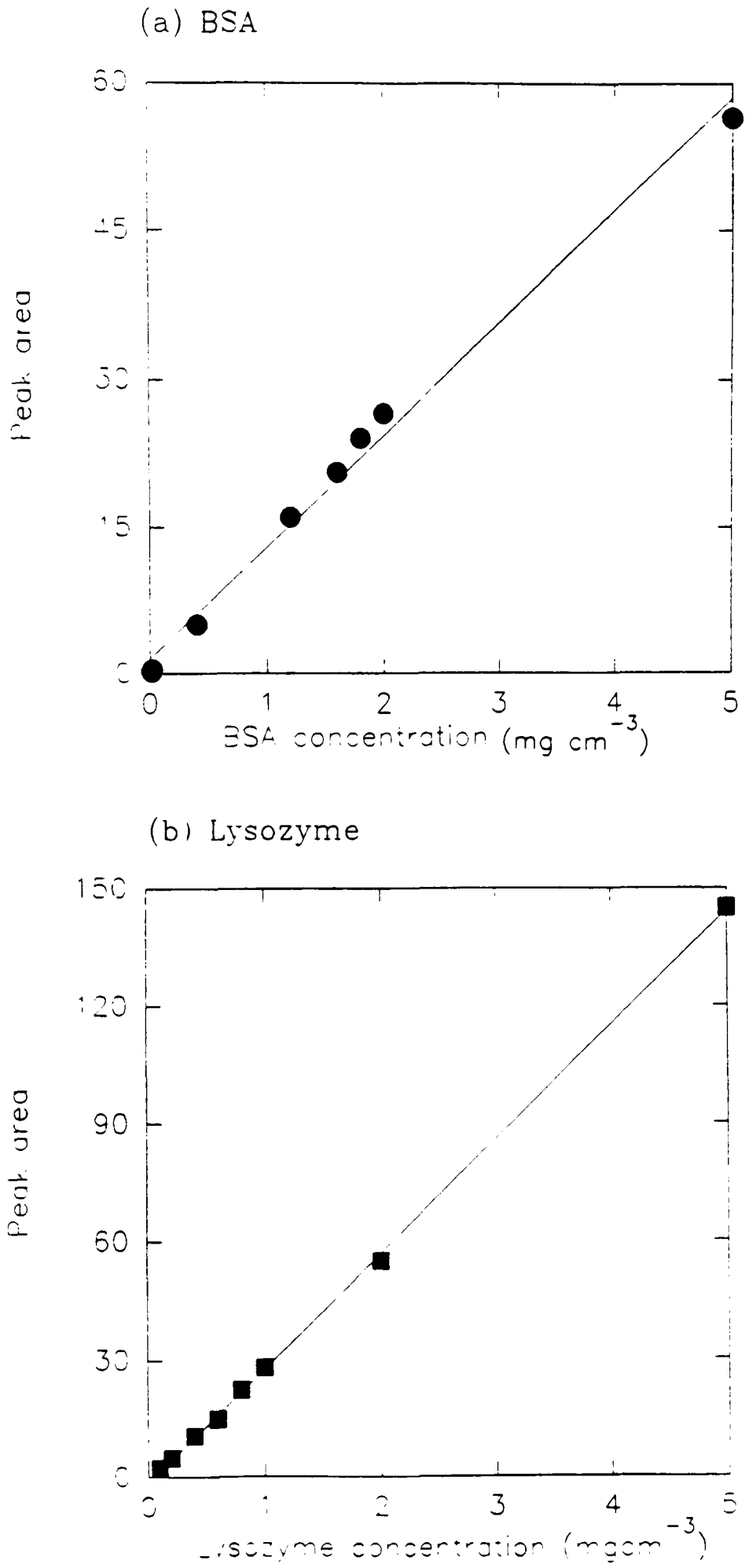

**Figure II3: Calibration Curve for Determination of BSA and Lysozyme Concentrations in Phosphate Buffer, pH 8.0, by HPLC Analysis; Range of Protein Concentration: 0-5 mg $cm^{-3}$** (see Chapter 2 (2.4.2))

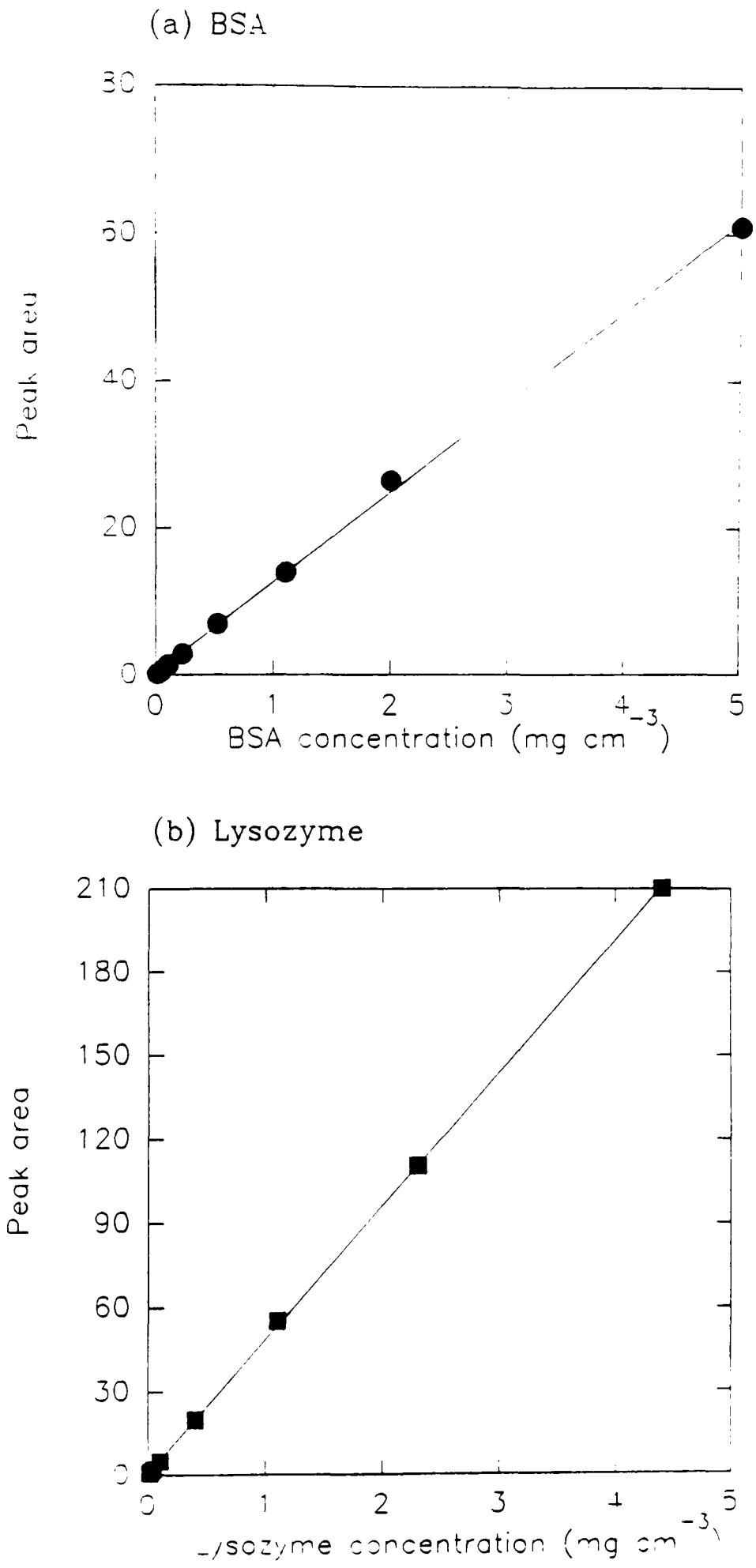

**Figure II4: Calibration Curve for Determination of BSA and Lysozyme Concentrations in Phosphate Buffer, pH 8.0, by HPLC Analysis; (a) Range of BSA Concentration: 0-0.25 mg $cm^{-3}$ and (b) Range of Lysozyme Concentration: 0-0.4 mg $cm^{-3}$;** (see Chapter 2 (2.4.2)).

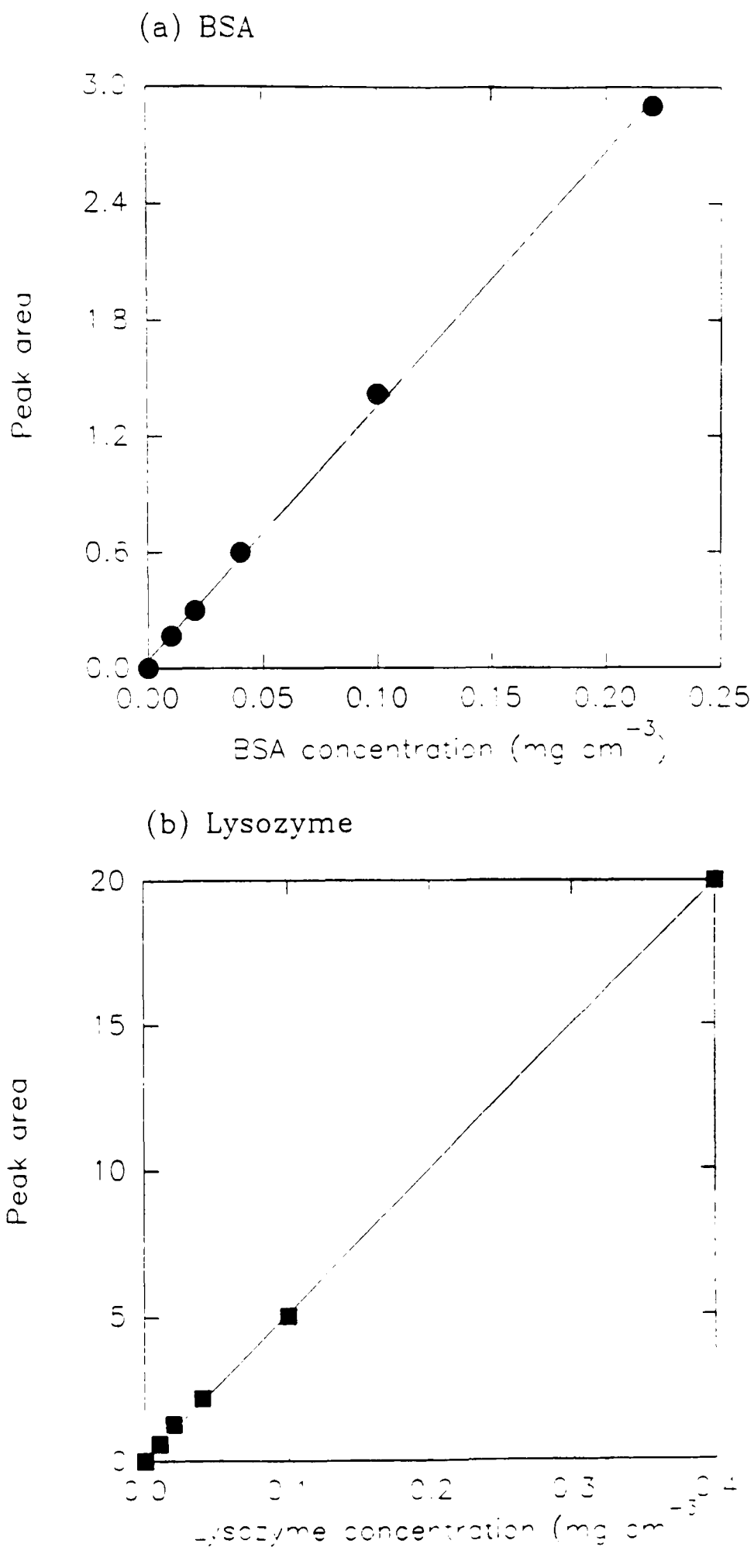

**Figure II5: Calibration Curve for Determination of Total Protein Concentration by Coomassie Blue** (see Chapter 2 (2.4.3))

(see Chapter 2 (2.4.3))

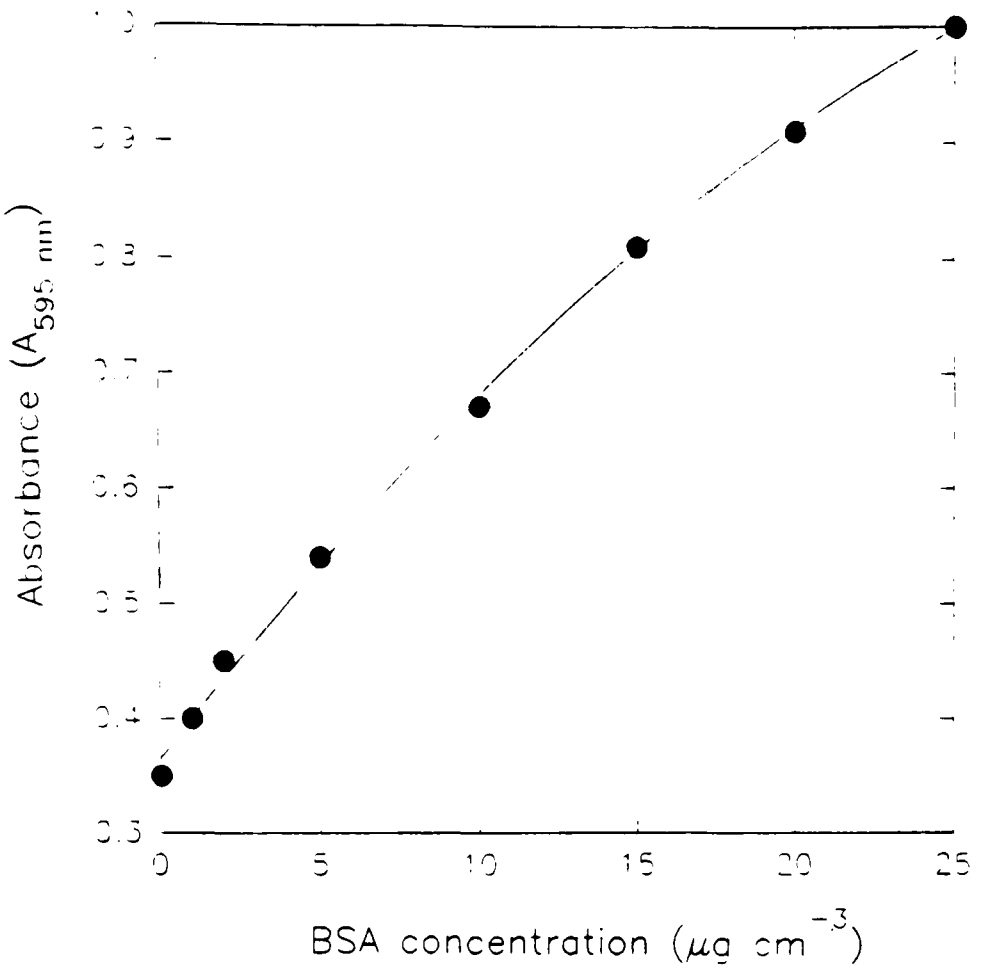


**Figure II6: Calibration Curve for Determination of RNA Concentration** (see Chapter 2 (2.4.4)

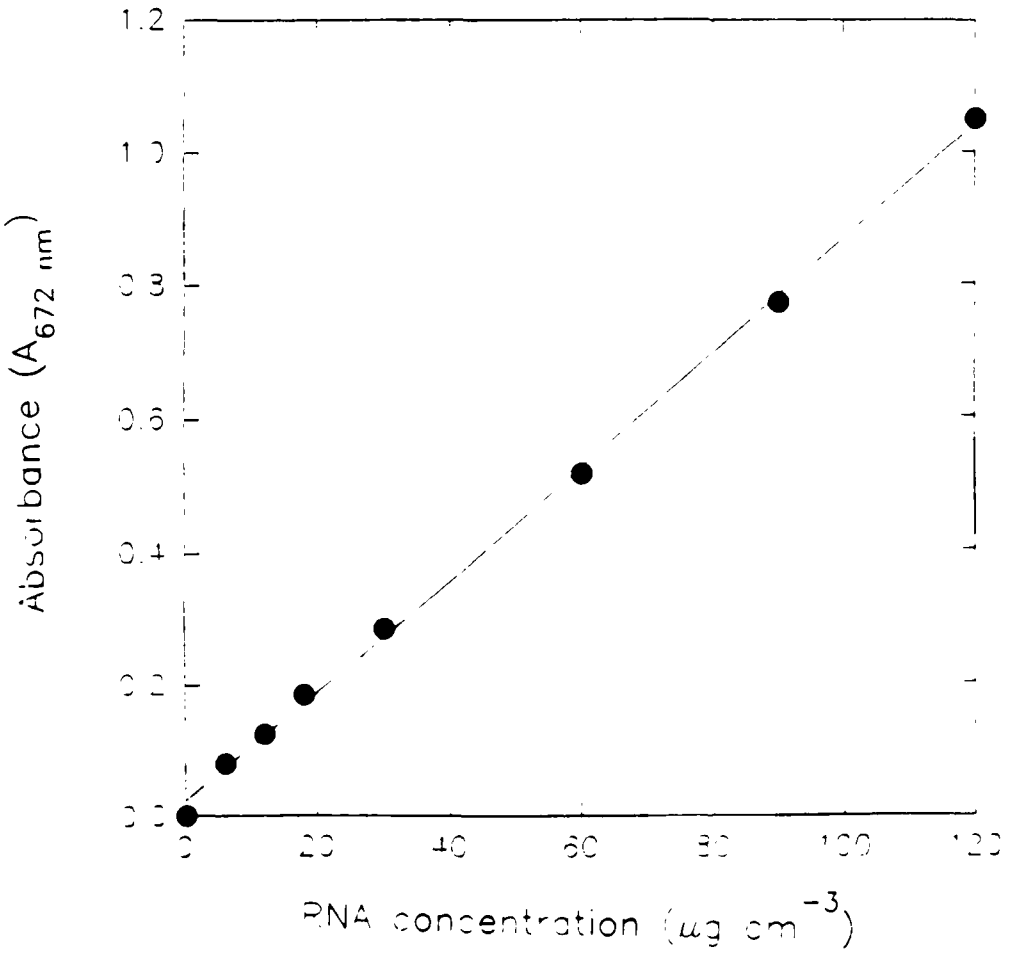

**Figure II7: Calibration Curve for Determination of Carbohydrate Concentration** (see Chapter 2 (2.4.5))

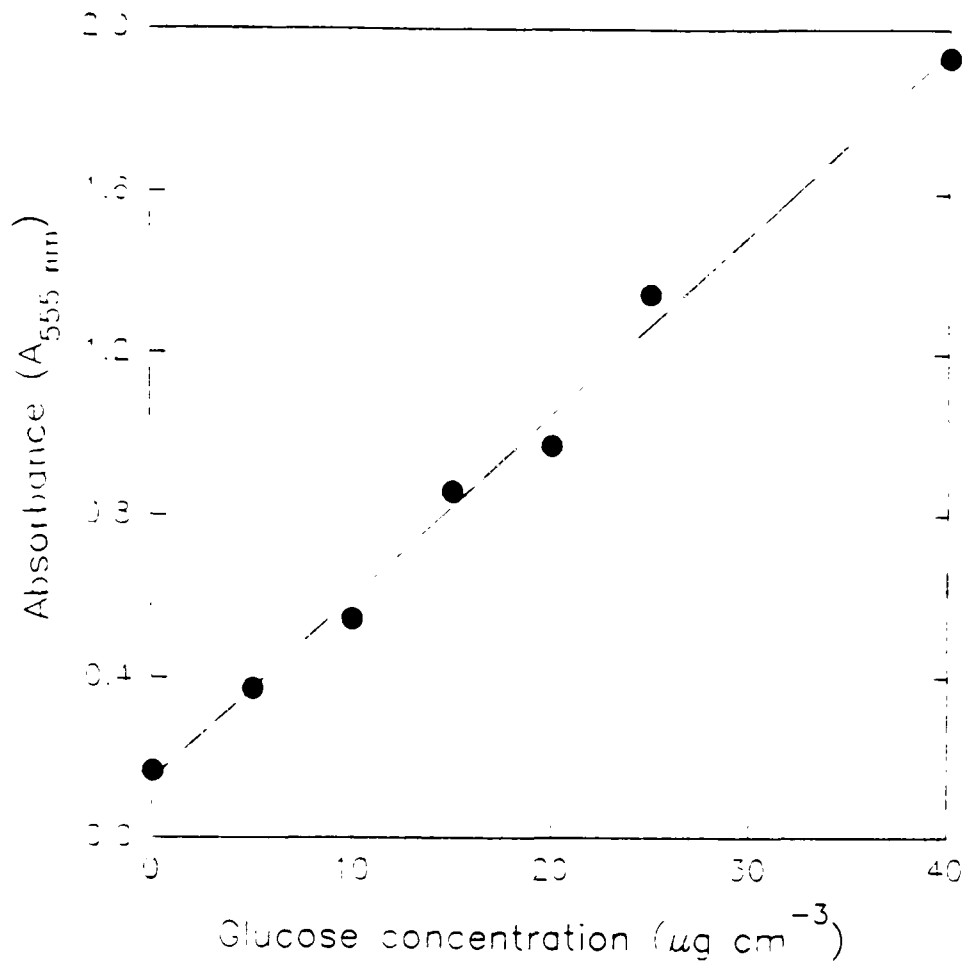


**Figure II8: Calibration Curve for Determination of Acidic Protease Concentration** (see Chapter 2 (2.4.6))

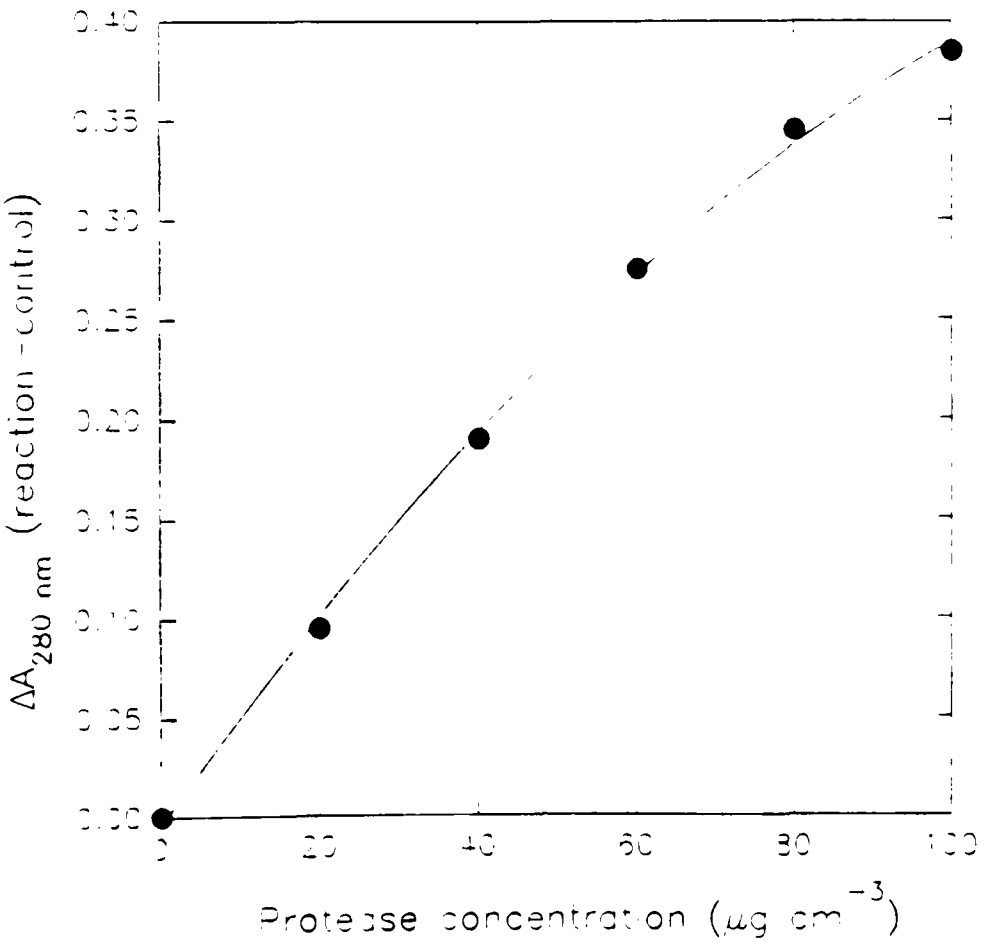

**Figure II9: Calibration Curve for Separation by Molecular Weight by SDS-PAGE of (a) Low Molecular Weight Standards and (b) Heavy Molecular Weight Standards**

(a) Low molecular weight (LMW) standards

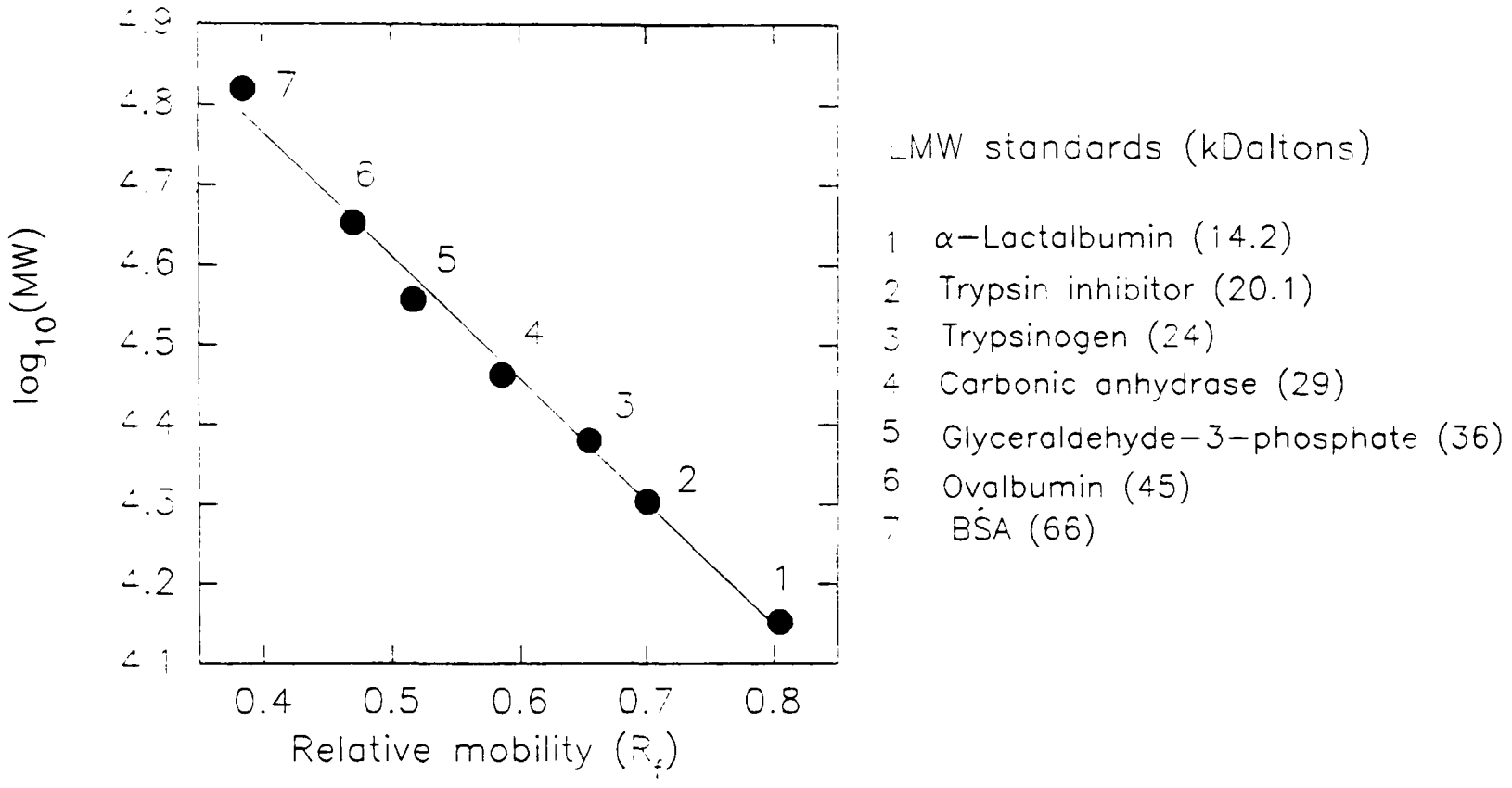


(b) Heavy molecular weight (HMW) standards

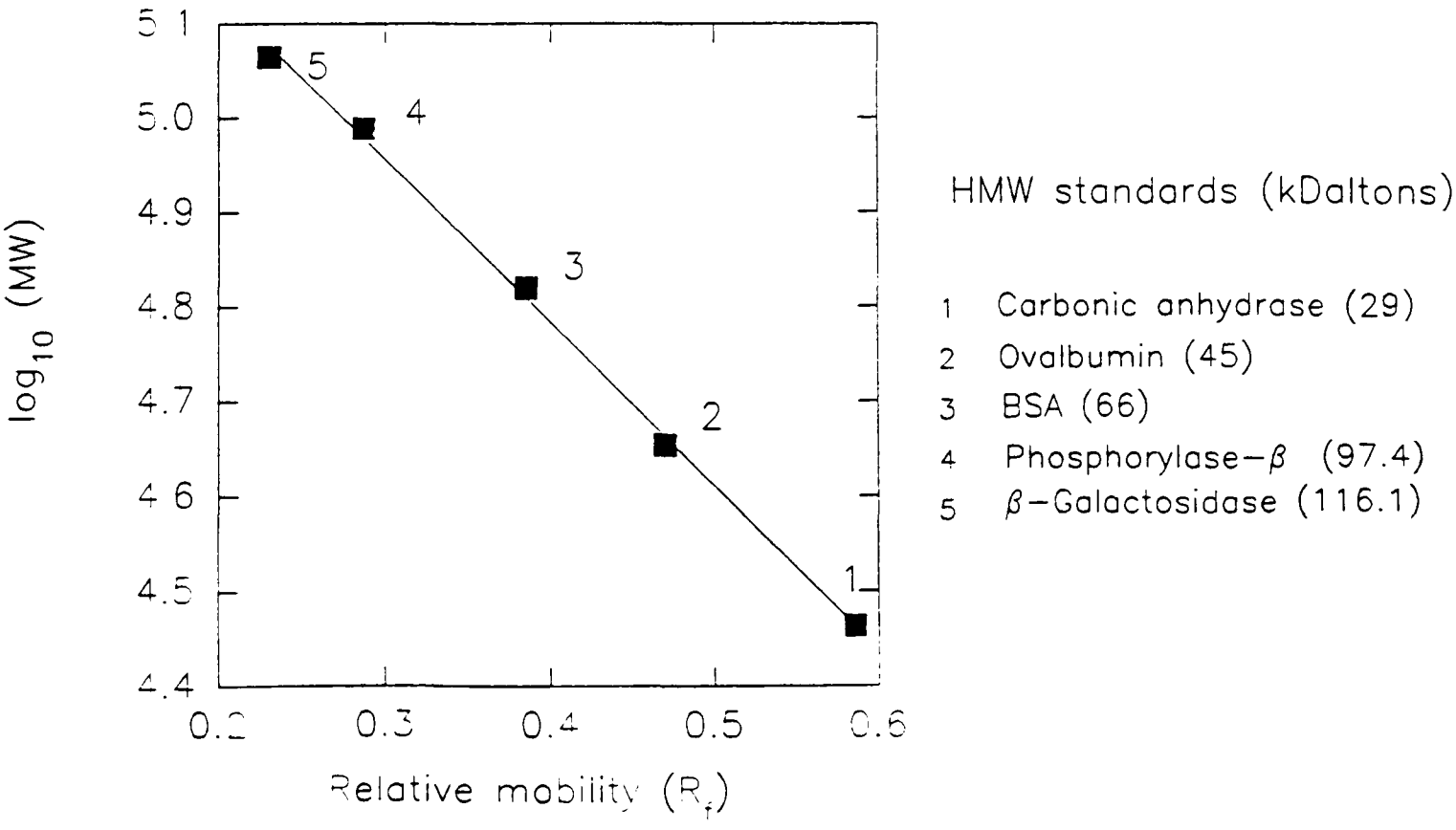

**Figure II10: Determination of the Ionic Strength of Citrate Buffer (pH 6.0), Phosphate Buffer (pH 8.0) and Solutions of Sodium Chloride by Measurements of the Conductivity of Respective Solutions of Varied Molarity** (Conductivity measurements were automatically compensated for variations in temperature)

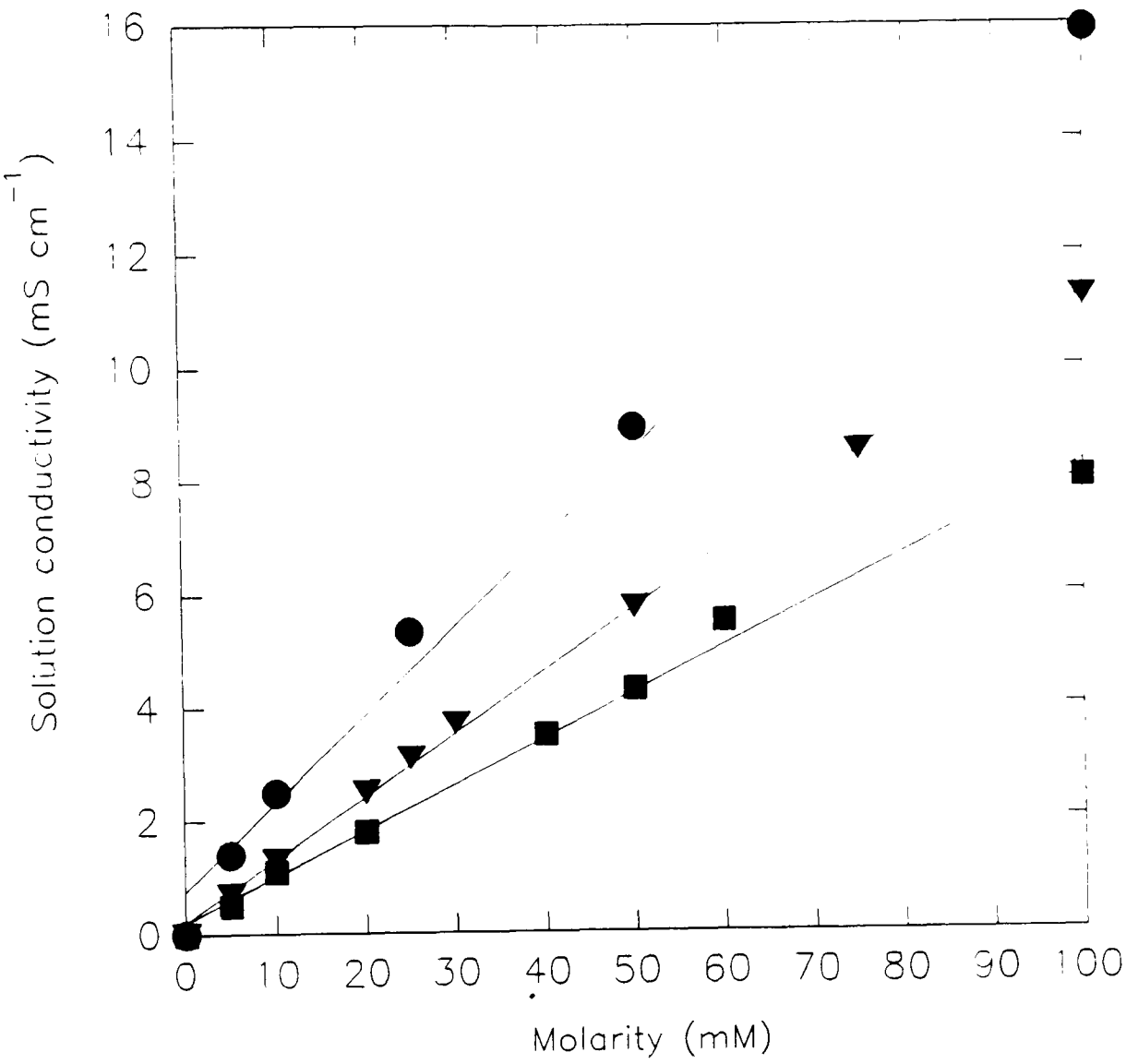

**Table II1: Determination of Cytochrome-*c* Concentration of Model Solutions in the Presence and Absence of Haemoglobin**

The influence of haemoglobin upon the accuracy of the cytochrome-*c* assay (Cole et al. (1972); see Chapter 2) is described for model solutions of cytochrome-c in the presence and absence of haemoglobin; **(a)** cytochrome-*c* solutions of varied concentration in the absence of haemoglobin, **(b)** solutions of varied cytochrome-*c* and fixed haemoglobin concentrations and **(c)** solutions of fixed cytochrome-*c* and varied haemoglobin concentrations.

**(a)**

| Sample Composition (mg $cm^{-3}$ dry w $v^{-1}$) | | Assay Determined Cytochrome-*c* |
|---|---|---|
| **Cytochrome-*c*** | **Haemoglobin** | **Concentration (mg $cm^{-3}$)** |
| 1.00 | 0.00 | 0.83 |
| 0.50 | 0.00 | 0.46 |
| 0.25 | 0.00 | 0.23 |
| 0.20 | 0.00 | 0.19 |

**(b)**

| Sample Composition (mg $cm^{-3}$ dry w $v^{-1}$) | | Assay Determined Cytochrome-*c* |
|---|---|---|
| **Cytochrome-*c*** | **Haemoglobin** | **Concentration (mg $cm^{-3}$)** |
| 1.00 | 0.50 | 0.79 |
| 0.50 | 0.50 | 0.44 |
| 0.25 | 0.50 | 0.22 |
| 0.20 | 0.50 | 0.18 |

**(c)**

| Sample Composition (mg $cm^{-3}$ dry w $v^{-1}$) | | Assay Determined Cytochrome-*c* |
|---|---|---|
| **Cytochrome-*c*** | **Haemoglobin** | **Concentration (mg $cm^{-3}$)** |
| 0.50 | 0.00 | 0.46 |
| 0.50 | 0.17 | 0.42 |
| 0.50 | 0.25 | 0.44 |
| 0.50 | 0.50 | 0.44 |

# *APPENDIX III*

## *SURFACE TENSION MEASUREMENTS OF PROTEIN SOLUTIONS*

**Figure III1: Surface Tension Measurements of Solutions of BSA and Lysozyme**

Surface tension ($\sigma$) measurements (see Chapter 2 (2.5.1)) of homogeneous solutions of BSA and lysozyme at varied concentrations. Protein solutions were prepared in 20 mM sodium phosphate buffer, pH 8.0. Measurements were undertaken at room temperature (22.5-22.8 °C) 90 min after preparation. In **(a)** surface tension is plotted against protein concentration, whilst in **(b)** surface tension is depicted as a function of the natural logarithm of protein concentration, thus indicating the CMC and threshold regions.

(a)

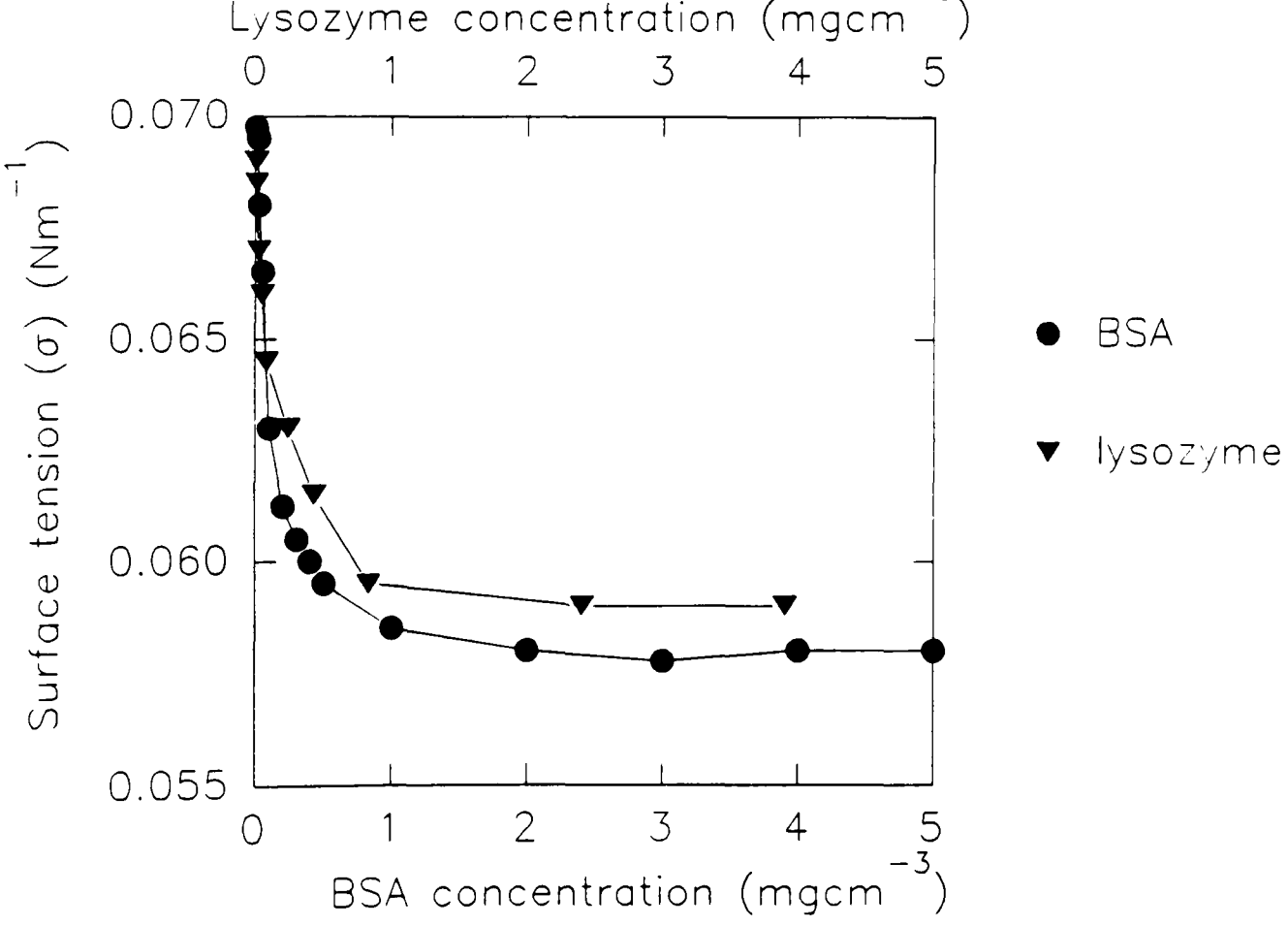

**Figure III1 continues**

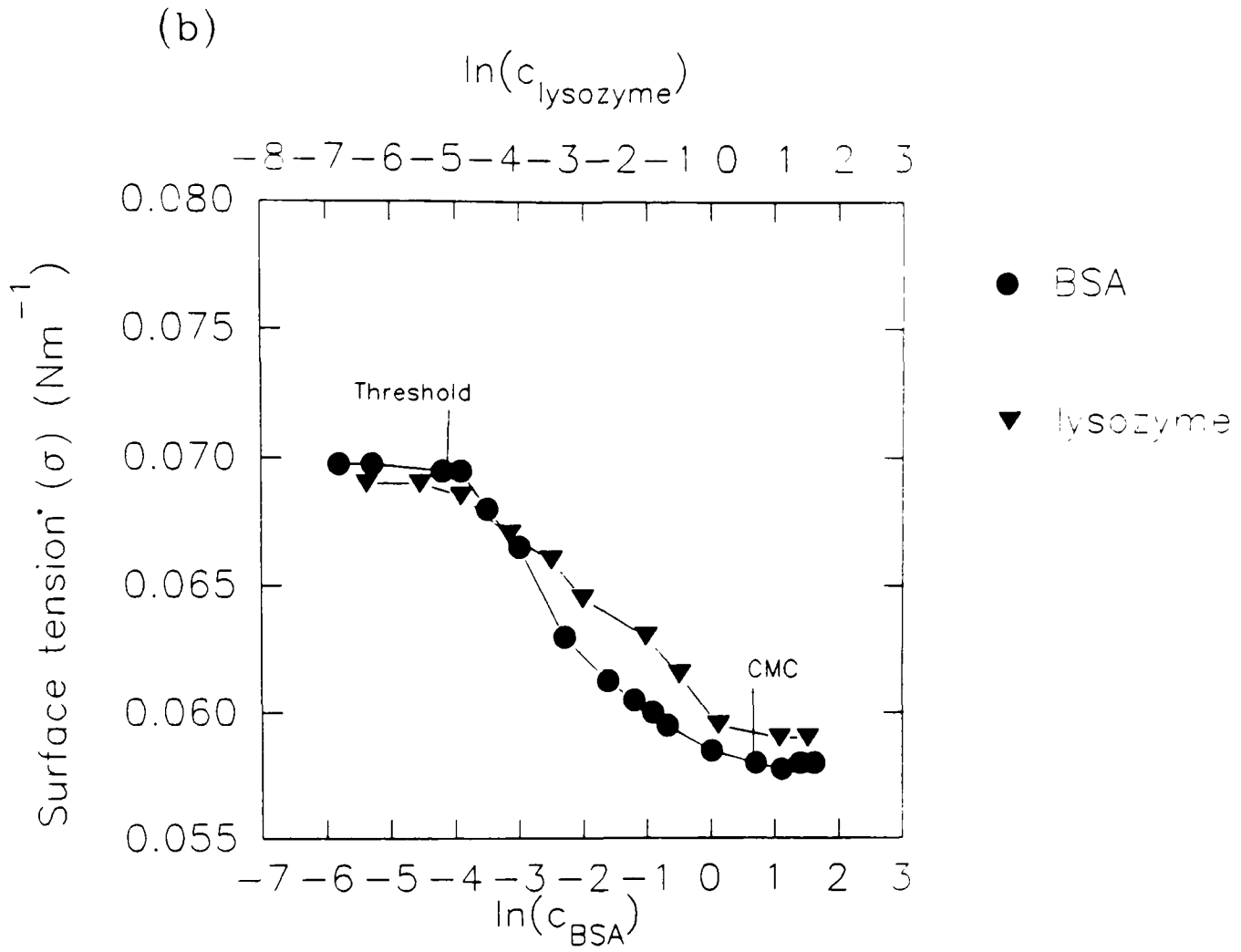

**Figure III2: Surface Tension of Brewer's Yeast Extracts**

Illustration of variations in surface tension ($\sigma$) of brewer's yeast extracts expressed as a function of yeast protein concentration. Samples were prepared in 20 mM potassium phosphate buffer, pH 8.0, and determination of surface tension was undertaken as described in Chapter 2 (2.5.1). Samples included fresh yeast extract (prepared as described in Chapter 6 (6.2)), resuspended freeze-dried yeast extract and resuspended freeze-dried yeast extract of low RNA content. This latter sample was the elution product at 0.2 M NACl (see Figure 6.11, Chapter 6) from yeast extract, treated by ion-exchange on a fixed bed of DEAE-52 cellulose as described in Chapter 6 (6.2).

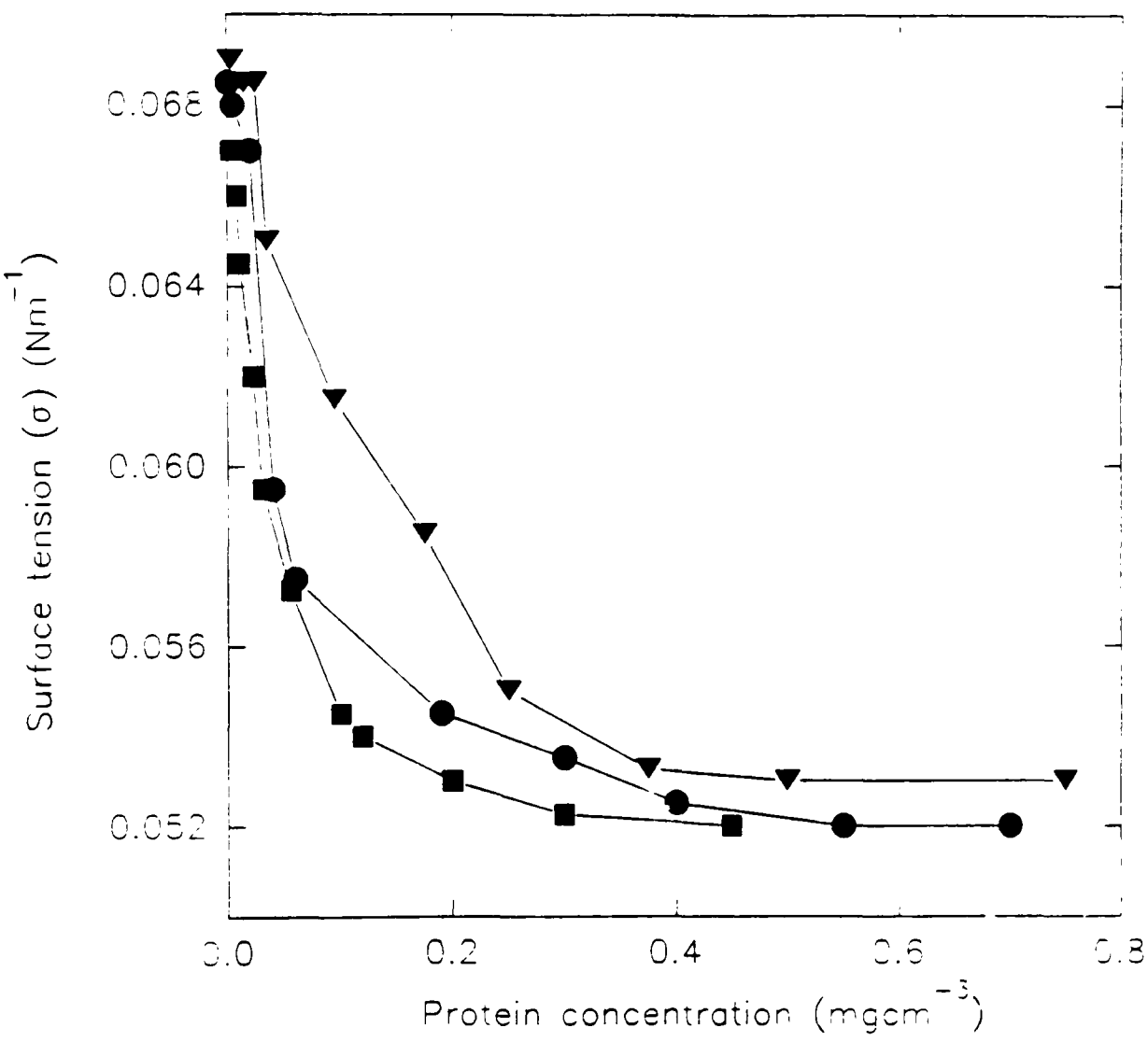

**Figure III3: Surface Tension of Brewer's Yeast Extracts Against the Natural Logarithm of Protein Concentration**

Surface tension ($\sigma$) of fresh brewer's yeast extract is described as a function of the natural logarithm of yeast protein concentration. Samples were prepared in 20 mM potassium phosphate buffer as described in Chapter 6 (6.2). Samples were prepared in 20 mM potassium phosphate buffer, pH 8.0, and determination of surface tension was undertaken as described in Chapter 2 (2.5.1).

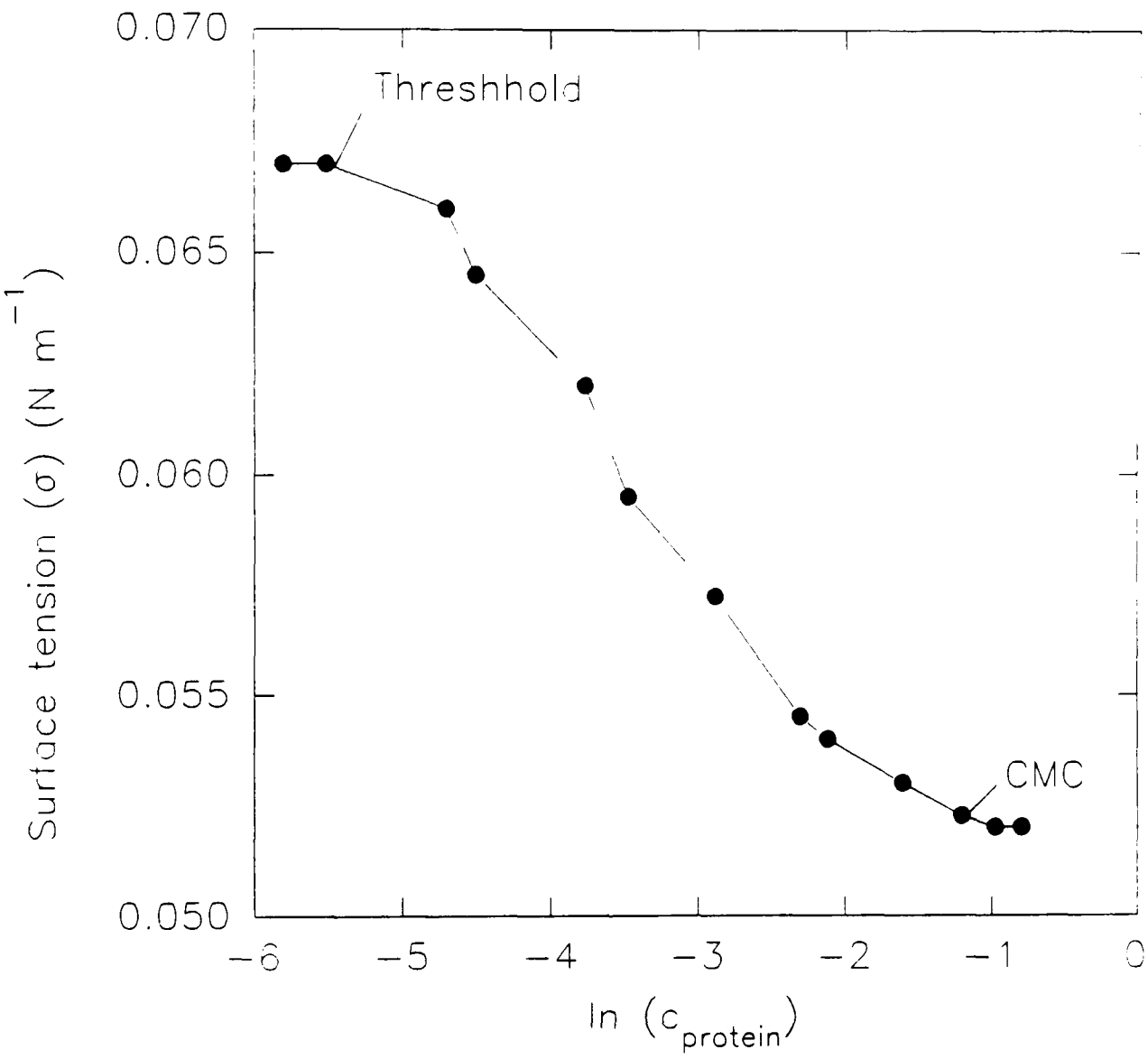

# *APPENDIX IV*

## IV1: Theoretical Model for the Performance Prediction of Continuous Foams Stabilised by BSA; Brown et al. (1990)

The model accounts for gravity drainage through the network of plateau borders. It also accounts for the thinning of the liquid lamellae due to Plateau border suction. Material balances are made on the liquid in the films and in the Plateau borders. Several assumptions are employed. First, it is assumed that the gas phase consists of dodecahedral bubbles of uniform size at a given height of the foam bed and that the foam bed ascends in plug flow. The Plateau borders are assumed to be randomly oriented. It is also assumed that the surface concentration of the protein is at equilibrium. This assumption is valid for high protein concentrations and prolonged residence times of the gas bubbles in the liquid pool.

$$e = c_F/c_0 = \{N_b n_f A_f \Gamma/(c_0 \varepsilon_l)\} + c/c_0 \qquad \text{(Equation IV1)}$$

where: e is enrichment

$c_0$ and $c_F$ are protein concentrations in feed and foam respectively

$N_b$ is the number of bubbles per unit volume of foam

$n_f$ is the number of thin films per bubble in a regular dodecahedron ; $n_f$=6 to avoid double counting

$A_f$ is area of film

$\Gamma$ is surface concentration of protein at equilibrium

$\varepsilon_l$ is liquid hold-up

c is bulk concentration of protein

$$\varepsilon_l = N_b(n_f A_f x_f + n_p a_p l) \qquad \text{(Equation IV2)}$$

where: $x_f$ is film thickness

$n_p$ is the number of plateau borders per bubble in a regular dodecahedron; $n_p$=10 to avoid double counting

$a_p$ is cross-sectional area of plateau border

$l$ is the length of plateau border

$$l = \delta R \qquad \text{(Equation IV3)}$$

where: $\delta$=0.816

R is the radius of the bubble ($R=\bar{d}_b/2$)

### (a) Material Balance for Liquid in Films

Liquid will tend to drain out of the films due to plateau border

suction. The drainage of liquid through a circular plane parallel film of radius $R_f$ and thickness $x_f$ can be described by the equations of continuity and motion. For the case of infinite viscosity (globular proteins), the no-slip boundary condition can be used and the Reynolds equation can describe the velocity of drainage U:

$$U = (2x_f^3\Delta P)/(3\mu R_f^2) \qquad \text{(Equation IV4)}$$

where: U is velocity of drainage

$\Delta P$ is the pressure difference between films and plateau borders

$\mu$ is the bulk liquid viscosity

$R_f$ is the radius of a planar phase film

$$A_f = 1.152R^2 = \pi R_f^2 \qquad \text{(Equation IV5)}$$

$$R_f = (1.152/\pi)^{0.5}R \qquad \text{(Equation IV6)}$$

$$\Delta P = \sigma/R_p - \Pi \qquad \text{(Equation IV7)}$$

where: $\sigma$ is the surface tension

$R_p$ is the radius of curvature

$\Pi$ is the disjoining pressure; $\Pi$ is negligible for films thicker that 100 nm and is considered to be negligible in the present study

$$R_p = \{-1.732x_f + \{1.453x_f^2 + 0.644\ a_p)^{0.5}\}/0.322;\ R_p > 0 \qquad \text{(Equation IV8)}$$

$$dn/dh_f = -\omega N_b/2 \qquad \text{(Equation IV9)}$$

where: n is the number of bubbles passing through a cross-sectional area of the foam column per unit time

$h_f$ is the height of foam bed

$\omega$ is coalescence frequency

$$n = u_g/v_b;\ N_b = (1-\varepsilon_l)/v_b \qquad \text{(Equation IV10)}$$

where: $u_g$ is superficial gas velocity

$v_b$ is the volume of a bubble

$$v_b = 4\pi R^3/3 \qquad \text{(Equation IV11)}$$

$$2\pi N_b R^4\omega/9u_g = dR/dh_f \qquad \text{(Equation IV12)}$$

The material balance for the liquid in the films is

$$-d(nn_fA_fx_f)/dh_f - N_bn_fA_fU - \omega n_fx_fA_fN_b/2 = 0;\quad dx_f/dh_f < 0 \qquad \text{(Equation IV13)}$$

**(b) Material Balance for Liquid in Plateau Borders**

There are four contributors to the material balance for liquid in the plateau borders, namely liquid sucked from the films, liquid from ruptured films, gravity and convection because foam is moving upwards. The velocity of gravity ($u$) drainage will be:

$$u = c_v \rho g a_p / 20\mu\sqrt{3} \qquad \text{(Equation IV14)}$$

where: $c_v$ is the ratio of the average velocity with finite surface viscosity to the average velocity with infinite surface viscosity. For infinite surface viscosity $c_v$ is one; $c_v$ is considered to be one for globular proteins such as BSA.

The average volumetric \ flowrate $q_p$ through a randomly orientated plateau border is:

$$q_p = 2a_p u/2 \qquad \text{(Equation IV15)}$$

The number of plateau borders per unit area of foam will be $2RN_b n_p/5$ and the change in flow due to gravity will be:

$$d(a_p)_g = d(4N_b n_p a_p uR/15)/dh_f \qquad \text{(Equation IV16)}$$

The material balance for liquid in the plateau borders is

$$-d(nn_p a_p l)/dh_f - d(N_b n_p a_p uR)/dh_f + N_b n_f A_f U + \omega N_b n_f A_f x_f/2 = 0$$

(Equation IV17)

**(c) Material Balance for Protein in Foam**

Protein concentration in foam changes with height due to coalescence and film rupture which lead to redistribution of liquid and protein in the plateau borders. If liquid entrained in foam is well mixed then protein concentration will be the same in films and plateau borders. This assumption tends to overestimate predicted concentrations but is reasonable when the liquid content of films is very small relative to the amount in plateau borders. If liquid in films is segregated from liquid in the plateau borders then only the concentration in the plateau borders is expected to change with foam bed height. When the former assumption is adopted then the material balance for protein is:

$$-d(nn_p a_p lc + nn_f A_f x_f c)/dh_f + d(4N_b n_p uRc/15)/dh_f + \omega N_b n_f A_f c/2 = 0$$

(Equation IV18)

For negligible coalescence, ie $\omega$=0, then $dc/dh_f$=0 and the number of

equations required to solve for $\varepsilon_l$ is reduced to two. Equation IV13 gives Equation IV19 and Equation IV17 gives Equation IV20.

$$dx_f/dh_f = -(1-\varepsilon_l)U/u_g \qquad \text{(Equation IV19)}$$

$$da_pY/dh_f = N_b n_f A_f U - Y^* dx_f/dh_f \qquad \text{(Equation IV20)}$$

where: $Y = nn_p l - N_b n_p a_p R\rho g/75\mu\sqrt{3} - 4N_b n_p uR/15$
$+ 4n_p^2 l a_p uR/\{15(v_b + n_f A_f x_f + n_p a_p l)^2\}$
$Y^* = 4n_f A_f n_p a_p uR/Y$

**(d) Boundary Conditions**

At the foam-liquid interface the rate of liquid uptake is rate of uptake = $u_g\varepsilon_{lo}/(1-\varepsilon_{lo})$ (Equation IV21) At $h_f$=0 the rate of drainage will be the rate of gravity drainage (rate of drainage at $h_f$=0) = $4/15N_{bo}n_p a_{po}R_o u_o$ (Equation IV22) At the foam-liquid interface the rate of uptake is approximately equal to the rate of drainage (Desai and Kumar (1983); Narsimhan and Ruckenstein (1986a)) and hence

$$u_g\varepsilon_{lo}/(1-\varepsilon_{lo}) = 4/15N_{bo}n_p a_{po}R_o u_o \qquad \text{(Equation IV23)}$$

Also,

$$x_{fo} = \varepsilon_{lo}\phi_{fo}/N_b n_f A_f \qquad \text{(Equation IV24)}$$

$$N_{bo} = 3(1 - \varepsilon_{lo})/4\pi R^3 \qquad \text{(Equation IV25)}$$

$$a_{po} = (1 - \phi_{fo})\varepsilon_{lo}/N_{bo}n_p\delta R_o \qquad \text{(Equation IV26)}$$

where: $\phi_{fo}$ is the fraction of foam liquid in the films at the foam-liquid interface.

From an overall material balance the pool (bottoms) concentration ($c_F$) can be related to the feed concentration ($c_0$) through:

$$c_B = c_0 - u_g n_f A_f \Gamma/v_b Q_0 \qquad \text{(Equation IV27)}$$

Application of this model to predict protein enrichment and recovery in foams from brewer's yeast extract (see Chapter 7 (7.3.1)) was hampered by unacceptable negatives values of $x_f$ as shown in Table IV1(a-b). Viscosity and density values are presented in Table 7.1 and bubble diameters at the foam-liquid interface are shown in Figure 7.1 in Chapter 7. Calculations of $x_{fo}$ and $a_{po}$ were based on Equations IV23 to IV26. Application of Equation IV27 enabled determination of protein surface excess at equilibrium ($\Gamma$) as shown in Figure IV2. It can be seen that $\Gamma$

increased with liquid pool concentration and it seems that this trend resembled Langmuir adsorption (see Figure 1.4 in Chapter 1) although more points are required to confirm such indication. Determination of $\Gamma$ in a dynamic system such as continuous foaming is expected to be more accurate than static determination of $\Gamma$ as described by Equation 1.3 (Chapter 1). In addition Equation IV27 enables determination of $\Gamma$ in mg $cm^{-2}$ as opposed to Equation 1.3, where $\Gamma$ is given in moles $cm^{-2}$. In multi-component systems such as yeast extract where the exact number and molar ratios of constituent components is unknown conversion of moles $cm^{-2}$ to mg $cm^{-2}$ would be very difficult if not impossible.

**Table IV1: Calculated Film thickness and Cross-Sectional Area of Plateau Border at the Foam-Liquid Interface in Foams Produced from Brewer's Yeast Extract.**

Film thickness and plateau border area at the foam-liquid interface ($x_{f0}$ and $a_{p0}$ respectively) were calculated by application of Equations IV23 to IV26 from the theoretical model from Brown et al. (1990). Negligible coalescence was assumed. Foams were produced continuously from brewer's yeast extract as described in Chapter 7 (7.2) and the height of the foam bed was 5 cm. Physical properties and bubble size values are presented in Chapter 7 (7.3.1).

**(a) Gas Flowrate G=40 $cm^3$ $min^{-1}$**

| Feedstock Protein Concentration ($c_{protein,0}$) (mg $cm^{-3}$) | $x_{f0}$ (mm) | $a_{p0}$ ($mm^2$) |
|---|---|---|
| 0.45 | $-1.41\times10^{-1}$ | $1.94\times10^{-2}$ |
| 0.25 | $-1.36\times10^{-1}$ | $2.06\times10^{-2}$ |
| 0.17 | $-1.10\times10^{-1}$ | $3.54\times10^{-2}$ |
| 0.10 | $-8.91\times10^{-2}$ | $4.55\times10^{-2}$ |

**(b) Feedstock Protein Concentration $c_{protein,0}$=0.45 mg $cm^{-3}$**

| Gas Flowrate (G) ($cm^3$ $min^{-1}$) | $x_{f0}$ (mm) | $a_{p0}$ ($mm^2$) |
|---|---|---|
| 40 | $-1.41\times10^{-1}$ | $1.94\times10^{-2}$ |
| 20 | $-8.96\times10^{-2}$ | $1.45\times10^{-2}$ |
| 10 | $-5.14\times10^{-2}$ | $1.06\times10^{-2}$ |

**(c) Feedstock Protein Concentration $c_{protein,0}$=0.25 mg $cm^{-3}$**

| Gas Flowrate (G) ($cm^3$ $min^{-1}$) | $x_{f0}$ (mm) | $a_{p0}$ ($mm^2$) |
|---|---|---|
| 40 | $-1.36\times10^{-1}$ | $2.06\times10^{-2}$ |
| 20 | $-8.11\times10^{-2}$ | $1.75\times10^{-2}$ |
| 10 | $-4.16\times10^{-2}$ | $1.40\times10^{-2}$ |

**Figure IV1: Surface Excess of Protein ($\Gamma_{protein}$) at Equilibrium**

Dependence of $\Gamma_{protein}$ (see Equation IV27) upon pool concentration in foams produced at comparable gas flowrates and various feedstock concentrations. The experimental conditions were the same as in Figure 7.1b.

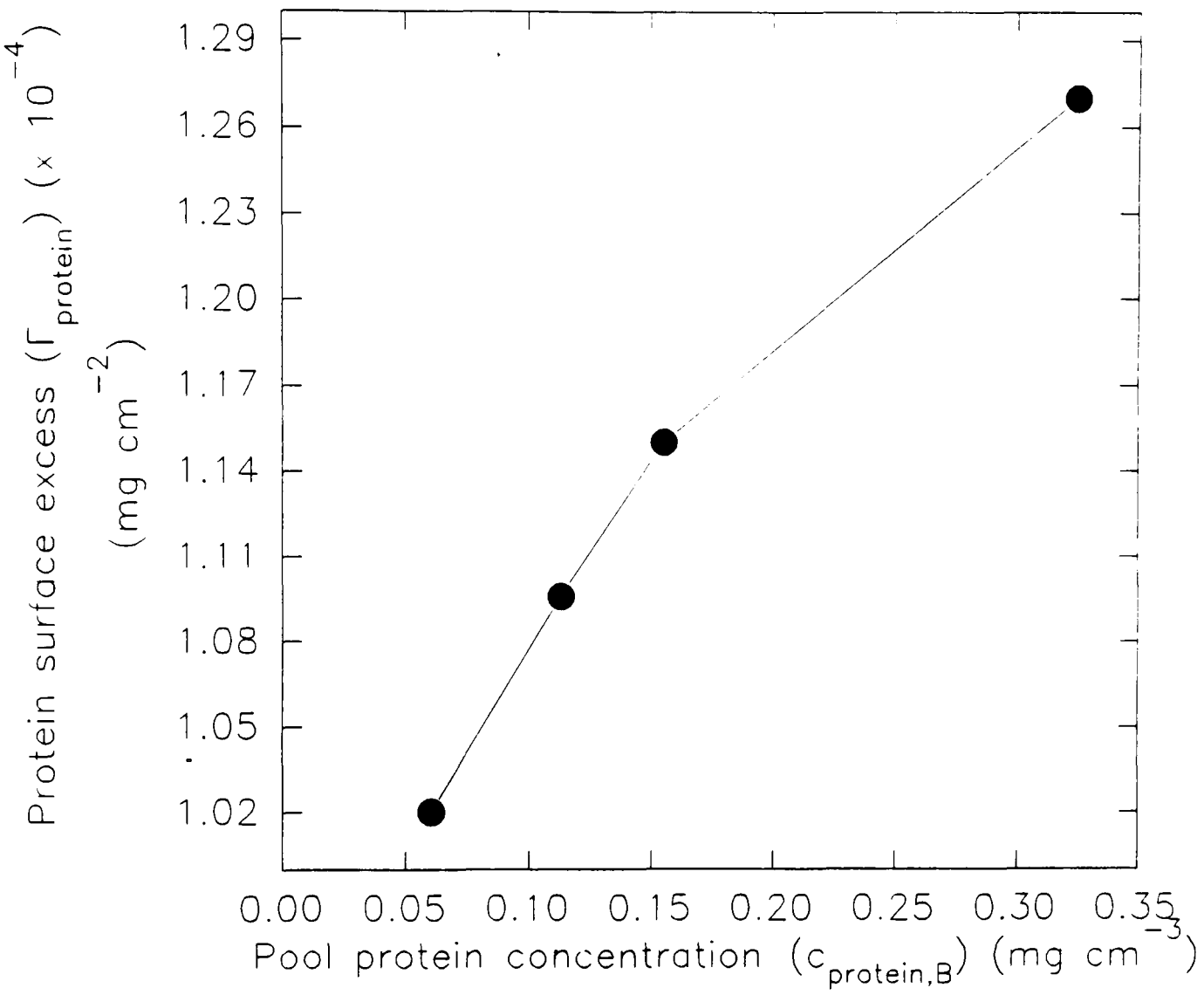

**IV2: Calculation of phase relative velocity ($u_{rel}$) in Equation 7.7**

The relative velocity between ascending bubbles and trickling liquid can be described by Equation IV28 (Marrucci (1965)) which applies for $1 < N_{Re} < 300$:

$$u_{rel}/u_{single} = \varepsilon_g/\{1-(1-\varepsilon_g)^{5/3}\} \qquad \text{(Equation IV28)}$$

The velocity of a single bubble ($u_{single}$) can be determined from Figure IV2 (Wace et al. (1969)) as a function of bubble diameter.

**Figure IV2: Rise Velocity of Air Bubbles in Aqueous Surfactant Solution** (from Wace et al. (1969))

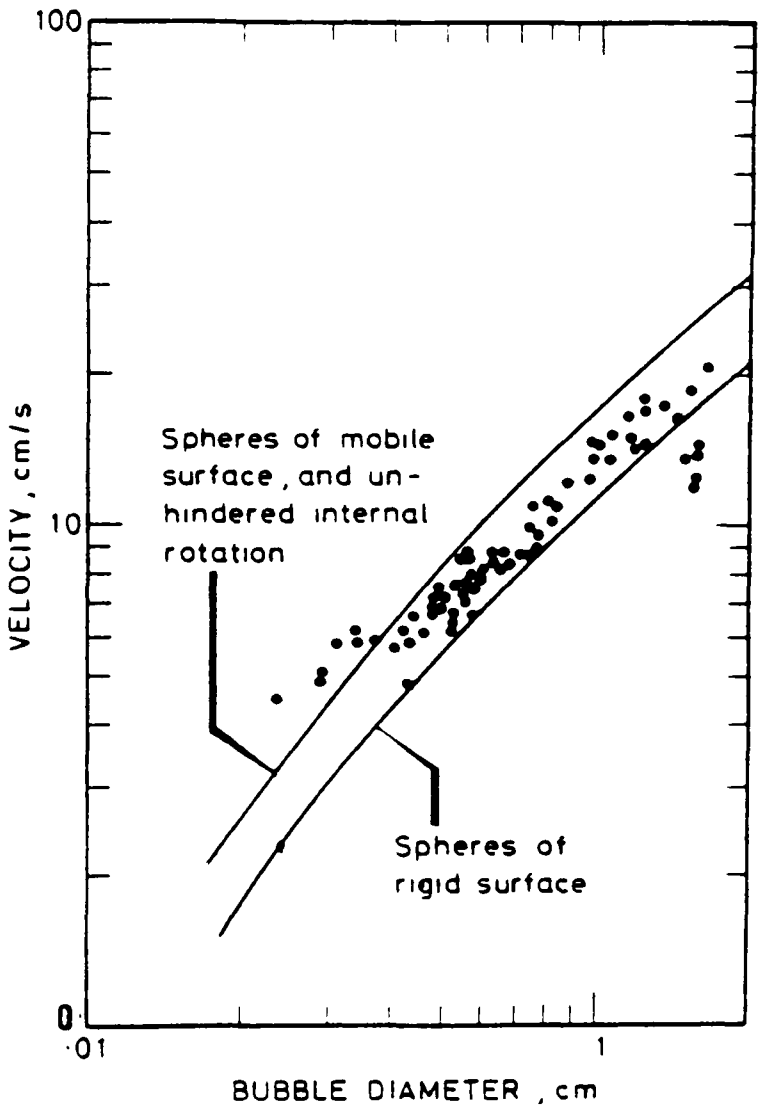


Rise velocity of air bubbles in aqueous surfactant solution.

**Plate IV1: Bubble Photographs in Foams at Various Heights of the Foam Bed**

Bubble photographs of foams at various heights of the foam bed. Foams were produced under various feedstock protein concentrations and gas flowrates. The total height of the foam bed was 5 cm; Also see Figures 7.1 to 7.3 in Chapter 7. Photograph scales are comparable.

$c_{protein,0}$=0.10 mg $cm^{-3}$ G=40 $cm^3$ $min^{-1}$

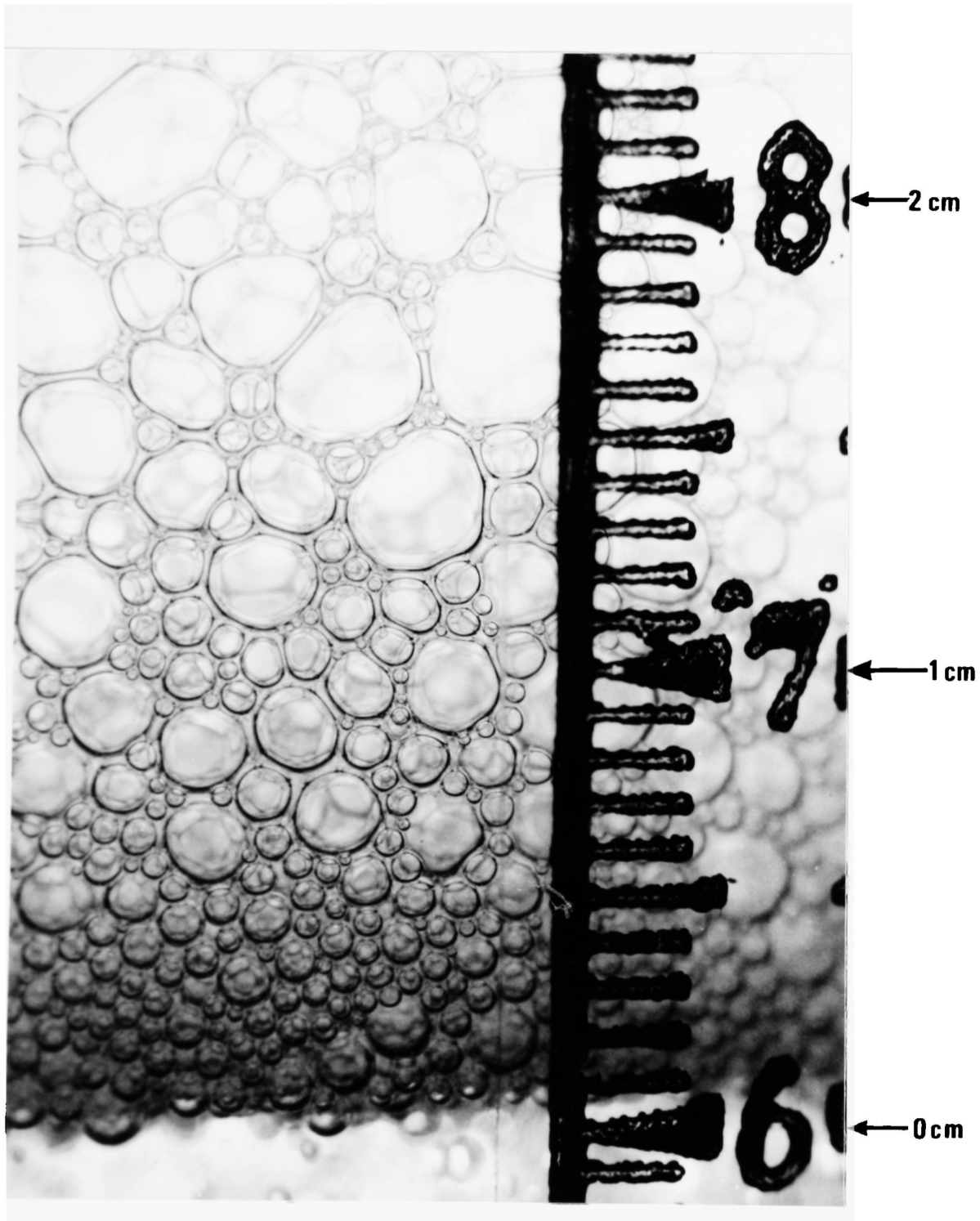


Total height of foam bed ($h_f$) = 5 cm

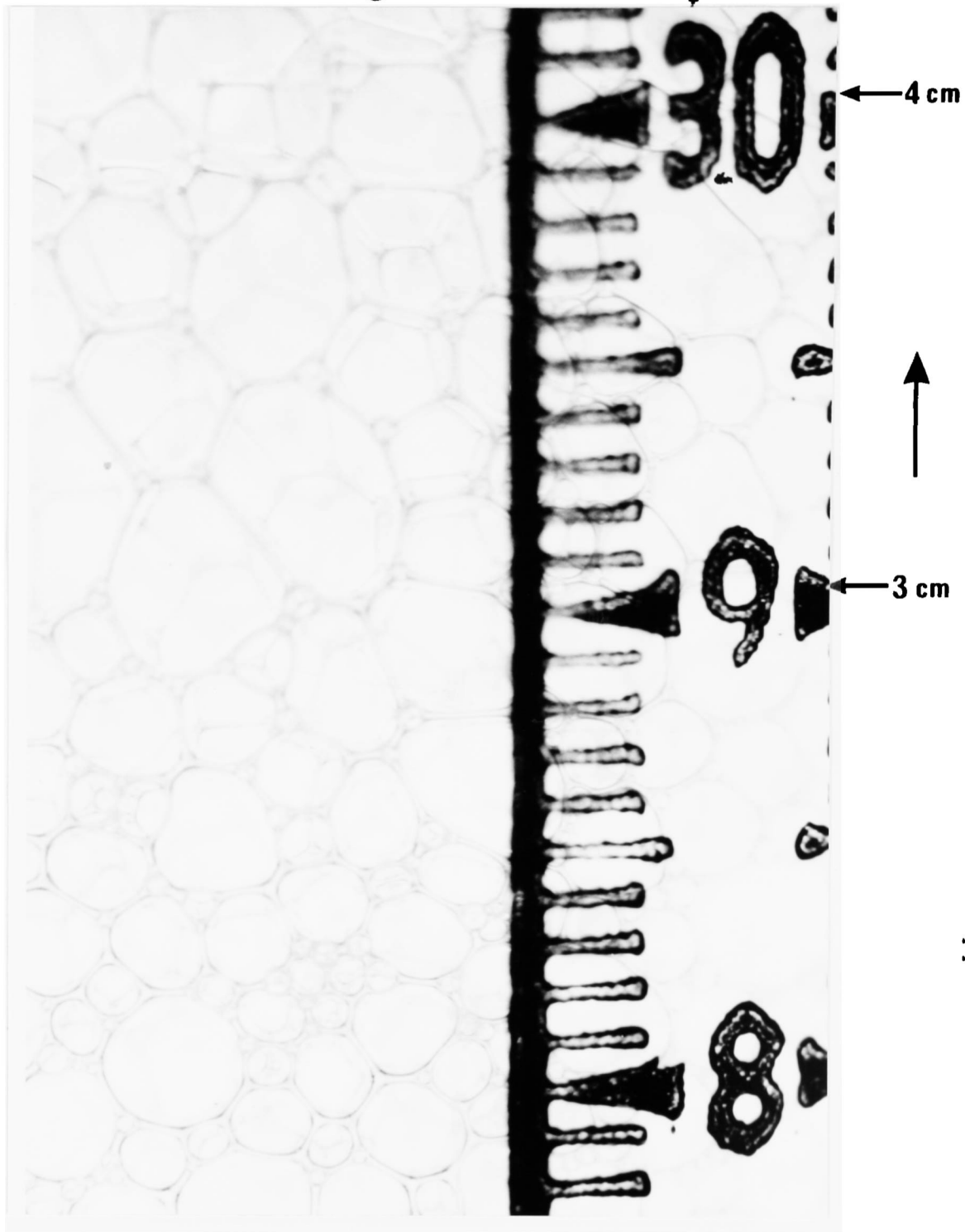

$c_{protein,0}$=0.45 mg $cm^{-3}$ G=40 $cm^3$ $min^{-1}$

Total height of foam bed ($h_f$) = 5 cm

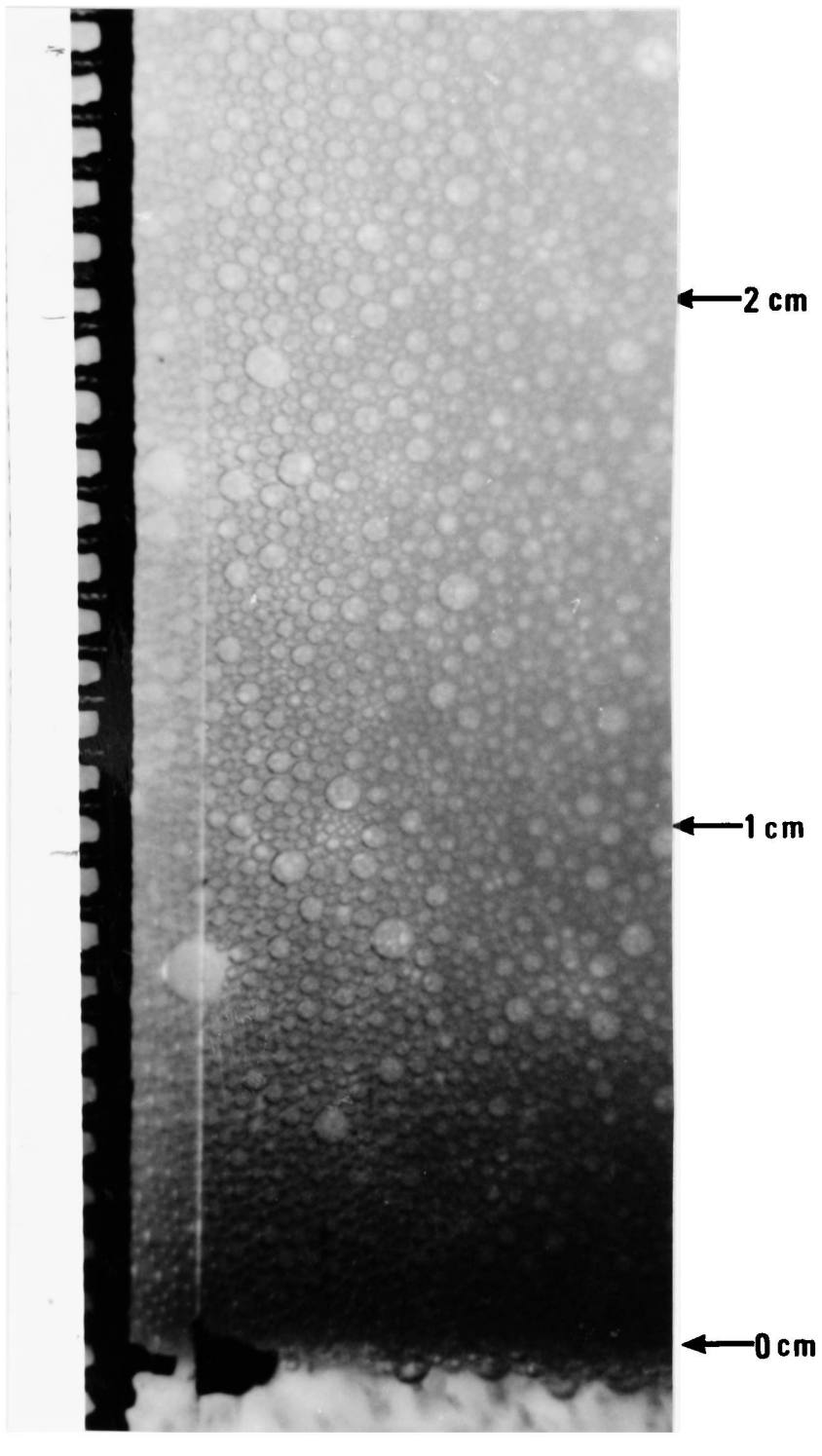


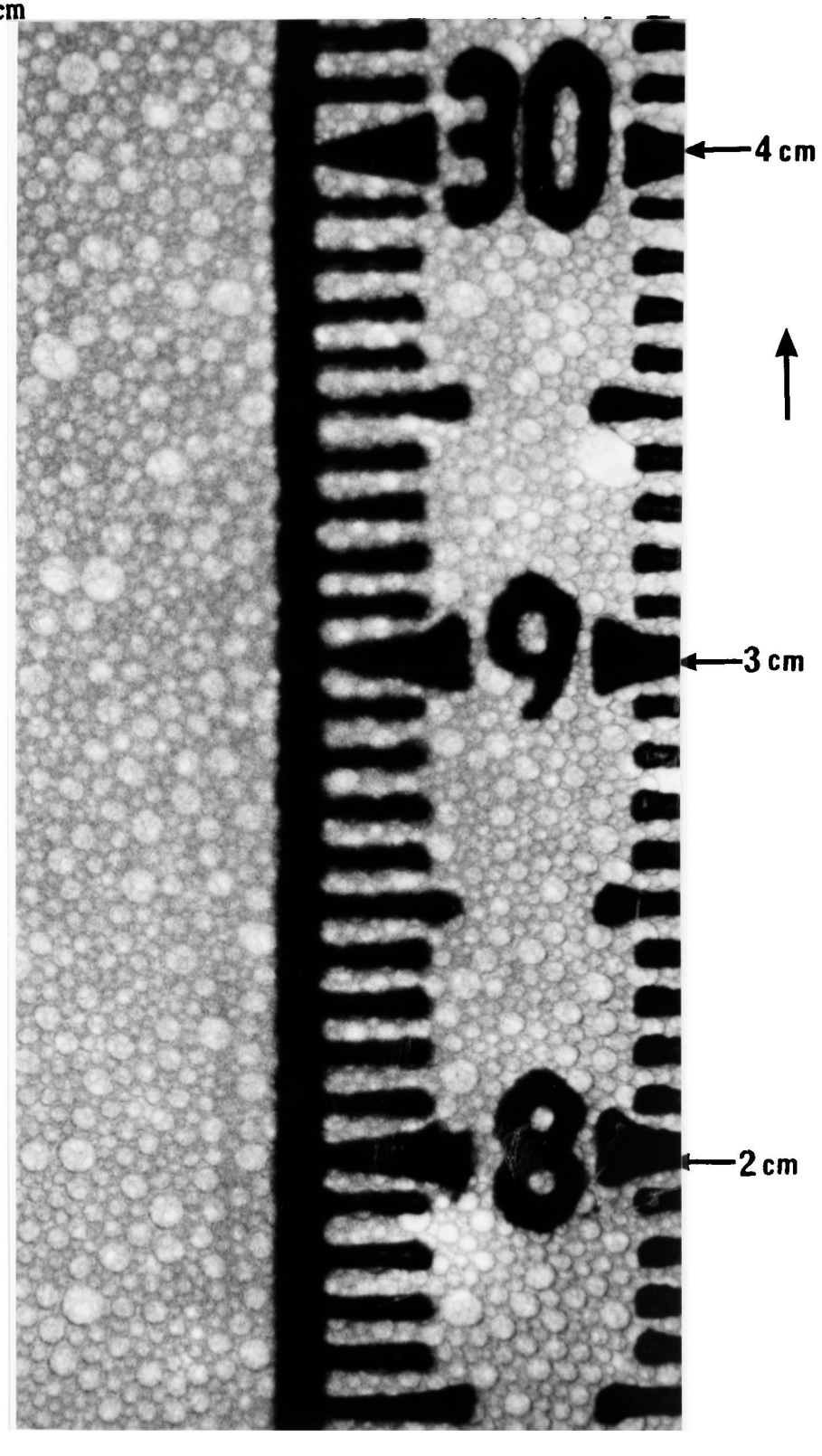

$c_{protein,0}$=0.25 mg $cm^{-3}$ G=10 $cm^3$ $min^{-1}$

Total height of foam bed ($h_f$) = 5 cm

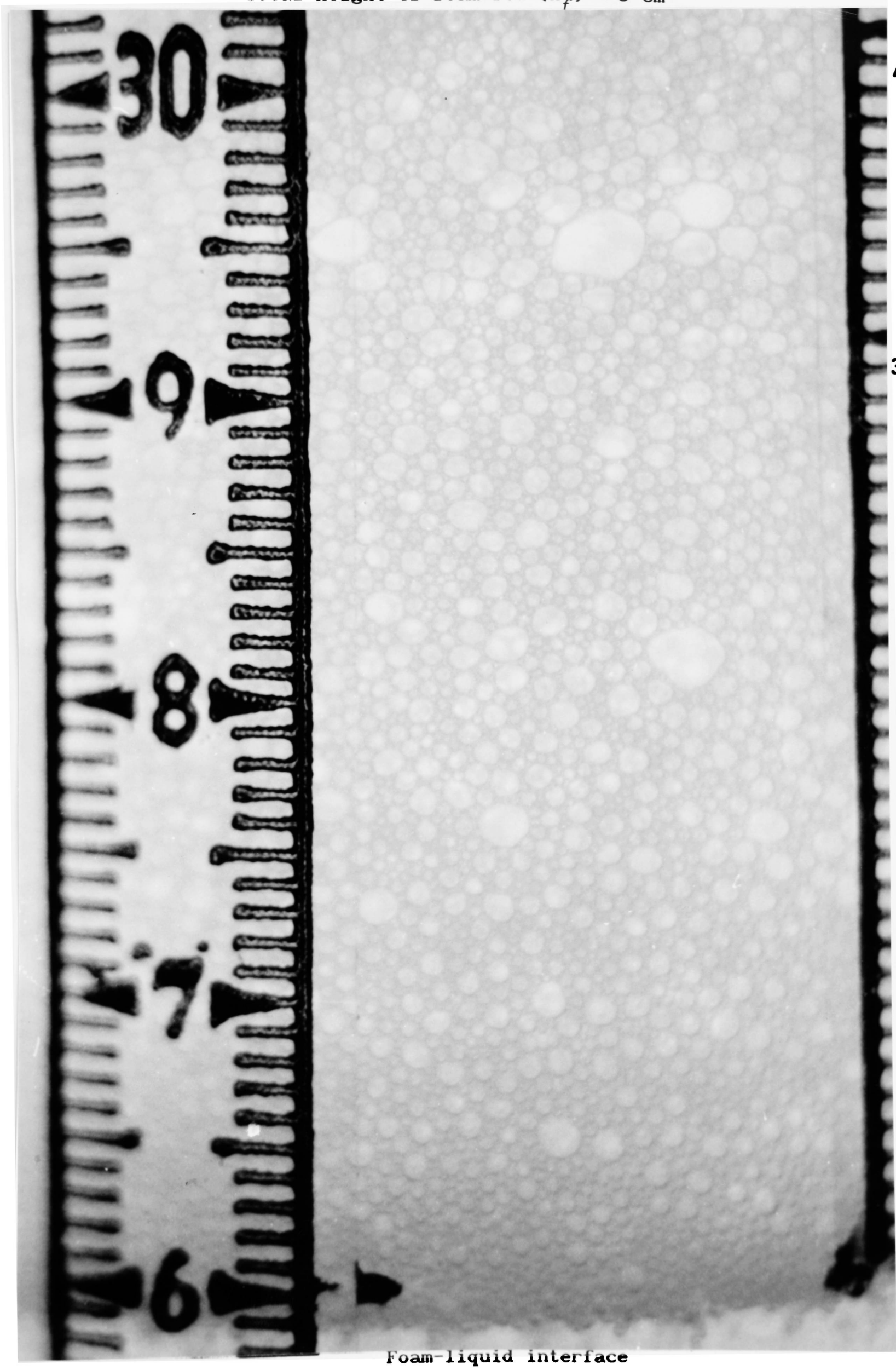


Foam-liquid interface

# *APPENDIX V*

## *BATCH FOAM PRODUCTION FROM BOVINE HEART MUSCLE HOMOGENATE*

### V.1 Cytochrome-*c* Collection in Foam

The excellent foaming properties of cytochrome-*c* (Velissariou (1988)), already discussed in Chapter 3, indicated a scope for investigation of the benefits of foam fractionation when applied as a preliminary step in the purification of mitochondrial cytochrome-*c*. Such benefits would include volume and time-scale reduction in further steps. These steps include collection of protein from a cation-exchange resin, ammonium sulphate fractionation and cation-exchange chromatography (Brautigan et al. (1978)). Thus bovine heart muscle homogenate was foamed batchwise (see Chapter 2) in the 1,600 $cm^3$ foam tower (see Figure 2.3 in Chapter 2). Fresh heart tissue was homogenised in 5 volumes of 0.3% w $v^{-1}$ $Al_2(SO_4)_3.17H_2O$ at pH 4.5 as described by Brautigan et al. (1978). The trivalent cations can effectively displace protein even at low ionic strength. Solids were removed by centrifugation at 30,000 g for 45 min and aliquots were were frozen. Prior to foaming aliquots were thawed overnight and diluted to predetermined concentrations in 0.3% w $v^{-1}$ $Al_2(SO_4)_3.17H_2O$; pH 4.5. Aluminium ions were then precipitated with 2 M NaOH at pH 8.2-8.5 and were removed by filtration through coarse fluted filter paper. Sample preparations were undertaken in the cold room at 4 $^{o}C$. Batch foaming was undertaken for comparative periods of time (45 min) at pH 8.5. The volume of the foamed sample was 400 $cm^3$ and the nitrogen flowrate was 80 $cm^3$ $min^{-1}$. The temperature was at 20$^{o}C$. The protein content and cytochrome-*c* concentration of the collected foams were determined by the Bradford assay (see Chapter 2 (2.4.3)) and the cytochrome-*c* assay (see Chapter 2 (2.4.8)).

Table V1 illustrates the dependence of protein concentration and cytochrome-*c* specific activity (ie mg of cytochrome-*c* per mg of total protein) in foam upon varied feedstock protein concentration. It can be seen that dilute feedstocks promoted protein concentration in foam but it appears that cytochrome-*c* fractionation did not occur. In contrast it seems that cytochrome-*c* specific activity was consistently slightly below that of the feedstock.

**Table V1: Partition of Total Protein and Cytochrome-*c* in Foam at Varied Feedstock Concentrations during Batch Foam Production from Bovine Heart Muscle Homogenate**

Variations in total protein concentration and cytochrome-*c* specific activity in foams generated from bovine heart muscle homogenate at various feedstock protein concentrations. Batch operations were applied at 4°C and nitrogen was sparged at a rate of 80 $cm^3$ $min^{-1}$. Samples were prepared in 0.3% w $v^{-1}$ $Al_2(SO_4)_3.17H_2O$; pH 4.5. Foaming solutions were free of aluminium cations and the pH was 8.5. Values in supersript describe apparent enrichement ($e_{i,app}$, see EquationS 3.1 and 6.1) of total protein and cytochrome-*c* specific activity.

| **Protein Concentration (mg $cm^{-3}$)** | | **Cytochrome-*c* Specific Activity (μg cytochrome-*c* $mg^{-1}$ total protein)** | |
|---|---|---|---|
| **Feedstock** | **Foam** | **Feedstock** | **Foam** |
| 1.20 | $1.35^{1.13}$ | 50.5 | $47.0^{0.93}$ |
| 0.80 | $1.20^{1.50}$ | 35.0 | $34.3^{0.98}$ |
| 0.39 | $1.18^{3.02}$ | 20.5 | $18.8^{0.92}$ |
| 0.16 | $0.82^{5.13}$ | 10.0 | $8.8^{0.88}$ |

The observed increase in protein enrichment agrees with results presented in Chapter 4 for model BSA systems and Chapters 6 and 7 for brewer's yeast extracts. The fact that no cytochrome-*c* fractionation occurred, although at the most dilute feedstock complete decolourisation of the bottoms was observed with simultaneous colour intensity of the foam, implies that the foam formation must be attributed to the combination of muscle proteins in solution rather than specific species. This is in line with conclusions presented in Chapter 6 for brewer's yeast extract. However, the slight reduction in cytochrome-*c* specific activity could be attributed to possible denaturation especially at low feedstock protein concentrations. Under such conditions it was visually observed that red aggregates were formed and such aggregates are expected to owe their colour to cytochrome-*c* and haemoglobin. Similar experiments at pH 4.5 led to extensive precipitation of cytochrome-*c*, while at pH 10.5 no improvement in cytochrome-*c* fractionation was observed. It was therefore concluded that foam fractionation of cytochrome-*c* under the present conditions was not feasible.

**V2: The Potential of Foam Fractionation of Myosin from Muscle Homogenates-Development of an Immunochemical Assay for Myosin Determination**

Considerable research in recent times has begun to unravel the

structural basis of the emulsifying properties of muscle proteins in meat products (Jones (1982); Fretheim et al. (1986); Dickinson et al. (1987)). Li-Chan et al. (1987) applied regression analyses to predict functionality of muscle proteins from physicochemical properties (ie pH, solubility, hydrophobicity, molecular structure). Morrissey et al. (1987) give a detailed account of the functional properties of muscle proteins, while O'Neill et al. (1989) studied the effects of pH and thermal treatment upon the surface activity of muscle proteins at gas-liquid interfaces. They demonstrated that heat-treatment at 60 °C and pH 11.0 resulted in enhanced surface activity, and showed that the rate of surface tension decline of heat treated myosin was fastest.

Such studies inspired the design of a series of foam experiments to investigate the partition of myosin in foam and assess the effects of foaming upon the food functional properties of the proteins collected in foam. Variations in foam quality at different buffer conditions would also provide information on the effects of myosin polymers (Godfrey and Harrington) and subunits (Gershman et al. (1969)), and actomyosin complexes (O'Neill et al. (1989) upon foaming. Design comprised homogenisation of very fresh bovine heart muscle (abattoir waste) in 0.6 M KCl (Frederisken and Rees (1982)) and solid removal, with subsequent foaming at lower buffer molarities (ie in the range of 0.1-.3 M KCl) and varied pH and temperature conditions. Application of well-established myosin assays (Pollard (1982)), namely ATPase assays and gel electrophoresis (Greaser et al. (1987)), would be very time-consuming since foam fractionation requires quantitation of a great number of samples for each set of experimental conditions. An ELISA assay was therefore devised (see Chapter 2 (2.4.9)) the results of which are depicted in Figure V1(a-b). Precipitation of myosin in 0.09 M sodium carbonate was tackled by preparing samples in 0.6 M KCl (Bandari and Trayer (1991)).

Experimentation was cancelled because of the limited availability of fresh bovine heart associated with the outbreak of BSE (Bovine Spongiform Encephalopathy). However, it would be possible to undertake such experiments by replacing the source of muscle. Thus, fresh porcine heart or thoratic aorta segments from hogs could be alternatively used . Valuable information on the role of protein-protein interactions upon foaming could also be derived from foaming studies of model systems comprising myosin and actin under conditions promoting the formation and dissociation of actomyosin complexes.

**Figure V1: ELISA Assay for Determination of Myosin Concentration**

Immunochemical assaying of myosin concentration by ELISA, as described in Chapter 2 (2.4.9); **(a)** Calibration curve for varied antigen and conjugate concentrations and **(b)** comparison between the antigenicity of commercially available myosin antigen (see Chapter 2 (2.1)) and myosin samples courtesy of Prof. I.P. Trayer and Dr. D. Bandari (Bandari and Trayer (1991)) at equivalent concentrations.

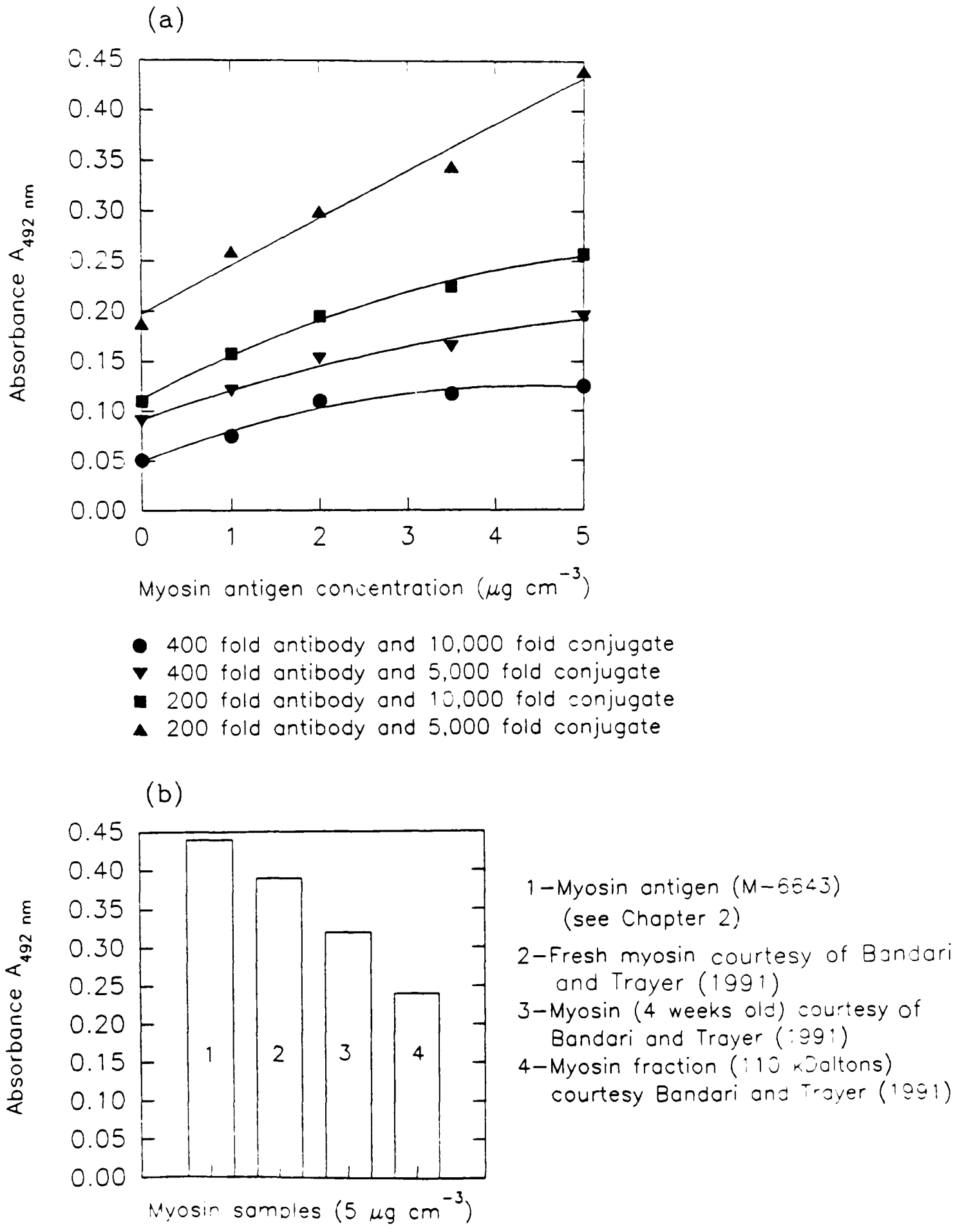

## *LIST OF ABBREVIATIONS*

BSA - Bovine Serum Albumin

CHL - Conductivity half-life

CMC - Critical micelle concentration

FP - Foaming power

HMW - High molecular weight

HRV - Head retention value

IEF - Isoelectric focusing

LMW - Low molecular weight

MW - Molecular weight

PB - Plateau border

PBS - Phosphate buffer saline

SP - Sampling port

# *BIBLIOGRAPHY*

AHMAD, S.I. (1975). *Separation Science*, **10**(6), 673.

AHMED, M. and DICKINSON, E. (1990). *Colloids and Surfaces*, **47**, 353.

ANDREWS, G. and SCHÜTZ, F. (1945). *J. Biochem.*, **39**, 1.

BADER, R., SCHUTZ, F. and STACEY, M. (1944). *Nature*, **154**, 183.

BAMFORTH, C.W. (1985). *J.Inst. Brew.*, **91**, 370.

BAMFORTH, C.W. (1989). In: *Food and Colloids*, eds. R.D. Bee, P. Richmond and J. Mingins, Royal Society of Chemistry, 48.

BANDARI, D. and TRAYER, I.P. (1991). *Personal Communication*, School of Biochemistry, University of Birmingham.

BIKERMAN, J.J. (1938). *Trans. Faraday Soc.*, **74**, 634.

BIKERMAN, J.J. (1973). *Foams*, Springer-Verlag, New York.

BIRD, R.B., STEWART, W.E. and LIGHTFOOT, E.N. (1960). *Transport Phenomena*, John Wiley & Sons Inc., New York-London.

BOHLEN, P., STEIN, S., DAIRMAN, W. and VOLENFRIEND, S. (1973). *Arch. Biochem. Biophys.*, **155**, 213.

BONAKDARPOUR, B. (1990). *Ph.D Thesis*, School of Chemical Engineering, University of Birmingham.

BOYLES, W.A. and LINCOLN, R.E. (1958). *Appl. Microbiol.*, **6**, 327.

BRADFORD, M.M. (1976). *Analytical Biochemistry*, **72**, 248.

BRASH, J.L. and UNIYAL, S. (1979). *Journal of Polymer Science: Polymer Symposium*, **66**, 377.

BRAUTIGAN, D.L., FERGUSON-MILLER, S. and MARGOLIASH, E. (1978). In: *Methods in Enzymology*, **LIII**(D), eds. S. Fleischer and L. Packer, Academic Press, 128.

BROOKER, B.E. (1985). *Food microfracture*, **4**, 289. (SEM Inc. AMF O'Hare, Chicago).

BROWN, L., NARSIMHAN, G. and WANKAT, P.C. (1990). *Biotechnology and Bioengineering*, **36**, 947.

BRUNNER, C.A. and LEMLICH, R. (1963). *I.&E.C. Fundamentals*, **2**(4), 297.

BUCHOLTZ, H., KALISCHEWSKI, K. and SCHÜGERL, K. (1979). *Eur. J. Appl. Microb. & Biotech.*, **7**, 321.

BUMBULLIS, W. and SCHÜGERL K. (1979). *Eur. J. Appl. Microb. Biotechnol.*, **8**, 17.

BUMBULLIS, W., KALISCHEWSKI, K. and SCHÜGERL, K. (1981). *Eur. J. Appl. Microb. Biotechnol.*, **11**, 110.

BUSHELL, C.H.G. (1962). *Transactions, Society of Mining Engineers*, September Issue, 266.

BURCKHART, R. and DECKWER, W.D. (1975). *Chemical Engineering Science*, **30**, 351.

CHARM, S.E., MORNIGSTAR, J., MATTEO, C.C. and PALTIEL, B. (1966). *Analytical Biochemistry*, **15**, 498.

CHARM, S.E. (1972). In: *Absorptive Bubble Separation Techniques* (Chapter 9), ed. R. Lemlich, Academic Press, New York and London, 157.

CLARK, D.C., MINGINS, J., SLOAN, F.E., SMITH, L.J. and WILSON, D.R. (1987). In: *Food Emulsions and Foams*, ed. E. Dickinson, Royal Society of Chemistry, London, 210.

CLARK, D.C., MACKIE, A.R., SMITH, L.J. and WILSON, D.R. (1988). *Food Hydrocolloids*, **2**(3), 209.

CLARK, D.C., MACKIE, A.R., SMITH, L.J. and WILSON, D.R. (1989). In: *Food Colloids*, eds. R.D Bee, J. Mingins, and P. Richmond, Royal Society of Chemistry, 97.

COLE, J.A. and RITTENBERG, S.C. (1971). *J. Gen. Microbiology*, **69**, 375.

COORRIER, R. and DOGNON, A. (1939). *C.R. Acad. Sci. Paris*, **202**, 242.

CROMPTON, I.E and HEGARTY, P.K. (1991). *Proceedings of the 3rd Conference on Malting, Brewing and Distilling*, 277.

DALGLEISH, D.G., EUSTON, S.E., HUNT, J.A. and DICKINSON, E. (1991). In: *Food Polymers, Gels and Colloids*, ed. E. Dickinson, Royal Society of Chemistry, Cambridge, 485.

DAVIES, J.T and RIDEAL, E.K (1961). *Interfacial Phenomena*, Academic Press, London.

DE FEIJTER, J.A. and BENJAMINS, J. (1987). In: *Food Emulsions and Foams*, ed. E. Dickinson, Royal Society of Chemistry, London, 72.

DE VRIES, A.J. (1972). In: *Absorptive Bubble Separation Techniques* (Chapter 2), ed. R. Lemlich, Academic Press, New York and London, 7.

DE WIT, J.N. and KLARENBECK, G. (1984). *J. Dairy Sci.*, **67**, 2701.

DER VILLAR, R., FINCH, J.A., GÓMEZ, C.O. and ESPINOZA-GOMEZ, R. (1992). *Minerals Engineering*, **5**(2), 169.

DESAI, D. and KUMAR, R. (1982). *Chemical Engineering Science*, **37**(9), 1361.

DESAI, D. and KUMAR, R. (1983). *Chemical Engineering Science*, **38**(9), 1525.

DESAI, D. and KUMAR, R. (1984). *Chemical Engineering Science*, **39**(11), 1559.

DESAI, D. and KUMAR, R. (1985). *Chemical Engineering Science*, **40**(7), 1305.

DICKINSON, E. and WOSKETT, C.M. (1989). In: *Food Colloids*, eds. R. D. Bee, J. Mingins, and P. Richmond, Royal Society of Chemistry, 74.

DICKINSON, E., MURRAY, B.S., STAINSBY, G. and BROCK, C.J. (1987). *Int. J. Biol. Macromol.*, **9**, 302.

DJABBARAH, N.F. and WASAN, D.T. (1985). *A.I.Ch.E Journal*, **31**(6), 1041.

DOUILLARD, R., LEFEBVRE, J. and TRAN, V. (1991a). In: *Food Polymers, Gels and Colloids*, ed. E. Dickinson, Royal Society of Chemistry, Cambridge, 564.

DOUILLARD, R. and TEISSIÉ, J. (1991b). *J.Colloid Interface Sci.*, **143**(1), 111.

DORMAN, D.C. and LEMLICH, R. (1965). *Nature*, **207**, 145.

EDWARDS, M., ESCHENBRUCH, R. and MOLAN, P.C. (1982). *Eur. J. Appl. Microbiol. Biotechnol.*, **16**, 105.

EMERY, A.N., BARKER, A.J. and HARGRAVE, A.L. (1977). *The Chemical Engineer*, July Issue, 506.

EXEROWA, D.and KASHCHIEV, D. (1986). *Contemp. Phys.* **27**(5), 429.

EVANS, M.T.A, MITCHELL, J., MUSSELLWHITE, P.R. and IRONS, L. (1970). In: *Advances in Experimental Medicine and Biology*, **70**, ed. M. Blank, 1.

FAIR, J.R., LAMBRIGHT, A.J. AND ANDERSEN, J.W. (1962). *Ind. Eng. Chem. Proc. Des. Dev.*, **1**, 33.

FANLO, S. and LEMLICH, R. (1965). *A.I.Ch.E.-I.Chem.E. Symposium Series*, No.9, 75.

FLANAGAN, J.A. and LYDDIATT, A. (1991): *Unpublished Data*, School of Chemical Engineering, University of Birmingham.

FREDERISKEN, D.W. and REES, D.D. (1982). In: *Methods in Enzymology*, **85**(B), eds. D.W Frederisken and L.W Cunningham, Academic Press, 292.

FRETHEIM, K., SAMEJIMA, K. and EGELANDSDAL, B. (1986). *Food Chemistry*, **22**, 107.

FUKAL, L., KÁš, J. and RAUCH P. (1986). *J. Inst. Brew.*, **92**, 357.

GEHLE, R.D. and SCHÜGERL, K. (1984a). *Appl. Microbiol. Biotechnol.*, **19**, 373.

GEHLE, R.D. and SCHÜGERL, K. (1984b). *Appl. Microbiol. Biotechnol.*, **20**, 133.

GERSHMAN, L.C., STRACHER, A. and DREIZEN, P. (1969). *The Journal of Biological Chemistry*, **244**(10), 2726.

GIANAZZA, E. and RIGHETTI, P.G. (1980). *Journal of Chromatography*, **193**, 1.

GIBBS, J.W. (1928). *Collected Works*, **1**, Longmans, Green, New York.

GODFREY, J.E. and HARRINGTON, W.F. (1970). *Biochemistry*, **4**(4), 886.

GONZALEZ, G. and MacRITCHIE, F. (1970). *J. Colloid Interface Sci.*, **32**, 55.

GRAHAM, D.E. and PHILLIPS, M.C. (1976). In: *Foams*, ed. R.J Akers, Academic Press, London, 237.

GRAHAM, D.E. and PHILIPS, M.C. (1979a). *J. Colloid Interface Sci.*, **70**(3), 403.

GRAHAM, D.E. and PHILIPS, M.C. (1979b). *J. Colloid Interface Sci.*, **70**(3), 415.

GRAHAM, D.E. and PHILIPS, M.C. (1979c). *J. Colloid Interface Sci.*, **70**(3), 427.

GRAHAM, D.E. and PHILIPS, M.C. (1980). *J. Colloid Interface Sci.*, **76**(1), 240.

GREASER, M.L., YATES, L.D., KRZYWICKI, K. and ROELKE, D.L. (1983). In: *Proceedings of 36th Reciprocal Meat Conference*, National Live Stock and Meat Board, Chicago, IL, 87.

GRIEVES, R.B. and WOOD, R.K. (1964). *A.I.Ch.E. Journal*, **10**(4), 456.

GRIEVES, R.B. and WANG, S.L. (1966). *Biotechnology and Bioengineering*, **8**, 323.

GRIEVES, R.B., BHATTACHARYYA, D. and CONGER, W.L. (1969). *Chem. Eng. Progr. Symp. Ser.*, **65**, 29.

HAAS, P.A. and JOHNSON, H.F. (1965). *A.I.Ch.E Journal*, **11**(2), 320.

HAAS, P.A. and JOHNSON, H.F. (1967). *I.&E.C. Fundamentals*, **6**(2), 225.

HALLING, P.J. (1981). *CRC Crit. Rev. Food Sci. Nutr.*, **15**(2), 155.

HANSEN, R.S. and DERDERIAN, E.J. (1976). In: *Foams*, ed. R.J Akers, Academic Press, 1.

HARPER, D.O. and LEMLICH, R. (1965). *I.&E.C. Process Design and Development*, **4**(1), 13.

HARTLAND, S. and BARBER, A.D. (1974). *Trans. Instn. Chem. Engrs*, **52**, 43.

HEGARTY, P.K., COPE, R., LEE, A.H. and BAMFORTH, C.W. (1989). *European Brewing Convention, Proceedings of the 22nd Congress, Zurich*, 553.

HEGARTY, P.K., CROMPTON, I.E. and WALLECH, E.R. (1991). *European Brewing Convention, Proceedings of the 23rd Congress, Lisbon*, 465.

HERBERT, D., PHIPPS, P.J. and STRANGE, R.E. (1971). In: *Methods in Microbiology*, **5B**, eds. J.R. Norris, and D.W. Ribbons, Academic Press, 282.

HERRINGTON, T.M. and SAHI, S.S. (1987). In: *Food Emulsions and Foams*, ed. E. Dickinson, Royal Society of Chemistry, London, 188.

HO, G.E. and PRINCE, R.G.H. (1971). In: *Proceedings of Symposium on Bubbles and Foams*, Nuremberg: Verein deutscher Ingenieure.

HOLLEMANS, M. and TONIES, A.R.J.M. (1989). *European Brewing Convention, Proceedings of the 22nd Congress, Zurich*, 561.

HOLMSTRöM, B. (1968). *Biotechnology and Bioengineering*, **10**, 551.

HOSTEN, Ç. and TEZCAN, A. (1990). *Minerals Engineering*, **3**(6), 637.

HUDSON, J.R. (1987). *The Brewers Digest*, July Issue, 86.

JACKSON, G. and BAMFORTH, C.W. (1982). *J. Inst. Brew.*, **88**, 378.

JACOBI, W.M. (1956). *Ind. Eng. Chem.*, **48**(11), 2046.

JENKINS, D., SCHERFIG, J. and ECKHOFF, D.W. (1972). In: *Absorptive Bubble Separation Techniques* (Chapter 9), ed. R. Lemlich, Academic Press, New York and London, 157.

JOHNSON, T.M. and ZABIC, M.E. (1981a). *Journal of Food Science*, **46**, 1226.

JOHNSON, T.M. and ZABIC, M.E. (1981b). *Journal of Food Science*, **46**, 1231.

JOHNSON, T.M. and ZABIC, M.E. (1981c). *Journal of Food Science*, **46**, 1237.

JOLLÈS JACQUELINE, PÉRIN JEAN-PIERRE and JOLLÈS PIERRE (1977). *Molecular and Cellular Biochemistry*, **17**(1), 39.

JONES, K.W. (1984). In: *Proceedings of the 37th Annual Reciprocal Meat Conference*, National Live Stock and Meat Board, Chicago, IL, 52.

KARGER, B.L., GRIEVES, R.B., LEMLICH, R., RUDIN, A.J. and SEBBA, F. (1967). *Separation Science*, **2**, 401.

KASSELL,B. and MEITMER, P.A. (1970). In: *Methods in Enzymology*, **19**, eds. G.E Perlmann and L. Lorand, Academic Press, London, 337.

KATO, A., OSAKO, Y., MATSUDOMI, N., KOBAYASHI, K. and NAKAI, S. (1983a). *Agric. Biol. Chem.*, **47**, 33.

KATO, A., TAKAHASHI, A., MATSUDOMI, N. and KOBAYASHI, K. (1983b). *Journal of Food Science*, **48**, 1983.

KESTER, J.J. and RICHARDSON, T. (1984). *J. Dairy Sci.*, **67**, 2757.

KHRISTOV, K., KRUGLJAKOV, P. and EXEROWA, D. (1979). *Colloid and Polymer Sci.*, **257**, 506.

KHRISTOV, K.I., EXEROWA, D.R. and KRUGLJAKOV, P.M. (1981). *J. Colloid Interface Sci.*, **79**(2), 584.

KHRISTOV, K.I., EXEROWA, D.R. and KRUGLJAKOV, P.M. (1983). *Colloid and Polymer Sci.*, **261**, 265.

KHRISTOV, K., MAŁYSA, K. and EXEROWA, D. (1984). *Colloids and Surfaces*, **11**, 39.

KIM, S.H. and KINSELLA, J.E. (1985). *Journal of Food Science* **50**, 1526.

KIM, S.H. and KINSELLA, J.E. (1987). *Journal of Food Science*, **51**(1), 92.

KINSELLA, J. (1981). *Food Chemistry*, **7**, 273.

KOCHWA, S., LITWAK, R.S., ROSENFIELD, R.E. and LEONARD, E.F. (1977). *Annals New York Academy of Sciences*, **283**, 37.

KOIDE, S., KATAO, S., TANAKA, Y. and KUBOTA, H. (1968). *J. Chem. Engng Japan*, **1**(1), 51.

KOULOHERIS, A.P. (1987). *Chemical Engineering*, October Issue, 88.

KRUGLJAKOV, P.M., EXEROWA, D and KHRISTOV, K. (1987). *Proceedings of the 31st International Conference of Pure and Applied Chemistry*, Section 7, Physical Chemistry and Electrochemistry, Sofia, Bulgaria, 116.

KUMAR, A., DEGALEESAN, T.E., LADDHA, G.S. and HOELSCHER, H.E. (1976). *The Canadian Journal of Chemical Engineering*, **54**, 503.

LALCHEV, Z., KHRISTOV, K., and EXEROWA, D. (1979). *Colloid and Polymer Sci.*, **257**, 1248.

LALCHEV, Z., DIMITROVA, L., TZVETKOVA, P. and EXEROWA, D. (1982). *Biotechnolology and Bioengineering*, **24**, 2251.

LEE, S.B. and RYU, D.D.Y. (1979). *Biotechnology and Bioengineering*, **21**, 2045.

LEESON, T.J. (1989). *PhD Thesis*, School of Chemical Engineering, University of Birmingham.

LEESON, T.J., VELISSARIOU, M. and LYDDIATT, A. (1991). In: *Food Polymers, Gels and Colloids*, ed. E. Dickinson, Royal Society of Chemistry, Cambridge, 194.

LEMLICH, R. and LAVI, E. (1961). *Science*, **134**, 191.

LEMLICH, R. (1972). In: *Absorptive Bubble Separation Techniques* (Chapter 3), ed. R. Lemlich, Academic Press, New York and London, 33.

LEMLICH, R. (1977). *J. Colloid and Interface Sci.*, **64**(1), 107.

LEONARD, R.A. and LEMLICH R. (1965a). *A.I.Ch.E Journal*, **1**(11), 18.

LEONARD, R.A. and LEMLICH R. (1965b). *A.I.Ch.E Journal*, **1**(11), 25.

LI-CHAN, E., NAKAI, S. and WOOD, D.F. (1987). *Journal of Food Science*, **52**(1), 31.

LLOPIS, J. and ALBERT, A. (1959a). *Arch. Biochem. Biophys.*, **81**, 146.

LLOPIS, J. and ALBERT, A. (1959b). *Arch. Biochem. Biophys.*, **81**, 159.

LONDON, M., and HUDSON, P.B. (1953). *Arch. Biochimica et Biophysica Acta*, **46**, 141.

LONDON, M., COHEN, M. and HUDSON, P.B. (1954). *Biochimica et Biophysica Acta*, **13**, 111.

LOWRY, O.H., ROSENBROUGH, N.Y., FARR, A.L. and RANDALL, R.Y (1951). *J. Biol. Chem.*, **193**, 265.

MALYSA, K. (1985). *Colloids and Surfaces*, **16**, 9.

MALYSA, K. (1987). *Bulletin of the Polish Academy of Sciences-Chemistry*, 35(9-10), 441.

MAMINOV, O.V. and MUTRISKOV, A. YA. (1969). *International Chemical Engineering*, 9(4), 642.

MARANGONI, C. (1871). *Nuovo Cimento*, **2** (5-6), 239.

MARRUCCI, G. (1965). *I.& E.C. Fundamentals* **4**(2), 224.

McGEE JAMIE (1989). *Chemical Engineering*, April Issue, 131.

MELANDER, W. and HORVATH, C. (1977). *Archives in Biochemistry and Biophysics*, **183**, 200.

MITCHELL, J.R (1986). In: *Developments in Food Proteins-4*, Chapter 8, ed. B.J.F. Hudson, Elsevier Applied Science Publishers, London, 291.

MIYAZU, Y. and YANO, T. (1974). *Agr. Biol. Chem.*, **38**(1), 183.

MOHAN, S.B., VELISSARIOU, M. and LYDDIATT, A. (1990). In: *Proc. Eur. Brewing Congress*, Dublin, ed. C.W. Bamforth, Zoeterwoude, Netherlands, EBC.

MOHAN, S.B. (1992). In: *Methods in Molecular Biology*, **11**, ed. A. Kennedy, The Humana Press Inc.

MOHAN, S.B., SMITH, L., KEMP, W. and LYDDIATT, A. (1992). *J. Inst.Brew.*, **98**, 187.

MOLAN, P.C., EDWARDS, M. and ESCHENBRUCH, R. (1982). *Eur. J. Appl. Microbiol.Biotechnol*, **16**, 110.

MORRISEY, B.W. (1977). *Annals New York Academy of Sciences*, **283**, 50.

MORRISSEY, P.A., MULVIHILL, D.M. and O'NEILL, E.M. (1987). In:*Developments in Food Proteins-5*, ed. B.J.F. Hudson, Elsevier Applied Science Publishers, London, 195.

MURRAY, E.K. (1987). In: *Food Emulsions and Foams*, ed. E. Dickinson, Royal Society of Chemistry, London, 170.

MYSELS, K.J., SHINODA, K. and FRANKEL, S. (1959). *Soap Films*, Pergamon Press.

NAKAI, S. (1983). *J. Agric. Food Chem.*, **31**, 676.

NARSIMHAN, G. and RUCKENSTEIN, E. (1986a). *Langmuir*, **2**(2), 230.

NARSIMHAN, G. and RUCKENSTEIN, E. (1986b). *Langmuir*, **2**(4), 494.

NARSIMHAN, G. (1987). *A.I.Ch.E.*, Summer National Meeting, August 16-19.

NARSIMHAN, G. (1991). In: *Food Polymers, Gels and Colloids*, ed. E. Dickinson, Royal Society of Chemistry, Cambridge, 207.

NIEUWOUNDT, D.J., VAN DEVENTER, J.S.J., REUTER, M.A. and ROSS, V.E. (1990). *Minerals Engineering*, 3(5), 483.

O'NEILL, E., MORRISSEY, P.A. and MULVIHILL, D.M. (1989). *Food Chemistry*,**34**, 295.

OSIPOW, L.I. (1962). *Surface Chemistry - Theory and Industrial Applications*, Reinhold Publishing Corporation, New York.

OSTERMAIER, K. and DOBIAS, B. (1984). *Flotative Separation of Protein in pH-Gradient*, Academic Press, NY, 1.

OSTWALD, W. and SIEHR, A. (1937). *Kolloid Z.*, **79**,11.

OUICHI, K. and AKUYAMA, H. (1971). *Agr. Biol. Chem.*, **35**, 1024.

OUICHI, K. and NUMOKAWA, Y. (1973). *J. Ferment. Technol.*, **51**, 85.

PARTHASARATHY, S., DAS, T.R. and KUMAR, R. (1988). *Biotechnology and Bioengineering*, **32**, 174.

PEGSON, E., ROBSON, E.W. and STAINSBY, E. (1985). *Colloids Surf.*, **14**, 135.

PELTONEN-SHALABY, R. and MANGINO, M.E. (1986). *Journal of Food Science*, **51**(1), 91.

PERRY, R.H. and GREEN, D.W. (1984). *Chemical Engineer's Handbook*, 6th Edition, McGraw Hill, New York.

PHARMACIA (1987). *Phast-system Manual*, Pharmacia Ltd., Uppsala, Sweden.

PHILLIPS, M.C. (1981). *Food Technology*, **35**, 50.

PIERCE, J. and SUELTER, C.H. (1977). *Analytical Biochemistry*, **81**, 478.

PLUMMER, D.T. (1978). *An Introduction to Practical Biochemistry*, 2nd Ed., McGraw Hill, London.

POLLARD, T.D. (1982). In: *Methods in Enzymology*, **85**(B), eds. D.W. Frederiksen and L.W. Cunningham, Academic Press, 123.

POOLE, S., WEST, S.I. and CLIFFORD, W.L. (1984). *J. Sci. Food Agric.*, **35**, 701.

PURSLOW PETER (1991). *Chemistry and Industry*, November Issue, 836.

RAO, S.R. (1974). Surface Forces in Flotation. *Minerals Sci. Engng.*, **6**(1), 45.

REISNER, A.H., MEMES, P. and BUCHOLTZ,C. (1975). *Analytical Biochemistry*, **64**, 509.

RICK, W. and FRITSCH, W.P. (1974). In: *Methods in Enzymatic Analysis*, ed. Bergmeter, 2nd edn, 1046.

ROBERTS, R.T. (1977). *Brewer's Digest*, June Issue, 50.

ROBERTS, R.T., KEENEY, P.J. and WAINWRIGHT, T. (1978). *J. Inst. Brew.*, **84**, 9.

RONTELTAP, A.D. and PRINS, A. (1989). In: *Food Colloids*, eds. R.D. Bee, J. Mingins, and P. Richmond, Royal Society of Chemistry, 39.

RONTELTAP, A.D., HOLLEMANS, M., BISPERINK, C.G.J., PRINS, A. (1991). *MBAA Technical Quarterly*, **28**, 25.

ROSE, M.W. and SEBBA, F. (1966). *J. Appl. Chem.*, **14**, 293.

ROY, R.B. (1989). *American Lab.*, **21**(3), 56.

RUDIN, A.D. (1957). *J. Inst. Brew.*, **63**, 506.

RUDIN, A.J.J. (1968). *Am. Water Works Assoc.*, **60**, 832

SARKAR, P., BHATTACHARYA, P., MUKHERJEA, R.N and MUKHERJEA, M. (1987). *Biotechnology and Bioengineering*, **29**, 934.

SAUTER, E.A. and MONTOURE, J.E. (1972). *Journal of Food Science*, **37**, 918.

SAWYER, W.H. (1969). *J. Dairy Sci.*, **52**, 1347.

SCHNEPF, R.W. and GADEN, E.L. (1959). *Journal of Biochemical and Microbiological Technology and Engineering*, **1**(1), 1.

SCHONFELD, E. and KIBBEY, A.H. (1967). *Nuclear Applications*, **3**, 353.

SCHUTZ, F. (1937). *Nature*, **139**, 630.

SEDMAK, J.J, and GROSSBERG, S.E. (1977). *Analytical Biochemistry*, **79**, 544.

SHAH, Y.T., KELKAR, S.P., GODBOL, S.P. and DECKWER, W.D. (1982). *A.I.Ch.E.Journal*, **28**(3), 353.

SHIH, F.S. and LEMLICH, R. (1971). *Ind. Eng. Chem. Fundam.*, **10**(2), 254.

SHIH NAN HSU and JER RU MAA (1985). *Ind. Eng. Chem. Process Des. Dev.*, **24**, 38.

SLACK, P.T. and BAMFORTH, C.W. (1983). *J. Inst. Brewing*, **89**, 397.

STEPHAN, D.G. (1965). *Civil Eng.* **35**(9), 46.

THOMAS, A. and WINKLER, M.A. (1977). In: *Topics in Enzyme and Fermentation Biotechnology 1*, (Chapter) 3, ed. A. Wiseman, Wiley, Chichester, 43.

THOMAS, C.R. (1990). In: *Critical Reports on Applied Chemistry*, **29** (Chemical Engineering Problems in Biotechnology), ed. M.A. Winkler, SCI, Elsevier Applied Science, 23.

TOWNSEND, A.A. and NAKAI S. (1983). *Journal of Food Science*, **48**, 588.

VELISSARIOU, M. (1988). *MSc Examination Thesis*, School of Chemical Engineering, University of Birmingham.

WACE, P.F. and BANFIELD, D.L. (1964) *Nature*, 113.

WACE, P.F., ALDER, P.J., and BANFIELD D.L. (1969). *Chemical Engineering Progress Symposium Series*, **65**(91), 19.

WANG, J.C. and KINSELLA, J.E. (1976). *Journal of Food Science*, **41**, 498.

WANISKA, R.D. and KINSELLA, J.E. (1985). *J. Agric. Food Chem.*, **33**, 1143.

WEARIE, D. (1989). In: *Food Colloids*, eds. R.D. Bee, J. Mingins, and P. Richmond, Royal Society of Chemistry, 25.

WEIJENBERG, D.C., MULDER, J.J, DRINKENBURG, A.A.H. and STEMERDING, S. (1978). *Ind. Eng. Chem. Process Des. Dev.*, **17**(2), 209.

WEST, S.I. (1984). *J. Chem. Tech. Biotechnol.*, **34B**, 176.

WEST, S.I. and WALTERS, C.L. (1984). *J. Sci. Food Agric.*, **35**, 701.

WHITE, W.F., BARLOW, G.H. and MOZEN, M.M. (1966). *Biochemistry*, **5**, 2160.

WILSON, P.J. and MANDY, A.P. (1984). *J. Inst. Brew.*, **90**, 385.

WILSON, A.J. (1989). *Microscopy and Analysis*, March Issue, 37.

WRIGHT, D.J. and HEMMANT, J.W. (1987). In: *Food Emulsions and Foams*, ed. E. Dickinson, Royal Society of Chemistry, London, 284.

WROBEL, S.A. (1953). *Mine & Quarry Engineering*, October Issue, 363.

YAGISAWA, S. (1975). *J. Biochem.*, **77**, 605.

ZITTLE, C.A., THOMPSON, M.P., CUSTER, J.H. and CERBULLIS, J. (1962). *J. Dairy Sci.*, **45**, 807.

ZLOKARNIK, M. (1986). *Ger. Chem. Eng.*, **9**, 314.

WILSON, P.J. and MANDY, A.P. (1984). *J. Inst. Brew.*, **90**, 385.

WILSON, A.J. (1989). *Microscopy and Analysis*, March Issue, 37.

WRIGHT, D.J. and HEMMANT, J.W. (1987). In: *Food Emulsions and Foams*, ed. E. Dickinson, Royal Society of Chemistry, London, 284.

WROBEL, S.A. (1953). *Mine & Quarry Engineering*, October Issue, 363.

YAGISAWA, S. (1975). *J. Biochem.*, **77**, 605.

ZITTLE, C.A., THOMPSON, M.P., CUSTER, J.H. and CERBULLIS, J. (1962). *J. Dairy Sci.*, **45**, 807.

ZLOKARNIK, M. (1986). *Ger. Chem. Eng.*, **9**, 314.